PHD

# Detection of instability in power systems using connectionism

Edwards, A. R.

*Award date:*
1995

*Awarding institution:*
University of Bath

Link to publication

# DETECTION OF INSTABILITY IN POWER SYSTEMS USING CONNECTIONISM

Submitted by A.R. Edwards, B.Eng.(Hons)
in partial fulfilment of the requirements
for the degree of
Doctor of Philosophy
at the University of Bath
1995



A. R. Edwards

Bath, September 1, 1995

# Summary

This thesis describes a new method for the detection of instability within large interconnected power systems. A novel feature extraction technique is used to provide inputs to a connectionist system which classifies the stability of the power system subject to a set of disturbances (contingencies). This method has been used to develop stability screens for use within on-line dynamic security assessment systems. At the core of a dynamic security assessor are functions to provide fast contingency screening for power system instability. A database of several thousand contingencies must be screened to detect those which may cause stability problems so that a more detailed evaluation of their effects can be presented to the power system operators. Such screens must be *conservative* and always detect those contingencies which will lead to stability problems even at the expense of mis-classifing some stable contingencies as potentialy unstable. Those contingencies which are detected by the stability screens as potential problems are then evaluated in detail, usually by a time domain simulation, and then ranked according to their severity. Future developments in this field will lead to the development of tools to advise the operators as to possible preventative or corrective control actions.

These screens are shown to be highly suited to on-line operation by integration within OASIS [1] , a state of the art dynamic security assessor which has been developed at the University of Bath. The overall improvement in the performance of OASIS using snapshots of the UK national grid system is shown to represent a significant step forward towards achieving full on-line dynamic security assessment of large power systems.

[1]Online Algorithms for System Instability Studies

# Acknowledgements

This work would not have been possible without the help, support and encouragement of many people. My supervisor Dr R.W. Dunn provided a great deal of support and advice, for which I am very grateful. I also thank Dr A. Ekwue of the National Grid Company, my industrial supervisor and the staff at the National Grid Control Centre, for their help and guidance.

Thanks are also due to my colleagues in the School of Electronic and Electrical Engineering, especially Mr A.R. Daniels, Dr K.W. Chan, Mr K.R.W. Bell, Dr C.G. Groom and Mr J.M. Grzejewski who all contributed to a pleasant and stimulating working environment.

I thank Professor A.T. Johns for permission to study in the School of Electronic and Electrical Engineering and for the provision of facilities. This project has been funded by an Engineering and Physical Science Research Council CASE[2] award in collaboration with the National Grid Company.

[2]Co-operative Award in Science and Engineering

# Contents


**1 Introduction** 1

1.1 Electrical Power Generation . . . 2
1.2 Electrical Transmission and Distribution . . . 3
1.3 Using Electrical Energy . . . 5
1.4 Modern Power Systems . . . 5
1.5 About this Thesis . . . 7

**2 Power System Operation** 9

2.1 Introduction . . . 9
2.2 UK national grid system . . . 11
2.2.1 Demand . . . 13
2.2.2 Generation Capability . . . 13
2.2.3 Economics . . . 14
2.2.4 The Future . . . 15
2.3 Power System Controls . . . 16
2.3.1 Frequency . . . 16
2.3.2 Voltage . . . 18
2.3.3 Protection . . . 20
2.4 Energy Management Systems . . . 20
2.4.1 SCADA Subsystem . . . 22
2.4.2 State Estimation . . . 23
2.4.3 Dispatch . . . 24
2.4.4 Security Assessment . . . 24
2.5 Chapter Summary . . . 26

**3 Dynamic Security Assessment** 29

3.1 Introduction . . . 29
3.2 Power System Stability . . . 31
3.2.1 Transient Instability . . . 33
3.2.2 Oscillatory Instability . . . 34
3.2.3 Steady State Stability . . . 36

3.2.4 Voltage Stability . . . . . . . . . . . . . . . . . . . . . . . . . 36
3.3 Current Operating Practice . . . . . . . . . . . . . . . . . . . . . . . 37
3.4 Dynamic Security Assessors . . . . . . . . . . . . . . . . . . . . . . . 38
3.4.1 Contingency Selection . . . . . . . . . . . . . . . . . . . . . . 41
3.4.2 Contingency Screening . . . . . . . . . . . . . . . . . . . . . . 41
3.4.3 Contingency Evaluation . . . . . . . . . . . . . . . . . . . . . 43
3.4.4 Contingency Ranking . . . . . . . . . . . . . . . . . . . . . . 43
3.4.5 Limit Calculations . . . . . . . . . . . . . . . . . . . . . . . 44
3.4.6 Operator Interface . . . . . . . . . . . . . . . . . . . . . . . 44
3.5 OASIS . . . . . . . . . . . . . . . . . . . . . . . . . . . . . . . . . 45
3.5.1 Client-Server Approach . . . . . . . . . . . . . . . . . . . . . 45
3.5.2 Parallel Evaluation . . . . . . . . . . . . . . . . . . . . . . . 47
3.5.3 Client Task . . . . . . . . . . . . . . . . . . . . . . . . . . . 48
3.5.4 Server Task . . . . . . . . . . . . . . . . . . . . . . . . . . . 51
3.5.5 Field Trials . . . . . . . . . . . . . . . . . . . . . . . . . . . 53

**4 Contingency Screening** **56**
4.1 Introduction . . . . . . . . . . . . . . . . . . . . . . . . . . . . . . 56
4.2 Traditional Approaches . . . . . . . . . . . . . . . . . . . . . . . . . 57
4.2.1 Numerical Integration . . . . . . . . . . . . . . . . . . . . . . 57
4.2.2 Energy Function Methods . . . . . . . . . . . . . . . . . . . . 58
4.2.3 Expert Systems . . . . . . . . . . . . . . . . . . . . . . . . . 62
4.2.4 Eigenvalue Analysis . . . . . . . . . . . . . . . . . . . . . . . 63
4.2.5 Pattern Recognition Method . . . . . . . . . . . . . . . . . . . 64
4.3 Chapter Summary . . . . . . . . . . . . . . . . . . . . . . . . . . . . 68

**5 Connectionism** **70**
5.1 Biological Basis for Neural Network Tools . . . . . . . . . . . . . . . 71
5.1.1 Structure . . . . . . . . . . . . . . . . . . . . . . . . . . . . 71
5.1.2 Operation . . . . . . . . . . . . . . . . . . . . . . . . . . . . 72
5.2 Artificial Neural Network Models . . . . . . . . . . . . . . . . . . . . 73
5.2.1 The Perceptron . . . . . . . . . . . . . . . . . . . . . . . . . 74
5.2.2 Multi-Layer Perceptrons . . . . . . . . . . . . . . . . . . . . . 75
5.2.3 The Self-Organisation Model . . . . . . . . . . . . . . . . . . . 77
5.2.4 The Hopfield Model . . . . . . . . . . . . . . . . . . . . . . . 78
5.3 Practical Issues . . . . . . . . . . . . . . . . . . . . . . . . . . . . . 78
5.3.1 Choice of Model . . . . . . . . . . . . . . . . . . . . . . . . . 79
5.3.2 Size of Model . . . . . . . . . . . . . . . . . . . . . . . . . . 79

5.3.3 Feature Extraction . . . . . . . . . . . . . . . . . . . . . . 80
5.3.4 Generalisation versus Memorisation . . . . . . . . . . . . . . 80
5.3.5 Inversion . . . . . . . . . . . . . . . . . . . . . . . . . . . 81
5.4 Performance Metrics for ANNs . . . . . . . . . . . . . . . . . . . 81
5.4.1 Percent Correct . . . . . . . . . . . . . . . . . . . . . . . . 81
5.4.2 Average Sum-Squared Error . . . . . . . . . . . . . . . . . . 82
5.4.3 ROC Curves . . . . . . . . . . . . . . . . . . . . . . . . . . 82
5.4.4 Chi-Square Test . . . . . . . . . . . . . . . . . . . . . . . . 84
5.5 Neural Network Tools . . . . . . . . . . . . . . . . . . . . . . . . 85
5.5.1 (N)eural (N)etwork (S)imulator . . . . . . . . . . . . . . . . 85
5.5.2 (S)tuttgart (N)eural (N)etwork (S)imulator . . . . . . . . . . . 85
5.6 Formal Methods . . . . . . . . . . . . . . . . . . . . . . . . . . . 86
5.7 Current Application Areas . . . . . . . . . . . . . . . . . . . . . 87
5.8 Sources of Information . . . . . . . . . . . . . . . . . . . . . . . 88
5.9 Chapter Summary . . . . . . . . . . . . . . . . . . . . . . . . . . 89

**6 Neural Network Contingency Screening 90**

6.1 Why use Neural Networks? . . . . . . . . . . . . . . . . . . . . . 90
6.2 Overview . . . . . . . . . . . . . . . . . . . . . . . . . . . . . . . 91
6.2.1 Advantages . . . . . . . . . . . . . . . . . . . . . . . . . . 92
6.2.2 Drawbacks . . . . . . . . . . . . . . . . . . . . . . . . . . . 93
6.3 Instability Indices . . . . . . . . . . . . . . . . . . . . . . . . . . 96
6.3.1 Transient Instability Indices . . . . . . . . . . . . . . . . . . 96
6.3.2 Oscillatory Instability Indices . . . . . . . . . . . . . . . . . 98
6.4 Composite Indices . . . . . . . . . . . . . . . . . . . . . . . . . . 102
6.4.1 Why use Composite Indices? . . . . . . . . . . . . . . . . . . 103
6.4.2 Set Notation . . . . . . . . . . . . . . . . . . . . . . . . . . 103
6.4.3 Base Indices . . . . . . . . . . . . . . . . . . . . . . . . . . 106
6.4.4 Statistical Functions . . . . . . . . . . . . . . . . . . . . . . 112
6.5 Selection Of Composite Indices . . . . . . . . . . . . . . . . . . . 115
6.6 Visualisation of Feature Space . . . . . . . . . . . . . . . . . . . . 117
6.6.1 Single feature suitability . . . . . . . . . . . . . . . . . . . . 117
6.6.2 Box Plots . . . . . . . . . . . . . . . . . . . . . . . . . . . . 118
6.6.3 Selected features' suitability . . . . . . . . . . . . . . . . . . 119
6.6.4 Sammon Plots . . . . . . . . . . . . . . . . . . . . . . . . . . 119
6.6.5 Edwards-Sammon Plot . . . . . . . . . . . . . . . . . . . . . 121
6.7 Screening Implementation Methods . . . . . . . . . . . . . . . . . 123

6.7.1 Multiple Contingency Screens . . . . . . . . . . . . . . . . . . 123
6.7.2 Voting Methods . . . . . . . . . . . . . . . . . . . . . . . . . 124
6.8 Performance Evaluation . . . . . . . . . . . . . . . . . . . . . . . 125
6.8.1 Performance of Screen . . . . . . . . . . . . . . . . . . . . . . 125
6.8.2 Improvement in overall DSA performance . . . . . . . . . . . 126
6.9 Chapter Summary . . . . . . . . . . . . . . . . . . . . . . . . . . 126

**7 Enhancements to OASIS 128**
7.1 Modifications to Client Task . . . . . . . . . . . . . . . . . . . . 128
7.1.1 Voltage Profile . . . . . . . . . . . . . . . . . . . . . . . . . 130
7.1.2 MW Injection Profile . . . . . . . . . . . . . . . . . . . . . . 131
7.1.3 MVar Injection Profile . . . . . . . . . . . . . . . . . . . . . 132
7.2 Modifications to Server Task . . . . . . . . . . . . . . . . . . . . 133
7.2.1 PVM Interface . . . . . . . . . . . . . . . . . . . . . . . . . 134
7.2.2 Load Flow Module . . . . . . . . . . . . . . . . . . . . . . . 135
7.2.3 Composite Indices Module . . . . . . . . . . . . . . . . . . . 136
7.2.4 Stability Screen Module . . . . . . . . . . . . . . . . . . . . 136
7.2.5 Operation . . . . . . . . . . . . . . . . . . . . . . . . . . . . 138

**8 Simulation Results 141**
8.1 100 Busbar Model . . . . . . . . . . . . . . . . . . . . . . . . . . 141
8.1.1 Transient Instability Screen . . . . . . . . . . . . . . . . . . . 142
8.1.2 Oscillatory Instability Screen . . . . . . . . . . . . . . . . . . 145
8.1.3 Performance Evaluation . . . . . . . . . . . . . . . . . . . . . 146
8.1.4 Contingency Allocation . . . . . . . . . . . . . . . . . . . . . 148
8.2 Full UK Power System Snapshots . . . . . . . . . . . . . . . . . . 149
8.2.1 Transient Instability Screen . . . . . . . . . . . . . . . . . . . 150
8.2.2 Oscillatory Instability Screen . . . . . . . . . . . . . . . . . . 152
8.2.3 Performance Evaluation . . . . . . . . . . . . . . . . . . . . . 154
8.2.4 Contingency Allocation . . . . . . . . . . . . . . . . . . . . . 155
8.3 Chapter Summary . . . . . . . . . . . . . . . . . . . . . . . . . . 156

**9 Conclusions 158**
9.1 Overall Approach . . . . . . . . . . . . . . . . . . . . . . . . . . 159
9.2 Composite Indices . . . . . . . . . . . . . . . . . . . . . . . . . . 159
9.3 Pattern Classifier . . . . . . . . . . . . . . . . . . . . . . . . . . 160
9.4 Performance . . . . . . . . . . . . . . . . . . . . . . . . . . . . . 161
9.4.1 Speedup . . . . . . . . . . . . . . . . . . . . . . . . . . . . . 161

9.4.2 Transient Instability Detection . . . . . . . . . . . . . . . . . . . 161
9.4.3 Oscillatory Instability Detection . . . . . . . . . . . . . . . . . . 162
9.5 Visualisation of Power System Stability . . . . . . . . . . . . . . . . . . 162
9.6 Edwards-Sammon Plots . . . . . . . . . . . . . . . . . . . . . . . 163
9.7 Practical DSA Implementation . . . . . . . . . . . . . . . . . . . . . . 163

**10 Suggestions for further work** **166**
10.1 Extensive on-line testing of screens . . . . . . . . . . . . . . . . . . . 166
10.2 On-line adaption of screens . . . . . . . . . . . . . . . . . . . . . . . 167
10.3 Development of Screens for unusual operating conditions . . . . . . . 168
10.4 Application to on-line limit calculation . . . . . . . . . . . . . . . . . . 168
10.5 Full on-line dynamic security assessment system . . . . . . . . . . . . 170
10.6 Application to other large engineering systems . . . . . . . . . . . . . 171

**A Box Plots** **192**
A.1 Transient Stabilty . . . . . . . . . . . . . . . . . . . . . . . . . . . 192
A.2 Oscillatory Stability . . . . . . . . . . . . . . . . . . . . . . . . . . 194

**B Published Work** **197**

# List of Tables

2.1 1994/95 Generation Capability . . . . . . . . . . . . . . . . . . . . . . 14

5.1 ROC Contingency Table . . . . . . . . . . . . . . . . . . . . . . . . . . 83
5.2 ROC Ratios . . . . . . . . . . . . . . . . . . . . . . . . . . . . . . . . 83
5.3 Neural Network Application Areas . . . . . . . . . . . . . . . . . . . . 88
5.4 Neural Networks in Power Systems . . . . . . . . . . . . . . . . . . . . 88
5.5 Neural Network URLs . . . . . . . . . . . . . . . . . . . . . . . . . . . 89

6.1 Screen Performance Table . . . . . . . . . . . . . . . . . . . . . . . . 125

8.1 Selected Composite Indices for Transient Instability Screen . . . . . . 143
8.2 Oscillatory Instability Screen Composite Indices for Laboratory Scale Model . . . . . . . . . . . . . . . . . . . . . . . . . . . . . . . . . . 145
8.3 Performance for Laboratory Scale Model . . . . . . . . . . . . . . . . 147
8.4 Transient Instability Screen Composite Indices for NGC Model . . . . 150
8.5 Oscillatory Instability Screen Composite Indices for NGC Model . . . 152
8.6 Performance the Instability Screens . . . . . . . . . . . . . . . . . . . 154

# List of Figures


2.1 The UK national grid system . . . . . . . . . . . . . . . . . . . . . . . . 11
2.2 Typical Winter Weekday Load Curve . . . . . . . . . . . . . . . . . . . 13
2.3 A Governor Control System . . . . . . . . . . . . . . . . . . . . . . . . 17
2.4 Connections for one phase of a Quadrature Booster . . . . . . . . . . 18
2.5 The place of an Energy Management System . . . . . . . . . . . . . . 21
2.6 Block Diagram of an EMS . . . . . . . . . . . . . . . . . . . . . . . . 22
2.7 Steps in State Estimation . . . . . . . . . . . . . . . . . . . . . . . . . 23
2.8 Power System Security Levels . . . . . . . . . . . . . . . . . . . . . . 28

3.1 Example of Transient Instability . . . . . . . . . . . . . . . . . . . . . 34
3.2 England Scotland Oscillatory Instability . . . . . . . . . . . . . . . . . 35
3.3 Relationship between power supplied and receiving voltage . . . . . . 37
3.4 DSAS Block Diagram . . . . . . . . . . . . . . . . . . . . . . . . . . . 39
3.5 Contingency Screening - The Filtering Process . . . . . . . . . . . . . 42
3.6 Block Diagram of OASIS . . . . . . . . . . . . . . . . . . . . . . . . . 46
3.7 An Example OASIS System . . . . . . . . . . . . . . . . . . . . . . . . 47
3.8 Ranked Contingency List . . . . . . . . . . . . . . . . . . . . . . . . . 50
3.9 Detail of Contingency . . . . . . . . . . . . . . . . . . . . . . . . . . . 51
3.10 Setup for OASIS Trials at NGCC . . . . . . . . . . . . . . . . . . . . 53

5.1 Biological Neuron . . . . . . . . . . . . . . . . . . . . . . . . . . . . . 72
5.2 Single-layer perceptron . . . . . . . . . . . . . . . . . . . . . . . . . . 74
5.3 Feed-forward Network Structure . . . . . . . . . . . . . . . . . . . . . 76
5.4 Example ROC curve . . . . . . . . . . . . . . . . . . . . . . . . . . . . 84
5.5 SNNS Screen Display . . . . . . . . . . . . . . . . . . . . . . . . . . . 87

6.1 Outline of the ANN Screening Approach . . . . . . . . . . . . . . . . . 92
6.2 Conceptual Stability Boundary . . . . . . . . . . . . . . . . . . . . . . 94
6.3 Slice Through a Stability Boundary . . . . . . . . . . . . . . . . . . . 95
6.4 Transient Decay Envelope . . . . . . . . . . . . . . . . . . . . . . . . 102
6.5 A good composite index for stability classification . . . . . . . . . . . 118

6.6 Box Plots for two composite indices . . . . . . . . . . . . . . . . . . . . 119
6.7 Sammon Plot for Iris Data Set . . . . . . . . . . . . . . . . . . . . . . . . 120
6.8 Edwards-Sammon Plot for Transient Stability . . . . . . . . . . . . . 121
6.9 Multiple Contingency Screens . . . . . . . . . . . . . . . . . . . . . . . 124

7.1 Security map with voltage profile . . . . . . . . . . . . . . . . . . . . . 130
7.2 Security map with MW injection profile . . . . . . . . . . . . . . . . . 131
7.3 Security map with MVar injection profile . . . . . . . . . . . . . . . . 132
7.4 Block diagram of new server task . . . . . . . . . . . . . . . . . . . . . 134
7.5 Control flow for composite index generation . . . . . . . . . . . . . . 140

8.1 100 Busbar Power System Model . . . . . . . . . . . . . . . . . . . . . 142
8.2 Transient Instability Screen Edwards-Sammon Plot for Laboratory Scale Model . . . . . . . . . . . . . . . . . . . . . . . . . . . . . . . . 144
8.3 Oscillatory Instability Screen Sammon Plot for Laboratory Scale Model 146
8.4 Contingency Allocation for Laboratory Scale Model . . . . . . . . . . 149
8.5 Transient Instability Screen Sammon Plot for NGC Model . . . . . . 151
8.6 Oscillatory Instability Screen Sammon Plot for NGC Model . . . . . 153
8.7 Contingency Allocation for Laboratory Scale Model . . . . . . . . . . 156

9.1 Setup for OASIS at NGCC . . . . . . . . . . . . . . . . . . . . . . . . . 164

10.1 Online Adaption of ANN Stability Screen . . . . . . . . . . . . . . . . 167
10.2 Transfer Limit Calculation using Stability Screens . . . . . . . . . . . 169

# List of Abbreviations

| | |
|---|---|
| AC | Alternating Current |
| ACC | Area Control Centre |
| ANN | Artificial Neural Network |
| ANSI | American National Standards Institute |
| BNN | Biological Neural Network |
| CCGT | Closed Cycle Gas Turbine |
| CTP | Contingency Termination Point |
| DC | Direct Current |
| DSA | Dynamic Security Assessment |
| DSAS | Dynamic Security Assessment System |
| EAC | Equal Area Criterion |
| EMC | Energy Management Centre |
| EMS | Energy Management System |
| EPRI | Electric Power Research Institute (USA) |
| EPSRC | Engineering and Physical Sciences Research Council (UK) |
| FN | False Negative (part of ROC) |
| FP | False Posotive (part of ROC) |
| GSP | Grid Supply Point |
| HCI | Human Computer Interface |
| LFR | Low Frequency Relay |
| MLP | Multi-layered perceptron |
| MOD | Mode of Disturbance |
| NGC | National Grid Company plc (UK) |

| | |
|---|---|
| NGCC | National Grid Control Centre |
| NNS | Neural Network Simulator |
| NNT | Neural Network Tool |
| OASIS | On-line Algorithms for System Instability Studies (a DSAS) |
| OCGT | Open Cycle Gas Turbine |
| OPF | Optimal Power Flow |
| PowSim | A real-time power system simulator |
| PVM | Parallel Virtual Machine |
| RASM | Stability analysis program developed by NGC |
| REC | Regional Electricity Company |
| ROC | Receiver Operating Curve |
| SNNS | Stuttgart Neural Network Simulator |
| SLP | Single-layered perceptron |
| SSA | Static Security Assessment |
| TEF | Transient Energy Function |
| TN | True Negative (part of ROC) |
| TP | True Posotive (part of ROC) |
| UEP | Unstable Equilibrium Point |
| UK | United Kingdom |
| URL | Uniform resource locator (WWW) |
| USA | United States of America |
| WWW | World Wide Web |

# List of Symbols

## General

| | |
|---|---|
| $C(\ldots)$ | Pattern classifier 'C' |
| P | Real power (MW) |
| p(t) | Envelope of rotor swing decays |
| Q | Reactive power (MVar) |
| S | Sensitivity value |
| t | Time (Seconds) |
| T | Temperature (Kelvin) |
| $V_a$ | Phase A voltage (Volts) |
| $V_{ab}$ | Voltage between phases A and B (Volts) |
| $x_i$ | X axis value of $i^{th}$ point |
| $y_i$ | Y axis value of $i^{th}$ point |
| $\Delta V$ | Transient energy margin |

## Neural Network Variables

| | |
|---|---|
| $d$ | Desired neuron output value |
| E | Error value |
| $I$ | Neuron input value |
| $O$ | Neuron output value |
| $w$ | Connection weight |
| $\alpha$ | Back-propagation momentum factor |
| $\delta$ | Back-propagation error gradient |
| $\eta$ | Back-propagation learning rate |

## Composite Index Variables

| | |
|---|---|
| a | Amplitude scale factor for transient decay |
| b | Time constant factor for transient decay |
| $I_o$ | Centre of inertia for all generators |
| $I_i$ | Inertia for $i^{th}$ generator |
| $N_b$ | Number of busbars |
| $N_g$ | Number of generators |
| $N_l$ | Number of transmission lines |
| $\delta_i$ | Rotor angular position at time $i$ $(Rad)$ |
| $\mu$ | Power system parameters |
| $\mu_o$ | Pre-contingency value of system parameters |
| $\omega$ | Rotor speed $(Rads^{-1})$ |
| $\dot{\omega}$ | Rotor acceleration $(Rads^{-2})$ |
| $\phi$ | Value of a composite index |
| $\phi_{ake}$ | Asynchronous Kinetic Energy |
| $\sigma$ | Standard deviation |

## Performance Metrics

| | |
|---|---|
| $N_c$ | Total number of selected contingencies |
| $N_o$ | Number of oscillatory unstable contingencies |
| $N_t$ | Number of transiently unstable contingencies |
| $\alpha_{xy}$ | Number of contingencies of class x classified as class y |
| $\eta_O$ | Efficiency of oscillatory instability screen |
| $\eta_T$ | Efficiency of transient instability screen |
| $\lambda_O$ | Speedup of oscillatory instability screen |
| $\lambda_T$ | Speedup of transient instability screen |

Chapter One

# Introduction

Lightning flashed, thunder rolled and pre-historic man gazed up into the heavens in wonder, and in those few split seconds began his fascination with electricity. Although such natural manifestations of electrical energy are virtually impossible to control, electricity is one of the key components of a modern industrial society as it can be easily generated, transported and converted into usable energy. There is a clear link between the energy consumption per head of population and the standard of living[1], and as we approach the $21^{st}$ century even more of this energy is being supplied in the form of electricity.

The pioneering work undertaken by Oersted, Ampere, Faraday, Tesla and Maxwell to mention but a few names has been well documented[2, 3] and has given rise to one of the most convenient forms of energy known to man. From the humble beginnings of the strange behaviour of current carrying wires has come the technological revolution that has seen the development of widespread interconnected power systems, factory automation, the micro-computer era and the age of space travel[4, 5]. All of these developments have arisen through the cheap[6], safe and secure transport of electrical power from generators through the transmission and distribution systems[7] to consumers. The equipment involved in the generation, transmission and distribution of electrical power form what is usually referred to as a *power system.*

## 1.1 Electrical Power Generation

With the exception of water driven turbines, virtually all prime movers used in the generation of electricity are *heat engines* and subject to the so-called Carnot Limitation[1]. This arises from the second law of thermodynamics which states that a temperature difference is essential before heat energy can be converted into work. This leads to the conclusion that the maximum possible thermal efficiency for *any heat engine* is:

$$\eta_{max} = \frac{T_1 - T_2}{T_1} \tag{1.1}$$

where $T_1$ is the temperature of the working fluid, normally steam, and $T_2$ is the minimum (condenser) temperature. In this case $T_1$ is limited to about $550^oC$,$823K$ and $T_2$ to $100^oC$,$373K$. This gives a maximum possible efficiency of only 55%, but in practice the efficiency is usually only about 40% due to other losses.

In the UK, electrical power generation comes from four main sources [8–11]. Coal has historically been the greatest contributor, but the exhausting of seams and the consequent need for deeper mines has led to a reduction in the economics of using this method. In recent years, the tight environmental controls have led to the closing of some coal fired power stations as the cost of *cleaning up* has been too costly. Nuclear power was conceived as the successor to coal and is fairly economic to operate. However, the high development and de-commissioning costs as well as the serious problem of the processing of nuclear waste has stunted its growth. Over recent years there has been a considerable growth in the number of gas turbine based power stations. These stations are useful to supply power during peak loading and have run-up times of only two to four minutes. Pump storage stations, such as those at Ffestiniog and Dinorwig in North Wales, provide a fast and economic method for providing peak loading power. During light loading conditions, water is pumped from a low to a high reservoir and this can be reversed to provide generation in about one minute. Other renewable sources of generation are continuously being sought, but have so far not been practical on a large scale. Of these tidal and wind power are the most promising methods. Research on using fusion power for electric power generation will, when successfully completed, lead to an almost inexhaustible supply of safe, clean energy.

## 1.2 Electrical Transmission and Distribution

The interconnection of power systems within the UK started in the North East and spread to the rest of the country through the National Grid. The motivation for this was to create economy by reducing the amount of spare machinery at power stations, to make use of diversity in times of maximum load and to provide an alternative source of supply in the event of failure of equipment at a power station. It is this last reason that ensures that an interconnected power system is operationally more secure than many separate power systems. Recently, it has enabled the operators of the power system to use generators in *Merit Order*, ie use the cheapest generation most of the time and bring in expensive generation to meet peak loading or security requirements.

The need for high voltage transmission systems arises from the fact that the per-unit loss of power transmission is inversely proportional to the transmission voltage. The maximum *safe* voltage for utilisation of electrical power has been considered to be 240V to earth, 415V three phase. For economic transfer of power between these different voltage levels, the use of AC transformers, and hence an AC power system is essential[12].

In the early days of electrical power generation, separate systems used different frequencies of generation. With the advent of an interconnected power system it was clearly necessary to standardise on a frequency and by an Act of Parliament in 1926, 50Hz was chosen, primarily because it was high enough to power lights with no observable flicker.

The choice between overhead transmission lines and underground cables has been traditionally made on economic grounds. Underground cables are approximately 20 times as expensive as overhead lines for the same distance, and suffer from capacitative problems, usually requiring shunt reactors for compensation. Overhead lines are naturally more exposed and frequently suffer from lightning strikes but due to the high degree of interconnection of the transmission system, and the development of protection relaying, these effects are minimised. However, with current planning laws it is becoming increasingly more difficult to obtain planning permission for overhead transmission lines and because underground cables are able to protect the aesthetics of the environment it is expected that their use will increase.

The protection of transmission lines, generators and transformers from damage due to faults on the transmission system is very important if one considers the capital cost of such items of plant and the operational costs involved of operation without these items in service[13].

## 1.3 Using Electrical Energy

Electrical energy can easily be converted into light, heat, or motive power. The work of Thomas Edison has led to the modern day light-bulbs, the work of Graham Bell has led to the worldwide communications breakthrough that has happened over the last few decades, and people such as Maxwell and Hertz began the developments into electrical machines.

For modern polyphase systems[14] there are two types of commonly used electric motor. The induction motor[15, 16] is the more simple of the two but its speed of rotation is not synchronised with the supply. The synchronous machine[17] is more complex but is synchronised to the electrical supply and is widely used for motors and generators. If synchronism is lost between the machine and the supply then a condition known as *pole-slipping* occurs which results in large electrical and mechanical stresses being exerted on the machine. This condition is labeled *instability* and must be avoided at all costs, due to the high capital cost of large synchronous machines and the potential for severe damage to occur.

Direct current machines are still used in certain applications, but the complex circuitry required to provide the direct current[18] make this an expensive option.

## 1.4 Modern Power Systems

The UK transmission system comprises of approximately 800 busbars and 1300 transmission lines, and 240 generating units. The system voltage is mainly 400KV, but falls to 275 or 132KV in places. There are some 11000 switches and circuit breakers on the system and protection systems on all items of equipment.

As the economic constraints on power utilities continue to increase [6], power systems are being operated ever closer to their stability boundaries. In addition, as sources of generation become more concentrated, often with large areas of generation geographically separated by large distances from centres of load, the stresses on the transmission network are increasing. In response to these pressures, extensive work is being carried out across the world to provide power system operators with tools within their energy management systems, EMSs, to enable them to operate the power systems securely.

One of the key functions within EMSs is security assessment, where the vulnerability of the power system to outside events, such as lightning strikes on the transmission network, are analysed. Several hundred of these events, or contingencies as they are known, have to be analysed within the constraints of real-time operation of the EMS.

One of the most widely used examples of a severe power system security problem occurred in the area of New York in 1963 and resulted in a complete blackout of the city[19]. This problem was caused by the maloperation of a relay on a transmission line from Canada, due to an incorrect setting, and led to cascade tripping of other lines into the New York area. Since that time considerable effort has been directed at determining the optimum relay settings for transmission lines as well as sympathy tripping. A smaller black-out occurred in Seattle in 1984 during a severe storm. In this case the hardware protection, ie the relays, functioned correctly but the result was similar. Japan has one of the most vulnerable power systems as regards lightning strikes, due to long transmission lines crossing mountainous areas. In the UK, transmission lines in the North Wales area are also vulnerable to lightning strikes although the effects are far less severe due to the more robust power transmission network.

Of the security problems caused by contingencies that of the stability of the power system is the most crucial. Loss of stability within the power system will invariably lead to loss of load with the appropriate associated industrial and social problems. Stability assessment of electric power systems is a highly computationally demanding task and considerable effort has been directed at realising fast methods for on-line stability assessment.

## 1.5 About this Thesis

Operator decision and control actions are hard to quantify in terms of numerical algorithms but the range of tools, that fall into the category of artificial intelligence, can be used to model human learning, reasoning and decision. The principle methods that are employed are expert systems[20], genetic algorithms[21], fuzzy logic[22] and connectionist techniques, such as artificial neural networks [23, 24].

The work described in this thesis details a new method for fast detection of power system stability problems using artificial neural networks. Information contained in the pre- and immediate post-contingency state vectors of the power system is used to construct an input pattern to an artificial neural network which has been trained to use this information to quickly identify potential stability problems in the power system. Using an approach such as this, on-line stability assessment can become a reality and the electric power utility can expect to be able to operate their power network closer to the stability limits with considerable economic savings through the use of less out of merit generation.

Chapter 2 provides a broad overview of the operation of a modern power system, and is followed by a detailed investigation into dynamic security assessment, the process by which the security of a power system is determined within the constraints of on-line operation. Chapter 4 describes the contingency screening process and the various approaches that have been used.

Neural networks are explained in chapter 5 together with some of the successful application areas both in the field of electric power systems and other practical areas.

Chapter 6 discuss the details of the new contingency screening method. This includes all aspects from the broad approach to the novel features and details of the neural network model. This is followed in chapter 7 by details of the implementation of this neural network stability screen into a dynamic security assessor.

The results of various laboratory simulations on a 20 machine 100 busbar reduced model of the UK National Grid System are presented in chapter 8. This is followed by simulation results obtained from real system snapshots of the full UK National Grid system, comprising approximately 920 busbars and 100 to 150 large generating units.

Conclusions and further work are given in chapters 9 and 10 respectively.

Chapter Two

# Power System Operation

The operation of an electric power system presents a wide variety of technical challenges to the engineering profession. The planning, construction, maintenance and operation of such systems requires a highly skilled workforce, who must increasingly rely on ever more powerful design and analysis tools. This chapter concentrates on explaining the engineering aspects involved in power system operation, in particular the tools used by the power system operators to maintain safe and economic operation.

## 2.1 Introduction

The real-time operation of an electric power system is a highly complex task, as the operators must control the system, with many thousands of states, reliably and economically. The electric power utility must strive to maintain a reliable supply to customers even in the event of possible contingencies, due to internal failures such as insulator breakdown or the loss of a large generating unit, and possible external effects such as lightning strikes.

An inter-connected power system is more robust to contingencies because there are multiple paths from areas of generation to load centres. A primary requirement for an interconnected power system is that the frequency of the AC generation is synchronised , at 50Hz in Europe and 60Hz in the USA.

The primary aim of the operators must be to supply the consumer demand for electricity. From the operational perspective, this requires the prediction of the probable demand so that generating sets are on-line to meet the demand changes as they occur. Historical records of demand over *similar* periods forms the basis of demand prediction and are used in day ahead studies to plan the generation patterns as well as for on-line operation as many stations have startup times of many hours.

Generating sets are becoming increasingly large and 2000MW capacity stations are normal. Such stations are often more efficient than smaller stations and hence, regardless of geographic position, it is more cost effective use these stations continuously and to transmit energy over large distances than it is to use less efficient local stations. For this reason the main *base load* is met by these large stations which must be inter-connected so that they feed into the system as a whole, as opposed to a particular load[25].

In order to meet the sudden increases in load a certain amount of generating capacity, known as *spinning reserve* is required. This consists of a number of generators, running at less than their full capacity, ready to supply more power at very short notice. Stationary generating units cannot be used to supply these fast changes in demand due to the long start-up times, approaching one hour for steam turbo-generators.

In order to maintain the security of supply, the power system must be operated in a manner that makes it robust to contingencies. Almost all utilities operate their power system to at least a security of $N-1$, ie to an extent that a single failure will not result in loss of load or damage to the system. Increasing the security level to $N-2$ and beyond results in a more secure power system but often at the expense of less economic operation. The trade-off between security and economy has to be chosen based on the *cost* of a serious problem versus the likelihood of such an occurance and is the subject of much debate within electric utilities.

## 2.2 UK national grid system

The UK national grid system is a highly interconnected transmission system with in excess of 7000 kilometres of overhead transmission lines and cables, 21,600 towers, 280 sub-stations and up to 200 large generating units operating at any time. There are two major power interconnections: the first a 275 and 400kV AC link to the Scottish power system and the second a 2000MW DC link with France[26, 27].

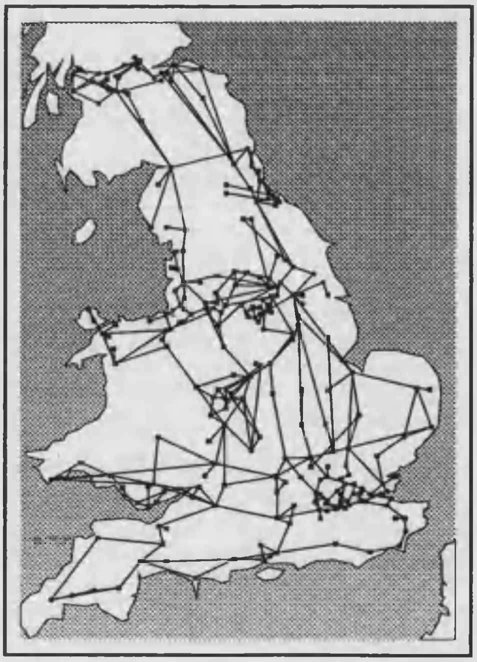

Figure 2.1: The UK national grid system

Figure 2.1 shows a schematic of the UK National Grid system. The transmission system is operated at voltages up to 400kV and is currently controlled through four Area Control Centres (ACCs) and the National Grid Control Centre (NGCC)[28].

The nodes on the transmission system where power is supplied to the customers, such as Regional Electricity Companies (RECs), are known as Grid Supply Points (GSPs) and such interconnected power systems have multiple paths from the generation areas to the GSPs, ensuring a high reliability of supply.

There are three main generating companies; PowerGen and National Power which operate the majority of the fossil fuelled stations and Nuclear Electric which runs the nuclear stations. The National Grid Company plc (NGC) are responsible for the maintenance, development and operation of the transmission system and also administer the *pool*[27][1] . Beyond the GSPs the responsibility for the electrical power distribution rests with the RECs, and is largely radial in nature.

NGC schedule and dispatch generation plant in England and Wales and power from Scotland and France according to a merit order based on bid prices submitted by the generating companies. Under the current system, NGCC instructs each of the four ACCs to maintain a defined import/export of power until a new instruction is given. This is known as the Inter-Area-Transfer System [29]. These power flows are initially calculated off-line and then modified on-line by the operators at NGCC to meet the actual operating condition. These flows can be adjusted by the ACCs in proportion to system frequency error and to reinforce the effect of governor control action. In addition, some of the generating sets at Dinorwig and Ffestiniog (pumped storage) usually operate an active low frequency relay. These sets will then start up automatically to maximum generation if there is a serious fall in the system frequency.

[1]The market place for buying and selling electrical power

### 2.2.1 Demand

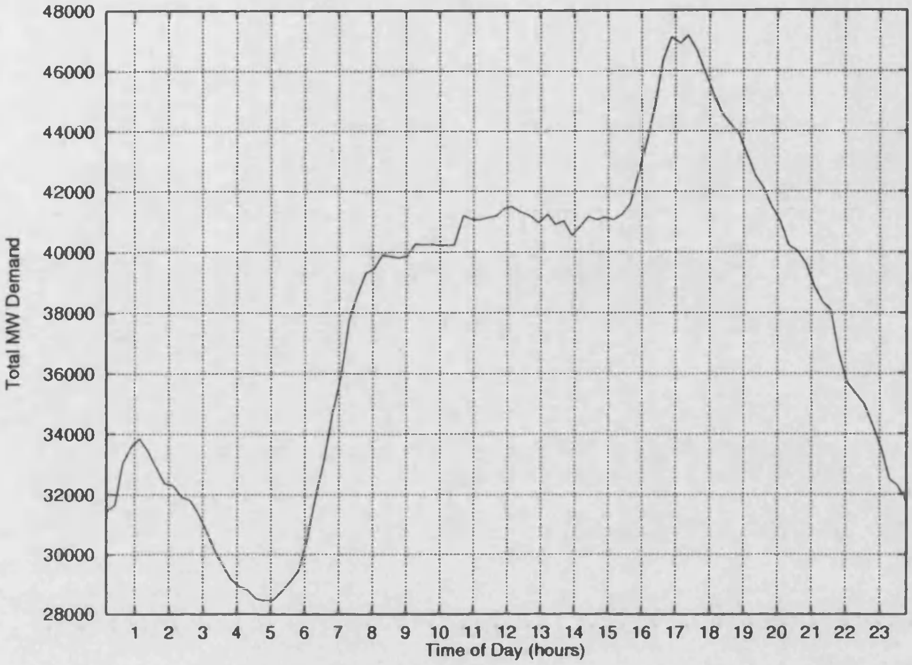


Figure 2.2: Typical Winter Weekday Load Curve

Figure 2.2 shows a typical winter weekday loadcurve on the UK National Grid System. In this example, the total demand ranges from 28GW to 48GW which requires between 100 and 160 separate generating sets to be operating: under summer nighttime conditions the demand falls to about 17GW.

### 2.2.2 Generation Capability

The generation capability within England and Wales encompasses fossil and nuclear fuelled plant, hydro electric schemes and pumped storage stations. Over recent years, with the introduction of fierce market forces into power generation, a large number of Open Cycle Gas Turbines (OCGTs), Combined Cycle Gas Turbines (CCGTs) and standard gas turbine plant have been commissioned which are used to meet peak demand.

| Generation Type | No Of Stations | Registered Capacity (MW) |
|---|---|---|
| Nuclear | 13 | 10633 |
| Small Coal | 7 | 1432 |
| Meduim Coal | 5 | 4306 |
| Large Coal | 12 | 22991 |
| CCGT | 29 | 8891 |
| Oil | 6 | 8489 |
| OCGT | 23 | 1938 |
| Hydro | 2 | 2100 |
| Scotland | - | 1200 (max) |
| France | - | 1976 (max) |
| Total | 97 | 63956 |

Table 2.1: 1994/95 Generation Capability

Table 2.1 shows the contribution to the total generating capacity from the various types of power station[11]. In general, the nuclear and some of the coal stations are used to meet the base load and the expensive gas turbines are used under peak loading conditions.

### 2.2.3 Economics

NGC facilitate the operation of the electricity market place, known as the *pool* [27] where power is bought from the generating utilities. At 10am every day all the generating companies who wish to trade the following day bid in their per MW hour prices for each of their available generating sets. They also declare the maximum output and operating parameters of each generator for security studies. Customers or 'demand side bidders' also submit bid prices at which they will reduce their demand. All of these bids are taken together to form the merit order of generation. This places the cheapest generating unit at the top and the most expensive at the bottom which then allows NGC to decide which units to run to meet the demand throughout the day. The generation cost passed onto the regional electricity companies and large commercial plant is comprised of the pool purchase price (basically determined by the most expensive generating unit being run) and uplift costs. This uplift cost takes into account factors such as system reserve, transmission constraints, demand forecast accuracy, generation availability and the cost of additional services such as voltage and frequency control.

As a consequence of the opening up of the electricity market place, the generator bid prices may vary considerably from day to day. This has a major effect on the constraint, or *uplift* costs as they are referred to within NGC, and is the key motivation behind moves to supply the power system operators with on-line stability information. This information will be provided by dynamic security assessors, which are described in chapter 3.

### 2.2.4 The Future

Submissions made by the RECs to NGC indicate that the winter peak demand in England and Wales is set to grow at an average rate of some 1.3% a year[11] over the next seven years; on this basis the peak demand will increase from 47.8GW in the winter of 1993 to about 53.3GW by 2000/2001.

The life expectancy of the aging Magnox (nuclear) station are unknown. In March 1993 a government white paper indicated that they would look closely at any requests from Nuclear Electric for approval of capital investment designed to extend the life of such stations.

## 2.3 Power System Controls

From a power system operator's perspective, their task is to alter the generation level to meet the load demand whilst keeping the system voltages and frequency within acceptable limits. In the UK, the NGC are bound by statutory regulations to operate the power system at ±5% of the nominal voltage level and ±2% of the system frequency, even under fault conditions.

As a consequence of these requirements and the need for continuous supply of electricity to consumers, both the transmission system and the generating units must remain *stable*. Maintaining a stable operating point requires good co-ordination of control actions, and the general topic of on-line security assessment is covered in detail in chapter 3.

To maintain the operation of the system within these constraints requires a combination of good planning, operator action and automatic control actions. In addition, coordinated protection schemes are needed to protect items of plant, such as lines and transformers, from damage under fault conditions.

### 2.3.1 Frequency

The power system frequency perturbations from nominal provide a clear indication of the imbalance between the real power generation and demand. A time history plot of the system frequency is one of the main tools used by a loading engineer in an Energy Management Centre (EMC) to alter the current generation level. Should the system frequency fall then there is a current shortfall in generation and vice versa. Due to the often rapid changes in system frequency some automatic frequency controls are present on the power system to control the short term, ie less than one minute, perturbations with the operators generation dispatch meeting the longer term generation requirement. One such automatic frequency control is provided by governor control action.

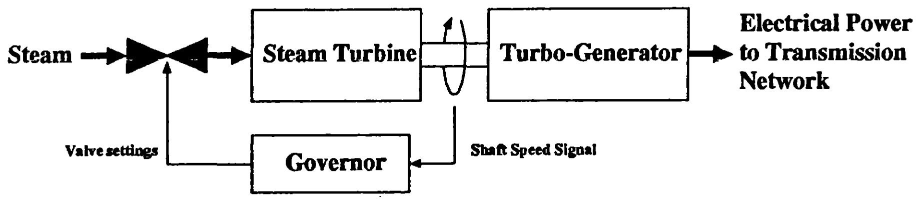


Figure 2.3: A Governor Control System

Figure 2.3 shows a schematic diagram of a speed governoring control system for a steam turbine. The function of the governor is to regulate the shaft speed of the turbine by controlling the high and low pressure steam valves on the turbine. The nature of the coupling between the steam turbine and the turbo-generator means that the frequency of the generator depends on the rotor speed of the turbine. Therefore, by trying to regulate the turbine speed the governor also has the effect of regulating the generator frequency. During normal operation some generating sets will not be operating at full load but will instead be operating on *free governor action*. As the system frequency changes the governors will strive to restore the frequency and the generating sets will alter their output power accordingly. In order for this to be effective, the generators must not be operating at full power because there will be no margin to increase the output power to restore the frequency

Low frequency relays (LFRs) are frequently used on large hydro generating units, such as Dinorwig and Ffestiniog in the UK, to provide emergency frequency control. A typical LFR setting of 49.85Hz, with a dead-time of 2.75 seconds, means that the relay will operate if the frequency drops below 49.85Hz for 2.75 seconds. This operation would then instruct its generating set to go to full generation, typically in less than ten seconds. This type of control action provides a rapid arrest of frequency fall in a time scale shorter than that possible by telemetered operator actions from an Energy Management System (EMS).

In the UK several 2000MVA, 400kV quadrature boosters have been installed to aid in the distribution of power across the transmission system. Although the generators constitute the only source of power in the system, the distribution of this power around the network can be influenced by the provision of phase changing equipment, namely quadrature booster transformers.

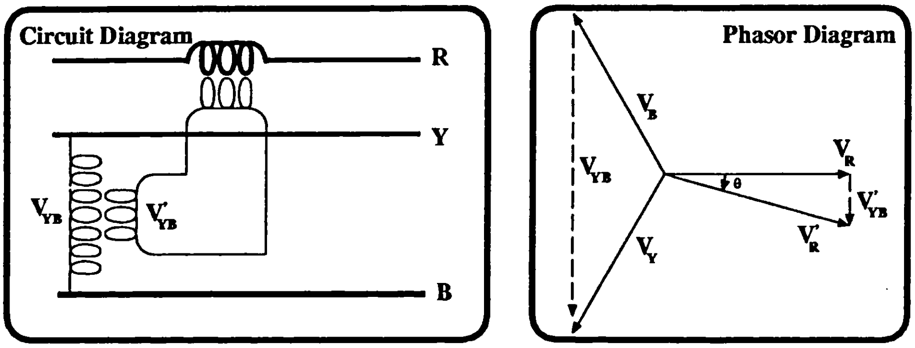


Figure 2.4: Connections for one phase of a Quadrature Booster

Figure 2.4 shows the connections in a quad-booster for the voltage injection into one of the three phases. Such devices produce a voltage phase change by adding a proportion of the voltage difference between two phases to the third. This is repeated for each of the phases and produces the net voltage phase change shown in the phasor diagram. By altering the tap ratio the level of voltage added to each phase can be adjusted and hence the voltage phase shift and real power flow can be controlled.

## 2.3.2 Voltage

With voltage levels constrained to be within 5% of nominal, even under fault conditions, the control of the voltage levels on the transmission system is of great importance. The effect of limiting the voltage ranges on busbars also provides a crude control to prevent *voltage instability* which is explained in detail in the following chapter. The main voltage controls are explained below:-

**Automatic Voltage Regulators** — AVRs are used to regulate the terminal voltage of a turbo-generator by setting the appropriate field voltage. The input signal is the desired terminal voltage, and the actual terminal voltage is used as the controlling feedback signal.

**Static Var Compensators** — SVCs are used to provide MVar injection in susceptible areas of many power systems. With a positive increase in MVar injection at a busbar, the voltage level will rise. Mechanically Switched Capacitor (MSC) banks provide this injection by the mechanical switching in and out of capacitor banks as the voltage level alters. Modern thyristor based SVCs switch capactitors on a frequency much greater than that of the AC system. This allow for a much finer grain control, but is a more expensive option.

**Synchronous Compensation** — This source of voltage control is again provided by a MVar injection. An over excited synchronous machine generates MVars while an under excited machine absorbs MVars[19] so by controlling the level of excitation the MVar injection, and hence voltage, can be controlled.

**Tap Changing Transformer** — By altering the tap ratio of the generator and transmission system transformers, the voltage level on the secondary side can be controlled. This constitutes the most popular and widespread form of voltage control at all voltage levels.

When overhead transmission lines are fully loaded they absorb MVars; with a current $I$ amperes for a line reactance per phase of $X$ ohms, the vars absorbed are $I^2X$ per phase. On lightly loaded lines the shunt capacitances become predominant and the lines become Var generators. This effect is amplified in cables where, due to the large susceptances, the Var generation becomes very large under light loading conditions. In the case of the UK system, this effect is significant in the London area where cables are sometimes taken out of service overnight to prevent high voltage problems.

### 2.3.3 Protection

With items of plant often costing many millions of pounds it is of paramount importance that they are protected from damage due to operation outside the normal ranges. Power system protection forms a highly complex engineering field in its own right, using modern computing hardware and fast communication links to achieve the desired security.

Transmission lines are usually protected by distance protection schemes and/or unit protection methods. Transformers are almost always covered by a unit protection system. For generators there are usually protection schemes for over current, under and over voltage as well as for under and over frequency. In addition there are protection systems to cover internal faults within the generator such as a stator earth fault.

## 2.4 Energy Management Systems

An Energy Management System (EMS) is a complex hardware and software system used by the power system operators to control the power system within the constraints of real-time operation[30, 31]. The modern EMS is the power industry's response to meeting the demands of running an economic and secure power system.

Figure 2.5 shows a schematic of how an EMS is related to the rest of the power

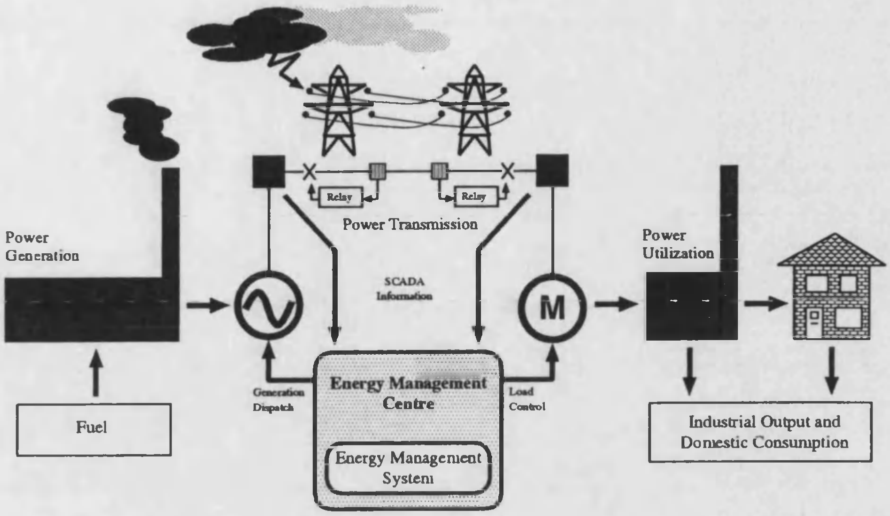


Figure 2.5: The place of an Energy Management System

system. It is based at the power utilities main Energy management Centre (EMC) and performs functions such as extensive on-line monitoring, security assessment and dispatch optimisation to minimise operational problems whilst maintaining economy of operation.

At the U.K. National Grid Control Centre[28] the EMS is based on a Cyber 960 dual computer system, with a third Cyber as an emergency backup. The Cyber computers support state estimation, security assessment software as well as retrospective data access. They are linked to and receive data from Cyber 960 computers at each of the ACCs. A Vax 6420 computer, with a Vax 6620 on standby, provides additional and complementary displays such as predictive demand and reserve management and provides advice for generation dispatch.

Figure 2.6 shows a typical block diagram of an EMS based on the UK system[28]. Each of these blocks is described in more detail in the following sections.

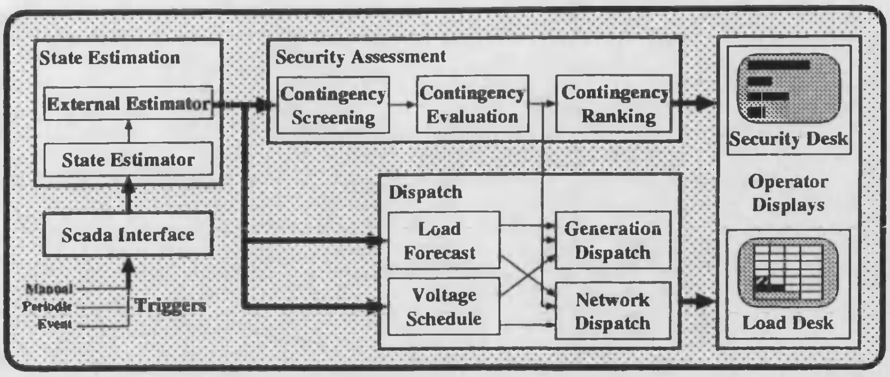


Figure 2.6: Block Diagram of an EMS

### 2.4.1 SCADA Subsystem

SCADA (Supervisory Control And Data Acquisition) is a generic term usually applied to the interface between an industrial plant and its control. Its primary function is to relay information on the state of the system back to the control centre and to dispatch control messages to the plant.

The SCADA subsystem of the EMS telemeters busbar voltage information, line power flows and switch statuses, relaying them back to the EMC. This telemetered information is often inconsistent due to noise and drift errors on the measuring devices, errors introduced in the analogue to digital conversion and communication errors. This problem is somewhat alleviated by incorporating redundancy into the system measurements; measurements are made at many points on the power network so that at the EMC although the received data is *noisy* there is sufficient redundancy such that the state estimation software can try to obtain a consistent power system state vector for the EMS functions.

## 2.4.2 State Estimation

As power systems become even more stressed it is essential for the power utilities to know the current power system state as EMS functions such as security assessment and generation dispatch rely on this information to maintain a secure and economic supply. The function of the state estimation subsystem of the EMS[32, 33] is to take the SCADA data, noise and all, and produce an accurate and consistent state vector that matches the power system state as closely as possible.

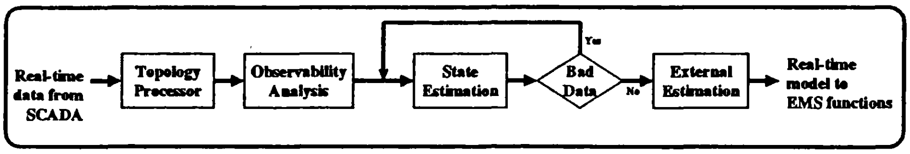


Figure 2.7: Steps in State Estimation

The function of a state estimator can be broken down into five separate stages as shown in figure 2.7. The topology processor picks out the statuses of the switches from the real-time data and determines the present network topology. Since the availability of real-time measurements can change, because of metering or communication failures, an observability check is made. This check normally only examines the observable areas of the network and identifies those busbars which may have become temporally unobservable. These busbars can then be made observable by adding *pseudo-measurements* or taken out of the state estimation calculation and added into the external network model.

The most common approach for the state estimation algorithm is to formulate the problem as a nonlinear weighted least squares minimisation[34, 35]. This problem is then solved for the observable part of the network in an iterative manner until the *best* system state vector is obtained. If any bad data is detected then it is removed from the input, marked as an *anomoly*, and the state estimation algorithm is re-run. The external estimator then adds in the *most likely* state of the external part of the network into the solution before the EMS real-time model of the power system is updated.

### 2.4.3 Dispatch

Given the current operating state of the power system and historical records, the total system load over the next few hours can estimated[36, 37]. The aim of the dispatch subsystem of the EMS is to set the generator MW and MVar outputs in order to meet this predicted load demand in as economic way as possible. Optimal dispatch[38, 39] software performs this task in real-time aiming to achieve a balance between economy and security of supply.

Optimal power flow (OPF) programs are often used in planning studies as well as for on-line operation. There have been a number of techniques employed[40, 41], but the most reliable method is based on a Quasi-Newton approach[42] although techniques based on fuzzy-expert systems seem promising[43]. Such optimisations must include constraints on busbar voltage limits, transformer and quad-booster tap positions, SVC and synchronous compensation limits as well as cost factors for each generating set.

### 2.4.4 Security Assessment

The aim of security assessment is to determine what effects certain contingencies will have on the power system should they occur[44, 45]. The selection of contingencies requires detailed knowledge of the power system concerned[46, 47] and varies depending on the loading and generation patterns. The selected contingencies are then *screened* to remove those contingencies which produce no violations [48]. The remaining contingencies then undergo detailed evaluation to determine the extent of the violations. Lastly, the contingencies are ranked in order of severity [49] and displayed to the operator.

Until recently the security monitoring software available with an EMS has only been able to perform static security analysis due to the computational restrictions on on-line algorithms. Static Security Analysis (SSA) is concerned with the post-contingency steady state condition of the power system. SSA is usually based on two main tools: DC and AC load-flows or neural networks[50–52].

DC load-flows, based purely on Kirchoffs Laws[53, 54], are often used to calculate line MW flows. The computational simplicity of such algorithms make it ideal for on-line use and its robustness to inconsistencies in the state estimation output make it a very reliable tool. Results from a DC load-flow can show if lines will be overloaded in the post-contingency state and if all the load can still be supplied.

Off-line studies are carried out in the planning stages to set maximum MW transfers across critical boundaries so that the operators can maintain system stability[55]. If results from the DC load-flow indicates that the post-contingency state will violate these *stability limits* then the system operators are warned so that they can plan preventative or corrective actions.

An AC load-flow provides information on both the line MW flows and busbar voltages in the post-contingency steady state condition. As an operational tool it may suffer from convergence problems if the state estimated solution is inconsistent. When functioning properly, it allows the post-contingency busbar voltages to be checked for limit violations.

In figure 2.8, Stott et al[44] have proposed a formal classification of power system security which they believe is necessary to define the relevant EMS functions. The normal mode of operation is at 'level one' where there are no problems on the system. Should the power system operating point change such that the current operating point is secure but a contingency may lead to an insecure condition then 'level two' has been reached. Should the situation become worse and loss of load is required to correct violations caused by a contingency then the system is in the *alert* state. The point of no-return occurs when the current operating limits are violated and loss of load is the only option. Following this loss of load the system operators will try to restore all loads and return to a secure operating condition.

Full on-line security assessment should look at the stability of the power system when subject to contingencies. Due to the highly computationally demanding nature of this problem, current on-line security assessors do not consider stability problems, but rely on planning studies to set MW transfer limits, often very conservatively, to ensure the system remains stable. Current research into full on-line dynamic security assessment, outlined in detail in the following chapter, aims to assess the stability implications of contingencies and to provide the power system operators with advice as to how to operate the system closer to the desired economic–security level.

## 2.5 Chapter Summary

The progression of electric power systems towards interconnection coupled with the ever increasing size of generating sets has led to more systems becoming limited by stability constraints.

The secure and economic operation of such power systems requires extensive on-line computer based tools to both assess the system security and to provide secure economic dispatch to meet all the load demand at all times.

The following chapter describes the new area of dynamic security assessment, where the stability of the power system subject to contingencies is determined within the constraints of on-line operation and operator advice is determined.

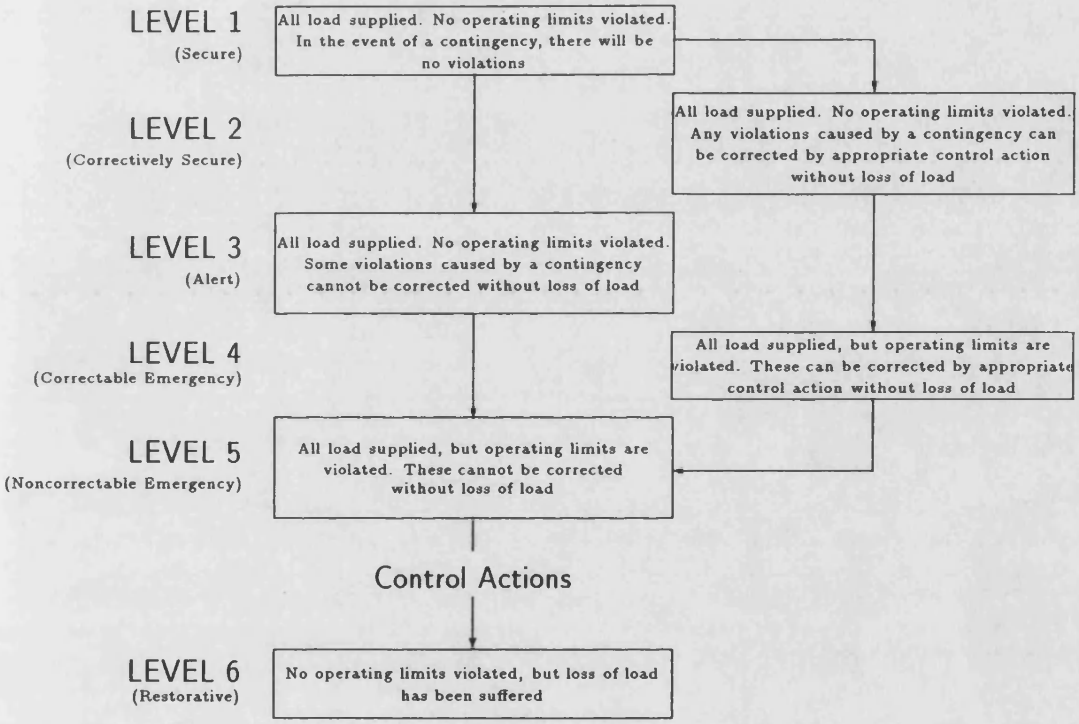


Figure 2.8: Power System Security Levels

Chapter Three

# Dynamic Security Assessment

The trends in modern interconnected power systems have resulted in heavier transmission loadings and hence operation closer to the steady-state limits. Increasing geographical dislocation of generation from load coupled with more unpredictable economic constraints sometimes means that large amounts of power are imported from external systems across weak boundaries which have made many power systems stability limited, i.e. the stability limits are reached prior to the steady state limits. A consequence of this is that the derivation of the on-line operational limits is crucial to allow the power system operators to operate the system closer to these limits and hence in a more economic manner. The aim of dynamic security assessment (DSA) is to provide the operators with information to enable them to run the power system closer to these limits in a secure manner.

## 3.1 Introduction

Over the last few years considerable effort has been and is being made to provide the power system operators with tools to enable the power systems to be operated closer to their stability limits. DSA tools will provide the operators with enough information on the power system stability to enable power system operators to run the power system closer to its stability limits with confidence. This has considerable economic benefits when less out of merit generation has to be used to meet stability limits. Cauley[56] gave an example where accurate knowledge of stability limits allowed 500MW of generation costing $50/MWh was replaced by remote generation costing only $20/MWh. The potential economic benefit to the utility, in this example of approximately $360,000 per day, is the main driving motivation for DSA. In the year 1993/4 the total cost due to all constraints[57, 58] on the UK national grid system was approximately £189M and therefore even a small percentage reduction in these constraint costs would lead to a substantial financial reward.

At the heart of a DSA system are the algorithms which analyse the transient and oscillatory responses of the power system for a set of credible contingencies. Of particular interest is the nature of the transition between the pre and post-contingency steady states in particular any potential instability problems. Also, during the transition between operating points, checks are made to ensure that the limits on busbar voltage fluctuations, transient line overloading and machine frequency limits are not violated.

The computational requirements for DSA are approximately three orders of magnitude greater than that required for static security analysis[44], which have made it infeasible to implement on-line dynamic security analysis until recently. DSA is one of the main areas of power systems research at the current time. EPRI[59] are undertaking a thorough investigation into the feasibility of implementing on-line DSA, and have proposed a route for the development of operator tools to meet this objective. Their perceived plan is to use an expert system based contingency selector, a neural network based contingency screen and transient stability analysis using the Transient Energy Function (TEF).

The recent application of artificial intelligence techniques to the field of dynamic security assessment has resulted in DSA moving from a theoretical tool to practical application. The application of expert systems to DSA is receiving a great deal of attention [60–66] and this seems to be the most promising way forward for contingency selection and on-line operator advice [43, 67–69]. Research into using neural networks for DSA[70–74] has been successful for small power systems, and currently much work is going into the application of this technology to larger power systems.

A recent collaborative venture between the University of Bath (U.K.) and the National Grid Company (U.K.) has led to the development of OASIS (On-line Algorithms for System Instability Studies), a state-of-the-art dynamic security assessor. OASIS has undergone recent field trials at the National Grid Control Centre with promising results.

## 3.2 Power System Stability

Dynamic Security Assessment aims to allow power system operators to run the system closer to its stability limits, whilst maintaining secure and economic operation. What do we mean by power system stability? The Oxford English Dictionary definition of stability is:

> Stability: In physical senses (a) Power of remaining erect; freedom from liability to fall or be overthrown. (b) Fixity of position in space; freedom from liability to changes of place. (c) Ability to remain in the same relative place or position in spite of disturbing influences; capacity for resistance to disturbance; the condition of being in stable equilibrium, tendency to recover the initial position after displacement. also, of a

> body in motion: Freedom from oscillation, steadiness. (d) Fixedness not fluidity. (e) Of a system of bodies: Permanence of arrangement; power of resisting change of structure. (f) Of a chemical compound or combination: Capacity to resist decomposition or disruption. Also of an atomic nucleus or sub-atomic particle. (g) Something fixed or settled.

This definition of stability [75] highlights many of features of the required dynamic response of a power system to a contingency. First and foremost the power system must be capable of surviving (a,c,e) the transition from the pre- to post-contingency operating condition. Ideally, all the load should remain supplied (b) and voltage and frequency within the statutory limits (d). The post-contingency operating point should be free from oscillations (g) and itself stable for further contingencies.

Power system operators need to know three aspects of the power system stability for every contingency. Firstly, will the power system survive the transition to the post-contingency operating point. If so the system is *transiently stable.* Secondly, is the transition to the post-contingency operating condition going to be sufficiently damped, i.e. is it *oscillatory stable.* Both of these forms of stability are electro-mechanical and are determined by the nature of the electro-mechanical oscillations between the transmission network and the machines connected to it.

The traditional concept of *dynamic instability* is not used in this work as it leads to confusion [75]. The concept of *steady state stability* concerns small fluctuations about the operating point of the system. In practice, if the post-contingency operating point has a poor degree of steady state stability, the pre- to post-contingency operating point will be characterised by poor damping or increasing oscillations and hence will be detected as oscillatory unstable.

The final stability aspect, ***voltage instability***, is a pure transmission network phenomenon concerned with widespread busbar voltage collapse. If there is a sudden increase in load then the busbar on the transmission network where the power is being drawn from will fall slightly. Under certain conditions this fall may be self-sustaining resulting in voltage collapse at the busbar. Rapid automatic or manual response is then required to shed load so that the transmission system voltage levels can be restored.

### 3.2.1 Transient Instability

Transient stability studies are carried out to examine the transient behaviour of the power system when moving from the pre to post-contingency operating point. The transient stability is then determined by the energy imbalances between the machines and the transmission system. Transient stability can be considered as the short term stability ($< 5$ seconds) of the system when subject to a large disturbance.

If a machine is unable to inject sufficient electrical power into the transmission system then its rotor will accelerate as the mechanical input power to the rotor will remain largely constant due to the relatively slow governor response. When the fault is removed, the machine rotor will experience oscillations and if these are too large then the machine will move towards ***pole-slipping***. At this point the machine pole-slipping protection schemes will operate and trip the generator to prevent any serious damage from occurring. Figure 3.1 shows the rotor angle plot for a machine with a contingency applied which causes the machine to pole-slip after half a second.

A recent conference [56] outlined the accomplishment of EPRI research projects and gave details of an actual on-line transient stability system at the Ontario Hydro Clarkson System Control Centre and contingency screening and ranking of these

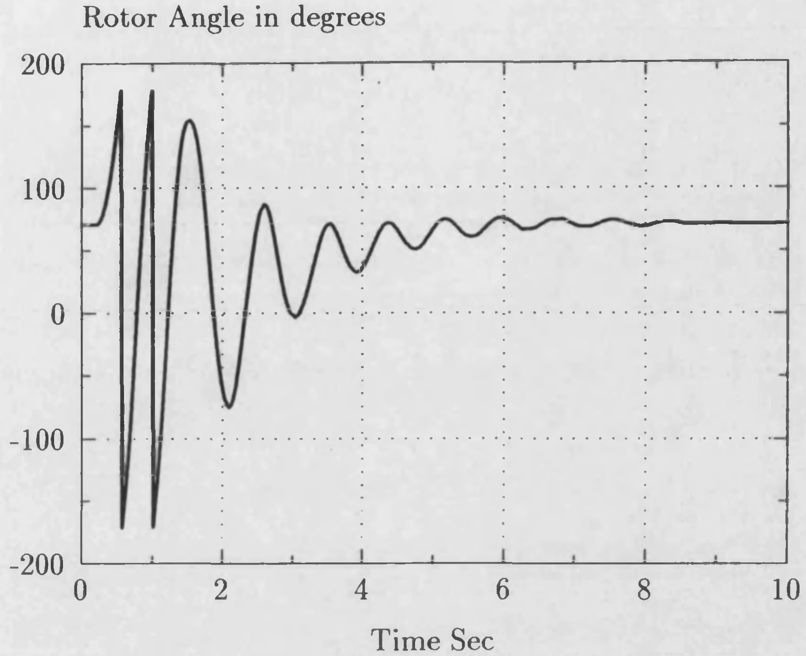


Figure 3.1: Example of Transient Instability

problems at Northern States Power. Transient instability problems are localised by nature and can usually only be solved by either the activation of an intertripping scheme or by transmission re-enforcement.

### 3.2.2 Oscillatory Instability

This is concerned with the nature of the post-contingency electro-mechanical oscillations between the machines and the transmission system. It is operationally desirable is these oscillations are fairly small and decay away within one minute [76].

Within the UK national grid system, such instability problems were known to exist when a large increase in demand was met by a large increased power import from the Scottish Power system. Figure 3.2 shows a simulation, using the laboratory scale model described in chapter 8.1, of a rotor angle of a generator in Scotland which is dynamically unstable when a 100ms busbar fault is applied to busbar DEES4.

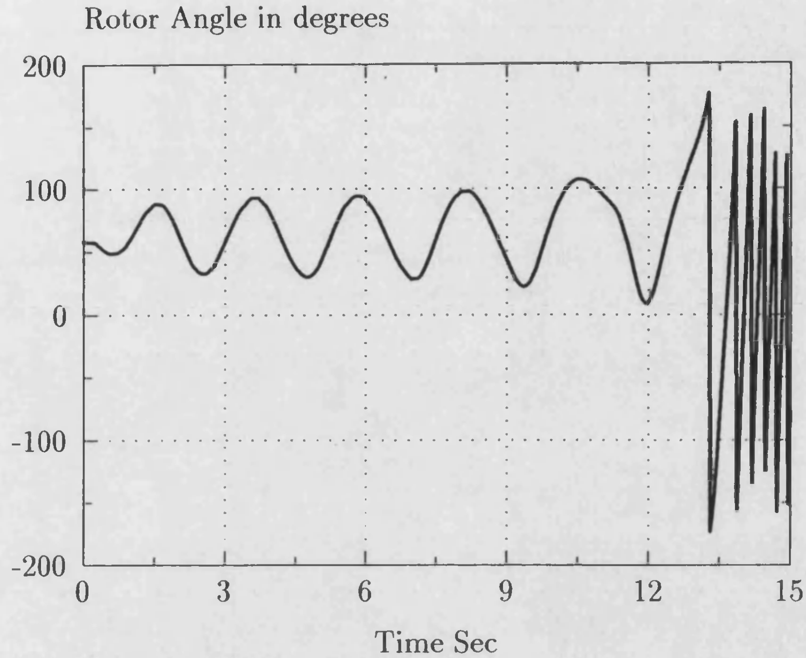

Figure 3.2: England Scotland Oscillatory Instability

The primary cause of the instability is because too much power is being transferred down two *weak* 275kV transmission lines to England. Simulations of this effect have shown that if control actions are not taken by the power system operators then the interconnection lines will be tripped and the UK power system split into two islands. This problem has been reduced by the recent addition of two 400kV transmission lines between the two systems. However, recent re-enforcement of this interconnection has considerably reduced this problem.

From an operational perspective, the system is operated in the oscillatory stable region by the application of MW transfer limits across critical boundaries in the system[58, 77]. Traditionally, these limits are calculated at the day ahead planning stage and are conservative to allow for variations between the actual and expected operating states of the power system. The use of these conservative limits leads to the running of out-of-merit generation and hence a large financial penalty. One of the aims of dynamic security assessment is to provide the power system operators with a better idea of the on-line transfer limit and hence reduce the economic penalty incurred as a result of such instability problems.

### 3.2.3 Steady State Stability

Steady state stability analysis concentrates on the stability of the power system when subject to small perturbations about its operating point [78, 79], i.e. its small signal stability. The transition to such an operating condition may lead to increasing long term oscillations and limit cycles, which if are not arrested will impair the power system security and may lead to islanding. From the practical perspective, this form of instability violation is alleviated by ensuring that the system is oscillatory stable.

### 3.2.4 Voltage Stability

Unlike transient, oscillatory and steady-state instability problems, voltage stability is not an electro-mechanical phenomena but a purely network phenomenon[80]. Consider the circuit shown in the upper right of figure 3.3. If the sending end voltage, $V_s$ is fixed, say at the nominal 1.0 per unit (pu) then as the power factor of the load varies, we obtain voltage versus MW transfer graphs of the form shown. The fact that there are two solutions of voltage for each MW supply can be thought of as by either a high voltage and low current or a low voltage and high current transmission.

The seasonal thermal ratings for the line are also shown and it is apparent that for power factors of less than unity the possibility exists that before the thermal limit is reached the operating power may be on that part of the characteristic where small changes in load cause large voltage changes. Under these conditions the system experiences *voltage instability.*

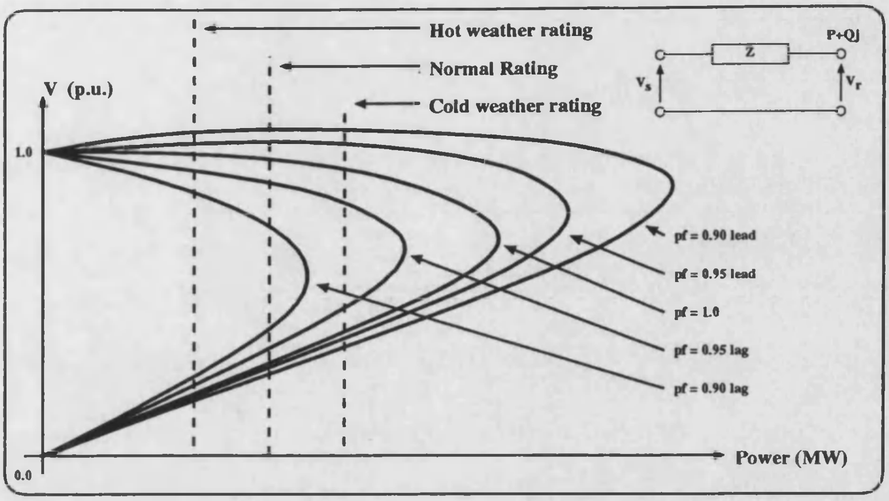


Figure 3.3: Relationship between power supplied and receiving voltage

Great caution has to be exercised in these conditions and depending on the type of load voltage collapse may occur. If the load is basically constant power (eg induction motors) the collapse is aggravated. For softer loads, i.e. those where the power drops off as the voltage drops, the situation is alleviated. The power factor across the line is a critical quantity and it is shown that a lagging power factor will precipitate voltage collapse. For long lines, it is therefore necessary to operate the system at above approximately 0.97pf, and the use of Var injection at the receiving end by SVCs or other devices becomes economically justifiable.

## 3.3 Current Operating Practice

Unacceptable stability conditions arise if any generator or group of generators falls out of synchronism with the remainder of the power system or if power/frequency oscillations do not decay within a time constant of typically 12 seconds[11].

The NGC operating standard, OM3, requires the power system to be stable following secured outages[57]. It is the practice of NGC to consider the following contingencies at the operating stage:-

① Three phase faults followed by a secured outage (i.e. single or double circuit faults perhaps with a circuit already out of service due to a planned outage).

② A fault clearance time assuming pessimistic operating times for both 1st main and 2nd main protection channels (the fastest of which will initiate tripping) plus the trip relay and circuit breaker operating time.

③ the worst fault location in terms of stability performance given the topology of the network and fault clearance time.

From an operational perspective, intertripping schemes are widely used to trip those generating sets that will go unstable as a result of transient instability problems. MW transfer limits, calculated in the day ahead planning stage are used to ensure that the system remains oscillatory stable.

## 3.4 Dynamic Security Assessors

At the heart of a modern on-line dynamic security assessment system (DSAS) is the ability to be able to evaluate the security implications of a set of contingencies on the current operating state of the power system. The operating state that is used by the DSAS is an approximation of the power system's operating state produced by the state estimation software[28] within the EMS. The reliability of the state estimator's output is highly dependent on both the accuracy of telemetered data from the power system, obtained by the SCADA system[28, 81, 82] and on the observability of the power system[83]. Hence it is vital that this issue is addressed before an on-line dynamic security assessor can be reliable.

The recent introduction of high performance low cost workstations has influenced the archetecture and design of EMS more than any other development[84]. The traditional aproach of using a single large computer to form the core of energy management systems is dogged by the problem of obtaining extra computing power for EMS applications without substantial alterations to the EMS computers. Energy management systems are being augmented with heterogeneous distributed computing systems[85] to perform the new EMS applications, such as dynamic security assessment. The flexibility and cost effectiveness of this approach is the driving motivation coupled with the minimal disruption to the existing EMS. The latest state estimation output is farmed out to the distributed computers which perform the evaluation. The results are sent back to the EMS for displaying through the standard EMS displays.

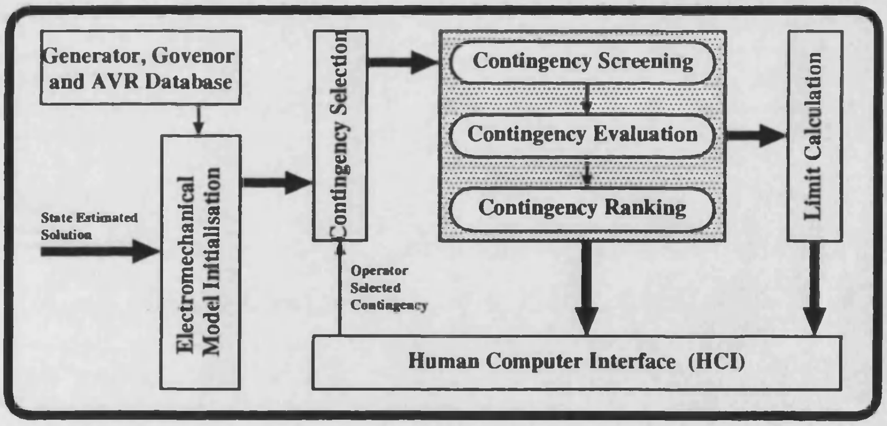


Figure 3.4: DSAS Block Diagram

Figure 3.4 shows a generic block diagram for a DSAS based on research being conducted at the University of Bath[86] and other work by CEGELEC ESCA[87–90]. In order that a large number of contingencies can be used it is vital to include some form of contingency screening to filter out those contingencies which cause little or no degradation of the system security. The remaining contingencies can then undergo detailed on-line evaluation for security violations such as line overloads, voltage violations and instability problems. These results are then presented to the power system operators in a clear and unambiguous manner to enable them to take preventative, or plan corrective, actions.

The continuous fluctuation of power system load in conjunction with the topology changes have a large effect on the ability of the power system to withstand contingencies. It is therefore vital that DSA tools should provide the system operators with up to date information. This requires the following conditions to be met.

① The DSA should be performed at a rate commensurate with the rate of change of system state. Hence, the DSAS should be triggered after any switching operations, after a new state estimation update or upon operator request.

② The DSAS cycle time should be short enough for the results to be still meaningful when the evaluation is completed. Cycle times of the order of 10 to 15 minutes were considered to be the aim for OASIS, but faster cycle times are obviously more desirable.

③ The DSAS should provide full diagnostics to the operator in the event of a failure of an algorithm. Typically, the failure of an AC loadflow to converge for a contingency should be reported to the operator as even the odd infrequent *quirky* result will reduce operator confidence in the DSAS.

The only aspects of stability that will be covered in the remainder of this discussion concentrate on transient and oscillatory instability problems – i.e. the nature of the electro-mechanical oscillations. This broad approach adopted for the electro-mechanical stability aspects can be expanded to cover voltage stability, although this is outside the scope of the current research associated with OASIS, which concentrates on the interaction between the EHV transmission system and the generating units.

### 3.4.1 Contingency Selection

The selection of the contingencies to be evaluated by a DSAS can be performed in one of two ways. Firstly, a static list of contingencies may be used, which encompasses all contingencies that may lead to potential instability problems under various operating conditions of the power system.

This approach leads to a large number of contingencies being selected and therefore increases the computational requirements for the DSAS and does not take into account valuable operator experience. This experience can form the basis of dynamic contingency selection, where only those contingencies that are likely to cause potential instability problems for the *current* operating condition are chosen.

This encompassment of power system performance and operator knowledge seems to be ideally suited to an expert system implementation [46, 91–94] as explicit rules can be developed to cover most of the operating conditions. In this way an automatic contingency selection can be implemented and augmented with other contingencies that the power system operators request.

### 3.4.2 Contingency Screening

For large power systems, such as the UK national grid system, it is possible that several thousand contingencies may be selected for evaluation. If a full time domain simulation is used to perform the detailed evaluation of each contingency, then even using a state of the art power system simulator, such as PowSim [95], it is not possible to meet the DSAS update time of 10 to 15 minutes without investing in substantial computing power. For example, performing a time domain simulation of 5000 contingencies using PowSim for 30 seconds each on the full NGC system takes approximately 11.5 hours using one DEC Alpha. To meet the desired update frequency would require approximately 70 DEC Alpha's.

Contingency screening aims to quickly filter out those contingencies which are very stable, only passing those unstable, or close to unstable, contingencies through for detailed evaluation. These screens must be lightweight computational processes so that as larger a speedup as possible can be obtained.

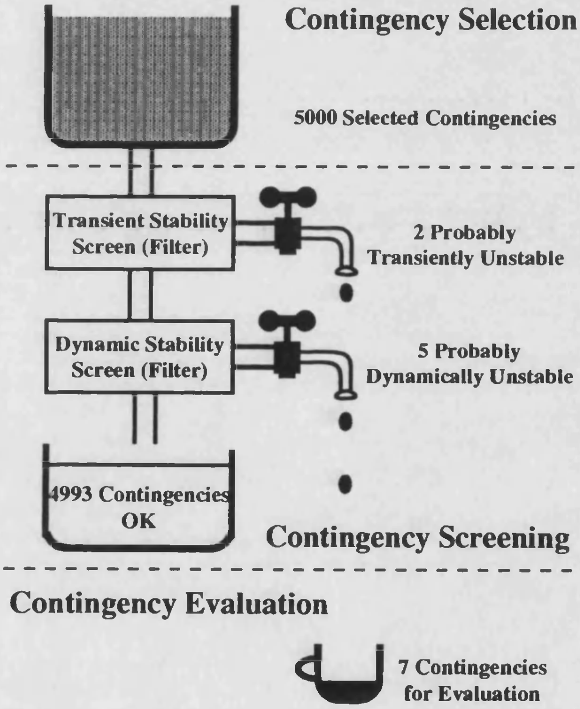


Figure 3.5: Contingency Screening - The Filtering Process

Figure 3.5 shows a typical case where the use of transient and oscillatory contingency screens filter out 4993 out of 5000 contingencies, and this approach can yield overall speedups in the DSAS operating time of 20 or more. The contingency screening process is explained in detail in chapter 4. Chapter 6 describes the design of the new artificial neural network based instability screens.

### 3.4.3 Contingency Evaluation

The detailed evaluation of the effect on a power system of one or many contingencies allows the severity of the contingencies to be assessed. The most accurate method for contingency evaluation uses a electro-mechanical time domain simulation with high order machine, AVR and governor models[96–98]. The effects of SVCs, quadrature boosters and other devices can be incorporated into the simulation to provide a realistic simulation.

A time domain simulation of approximately 30 seconds will detect any transient instability problems and will provide information on the decay of machine rotor angle oscillations following the contingency[99]. From an operational perspective, an acceptable transition from the pre to post contingency state occurs if the system remains (transiently) stable and if the rotor oscillations decay away in under one minute. Bearing the latter decay conditions in mind, we can conclude that the envelope of the decay of acceptable oscillations has a time constant of approximately 12 seconds. If the post contingency operating point of the system is steady-state unstable then it is highly likely that the decay time constant will exceed the required 12 seconds, and it is the author's opinion that this decay rate may be used as an indicator of an acceptable dynamic post contingency operating state.

### 3.4.4 Contingency Ranking

The aim of contingency ranking is to sort the selected contingency list into a severity order, with the most severe contingency at the top. In this way the power system operators can quickly see what the worst contingencies are and what instability problems would be caused.

Numerous contingency ranking algorithms have ben developed[49, 100] but most of them deal with the aspects of voltage and thermal overloads investigated by SSA. The contingency ranking algorithm used within OASIS[86] has been shown to produce good results for transiently unstable contingencies and those with a poor oscillatory response.

### 3.4.5 Limit Calculations

Traditionally the MW flow limits, which are set to ensure that the system remains oscillatory stable, are calculated by an off-line trial and error process and are made conservative to take into account possible changes in the operating point of the system.

The natural conservativeness of these limits leads to large constraint costs which will hopefully be reduced when dynamic security assessment systems are used. The development of on-line algorithms to calculate the actual safe MW transfer limits is an area for future research.

### 3.4.6 Operator Interface

The operator interface for a DSAS should appear in a similar format to the other EMS displays and be developed in conjunction with power system operators. The inclusion of the *end users* into the design process at the earliest opportunity is to be encouraged as this will tend to reduce the amount of time and effort spent in tailoring the displays to the operators requirements during the commissioning of the DSAS.

Typically the displays are *window* based, and of the application technologies available, the X-Window system[101] is the most popular. Most of the displays at NGCC are based on the X-Window system, and the future DSAS displays will almost certainly be the same.

Mahadev[102] and others have investigated various methods for envisioning power system security information. The author has developed a simple method for envisioning the current stability problems on a power system, which is explained later in 7.1.

## 3.5 OASIS

OASIS[86, 103, 104] is a state-of-the-art dynamic security assessor developed in a collaborative project between the Power and Energy Systems Group, in the University of Bath School of Electronic and Electrical Engineering (U.K.), and the NGC (U.K.). This work is also funded by EPSRC. Within NGC, the on-line static security assessment software within EMSs[28] is triggered on completion of the state estimation and concentrates on line overloads and voltage problems following contingencies on the system. The OASIS project was motivated by NGCs future requirement of an on-line dynamic security assessor and was to concentrate on the detection of transient and oscillatory instability problems.

### 3.5.1 Client-Server Approach

Contingency evaluation is at the heart of a dynamic security assessment system and is parallelisable at the contingency level[105] and therefore ideally suited to distributed processing. The seperate cases in the contingency list can be shared between multiple inexpensive processors. A client-server architecture therefore lends itself to this type of application where a single client task can control a large number of server processes, each of which performs contingency evaluation.

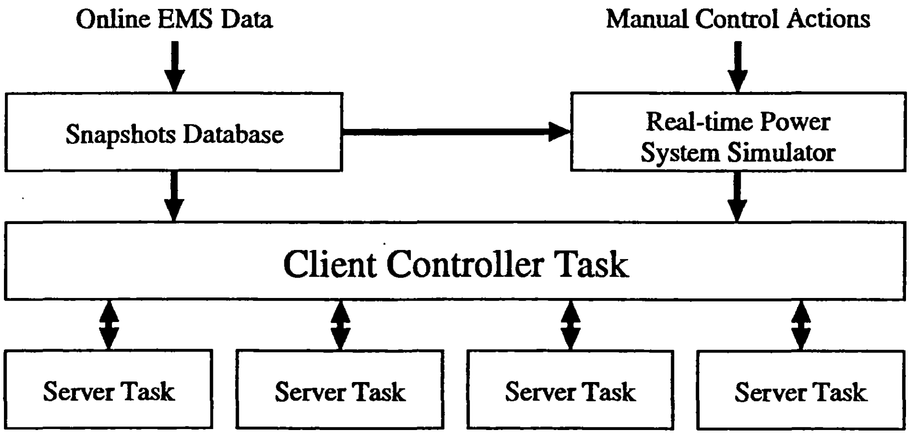


Figure 3.6: Block Diagram of OASIS

Figure 3.6 shows the block diagram of the OASIS system. The data input can come from either saved power system snapshots, obtained from on-line EMS data or off-line studies, or from a real-time power system simulator mimicking the *real* power system. This facility allows the effects of simulator operator control actions to be evaluated by OASIS and provides the basis for *closing the loop* on power system operation where automatic on-line advice can be directly implemented without any operator intervention.

The server tasks, executed on each of the host computers, are based on a real-time power system simulator[95, 106] and perform the contingency screening and evaluation. The client controller task distributes the contingencies to the server tasks, collects the results and displays them to the operators through X-Window[101, 107] displays.

### 3.5.2 Parallel Evaluation

During the design of OASIS, a number of practical implementation technologies were investigated for their suitability for forming the client-server backbone of OASIS. Of these technologies, PVM (Parallel Virtual Machine), developed by Oak Ridge National Laboratory[108–111], offered the best practical solution and hence was chosen. PVM allows a parallel machine to be dynamically constructed from a number of heterogeneous computing platforms on which client–server software tasks can run.

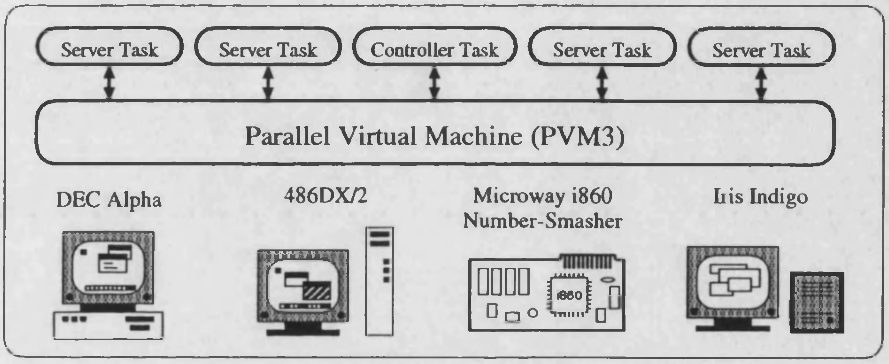


Figure 3.7: An Example OASIS System

The OASIS system falls into several distinct yet interacting layers as shown in figure 3.7. The hardware level is comprised of the physical machines available to form the heterogeneous computing system. Residing on each of these machines is the PVM daemon forming the linking layer between the hardware and PVM. Finally, the PVM task layer allows the tasks to be distributed across the parallel virtual machine. PVM then allows the client task and a number of server tasks to be run across the heterogeneous computing system

### 3.5.3 Client Task

In OASIS the client has to perform the tasks of server initialisation, contingency processing control and HCI for the DSAS. In addition the client has to be able to register OASIS with PVM and to gracefully leave PVM once all the contingencies have been evaluated.

#### 3.5.3.1 Server Initialisation

The vast majority of UNIX schedulers[112] operate on a *round robin* basis swapping between tasks that are not waiting on IO. The server task was designed to be a purely computational process and therefore will not be waiting on any IO and hence there will be no benefit of using multiple server tasks on one architecture as they will be competing to use the same (cpu) resource. Indeed, there will be a slight degradation in performance if multiple worker tasks are spawned as there will be an overhead associated between swapping between the multiple tasks as well as the other processes running on the architecture. The OASIS system was therefore designed to create one instance of the server process on each of the architectures registered with PVM during its initialisation. Once the sever tasks have been created, the client task sends the current power system state and contingency database to each server task, each of which then waits for the client to inform it of which contingency to evaluate.

#### 3.5.3.2 Contingency Processing

The controller task distributes server tasks over the PVM system using a flood-fill algorithm. The server tasks are firstly initialised with the current system states obtained from the on-line EMS, power system simulator or saved power system snapshots. The controller task then enters the main service loop which controls the contingency processing.

Inside the service loop, contingencies are allocated to the server tasks using the 'pool of tasks' paradigm since the number of contingencies to be evaluated is normally at least one order of magnitude more than the number of host computers. Under this condition, the system is inherently load balanced with each server task making full use of its host processing resource. The controller task then waits for a message from one of the server tasks containing information about the contingency evaluation. These results are stored and a new contingency is allocated to the server task until all the contingencies have been evaluated. When the last contingency has been allocated to a server task, the other server tasks are also allocated the last contingency for evaluation. In this manner OASIS will not be left waiting for the results of one server task running on a very slow computer as one of the faster server tasks may return the results first.

Once the evaluation is complete a ranked list of contingencies is displayed to the user in the main window. A new evaluation cycle is then started using the latest power system state. If a manual trigger signal is received, the current evaluation cycle is aborted and a new cycle started using the current power system states. The contingency evaluation cycling continues indefinitely.

#### 3.5.3.3 Human-Computer Interface

The HCI is provided through an X-Window interface based on MOTIF [107] comprising two windows and was developed using valuable input from NGC shift engineers resulting in clear unambiguous displays. The top section of both windows displays information on the total system load, the percentage of contingency processing that has been completed and provides various buttons to control the processing.

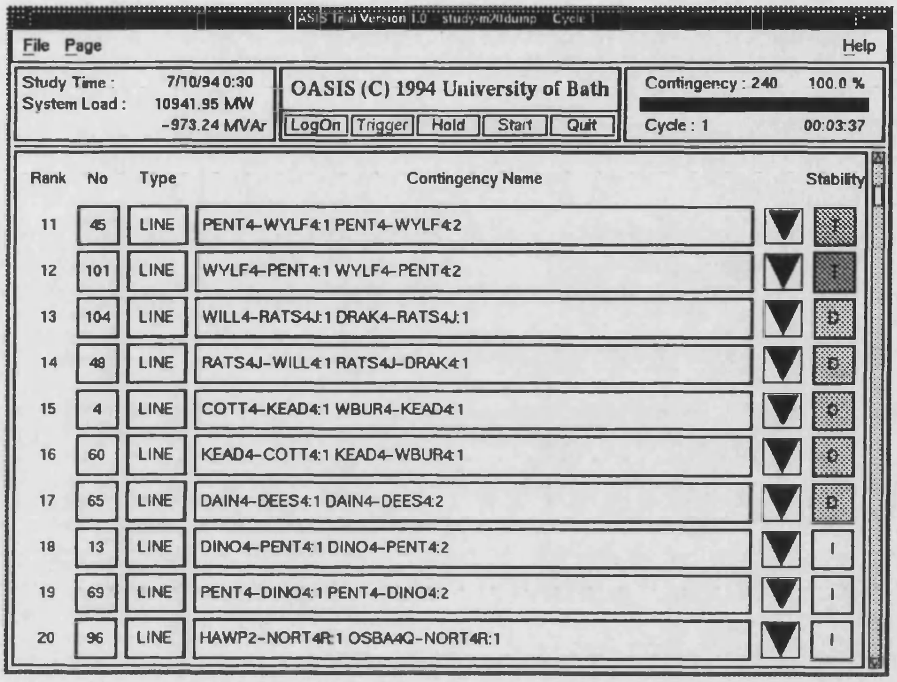


Figure 3.8: Ranked Contingency List

The main window is shown in figure 3.8 and displays a ranked list of contingencies. The stability information for each contingency is provided at the right of the contingency and displays a 'T' on a red background for transiently unstable contingencies, 'D' on a green background for poorly damped contingencies and nothing for contingencies which do not lead to either of these problems. In addition an 'I' is displayed if any node of the system becomes islanded as a result of the contingency. *Poke points* are provided which upon activation change the display to show the more detailed information about a particular contingency.

The more detailed display of a single contingency, shown in Figure 3.9, is split into two areas. The upper area displays the details of the contingency including affected plant, breaker operation times and fault location. The lower area displays information from four of the machines connected to the power system. The machines

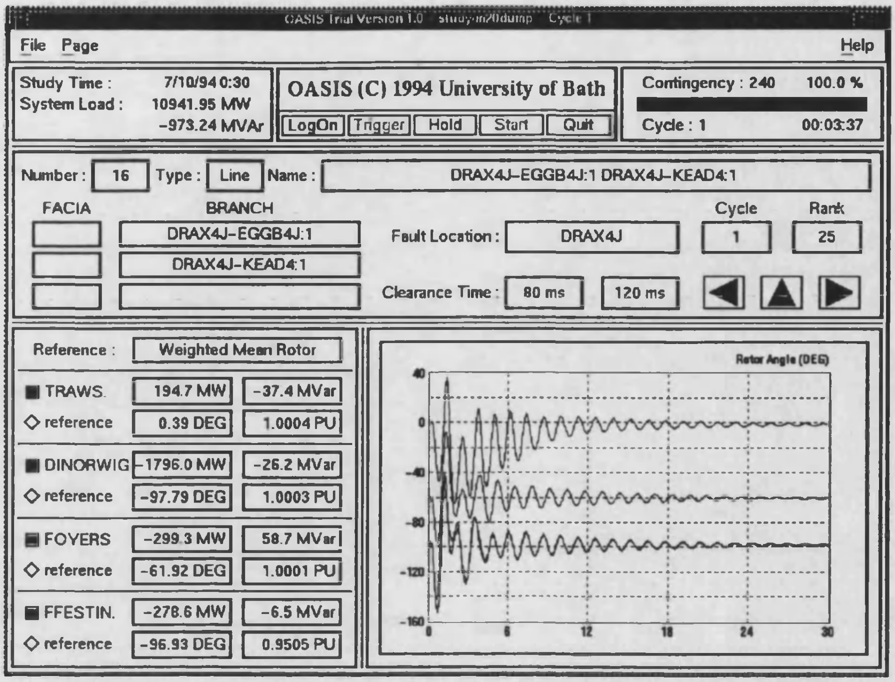


Figure 3.9: Detail of Contingency

that are automatically displayed are those four with the largest rotor swings in the system, but other machines can be specified by the user in the contingency database. Since the rotor swing curves only provide qualitative information, only one machine is selected per busbar to allow plots from other machines elsewhere in the system to be displayed. For each machine the pre-contingency MW and MVAr loadings, rotor angle and terminal voltage are shown and the rotor angle time histories are plotted. By default, the rotor angles are referenced to the weighted mean rotor angle of the system but any one of the four machines may also be used as a reference.

### 3.5.4 Server Task

The function of the server task is to perform the contingency screening and evaluation and report the results to the controller task. The server task is a pure calculation engine requiring no disk or IO access other than the communications provided through the PVM library. Since the task is coded in ANSI standard 'C', the server task can be ported easily to a wide variety of hardware platforms.

#### 3.5.4.1 Contingency Screening

One of the key areas to be addressed by such dynamic security assessors is the contingency screening required for these instability problems in order that most of the mild contingencies can be filtered out, with the remaining ones being left to undergo a detailed time domain simulation to determine their severity.

The work described in this thesis has been aimed at developing both transient and oscillatory instability screens for OASIS. These screens have been incorporated into the server task and result in an overall speedup of approximately 20 times.

#### 3.5.4.2 Contingency Evaluation

The contingency evaluation is based on PowSim, an enhanced real-time power system simulator which has been developed at the University of Bath over a number of years [113, 114]. The simulation algorithm is based on the partitioned implicit trapezoidal method. Each machine group is represented by a fifth order 'voltage behind subtransient reactance' model. Together with a first order excitation model and a fourth order prime mover model, this results in a set of ten first order differential equations including valve rate and position limits, AVR ceiling limits and magnetic saturation. The network models balanced conditions using positive phase sequence nodal admittance analysis. Loads are modelled by lumped fixed impedances while circuit branches are represented by a general purpose equivalent $\pi$ circuit that models either lumped parameter transmission lines or power transformers. Previous work has successfully verified PowSim against RASM [115], the off-line professional stability analysis package developed and used by the NGC.

When the contingency evaluation is complete, a severity index is calculated and, together with the stability information and the selected machine rotor time history plots, sent back to the client for displaying to the operators using the HCI.

### 3.5.5 Field Trials

Field trials were carried out at the NGCC between 7th and 24th November, 1994. OASIS was installed on a Silicon Graphics Indy with access to the operational ethernets at the NGCC.

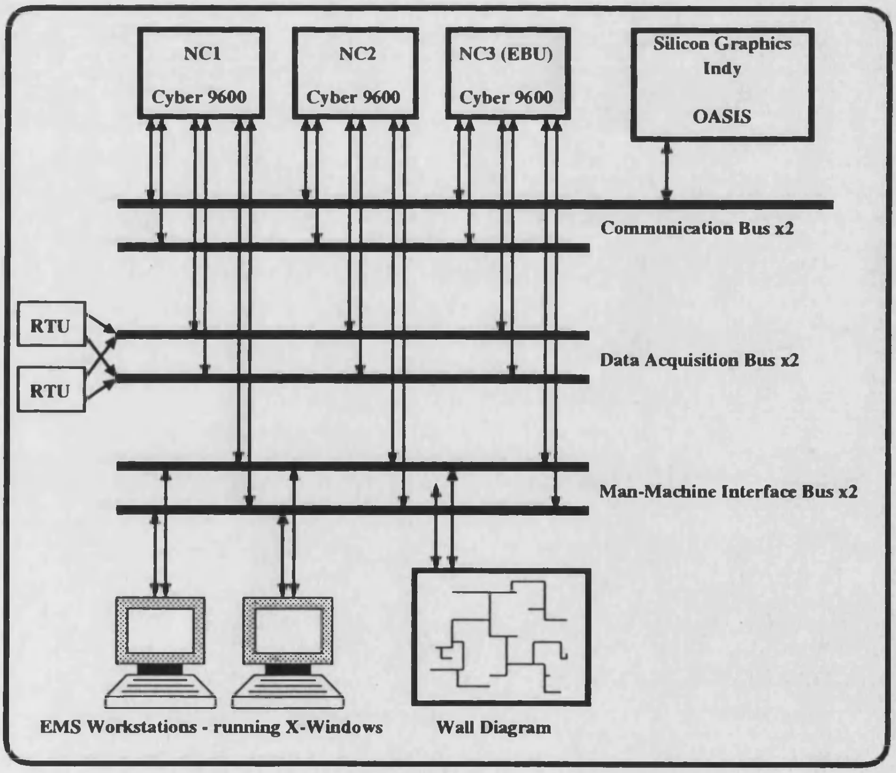


Figure 3.10: Setup for OASIS Trials at NGCC

Figure 3.10 shows the basic hardware configuration at NGCC. The main EMS computers are Cyber 9600's: NC1 and NC2 are the operational and standby computers with NC3 being used as the engineering backup computer, where software modifications are first implemented. The remote telemetry units (RTUs) provide the SCADA interface to the power system and this SCADA data is distributed by the data acquisition busses. The system reliability is enhanced by having two operational EMS computers and two of the communication, data acquisition and man-machine interface busses.

For the field trials, the Indy which was used was connected to one of the main communication ethernets, which allowed the latest state estimated power network solution, in IEEE format, to be down-loaded using `ftp` from NC3. A utility running on the Silicon Graphics Indy combined this file with a static database of machine, governor and AVR parameters to produce an OASIS input file.

Since only one Silicon Graphics Indy was being used during the trials, the PVM consisted of only this machine. Hence both the client and the one server task were running on the Indy. Typical cycle times for OASIS were of the order of 2.5 minutes for the ten contingencies, using a full 30 second time domain simulation.

For a practical implementation of approximately 5000 contingencies within a 10 minute cycle time, the hardware requirement would require approximately 125 Indy's. The contingency screening technique described in this thesis would reduce this requirement to only 4 Indy's, which would represent a more feasible investment.

The X-Window interface was shown to a number of power system operators and managers from NGCC and numerous other personnel from other sections of NGC. The feedback that was received was very favourable and moves are now underway to produce a full control-room DSAS as soon as possible.

As a requirement of the field trials, the results from OASIS for the ten contingencies were stored for a later off-line comparison with RASM. The report[103] describes the details of these results.

Chapter Four

# Contingency Screening

The aim of contingency screening is to filter out those contingencies which pose little or no security problems so that only the few potentially severe contingencies undergo detailed evaluation. This detailed evaluation is usually performed by a time domain simulation and is used to determine the severity of the contingency so that possible preventative actions may be taken and/or corrective actions determined. The research described in this thesis concerns the development of artificial neural network based electro-mechanical stability screens for use within a OASIS[86, 104], the online dynamic security assessment system developed at the University of Bath.

## 4.1 Introduction

In order that a large number of contingencies can be processed by an online dynamic security assessor it is necessary to include some form of contingency screening to filter out those contingencies which lead to little or no degradation of the system security.

All the selected contingencies will be processed by the contingency screens and therefore it is important that the screening process is simple. This will reduce the time spent filtering out the potentially severe contingencies and reduce the update time of the dynamic security assessment system. At the same time, it is very important that all the contingencies that will lead to stability problems are identified, i.e. that the screening process is *conservative.*

The potentially severe contingencies can then undergo detailed online evaluation for security violations such as line overloads, voltage violations and stability problems. These results are then presented to the power system operators through the DSA displays to enable them to take preventative or plan for corrective actions.

## 4.2 Traditional Approaches

There are several broad approaches that can be used for stability assessment: numerical integration methods, energy function approaches, expert systems, eigenvalue analysis and pattern recognition methods.

### 4.2.1 Numerical Integration

Digital power system simulators[95] perform a step by step solution of the network and machine equations at discrete intervals in time using numerical integration methods to solve the differential equations. Considerable progress has been made to speed up the numerical integration functions and combined with the use of modern sparse matrix techniques[116] the speed of numerical integration methods has improved considerably.

This approach can be used to perform a full time domain simulation of the effect of the contingency on the power system, and is the ideal method for contingency evaluation. The transient stability of the system can be determined and the decay rate of machine rotor oscillations can be calculated, giving a good indication of the degree of oscillatory instability of the post-contingency operating point.

The principal advantage of this approach is that complex high order models of AVRs, governors, boilers, SVCs and other items of plant can be used giving very accurate results which form the benchmark against which the other stability assessment methods are judged. However this method remains too slow to be used for contingency screening in an on-line environment such as a DSA.

## 4.2.2 Energy Function Methods

In these methods the post-contingency integration period is replaced by a stability criterion based on the construction of a Lyapunov function[117] in order to determine the stability domain surrounding the stable equilibrium point of the post-contingency system. If the value of the Lyapunov function is less than a pre-determined value then the system remains stable for the contingency. The transient energy function method[118] and the Equal Area Criterion (EAC) are the most widely used techniques for transient stability analysis.

### 4.2.2.1 Transient Energy Function

The basis of this method is that at the end of the disturbance of interest a certain function, in this case describing the transient energy of the system, is calculated and compared with a critical value. The difference between these values is the *transient* *energy margin.* This energy margin must be related to the parameter of interest in assessment of the systems transient behaviour, usually that of loss of synchronism associated with the pole-slipping of a machine.

The transient energy function[119, 120], which describes the system transient energy at the point of interest, contains potential and kinetic energy components. The former is made up of three components; position energy, magnetic energy and the energy associated with the networks transfer conductances. In the post disturbance period the total transient energy is considered constant, and the transient kinetic energy is converted into potential energy. If all the kinetic energy is converted then the system remains stable.

The critical energy is the threshold value of the transient energy against which transient stability assessment is made. It is the value of the potential energy at the controlling unstable equilibrium point, UEP, for the particular disturbance under investigation. The value of the potential energy at the UEP depends on the identity of the severely disturbed machines and since this in turn determines the kinetic energy correction, the UEP determination is the *key step* in the use of the TEF method in transient stability assessment. The determination of the controlling UEP is complicated by the following difficulties:

- The desired UEP is system and disturbance-specific.
- It is one among many possible UEPs.
- It is to be solved for in systems which are often numerically ill-conditioned.

Solving for the UEP can be viewed as involving the following steps:

① Identifying the critical machines; this determines the specific UEP to be solved for (if the critical machines are known then this step can be by-passed).

② Starting the solution procedure, in the angle space, near the desired UEP (to avoid solving for the wrong UEP)

③ Using a robust solution technique to solve for the UEP.

At present there are two procedures which can be used for determining the UEP. The first is the *mode of disturbance* (MOD) procedure which involves the three distinct steps mentioned above. This method is reliable but is computationally cumbersome if there are many machines in the UEP. The second procedure is the so-called *exit point method*, based on the concept of the stable manifold of the controlling UEP and the associated gradient system.

The assessment of the system transient behavoir is accomplished via computing the transient energy margin $\Delta V$, given by:

$$\Delta V = (E_{cr} - E_{eod}) \tag{4.1}$$

$$= \left(E^P_{uep} - E_{eod}\right) \tag{4.2}$$

where $E_{cr}$ is the critical energy, $E_{eod}$ is the energy at the end of the disturbance and $E^P_{uep}$ is the potential energy at the UEP.

For transient stability assessment:

$$\Delta V > 0 \quad \Rightarrow \quad \text{System is stable} \tag{4.3}$$

$$\Delta V = 0 \quad \Rightarrow \quad \text{System is critically stable} \tag{4.4}$$

$$\Delta V < 0 \quad \Rightarrow \quad \text{System is unstable} \tag{4.5}$$

The normalised $\Delta V$ is the energy margin divided by the corrected kinetic energy and is indicative of the degree of stability of the system.

The concept of system vulnerability [121] is concerned with the change in $\Delta V$ to a changing system parameter, $P$, hence the sensitivity of the control parameter $P$ is given by:

$$S_p = \frac{\delta \Delta V}{\delta P} \tag{4.6}$$

This approach may provide one route for determining control actions to move the system towards a more secure operating condition. To summarise, the *advantages* of using the TEF method are:

- Contains qualitative information on the degree of stability and instability.
- Gives sensitivity of stability-related information to changes in key system parameters or operating conditions.
- Detects structural attributes of the (post disturbance) network which influences the transient system behavoir even beyond the inertial transient.
- Suited for applications in which large amounts of data need to be processed, i.e. on-line operation.

The three main drawbacks to this approach are that if the post-contingency operating point is outside the estimated stability region then the post-contingency stability cannot be determined for certain. Secondly the computational overhead of determining the stability boundary for large multi-machine power systems is very time consuming and, finally, reduced order models have to be used, so that the accuracy of a numerical integration method is not achieved. However, this method is considerably less processing intensive than the numerical integration method and is being considered for use as transient stability screen within dynamic security assessment systems.

#### 4.2.2.2 Equal Area Criterion

This method[122–124] falls into the *direct methods* category of fast transient stability assessment. It is based on a particular application of the Lyapunov direct method and an extension of the equal–area criterion applied to a multi–machine case. For a given contingency it consists of:

- Dividing the machines in the system into two groups; that of the *critical machines* which are responsible for the loss of synchronism, and the remaining *non–critical machines.*
- Replacing the two groups by two equivalent machines.
- Further replacing this by a single machine infinite bus system.
- Evaluating the system robustness for the contingency using the equal–area criterion.

The system robustness is quantified by two measures. The *stability margin*, $\eta$, corresponding to a given fault clearing time and the *critical clearing time* for which the stability margin is reduced to zero. This technique suffers from similar problems to the TEF method. Above all, the use of reduced models and problems with accuracy after the first swing make this method an unlikely candidate for a transient stability screen within a DSA system.

### 4.2.3 Expert Systems

Expert systems have been sucessfully applied to many areas of power engineering where a well defined set of rules can be derived [63]. Applications include alarm processing [125], stability assessment [126] and dynamic security assessment [62]. Expert systems are highly suited for assisting operator control actions [43, 66, 127, 128] because it is possible to model the majority of operators actions by a set of rules.

The use of decision trees [129–131] has been widely investigated for stability assessment. This work has produced a reliable method for stability assessment, although the size of the decision trees becomes very large for large power systems. Work remains to be done on sensitivity and control for different security regions as well as practical strategies for implementing this technique. A comparison of decision trees versus the pattern recognition technique for stability assessment [132] concluded that the pattern recognition technique was slightly more reliable/accurate than the decision tree approach.

### 4.2.4 Eigenvalue Analysis

The most widely used technique for steady-state stability studies is eigenvalue analysis[133–135], which involves determining the most critical eigenvalues of the power system. An eigenvalue with a real part greater than zero corresponds to a system pole in the right hand half of a root locus diagram and is a characteristic of an unstable system. Power systems with a poor oscillatory stability response can also be detected by this approach. The positioning of system poles close to the imaginary axis (i.e. having a small real part) will experience poor damping, and hence produce a poor oscillatory stability response.

Studies carried out by Chan[136] showed that for the full NGC system (900 busbars and 10th order machine models) a standard eigenvalue analysis using a QR solver would take approximately seven minutes to calculate all eigenvalues when running on a Silicon Graphics Indigo (SPECMark 60.3). This indicates that this approach is considerably slower than required for a fast contingency screen.

### 4.2.5 Pattern Recognition Method

This method relies on reducing the on-line computational overhead to a minimum at the expense of intensive off-line studies. By performing offline training of a pattern classifier using results obtained from a time domain simulator, the accuracy of a numerical integration method may be achieved within the computational and time constraints of on-line operation making this approach an ideal choice for stability screening.

The classical task of pattern recognition consists of defining a pattern vector, $I$, whose components contain sufficient information about the stability of the power system so that a classifier can decide purely on the basis of $V$ what the system stability will be. This vector is then evaluated at many different *representative* operating points of the power system to generate a training data set. The final step is then to determine the classifier function $C(I)$ such that the pattern recognition task becomes:

$$C(I) = \begin{cases} \geq 0 & \text{for a secure I} \\ < 0 & \text{for an insecure I} \end{cases} \tag{4.7}$$

The lower limit for the classification error depends on the choice of the primary inputs and the feature selection process to determine the inputs to the classifier.

In 1974 Pang[137] described a pattern recognition approach to security assessment and included results for the 225kV 10 bus CIGRE test network. Most of the selected features were related to particular items of plant, such as bus 4 voltage magnitude, and therefore do not scale well to systems with approximately 1000 busbars. However, the broad approach of using a steady state classifier followed by a transient security classifier remains the basic approach adopted within OASIS.

This work was followed in 1975 by Koizumi[138] which described a pattern recognition approach to transient stability screening. The network that was used for the studies was an 78 busbar model with 24 generating units and 88 lines. As before, the features are related directly to the power system state vector, and the feature extraction process selected 30 features to be used as inputs to a classifier and achieved good results.

In 1983 the work of Hakimmashhadi[139] outlined a method for fast transient stability assessment. This work mentioned the use of transient data as features for stability assessment and in particular the use of **accelerating energy** as a feature for transient stability assessment. The example system that was used was a nine bus reduction of a 230kV network and resulted in classification errors of less than 2%.

Yamashiro[140] described a method for transient stability assessment using only two features. The **asynchronous kinetic energy** of the generators and the **transmission power margin** are shown to be sufficient for the classification of one particular contingency on the IEEE 118 bus network. These features have been shown by the author to provide poor discrimination on larger systems, such as the UK National Grid System.

The application of pattern recognition techniques to transient security assessment was comprehensively detailed by Hakim[141] The application of a pattern recognition technique to security analysis is described by Chang[46]. Again, specific elements of the power system state vector were used as inputs to a classifier to detect post-contingency voltage problems. This approach was tested on a 22 bus network, and the authors indicated that further work is needed to ascertain the feasibility of this approach to larger networks.

In 1993 Fidalgo[142] described an approach for using an ANN to predict the transient stability margin. This approach was tested on the 11 bus CIGRE test system and used plant specific features, which will not easily scale to large power networks.

The use of adaptive pattern recognition proposed by Sobajic[143] coupled with a neural network approach has been shown to produce good results on a 4 bus system, but this technique still has to be applied to large power networks.

Over recent years, the application of ANNs as pattern classifiers has become widespread. In particular, the application of ANNs for power system security assessment is of particular interest.

#### 4.2.5.1 Neural Network Classifiers

The work of Niebur[52, 144] formed the basis for the adoption of self-organising ANNs to the task of security assessment. In particular, the use of Kohonen networks for static security assessment on a 5 bus system has produced encouraging results. Similar work by Pao[50] has also been performed.

The work of Sobajic[48, 72] forms one of the core references for the application of supervised learning ANN models to power system security assessment, although the work was only applied to a 6 busbar power system. Chowdhury[145] also discussed the application of ANNs to security assessment and concluded that this approach is significantly less computationally demanding that a numerical integration approach. The problem of extending this technique to larger systems was outlined, including the much larger input vector size.

Similar work by Song[146], Aggoune[147], Thomas[148], El-Sharkawi[51], Mori[149] and Hobson[150] has applied neural nets to security assessment, although the latter paper raised into doubt the ability of ANNs to generalise over different operating conditions. The use of ANNs and a transient energy function approach has been extended to include the concept of **vulnerability assessment** [102, 121, 151], where the inputs to an ANN are used to indicate corrective actions to move the power system closer to stability.

#### 4.2.5.2 Dimensionality Problems

The traditional problem with applying pattern recognition methods to stability assessment of large power systems is due to the *curse of dimensionality.* Put simply, this problem is due to a large number of features being required to classify the stability of a large power system. This makes it almost impossible to design a classifier which will be robust to changes in the system loading and topology. This problem is well described by Hobson [150] where the conclusion that current pattern recognition methods cannot be sucessfully applied to large power systems.

Cauley[70] outlined a method for contingency screening using features based on the deviation between parameters calculated at the pre- and immediate post-contingency (fault clearing) operating conditions. These features, or composite indices as they are termed, are system wide and not all limited to particular items of plant. This approach was applied to a 436 bus network and 24 features were selected as inputs to a classifier. A MLP was trained to perform the classification and good classification results were obtained. This work is being taken forward by EPRI[56] and shows promising results. The principle difference between this work and the rest is that actual power system parameters, such as generation levels and line power flows are not used as inputs to the MLP.

#### 4.2.5.3 The new method

The contingency screening method described in this thesis is based on the pattern recognition approach. As with the previous methods, an ANN is used as the basis of the pattern classifier. These screens are shown to be easily scaled to large power systems by the use of a novel set of features which overcome the curse of dimensionality. The approach is also extended to detect both transient and oscillatory instability. Results are presented for the application of these screens to a 100 busbar, laboratory scale, power system model as well as to snapshots of the full UK national grid system. In addition, the screens are integrated into a dynamic security assessor, allowing the real benefits of this fast contingency screening to be realised.

## 4.3 Chapter Summary

The provision of fast and reliable contingency screens within a dynamic security assessment system is critical to enable the time constraints for on-line operation to be met. A wide number of techniques can be used to detect those contingencies which may lead to instability, but few are suitable for contingency screening due to their complexity.

The pattern recognition approach is ideally suited for on-line operation and has been chosen to form the basic approach for this work. The traditional problem of applying such a technique to large power systems has been solved and is described in detail in the next chapter. This is followed in chapter 7 by details of their implementation within OASIS.

## Chapter Five

# Connectionism

Connectionist systems consist of many primitive units which are working in parallel and are connected via directed links (connections). The main processing principle of these units is the distribution of activation patterns across connections similar to the basic mechanism of the human brain. This kind of processing is also known as parallel distributed processing. Neural networks are one such connectionist system and are being touted as one of the greatest computational tools ever developed [23, 24, 152]. Although there is substantial hype, most of the excitement is due to a neural networks apparent ability to imitate the human brain's ability to make decisions and at a primitive level to imitate the brain's *creative* processes.

Neural networks, or to be more precise Artificial Neural Networks, ANNs, have been found to be exceptionally suited to some tasks where there is either no, or no effective, algorithmic solution. These tasks are primarily that of pattern recognition and optimisation. Before going into these areas in more detail the relationship between an ANN and the biological neural networks, BNNs, will be outlined.

# 5.1 Biological Basis for Neural Network Tools

Every day of our lives, each of us carries out thousands of tasks that require us to keep track of many things at once. Relatively simple actions, such as picking up a glass involve memory, learning and physical co-ordination. The complexitivity of even these *simple* tasks, which we often do without *thinking*, is underscored by the difficulty of building a robot to perform the same operation. It is the complex biological systems within us that make performance of these tasks possible.

The operating time for biological neurons is of the order of one millisecond, which is many times slower than that provided by modern silicon technology. However it is the vast parallel operation of information flow from dendrites through the cell body to the axons that makes biological neural nets far superior.

## 5.1.1 Structure

Over the past few decades detailed studies have been carried out on the construction and operation of our brains and nervous systems. The basic building block of the nervous system is the neuron, see figure 5.1 for a conceptual diagram, which is comprised of a cell body, dendrites and an axon. There are many different types of neuron[152]; the neuron shown is most like a ***motor neuron*** but is meant only to convey the basic configuration and terminology. The signal flow goes from left to right, from the dendrites through the cell body and out through the axon. The signal from one neuron to another is passed on by the connection of one neurons axon and the other neurons dendrite at a connection called a synapse.

The human brain has a large number of neurons: typical estimates are of the order 10

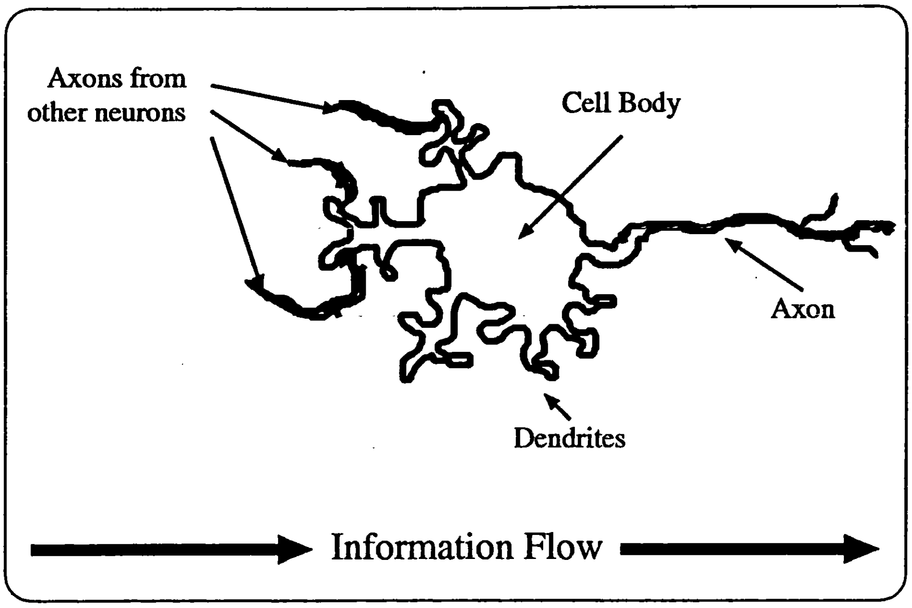


Figure 5.1: Biological Neuron

to 500 billion[152]. According to one estimate by Stubbs[153], neurons are arranged into about 1000 main modules, each with about 500 neural networks. Each neural network has of the order of 100,000 neurons and each axon connects to on average 100 dendrites. The perceived operation of the brain is that neurons communicate with each other by means of electrical impulses[154].

### 5.1.2 Operation

The signals reaching a synapse and received by the dendrites are converted into electrical energy. The inter-neural transmission is sometimes electrical but more often effected by the release of chemical transmitters in the synapse. The neuron then either generates an impulse (fires) to its axon if the input is sufficiently *excitatory* or fails to do so if the input is *inhibitory*. More precisely, for the neuron to fire, the excitation must exceed the inhibition by a value equal to the *threshold* value.

After carrying a pulse, an axon fibre moves to a state of non-excitability for a certain time known as the *refractory period.* This duration varies between different types of neurons and results in the brain being a dense interconnection of neurons which release asynchronous signals. The signals are not only fed forward to other neurons within the spatial neighbourhood but also back to some of the generating neurons.

This explanation of the biological operation is greatly simplified when seen from a neuro-biological point of view, although it explains the basic principles involved. Artificial neural networks are much more simplified than their biological counterparts are described in the following section.

## 5.2 Artificial Neural Network Models

Vast discrepancies exist between both the architectures and capabilities of artificial and biological neural networks. Knowledge about actual brain functions is so limited that there is little to guide those who try to emulate them. In ANNs, the processing elements are often called neurodes or neurons, and in this thesis the latter will be used. The main differences between BNNs and ANNs are outlined below:-

- In a typical implementation of a ANN, connections among neurons can either have positive or negative weights.
- Information about the state of activation, or excitation, of a neuron is passed to other neurons to which it is connected as a single numeric value.
- There are many kinds of neurons in biological systems. A ANN is usually implemented with only one type of neuron, although occasionally two or three types are used.

- BNNs typically operate on a cycle time of about 10-100 milliseconds. ANNs implemented on even a basic IBM PC386 operate with a cycle time of 1-10 micro seconds.
- There is a significant difference between the number of neurons in a BNN and and a typical ANN. Typically ANNs are implemented with less than a few hundred neurons.

None of the models that exist today have been successful in duplicating the performance of the human brain but they been very successful in limited application areas[23, 24, 155]. Of the different types of ANN, that of the feed-forward, multi-layer perceptron (MLP) model is the most widely used.

### 5.2.1 The Perceptron

The *perceptron* is the simplest form of neural network used for the classification of a special type of patterns said to be linearly separable. Figure 5.2 shows a single-layer perceptron (SLP) which is composed of a single artificial neuron with adjustable synaptic weights and threshold.

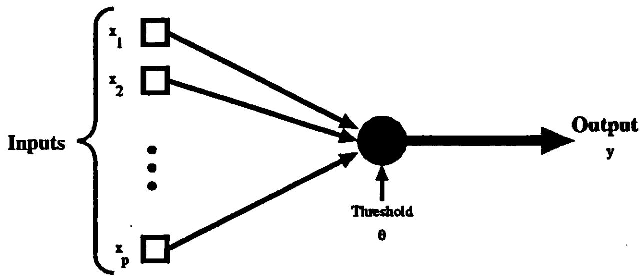


Figure 5.2: Single-layer perceptron

The output of the SLP is given by a linear combination of the inputs multiplied by the connection weights, $w$, as well as the threshold $\theta$ as shown in equation 5.1

$$O = \sum_{i=1}^{p} w_i I_i - \theta \tag{5.1}$$

The work of Rosenblatt[156] on his perceptron brain model forms the basis for the whole field of ANNs. Rosenblatt proved that if the input patterns (vectors) used to train the perceptron are drawn from two linearly separable classes, then the perceptron algorithm converges and positions the decision surface in the form of a hyper-plane between the two classes.

### 5.2.2 Multi-Layer Perceptrons

The Multi-layer perceptron model consists of a set of input neurons that constitute an *input layer*, a set of hidden neurons and a set of output neurons that form the *output layer*. These class of ANNs are a generalisation of the SLPs described previously, but are far more powerful.

A simple three layer MLP is shown in figure 5.3. Each neuron is represented by a circle with the icon in the circle representing the transfer function of the neuron. The neurons are grouped together in slabs, or layers. The connections between neurons are represented by straight arrowed lines. The input neurons are on the left and the output neurons are on the right.

To train an ANN requires an algorithm that adapts the connection weights in such a manner that successive presentations of the training data to the input neuron produces outputs that are close to the desired response. This form of *learning*, where the output is changed towards a desired value is known as *supervised learning*, and is usually performed by a variant of the back-propagation algorithm[23].

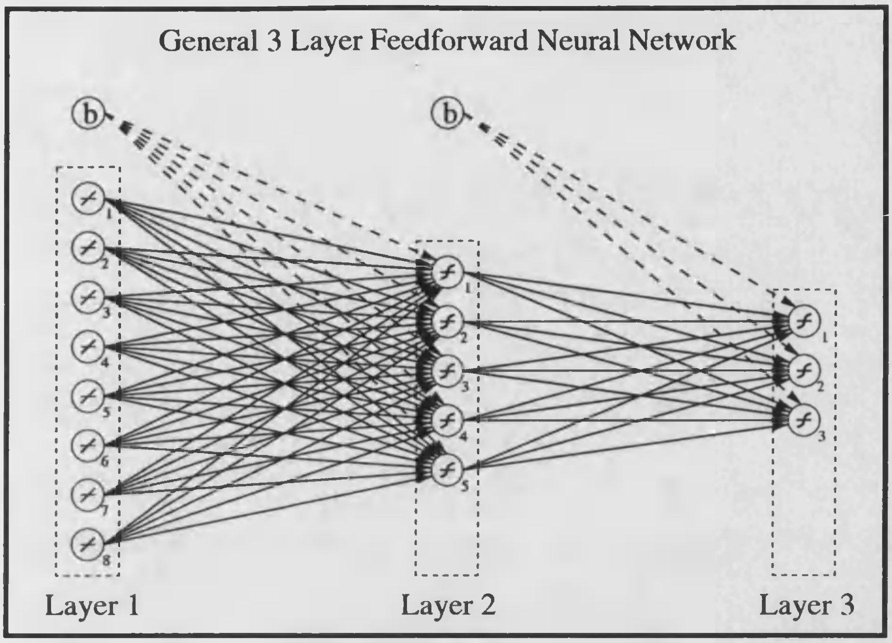


Figure 5.3: Feed-forward Network Structure

#### 5.2.2.1 The Back-Propagation Learning Algorithm

The back-propagation training algorithm is an iterative gradient algorithm designed to minimise the mean squared error between the actual output of a multi-layer feed-forward ANN and the desired output. It requires that the transfer function for each neuron is continuous and differentiable. The algorithm is explained below:

**STEP 1** – Initialise Weights and Offsets. Set all weights and node offsets to small random values.

**STEP 2** – Present Inputs and Desired Outputs. Present a continuously valued input vector space to the input neurons, $\vec{I}$, and get the desired output, $\vec{d}$.

**STEP 3** – Calculate Actual Outputs. Use the neuron transfer functions to propagate the network input vectors through to the output layer neurons.

**STEP 4** – **Adapt Weights.** Use a recursive algorithm starting at the output neurons and working back to the first hidden layer to adjust the weights. Adjust the weights by:

$$w_{ij}(t+1) = w_{ij}(t) + \eta\delta_j I_i + \alpha\left(w_{ij}(t) - w_{ij}(t-1)\right)$$

In this equation, $w_{ij}(t)$ is a weight from neuron $i$, in layer $n-1$, to neuron $j$ in layer $n$ at iteration $t$. $0 \leq \eta \leq 1$ is the learning factor, which controls how much of the error is used to adapt the weights, and $0 \leq \alpha \leq 1$ is the momentum factor which controls how much of the previous weight change is used for the current weight change.

If neuron $j$ is in the output layer, and assuming all neuron transfer functions are **Sigmoid**, then:

$$\delta_j = O_j(1 - O_j)(d_j - O_j)$$

where $d_j$ is the desired output of neuron $j$, and $O_j$ is the actual output. If node $j$ is a hidden layer neuron then:

$$\delta_j = I_j(1 - I_j)\sigma_k\delta_k w_{jk}$$

where $k$ goes from 1 to the number of nodes in the layers above node $j$. Bias thresholds are adapted in a similar manner by assuming that they are connections from a constant valued (1) bias neuron.

**STEP 5** – **Calculate Average Sum Squared Error.** If the average sum squared error is less than a threshold then the learning is complete, else return to step 2.

### 5.2.3 The Self-Organisation Model

This neural network model was made famous by the work of Dr. Teuvo Kohonen of Helsinki University of Technology in Finland, and is often referred to as the Kohonen model.

The most significant difference between this model and the feed-forward model is the fact that this model is trained without supervision: only the input patterns are presented, and the network trains itself. The best description of this model is given by Dr Kohonen[157].

### 5.2.4 The Hopfield Model

This model[158] is a recurrent, single layered, neural network. Unlike the previous models, the main use of these networks is for optimisation problems[159]. The network is not *trained*, but inter-neuron connection weights can be explicitly set so that the network performs optimisation.

Recent papers[160–162] have shown that these networks can be used for constrained, non-linear, quadratic optimisation with boundary constraints. The major advantages of optimisation methods employing these neural networks are:

- Exponential convergence.
- Amenable to parallel implementation.
- Only yields feasible solutions.

## 5.3 Practical Issues

The inclusion of an ANN within a software or hardware module is often perceived to be surrounded by some vague guidelines and guesswork. This section provides broad guidelines for practical issues surrounding the design, training and testing of ANN based systems.

### 5.3.1 Choice of Model

The choice of model is usually made on the type of data available for training. If the desired output of the ANN is known for each of the training patterns then a form of supervised learning is likely to be the most suitable. The most obvious choice for an ANN model that supports this type of learning is the MLP, trained using some variant of the back-propagation algorithm. Other choices may include ANN models derived from an self-organising input stage and an output stage using a supervised learning technique to achieve the desired transfer function. Otherwise, an ANN model supporting a un-supervised learning algorithm would be more appropriate, such as the self-organising models described earlier.

### 5.3.2 Size of Model

The degree of freedom of an ANN is equal to the number of interconnections and therefore proportional to the number of hidden neurons in a 3 layer MLP. The number of hidden neurons must therefore be matched in some sense to the complexity of the decision boundary. Currently, the only reliable method is to use a comparison of the performance of ANNs with different numbers of hidden neurons. The time to achieve a desired training error can be used as a metric, and usually a *bath* type curve of training error against the number of hidden layer neurons is achieved. For a small number of hidden layer neurons the ANN will be unable to learn the training data. As this number is increased the training error will reduce until a very large number of neurons are used, when the error will increase again.

### 5.3.3 Feature Extraction

For pattern recognition problems, the inputs to the pattern classifier should have a high correlation with the desired classification. The process by which the inputs to an ANN classifier are determined is called feature extraction. The mathematical approach to feature selection is to identify certain invariant properties of the pattern classes. These properties are then used to reduce the dimensionality of the pattern vectors either through a linear transformation or through the preferential choice of a subset of the attributes.

The selection of features with a low correlation to the problem should be avoided as the ANN will try to force a mapping between the feature and the output. In this case, the performance ANN may depend heavily on a feature with weak correlation.

### 5.3.4 Generalisation versus Memorisation

The ability of an ANN to classify inputs that it has not seen before is referred to as *generalisation*. Memorisation, on the other hand, guarantees that when the ANN is presented with a particular pattern in the training set then the output of the ANN will be as desired. However, the performance of such an ANN on data that it has not seen before is likely to be poor. The ability to interpolate among the training data does not necessarily imply good generalisation. A properly trained ANN classifier should respond with roughly the same error for both the training and test cases.

### 5.3.5 Inversion

The process of inversion can be used to enhance the performance of an ANN close to a decision boundary. A query-based mechanism has been proposed[24, 163] which requires a set of inversion data points from a partially trained ANN. These points are then used to calculate further input patterns in the vicinity of the decision boundary. The desired output of the classifier for these patterns is determined using the techniques used to generate the training patterns, and hence the performance of the ANN is improved in the vicinity of the decision boundary.

## 5.4 Performance Metrics for ANNs

Most of the time, measuring how well a system performs is relatively straightforward, for example by calculating the percentage of all answers that are correct. Measuring the performance of ANNs is usually not this simple.

Consideration has to be given to the choosing of a *representative* testing data set, and should not just be the *standard* examples, but should include examples close to decision boundaries. The examples should ideally be chosen by *experts* in the field and not just the programmer or engineer.

### 5.4.1 Percent Correct

This is probably the most simple performance metric. Care should be taken when interpreting results if a number of different examples were chosen for each class.

### 5.4.2 Average Sum-Squared Error

This is a convenient metric for monitoring the learning of a network as training progresses and the testing of the network once the training phase is complete.

The average sum squared error is obtained by computing the difference between the output value of an output neuron, $o_i$, and its desired value, $t_i$. This value is then squared and summed with the values for all output neurons for all $P$ patterns. This grand total sum over all output neurons and patterns, multiplied by 0.5 and divided by the total number of patterns yields the average sum squared error, $E_{asse}$:

$$E_{asse} = \frac{1}{2 * P} \sum_{l} \sum_{p} (t_{pl} - o_{pl})^2 \tag{5.2}$$

### 5.4.3 ROC Curves

Another way to measure the performance of a neural network system is with receiver operating characteristic, ROC, curves. The use of these curves has dated back to the 1940's for electronic communication systems and has been more recently used for measuring the performance of neural networks and other expert systems.

ROC curves are particularly valuable tools when used with neural network systems because the results obtained are not sensitive to the probability distribution of the training/test set patterns or decision bias. A ROC curve is generated for, and reflects, the performance of a neural network for one given result. It indicates how well the system did compared with a *gold standard*, in making a decision.

For a given decision, indicated by a given output neuron, four possible alternatives exist as shown in the ROC contingency table in figure 5.1. The first alternative is a

| System Diagnosis | "Gold Standard" diagnosis | |
|---|---|---|
| | Positive | Negative |
| Positive | TP (true positive) | FP (false positive ) |
| Negative | FN (false negative) | TN (true negative) |

Table 5.1: ROC Contingency Table

true positive decision, TP, in which the positive decision of the system coincides with a positive diagnosis according to the gold standard. The second is a false positive decision, FP, in which the system made a positive diagnosis that was not in the gold standard. Similarly, a false negative decision, FN, is made when the gold standard diagnosed a positive diagnosis that was not made by the system, and a true negative decision is made when both the system and gold standard indicate the absence of a positive diagnosis.

The ROC curve makes use of two ratios involving these four possible decisions, as shown in table 5.2.

| Ratio | Construction |
|---|---|
| True Positive Ratio | $\frac{TP}{TP+FN}$ |
| False Positive Ratio | $\frac{FP}{FP+TN}$ |

Table 5.2: ROC Ratios

The ROC curve is then a plot of the true positive ratio versus the false positive ratio. When applied to the performance of neural network tools, the curve is usually obtained by plotting points for various values of the threshold and then connecting the points. A typical way to proceed is to plot points for a number of threshold values, for example 0.1, 0.2, $\cdots$, 0.9. Both ratios are then calculated for each point. Figure 5.4 illustrates a hypothetical case involving two configurations of an ANN, giving the two ROC curves shown. The curve representing the configuration of ANN2 reflects a better overall system performance than that of ANN1. The dotted line represents

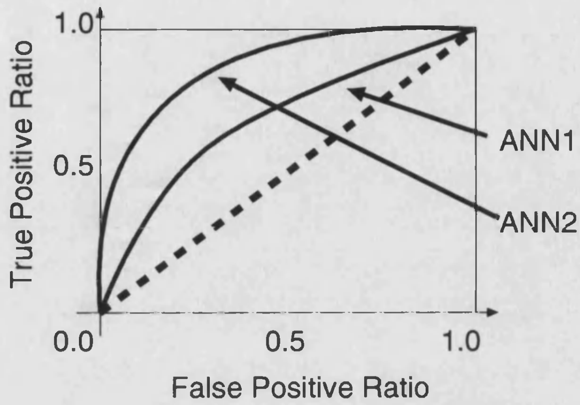


Figure 5.4: Example ROC curve

the situation in which no discrimination exists, ie a system could only achieve this by chance. When the curve follows the left vertical and upper horizontal axes, the system is discriminating perfectly.

The ROC curve therefore always lies above the major diagonal, and the area under the ROC curve can be used as a single value performance metric.

### 5.4.4 Chi-Square Test

The chi-square test examines the frequency distribution of all the categories that it is possible to obtain from a particular network system. That is, it looks at how often each category is expected to occur versus how often it actually occurs.

## 5.5 Neural Network Tools

A Neural Network Tool, NNT, is an analysis tool which allows artificial neural networks to be designed, trained and tested. Such tools are invariably software based although the majority of ANNs that are developed are coded in software high speed ANNs can be achieved by constructing hardware ANNs. Two NNTs were used in this research and are described below.

### 5.5.1 (N)eural (N)etwork (S)imulator

NNS is a NNT designed and written by the author to provide an effective method for training neural networks in an offline environment. The features of NNS of interest are:

① The ability to train and test general *N layer* neural networks.

② Training by the back-propagation algorithm.

③ Designed for processing large networks offline.

④ Utility to generate Hinton diagrams.

⑤ Utility to produce high quality network diagrams.

### 5.5.2 (S)tuttgart (N)eural (N)etwork (S)imulator

SNNS is a simulator for neural networks developed at the Institute for Parallel and Distributed High Performance Systems at the Universität Stuttgart since 1989. The goal of the project was to create an efficient and flexible simulation environment for research on and application of neural nets. It is the authors opinion that SNNS is an extremely good NNT.

SNNS is a NNT which runs under an X Window System environment on a wide range of computing architectures. The features of SNNS which made it suitable for use in this project are briefly described below.

① Full Windows-Icon-Mouse-Pointer interface, allowing fast and convenient modification of neural networks.

② Ability to handle a wide range of ANNs with a wide selection of neurons and training algorithms.

③ A graphical network editor which allows for easy modification and monitoring of an ANN.

④ Ability to produce Hinton diagrams.

Figure 5.5 shows a typical screen display of SNNS being used to train a pattern classification ANN. SNNS was used wherever possible for all interactive design of neural networks as the very effective graphical user interface allowed greater productivity than offline neural network design. SNNS can be freely obtained by anonymous ftp from `ifi.informatik.uni-stuttgart.de`.

## 5.6 Formal Methods

Some work has been done on arriving on a method for neural network formalisation[164] based on the concept of layers. It comprises a mnemonic notation, a uni-

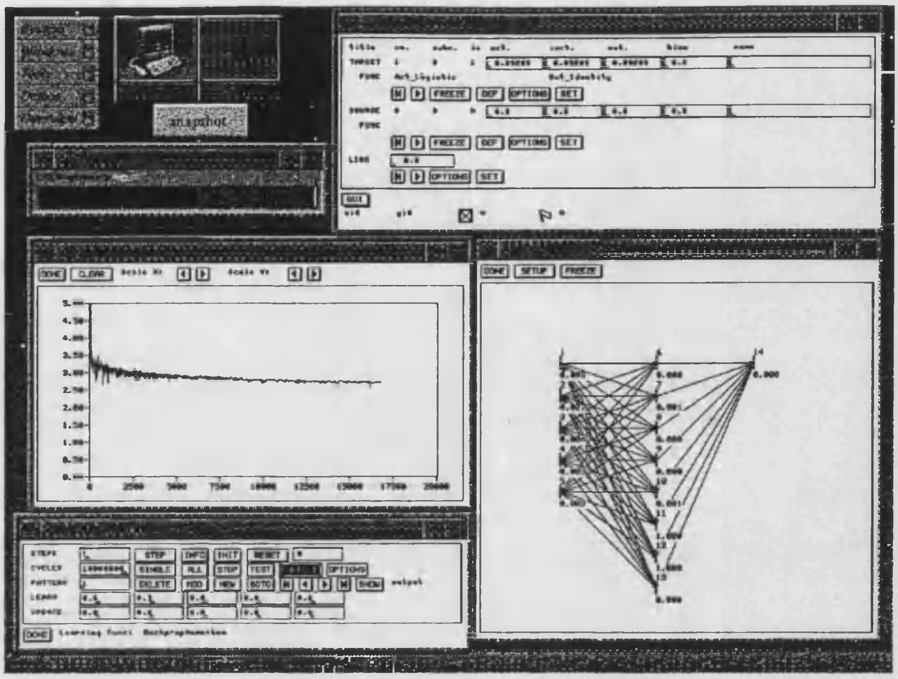

Figure 5.5: SNNS Screen Display

form nomenclature and a topological taxonomy, supplemented with both a hierarchical and a universal mathematical definition of a neural network. This method has not been adopted in this work at the present time due to its complex notational requirements, but its merits are noted by the author.

## 5.7 Current Application Areas

The application of ANNs to current science and engineering problems is a widespread area, and is expanding rapidly. Table 5.3 outlines **some** of the current application areas; it is not supposed to be complete, but merely to provide a feel for the current wide range of applications.

The application of ANNs to tools within energy management systems is another of these main application areas[124]. This is a rapidly expanding area and table 5.4

| | |
|---|---|
| Analysis of medical tests | Circuit board problem diagnosis |
| EEG waveform classification | Analysis of loan predictions |
| Stock market prediction | Military target tracking and recognition |
| Oil exploration | Process control |
| Psychiatric evaluations | Optimising scheduled machine maintenance |
| Composing music | Explosives detection in airline luggage |
| Speech recognition | Test-to-speech conversion |
| Optical character recognition | Spectral Analysis |

Table 5.3: Neural Network Application Areas

shows the topics which have been investigated at the present time.

| | |
|---|---|
| Load Forecasting | Contingency Screening |
| Contingency Selection | Optimal Power Flow |
| Transient Stability Studies | Dynamic Stability Studies |
| Unit Commitment | Corrective Actions |
| State Estimation | Restorative Actions |

Table 5.4: Neural Networks in Power Systems

## 5.8 Sources of Information

Current *hot news* on neural networks can be obtained from the internet news group `comp.ai.neural-nets`[165], the IEEE transactions on Neural Networks or any of the international neural network bodies.

Table 5.5 shows some uniform resource locators (URLs) which provide usefull on-line neural network information via the WWW (internet).

http://www.emsl.pnl.gov:2080/docs/cie/neural/
http://http2.sils.umich.edu/Public/nirg/nirg1.html
http://www.neuronet.ph.kcl.ac.uk/
http://vasarely.informatik.uni-stuttgart.de/snns/snns.html
http://physig.ph.kcl.ac.uk/cnn/cnn.html
http://www.lpac.ac.uk/SEL-HPC/Articles/GeneratedHtml/neural.appl.html
http://www.mindspring.com/ zsol/nnintro.html
http://www.lpac.ac.uk/SEL-HPC/Articles/NeuralArchive.html
http://www.eeb.ele.tue.nl/neural/index.html

Table 5.5: Neural Network URLs

## 5.9 Chapter Summary

The broad topic of artificial neural networks has been covered, with particular emphasis on multi-layer perceptrons and the back-propogation algorithm that is used to adapt the weights to achieve the desired non-linear mapping function from inputs to output. Practical issues surrounding the design and training of such networks have also been covered.

The following chapter describes the details of the application of this type of neural network to contingency screening.

Chapter Six

# Neural Network Contingency Screening

The previous chapters have outlined the requirement for fast contingency screening within dynamic security assessment systems and have described the technology of neural networks. This chapter brings these two strands together and describes a new pattern recognition method for fast contingency screening of large interconnected power systems. A novel way of generating and selecting features which are highly correlated to the stability of the power system is presented. It is shown that these features can be used to overcome the dimensionality problems associated to applying pattern recognition techniques to large systems. This is preceeded with a brief justification of the reasons for using neural networks as the core of a pattern classifier.

## 6.1 Why use Neural Networks?

Pattern recognition problems can be solved in a variety of ways. If rules can be generated to perform the classification then a rule-based pattern classifier will be appropriate. Such classifiers could then be based on expert or fuzzy-expert systems, decision trees or other similar techniques. However, in many cases such as contingency screening, the rule-base is difficult or impossible to generate and therefore another approach needs to be adopted.

Such approaches rely on using past experience or historical records to develop the pattern classifiers. Neural networks are one such example of this technique. Their ability to *learn* examples of the pattern classification and then to be able to *generalise* for patterns that it has not seen before make them the leading contender for such classifiers. For these reasons, neural networks were chosen to form the core of the pattern classifier for this application.

## 6.2 Overview

The broad approach of using neural networks for contingency screening is shown in figure 6.1. A power system simulator is used to perform a time domain simulation of the contingency up until the power system topology changes are complete. This point in the simulation is referred to as the contingency termination point (CTP). At the CTP a set of features, called *composite indices*, are calculated from the power system state vector and presented as inputs to an ANN. The ANN then predicts an instability index which is compared to a threshold value to determine whether the system remains stable.

If the time domain simulation is continued beyond the CTP then the effect of protection equipment may be to alter the topology of the power network. However, these effects are due to the influence of the contingency on the power system and not to the contingency itself and hence do not effect the position of the CTP. In

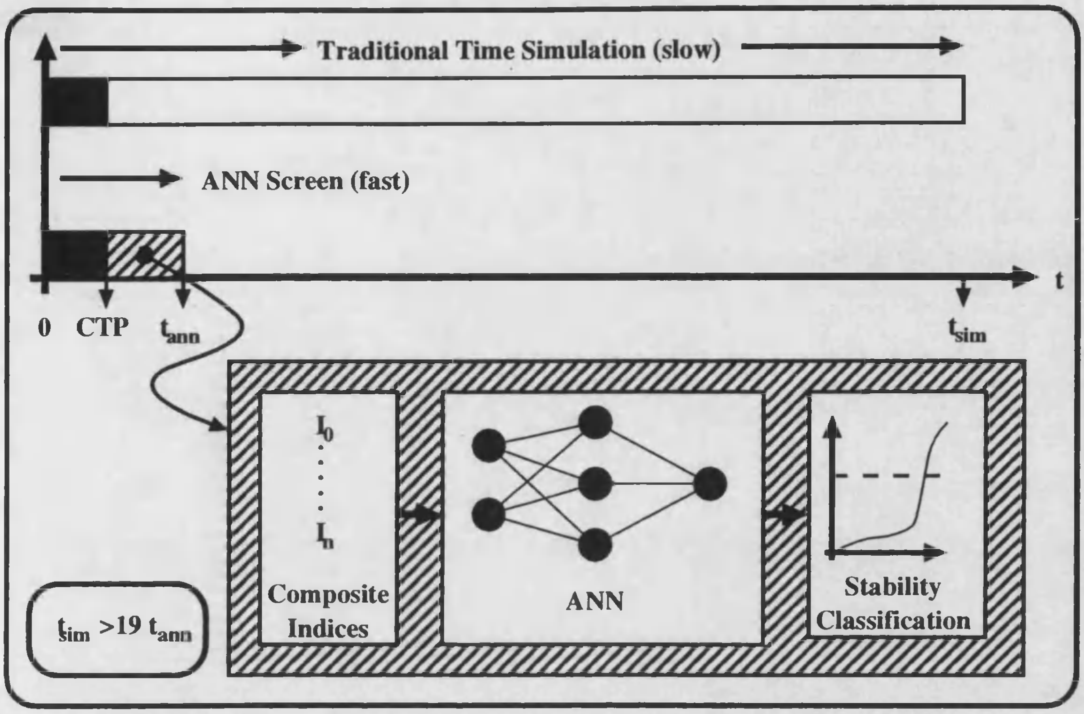


Figure 6.1: Outline of the ANN Screening Approach

practice, two sets of composite indices and ANNs are used, one for transient and one for oscillatory instability.

### 6.2.1 Advantages

The primary advantage of this approach is that the computationally intensive operation of simulating the post-contingency state of the power system, beyond the CTP, is replaced by the relatively un-intensive process of calculating the composite indices, propagating them through the ANN and comparing the output with a threshold value. This property makes this method an ideal candidate for use as an online stability screen, having an accuracy close to that of a numerical integration approach coupled with the speed advantages of a pattern recognition approach.

### 6.2.2 Drawbacks

A feature of pattern recognition techniques is that although they are faster than a full time domain simulation, their reliability can be questioned. In particular, the classifier must be designed to function across the range of expected operating points, maintaining efficiency and conservativeness of operation.

The robustness of this approaches to changes in the power system topology depends on:

① Selection of features (composite indices) that are as topology and loading independent as possible.

② The use of training data that covers the expected range of operating conditions.

③ The reliable performance of the classifier in the vicinity of stability boundaries.

The first two points can be dealt with by ensuring that the training data set is (1) representative of the problem to be solved and (2) covers the expected range of operating conditions. The third point has been dealt with in the following way.

Figure 6.2 shows a conceptual stability boundary. Those contingencies close to the boundary will in practice be either just stable or just unstable and the conventional binary classification into stable or unstable classes looses this information. By training the ANN to predict the instability index the errors close to these stability boundaries are greatly reduced as the ANN *surface* is much smoother and consequently the prediction errors in the vicinity of the stability boundary are reduced.

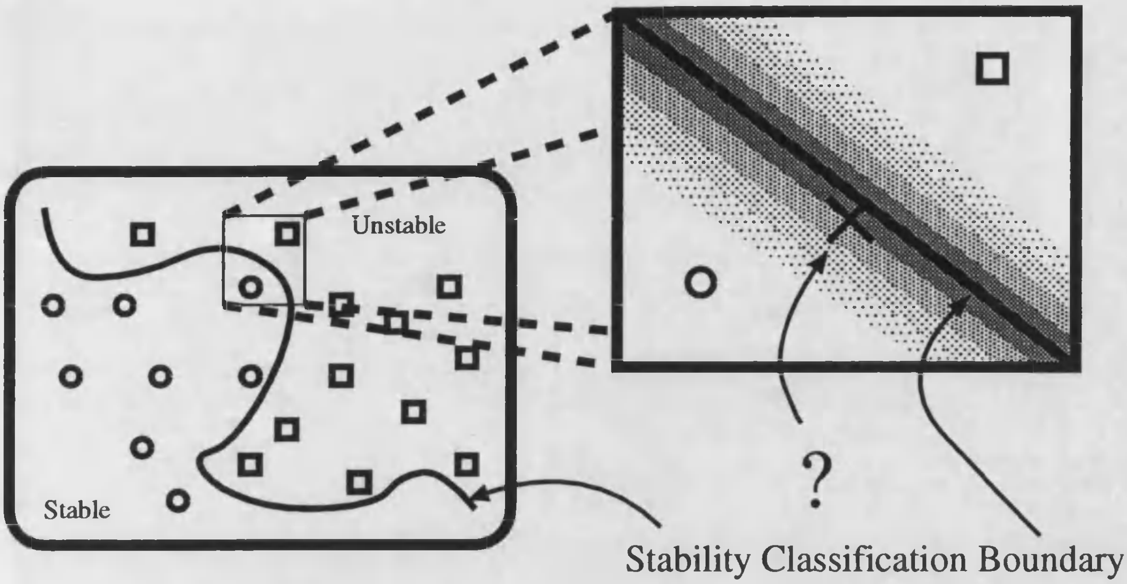


Figure 6.2: Conceptual Stability Boundary

Figure 6.3 shows an imaginary cross section through a stability boundary with the associated stability index profile. A contingency which should produce an output at position **X** would normally be classified as unstable. However, if the neural network output occurs at position **X'** then the contingency would be classified as stable, resulting in a serious mis-classification. This mis-classification is avoided if the threshold (**T**) is set to 0.3 and the neural network is trained to predict the stability index. Although the stability index falls from 0.7 to 0.5, the contingency will still be classified as unstable. This example shows how the number of mis-classifications of unstable contingencies as stable is reduced. The negative side of this approach is that a contingency with a real output of **X'** will be classified as unstable but this is not a serious classification error.

By adopting a continuous valued instability index we can also control the issue of the *conservativeness* of the screen. Varying the level of the threshold for stability comparison has the effect of varying the severity of the contingencies which are passed on for detailed time domain simulation evaluation.

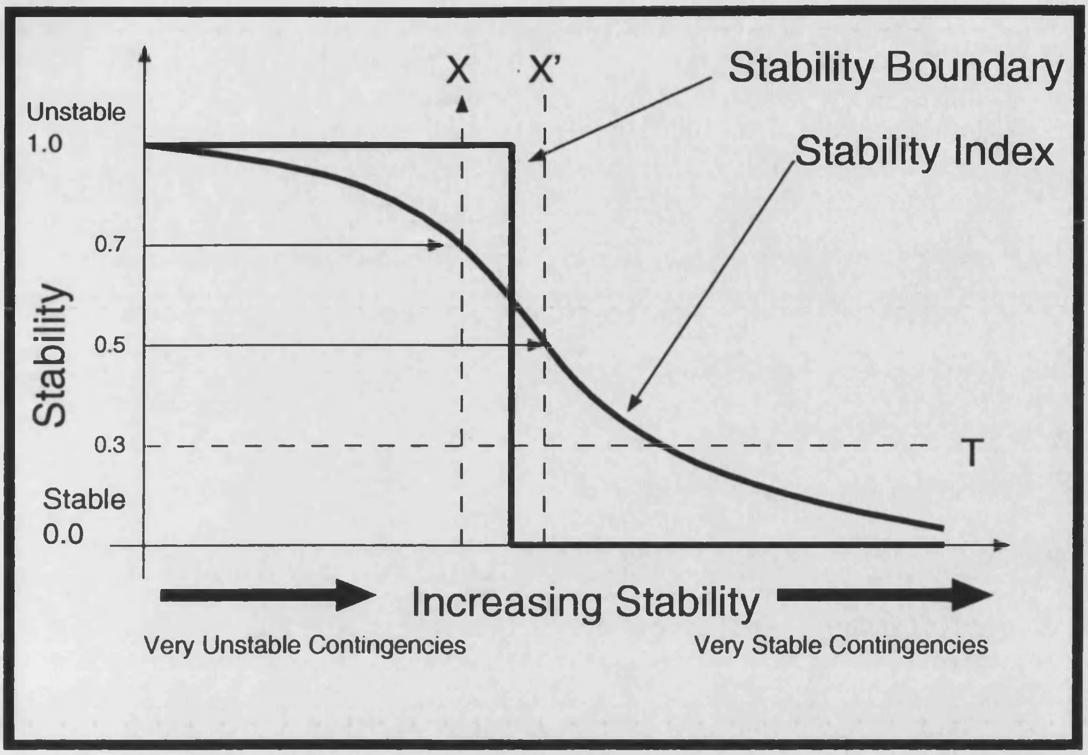


Figure 6.3: Slice Through a Stability Boundary

Various methods have been proposed to improve the performance of ANNs in the vicinity of decision boundaries by a technique known as inversion [166]. This technique uses a query-based training mechanism[24] where new patterns close to the decision boundary are determined. These patterns can then be evaluated, by the offline pattern generation process, to determine the class of the pattern. This technique cannot be used in this case as there is no mechanism to obtain the operating condition of the power system from the selected features, due to the high dimensionality reduction performed by the composite indices.

## 6.3 Instability Indices

The purpose of a stability index is to indicate how far the system operating point is from the stability boundary, not just the binary stability classification. For the purposes of this work both transient and oscillatory instability indices were required preferably using information derived from a time domain simulation. The advantage of this is that as the time domain simulator is improved to include higher order AVR's, governors, quadrature boosters, SVC's, protection modelling etc then no further changes are needed to get the instability index. Also this method does not rely on *simplified* models as do most of the energy function methods.

### 6.3.1 Transient Instability Indices

By its very nature, transient stability is a localised effect based on local energy imbalances between generating sets and the transmission system. A variety of transient instability indicators were investigated, as detailed below.

#### 6.3.1.1 Stability Indicator

This is a simple binary index which is set to zero if the system is transiently stable or to one if the system is transiently unstable. Although this index is simple it suffers because there is no indication of how close the system is to losing synchronism for a particular contingency, and because in practice power system operators would be interested in those contingencies with long decay constants as well as those leading directly to transient instability.

#### 6.3.1.2 Proximity to Pole Slip

Considering a 2 pole machine model, the distance of the rotor angle from 180 degrees can be used as a measure of the proximity of the machine from pole–slipping, and hence as a measure of the transient behavoir of the power system.

#### 6.3.1.3 Transient Energy Margin

This is a useful indicator as the transient performance of a system, but suffers as it relies on using simplified power system models. As one of the key aims in selecting a transient stability index was that it should be able to use the full modelling detail provided by the time domain simulation, this index was rejected.

#### 6.3.1.4 First Swing Magnitude

The maximum magnitude of the first rotor swing of all the machines connected to the transmission system provides a measure of the transient susceptance of the power system to the contingency. NGC consider any swing in excess of 100 degrees to be unacceptable as regards the operation of the UK power system.

#### 6.3.1.5 Maximum Rotor Swing

The maximum rotor angle swing occurring on a machine in the power system is a useful indicator of the transient period following a contingency. For a mild contingency the rotor angles swings on the machines would be expected to be slight but for a more severe contingency large rotor angle swings may be experienced by some of the machines. In the case of a machine which loses synchronism, the rotor angle swing, on a two pole model, would be a full 360 degrees.

This index has been adopted by NGC[76] as a guide to the transient performance of the system. It is suggested that swings of over 100 degrees are unacceptable. Because this index also provides a continuous valued stability index which is related directly to desired operational performance, it was chosen as the transient stability index.

### 6.3.2 Oscillatory Instability Indices

Oscillatory instability problems affect large area's of the system and are frequently due to too much real power being transmitted through weak lines connecting two area's of the power system. The transition to a dynamically poor operating state will be characterised by slow and/or oscillatory effects and in the extreme case pole-slipping of a number of machines or the outaging of overloaded lines by protection schemes. Two oscillatory instability indices were considered, as shown below.

#### 6.3.2.1 Most Positive Eigenvalue

The evaluation of the small signal, oscillatory, instability of power systems can be achieved by the calculation of the eigenvalues of a very large unsymetrical and non-sparse matrix derived from a linearisation of the current operating point of the power system[79, 135]. For a practical sized power system, say of over 100 busbars, this results in a heavyweight computational process which is not suited to online operation within an EMS. However, for offline studies this method is the main approach and results in the determination of the system eigenvalues in the complex plane.

Traditional control theory tells us that if any of the eigenvalues have a positive real part then the system can, under some operating condition, lead to instability. The most positive real part of all the eigen vectors can therefore be used as an indicator of the proximity to oscillatory instability.

Some work has been done on using ANN's to predict the most positive eigenvalue for power systems[149] but this has been limited to small power systems, typically less than 20 busbars, using actual power system measurements as inputs. Such an approach is not easily scaled to a power system of approximately 100 busbars, such as the UK National Grid System, as a very large number of inputs would be needed, which would make an ANN difficult to train.

#### 6.3.2.2 Transient Decay Rate

As a quantitative measure of the decay of transients in a power system we may consider the exponential decay rate of an envelope of power system parameters of the form given in equation 6.1.

$$p(t) = Ae^{bt} = e^{(a+bt)} \tag{6.1}$$

In practice, the envelope of power system parameters such as rotor angle swings will not be a true exponential, however their decay can be approximated by an exponential envelope of this form.

The transient decay rate corresponds to the value of $b$ which is a *best fit* on the discrete data obtained by simulation. Consider a situation in which $N_{tot}$ points of simulated data for a machine rotor angle are known.

The decay rate, $b$, can be found by considering a time series of amplitudes of the $N$ power system parameter $p$ associated with a machine. $p$ may be the rotor angle, MW generation or any other parameter related to the transient behavoir of the machine. Taking a logarithm of equation 6.1 gives:

$$ln\left(p\right) = bt + a \tag{6.2}$$

This equation yields a linear graph of the logarithm of the power system parameter, $p$, versus the simulation time. Hence, given discrete values of $p$ during a time domain simulation, we can use the method of least squares to fit a *best line* through these points, which will correspond to our desired decay envelope. The gradient of this line is equal to the decay rate $b$.

Let the function $\chi$ be the sum of the squares of the errors between the *best fit line* and the data obtained by simulation, hence:

$$\chi^2\left(a, b\right) = \sum_{i=1}^{N}\left(y_i - a - bx_i\right)^2 \tag{6.3}$$

The optimal solution of $a$ and $b$ to minimise this error is found when the constraint equations given below are met.

$$\begin{aligned}
\frac{\partial\chi}{\partial a} &\equiv -2\textstyle\sum_{i=1}^{N}\left(y_i - a - bx_i\right) &= 0 \qquad (6.4)\\
\frac{\partial\chi}{\partial b} &\equiv -2\textstyle\sum_{i=1}^{N} x_i\left(y_i - a - bx_i\right) &= 0 \qquad (6.5)\\
\frac{\partial^2\chi}{\partial a^2} &\equiv 2\textstyle\sum_{i=1}^{N} 1 &> 0 \qquad (6.6)\\
\frac{\partial^2\chi}{\partial b^2} &\equiv 2\textstyle\sum_{i=1}^{N} x_i^2 &> 0 \qquad (6.7)
\end{aligned}$$

(6.8)

Of the equations above, 6.6 and 6.7 are clearly met, a fact which implies that the only sensible solution leads to a minimum error. Rewriting equations 6.4 and 6.5 gives:

$$\sum_{i=1}^{N} y_i = aN + b\sum_{i=1}^{N} x_i \tag{6.9}$$

$$\sum_{i=1}^{N} x_i y_i = a\sum_{i=1}^{N} x_i + b\sum_{i=1}^{N} x_i^2 \tag{6.10}$$

$$\tag{6.11}$$

The solution of these two simultaneous equations yields the parameters $a$ and $b$ which define the decay envelope of the transient. The particular advantage of this index is that it describes how quickly the transients decay away following a contingency.

This index has been applied to the 100 busbar, 20 machine reduced model of the UK National Grid. The results have been very encouraging, showing that the transient decay of the machine rotor angle transients tends to fit an exponential response well from 10s after the end of a contingency. Figure 6.4 shows the *best fit* exponential envelope plotted against 30 seconds of discrete rotor swing amplitudes.

If a decay time constant was of the order of 12 seconds then this implies that the transient should have reduced by 99% after one minute. The direct relationship of this decay rate to a power system operational perspective is very useful as a *meaningful* threshold can be put on decay rates and hence contingencies which may lead to unacceptable decay rates can be identified[76]. OASIS uses this stability index to highlight those contingencies with an unacceptable dynamic performance.

#### 6.3.2.3 Selected Oscillatory Instability Index

The selected oscillatory instability index was the *transient decay rate* as (1) it provides both a continuous valued stability index and (2) it is directly related to the desired

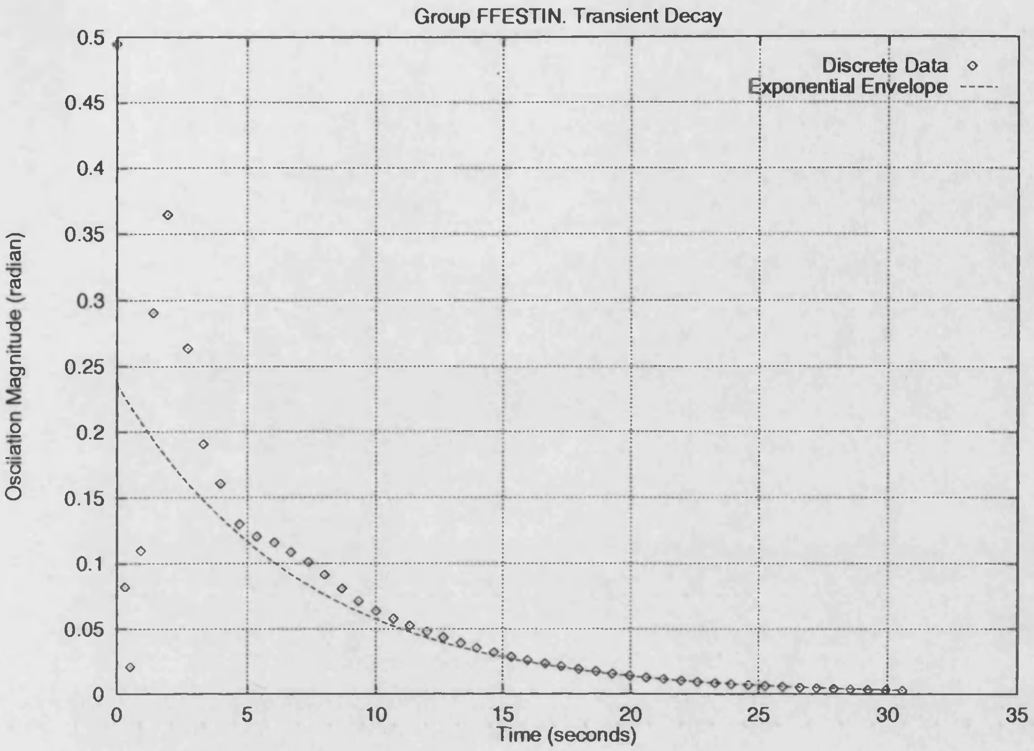


Figure 6.4: Transient Decay Envelope

operational performance of the power system.

## 6.4 Composite Indices

In everyday life we are confronted with statistical indicators of the health of the economy and combinations of these indicators can be successfully used to provide a clear indication of the overall economic health of the country. In this manner a system with many millions of states is successfully classified by a few tens of numbers. This form of feature compression, based on using statistical indicators is the motivation behind using composite indices as features for stability assessment and is justified by the results that have been obtained.

### 6.4.1 Why use Composite Indices?

Much of the previous work on the application of ANNs to power system security assessment (described in 4.2.5.1) has concentrated on small power systems. Due to their small size, individual elements of the power system state vector have a good correlation to the system security, or stability. However, as the size of the power systems increase the correlation of an individual element of the state vector to the power system stability falls to such an extent that they are un-usable as features for security assessment.

Composite indices provide a method for describing in numerical terms certain properties of the power system that are highly correlated to the power system security. The following section outlines how they are constructed and methods that are used to select the most suitable indices for stability assessment.

### 6.4.2 Set Notation

Information regarding the post-contingency stability of a power system can be captured by use of a number of composite indices generated in the following manner.

$$i = A \wedge B \wedge C \wedge D \wedge E \tag{6.12}$$

Equation 6.12 describes how a composite index, $i$, is formed where $A$, $B$, $C$, $D$ and $E$ are elements of sets where:-

$$A : A \in U_a \tag{6.13}$$

$$B : B \in U_b \tag{6.14}$$

$$C : C \in U_c \tag{6.15}$$

$$D : D \in U_d \tag{6.16}$$

$$E : E \in U_e \tag{6.17}$$

**Set** $U_a$ is a set of statistical functions to be used to create the composite index. The members **MIN** and **MAX** are the minimum and maximum functions respectively and **SUM** is the sum of the values across all items of plant. **RMS** allows the use of the root mean square function, **RNG** determines the range of the variable and **VAR** calculates the variance. **MEAN** is the mean of all the variables, **SKEW** is the skew and **ADEV** is the absolute deviation. The remaining two use the modulus function: **MMAX** is the maximum modulus of the variable and **MSUM** is the sum of the modulus of all the variables. These are explained in detail in section 6.4.4.

**Set** $U_b$ defines which parameters are to be used in the construction of the composite index. Element **N** indicates that the index is to be built using the appropriate measurement at the CTP. **G** indicates that the gradient of the measurement at the CTP is to be used. **C** signifies that the change between the pre-contingency value and the measurement at the CTP is to be used. The set member **S** defines the post contingency steady state value of the composite index, determined by a loadflow, to be used.

**Set** $U_c$ defines the items of plant which are related to the composite index. These may be **B**usbars, **L**ines or **M**achines. For the purposes of the modelling all transformers, SVCs and quadrature boosters are modelled as lines.

**Set** $U_d$ defines the measurements (base indices) to be constructed from the CTP state vector to form the basis of the composite index. **VM** and **VP** are the voltage magnitude and phase respectively, **MW** and **MV** are the MW and MVAr measurements and **MVA** is the MVA measurement. **OL** is the overload which is the current MVA value divided by the approximate rating. **KE** is the kinetic energy of a machine, **RA**, **RS** and **RC** are the rotor angle, speed and acceleration of machines and **RAM** is the rotor angular momentum. **RAP** calculates the rotor accelerating power, **AVE** is the machine's AVR voltage error and **TI** is the estimated time to instability assuming constant rotor acceleration. The derivation of these base indices is described in detail in section 6.4.3.

**Set** $U_e$ contains two members. The first member **V** limits the scope of generation of composite indices to the immediate vicinity of a contingency. Since transient instability problems are local phenomena, the effects on parts of the power system remote from the contingency area are negligible. Our work has shown that defining the *vicinity* as a topological distance of four busbars from an item of plant involved in the contingency produces good results. The other member of the set **S** forces the indices to be built from all items of plant in the power system, i.e. the index is system wide.

This is best clarified by considering the example index shown below

$$i = \{\text{SUM}\ ,\ \text{C}\ ,\ \text{M}\ ,\ \text{KE},\ \text{S}\} \tag{6.18}$$

which corresponds to the *sum of the changes in machine kinetic energy changes across the whole system.* In practice, each composite index was divided by the number of items of plant involved in its construction, i.e. the above was divided by the number of machines, in order to reduce the sensitivity of the composite indices to changes in the number of equipment. In this manner, the composite indices are made even more robust to changes in the power system topology and loading.

### 6.4.3 Base Indices

Previous research [137, 138] has shown that parameters such as generator real power output, generator bus voltage, generator rotor angle, real and reactive power flows and the speed and kinetic energy of generators are likely to be suitable inputs for a transient stability classifier for multi-machine power system studies. In addition features used for the TEF method for power system stability studies have been used as well as those thought to be potentially useful by the author. These type of features are referred to as *base indices.*

The following sections define the base indices and are related to a system with $N_b$ busbars, $N_l$ lines and $N_g$ generators. For convenience, they are split into three categories: network, machine and local.

#### 6.4.3.1 Network Indices

**Busbar Voltage Magnitude** Low voltages on or near generator terminals tends to make the generators more susceptible to transient instability. The reason for this is that the available electrical output power from a generator is proportional to the terminal voltage; a low terminal voltage will reduce the electrical power output causing the rotor to increase speed above nominal. Work presented by EPRI[56] indicated that this is a very useful index for transient stability classification.

**Busbar Voltage Phase** Power systems with a large variation in busbar voltage phase angles are likely to be more susceptible to oscillatory instability problems due to large MW transfers between area's of the power system. This index is therefore quite useful for oscillatory instability classification.

**Transmission Line MW flow** As mentioned in (3.2.3) one characteristic of a oscillatory unstable system is large MW transfers across critical boundaries. This index is the direct indicator of these problems and is likely to be useful for oscillatory instability classification.

**Transmission Line MVar flow** Overloaded lines tend to have large MVar generation which can be used as an indicator of potential dynamic stability problems. Also localised MVar flows provide a good indication of the voltage situation and may be used for transient instability classification.

**Transmission Line Phase Difference** As the voltage phase difference over a transmission line increases the MW flow through the line will increase. When the line becomes overloaded the system will tend to be more susceptible to oscillatory instability problems. In the UK, overloading on the transmission lines from Scotland to England can lead to such problems.

**Transmission Line Potential Energy** If the potential energy of the transmission lines is low enough to absorb the excess kinetic energy of the machines during the transient phase of the contingency, then the system is liable to be transiently stable. If this is not the case then the transmission system will be unable to absorb the injected kinetic energy and some generating units may pole-slip as a result.

**Excess Generation** This index provides information on the level of excess generation in the system. If this is high then the machine frequencies will be high and the system will be closer to transient instability.

**Topology Change** The outaging of a line due to a contingency will cause a significant amount of power re-routing in the locality of the outaged line. The resulting increase in loading of neighbouring lines may make the system more susceptible to transient instability problems.

#### 6.4.3.2 Machine Indices

**Terminal Voltage Magnitude** Machines which experiencr transient instability problems are usually associated with a low terminal voltage magnitude which reduces the possible electrical power output. Hence, this base index is very useful for transient instability classification.

**Terminal Voltage Phase** If a machine is forced to change its MW output considerably then there is likely to be a significant change in its terminal voltage phase angle. This change may be used to indicate transient instability problems.

**AVR Voltage Error** The AVR voltage error, the terminal voltage minus the desired terminal voltage, can be used to provide information on how much effort the machine AVRs are making to keep the terminal voltage at the set point. As the transient problems increase, the error will increase until the AVR fails to maintain the terminal voltage. Once this condition is reached, it is likely that the machine will pole-slip.

**MW Output** The change in MW output of a machine during a contingency is a good indicator of the severity of the contingency. Large localised MW variations indicate that the electrical power output of the machine has change significantly, moving the system towards transient instability.

**MVar Output** The change in MVar output of a machine during a contingency provides indication on the voltage support at the generator terminals. Therefore this provides a useful indicator of transient stability problems.

**Rotor Angle** The change in machine rotor angles during the contingency, and their proximity to 180 degrees is by its very nature a good indicator of stability, which is due to large rotor angle swing on affected machines.

$$s = s_0 + ut + \frac{1}{2}at^2 \tag{6.19}$$

$$\delta_p = \delta_{clearing} + \omega * 1 + \frac{1}{2}\dot{\omega} * 1^2 \tag{6.20}$$

In addition, three composite indices were selected based on the projected rotor angle, $\delta_p$ defined above. Equation 6.19 is one of the standard Newtonian equations of motion, from which its rotational equivalent (6.20) is derived. An estimate of a machines rotor angle one second after the end of a contingency could be made by considering the rotor acceleration to remain constant during this period. The functions MAXi and MINi are the used to provide estimates of the maximum and minimum projected rotor angle one second after the end of the contingency.

$$t_i = \frac{-\omega \pm \sqrt{\omega^2 + 2 * \dot{\omega} * \delta_i}}{\dot{\omega}} \tag{6.21}$$

The projected time to instability, $t_i$, is based on equation 6.20, but in this case the distance of the rotor angle from $\pi$ is known and hence the estimated time for the machine to pole slip assuming constant acceleration is calculated. The minimum of the projected times for all machines in the system is likely to be a good indicator of potential transient stability problems. Although in practice the rotor acceleration will not remain constant this index could provide a useful indicator of the proximity of a machine from a pole slipping situation.

**Rotor Kinetic Energy** As a machine approaches a pole-slip it will have a noticeable difference from its steady state kinetic energy. Machines with high kinetic energies are likely to be unstable as the transmission network is less likely to be able to absorb the excess kinetic energy before a pole-slip situation is reached.

**Rotor Potential Energy** For completeness, an estimate of the rotor potential energy is used to provide an idea of how much margin there is for kinetic energy increase.

**Rotor Angular Momentum** The angular momentum of a rotating body is a key indicator of how much energy is required to stop the rotation. In this case the excess angular momentum at the end of the contingency must be removed by the interaction with the network or the machine will pole-slip.

**Asynchronous Kinetic Energy[140]** Asynchronous Kinetic energy, $\phi_{ake}$, is an index which shows the degree of dispersion of the kinetic energy among generators and is hence expected to be a useful index for transient stability assessment.

$$I_0 = \sum_{i=1}^{N_g} I_i \tag{6.22}$$

$$\delta_0 = \frac{\left(\sum_{i=1}^{N_g} \delta_i I_i\right)}{I_0} \tag{6.23}$$

$$\phi_{ake} = \frac{1}{2}\sum_{i=1}^{N_g} I_i \dot{\delta}_i^2 - \frac{1}{2} I_0 \dot{\delta}_0^2 \tag{6.24}$$

The first equation calculates the *centre of inertia of the system* and the second and third combine to calculate the asynchronous kinetic energy.

**Machine lines outaged** This index is one if any lines have been outaged from the generator terminals by the contingency, otherwize zero. In general, the loss of a line from a generator will overload the remaining lines (if any) and send the generator towards instability.

**System Frequency** The deviation of the system frequency from the nominal 50Hz is a good measure of the degree of disturbance present in the system.

**Negative Pole Slip Likely** This index is one if the post contingency rotor angle is less than 1.5 radian (on two pole model) and both the rotor angular velocity and acceleration are negative, otherwize zero.

**Positive Pole Slip Likely** This index is one if the post contingency rotor angle is greater than 1.5 radian (on two pole model) and both the rotor angular velocity and acceleration are positive, otherwise zero.

**Capacity Reduction** This index provides a measure of the percentage of transmission capacity that is lost from a generation group due to the outaging of lines connected directly to the generating groups terminals.

$$CR = \frac{\sum_{i=1}^{n} P_i}{P_{G0}} \tag{6.25}$$

Equation 6.25 is used to calculate the capacity reduction for a generation group with a pre–contingency generation of $P_{G0}$ MW which has $n$ lines connected to its terminals. The term $P_i$ corresponds to the outaged MW pre–contingency capacity of one of the $n$ lines. Hence, if the line is not outaged then $P_i$ is zero else it is equal to the pre–contingency MW flow of the line.

### 6.4.3.3 Local Indices

**Critical MW Interface Flows** Past experience of power system operators has revealed critical interface flows, which if exceeded will move the system towards instability. The choice of these flows as inputs to a neural network classifier seems sensible.

**Critical MVar Interface Flows** This is similar to above and used for completeness.

**Local Area MW Generation** The total MW generation within a particular part of the overall system can have a big effect on stability.

**Local Area MVar Generation** The total MVar generation within a particular area has a big effect on the voltage profile within that area. If the voltage profile is low then the area will be more susceptible to transient instability problems.

**Generator Kinetic Energy** The kinetic energy of a small generator will not have much effect on a system wide total kinetic energy index. Choosing this index will allow the neural network more information on a susceptible generator.

**Generator Angular Acceleration** This is used for similar cases to the index above, and provides information on a small machine whose input to the global index would otherwise be negligible.

### 6.4.4 Statistical Functions

The purpose of the statistical functions is to provide a mapping from a number of base indices to a single numerical composite index that may be useful for the stability classification problem. In this manner a dimensionality reduction is achieved without the loss of discriminatory power.

Consider an example where we can determine the voltage magnitudes at all $N_b$ busbars in the power system. A *standard deviation* function will perform a mapping from $\Re^{N_b}$ to $\Re$: i.e. $N_b$ busbar voltage magnitudes are mapped onto a single value.

The indices are formed by using a number of functions on the power system parameters, $\mu$ at the immediate post-contingency state. The functions used to produce the composite indices $\phi$ are detailed below, where $\mu_0$ represents the pre-contingency value of $\mu$ :

**Maximum Value** — this is the maximum value of $\mu$ across all the equipments in the network.

$$\phi = \mathsf{MAXi}\,(\mu) = \mathtt{max}\ \mu_i \Big|_{\ i = 1 \cdots N_g} \tag{6.26}$$

**Minimum Value** — this is the minimum value of $\mu$ across all the equipments in the network.

$$\phi = \mathsf{MINi}\,(\mu) = \mathtt{min}\ \mu_i \Big|_{\ i = 1 \cdots N_g} \tag{6.27}$$

**Maximum Change** — this is the maximum value of the change in $\mu$ between the pre and immediate post-contingency state across all the equipments in the network.

$$\phi = \mathsf{MAXDi}\,(\mu) = \mathtt{max}\ \left(\mu_i - \mu_i^0\right) \Big|_{\ i = 1 \cdots N_g} \tag{6.28}$$

**Minimum Change** — this is the minimum value of the change in $\mu$ between the pre and immediate post-contingency state across all the equipments in the network.

$$\phi = \mathsf{MINDi}\,(\mu) = \mathtt{min}\ \left(\mu_i - \mu_i^0\right) \Big|_{\ i = 1 \cdots N_g} \tag{6.29}$$

**Maximum Modulus of Change** — this is the maximum value of the modulus of the change in $\mu$ between the pre and immediate post-contingency state across all the equipments in the network.

$$\phi = \mathsf{MAXMDi}\,(\mu) = \mathtt{max}\ \left(\mid \mu_i - \mu_i^0 \mid\right) \Big|_{\ i = 1 \cdots N_g} \tag{6.30}$$

**Sum of Modulus of Change** — this is the sum of the modulus of all the changes of $\mu$.

$$\phi = \mathsf{SUMDi}\,(\mu) = \sum_{i=1}^{N_g} \left(\mu_i - \mu_i^0\right) \tag{6.31}$$

**Maximum Gradient** — this is the maximum gradient of $\mu$ at the immediate post-contingency state across all the equipments.

$$\phi = \mathsf{MAXGi}\,(\mu) = \mathtt{max}\ \dot{\mu}_i \Big|_{\ i = 1 \cdots N_g} \tag{6.32}$$

**Minimum Gradient** — this is the minimum gradient of $\mu$ at the immediate post-contingency state across all the equipments.

$$\phi = \mathsf{MINGi}\,(\mu) = \mathtt{min}\ \dot{\mu}_i \Big|_{\ i = 1 \cdots N_g} \tag{6.33}$$

**Maximum Modulus of Gradient** — this is the maximum value of the modulus of the gradient of $\mu$ between the pre and immediate post-contingency state across all the equipments in the network.

$$\phi = \mathsf{MAXMGi}\,(\mu) = \mathtt{max}\ \mid \dot{\mu}_i \mid \Big|_{\ i = 1 \cdots N_g} \tag{6.34}$$

**Sum of Modulus of Gradient** — this is the sum of the modulus of the gradient of $\mu$ at the immediate post-contingency state.

$$\phi = \mathsf{SUMGi}\,(\mu) = \sum_{i=1}^{N_g} \dot{\mu}_i \tag{6.35}$$

**Mean** — this is the mean values of $\mu$ at the immediate post-contingency state across all the equipment and is denoted by $\bar{\mu}$.

$$\phi = \mathsf{MEAN}\,(\mu) = \frac{1}{N_g} \sum_{i=1}^{N_g} \mu_i \tag{6.36}$$

**Variance** — this is the *variance* of $\mu$ over all the items of equipment and provides a measure of of the *width* or *variability* of $\mu$ about this value and is represented as $\sigma^2$ where $\sigma$ is the *standard deviation.*

$$\phi = \mathsf{VAR}\,(\mu) = \frac{1}{N_g - 1} \sum_{i=1}^{N_g} (\mu_i - \bar{\mu})^2 \tag{6.37}$$

As the mean depends on the first moment of the data, the variance depends on the second moment. It is not uncommon in real life to be dealing with a distribution whose second moment does not exist (i.e. is infinite). In this case, the variance is useless as a measure of the data's width around its central value: the values obtained by 6.37 will not converge with increased numbers of points, nor show any consistency from data set to data set drawn from the same distribution. A more robust estimator of the *width* is the *mean absolute deviation.*

**Mean Absolute Deviation** — This is a more robust estimator of the *width* of a distribution.

$$\phi = \mathsf{ADEV}(\mu) = \frac{1}{N_g}\sum_{i=1}^{N_g}|\mu_i - \bar{\mu}| \tag{6.38}$$

**Skewness** — This characterises the degree of asymmetry of a distribution around its mean. While the mean, variance and absolute deviation are *dimensional* quantities, that is, have the same units as the measured quantities, $\mu$, the skewness is defined in such a way as to make it *non-dimensional.* It is a pure number that characterises only the shape of the distribution.

$$\phi = \mathsf{SKEW}(\mu) = \frac{1}{N_g}\sum_{i=1}^{N_g}\left[\frac{\mu_i - \bar{\mu}}{\sigma}\right] \tag{6.39}$$

## 6.5 Selection Of Composite Indices

From the set of composite indices considered a number of standard filters were used to select the *best* composite indices to use as inputs to a direct neural network classifier. The aim of this selection procedure is to provide a structured method for ranking the composite indices on their effectiveness for stability assessment. In this way a selection of the *best* composite indices can be used to as inputs to the neural network classifier.

The filters that were used performed a ranking of the indices using the inter-class Euclidean distance as the metric. Both a *best features* and a *sequential forward search* technique were used, and the best 5 indices considered for selection. These filters were implemented in a software package called TOOLDIAG[167], which is freely available.

A utility program was also written to perform this automatic selection by calculating a number of ranking coefficients, $C_1 \cdots C_{10}$, for each composite index. The best composite index for each of these ranking criteria was then chosen, resulting in a small number of automatically selected composite indices.

Let $\phi_i$ be the value of the composite index $c$ for the $i^{th}$ contingency. If the stability index for contingency $i$ is given by $s_i$ and the stability classification is $S_i$ then:-

$$C_1 = \sum_{i=1}^{N_{ctg}} (\phi_i - s_i)^k \quad (6.40)$$

$$C_2 = \sum_{i=1}^{N_{ctg}} (\phi_i - S_i)^k \quad (6.41)$$

$$C_3 = \sum_{i=1}^{N_{ctg}} (\phi_i - s_i)^{k+1} \quad (6.42)$$

$$C_4 = \sum_{i=1}^{N_{ctg}} (\phi_i - S_i)^{k+1} \quad (6.43)$$

$$C_5 = \sum_{i=1}^{N_{ctg}} (\phi_i - s_i)^{k+2} \quad (6.44)$$

$$C_6 = \sum_{i=1}^{N_{ctg}} (\phi_i - S_i)^{k+2} \quad (6.45)$$

$$C_7 = \mathsf{MAX}_{i=1}^{N_{ctg}} (\phi_i - s_i)^2 \quad (6.46)$$

$$C_8 = \mathsf{MAX}_{i=1}^{N_{ctg}} (\phi_i - S_i)^2 \quad (6.47)$$

(6.48)

where $k$ is the *error power*. The higher the value of $k$ the more a single large error is penalised compared to a number of smaller errors. The values of $k$ that were used were one, five and ten in order to achieve a balance between composite indices showing a general trend and ones with a good correlation to the stability indices but with the occasional large error. Values of $k$ greater than ten were found to produce negligible changes in the selected composite indices.

Similarly, ranking coefficients $C_9 \cdots C_{16}$ were generated by replacing $S_i$ by $1-S_i$ and $s_i$ by $1-s_i$. This allows those indices with a good correlation to the inverse of the stability index to be selected.

## 6.6 Visualisation of Feature Space

Once a set of composite indices have been selected as features for the stability assessment, it is desirable if their suitability at performing the desired classification can be displayed. This has the effect of confirming the suitability of the selected indices and of highlighting any errors in the selection process. With the time required to validate the screens being several hours, this quick check can save a lot of time.

### 6.6.1 Single feature suitability

The correlation of a single composite index (feature) to the instability index can be shown by a plot of the value of the composite index against the instability index for all patterns in the training data set.

Figure 6.5 shows a graph of the value of one automatically selected composite index versus the stability index for all the contingencies in the training set. There is a clear correlation between this index and the stability, confirming the usefulness of the automatic selection program. Another technique that performs a similar function is that of boxplots.

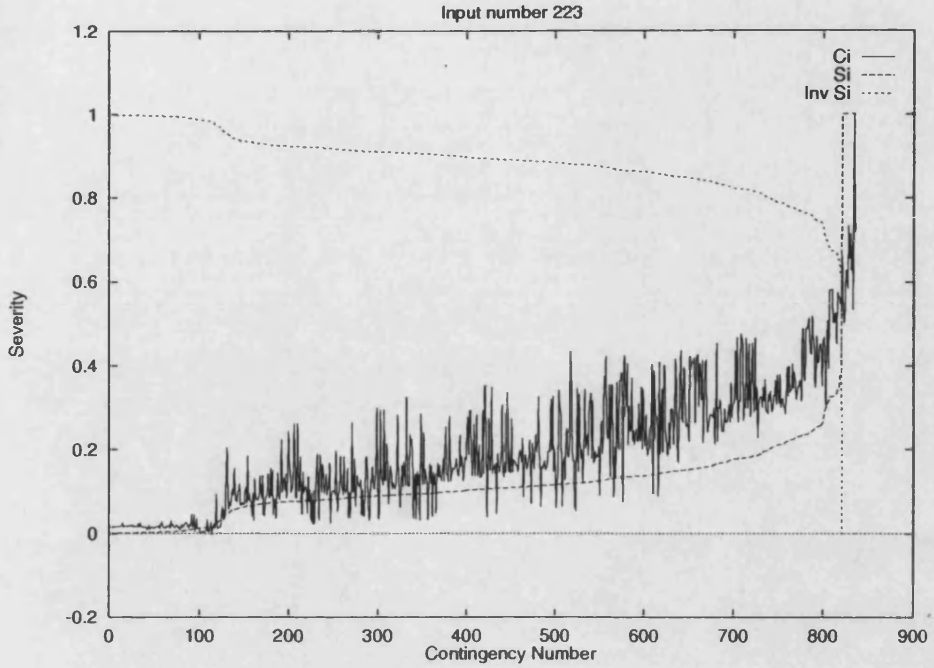


Figure 6.5: A good composite index for stability classification

### 6.6.2 Box Plots

Box plots[168] provide a powerful graphical tool for visualising the range and distribution of a composite index for the stable and unstable classes. Figure 6.6 shows a box plot for two typical composite indices. The plots show the bounds, interquartile ranges and medians of the composite index, on the same scale for the stable and unstable contingencies. The *good* index shows a clear difference in the composite index between the stable and unstable cases, but the *poor* index lacks this discrimination and is therefore likely to be of little use for transient stability classification.

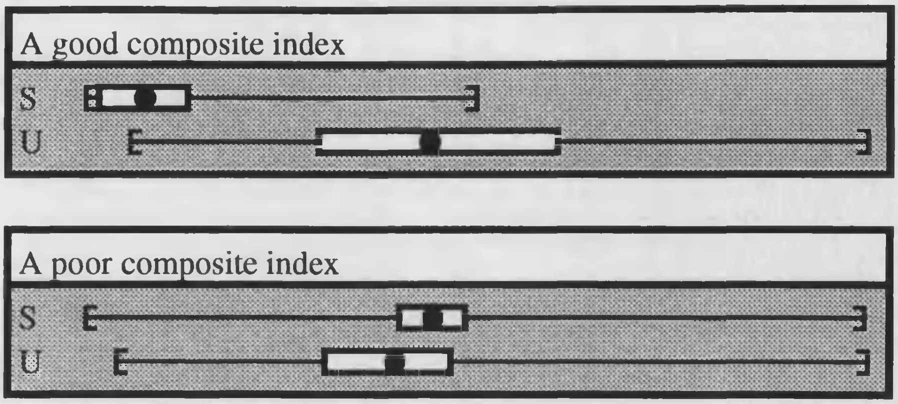


Figure 6.6: Box Plots for two composite indices

### 6.6.3 Selected features' suitability

In order to visualise the suitability of the selected features for describing the power system stability, some method must be used to transform the high dimensional feature space onto a two dimensional piece of paper. The techniques have been adopted that are based on Sammon plots.

### 6.6.4 Sammon Plots

The Sammon algorithm [169] allows the visualisation of a multi-dimensional set of inputs to a neural network on a two dimensional piece of paper allowing the relative geometric separation between patterns from different classes to be compared. This algorithm performs a dimensionality reduction from a high order space, equal to the number of selected composite indices, to a lower dimensional space, in this case two dimensions. The criteria for the dimensionality reduction is to reduce, by a gradient descent approach, the differences in the Euclidean distances between patterns in the the high and low spaces as much as possible. In this way the *geometric* separation of the patterns is maintained.

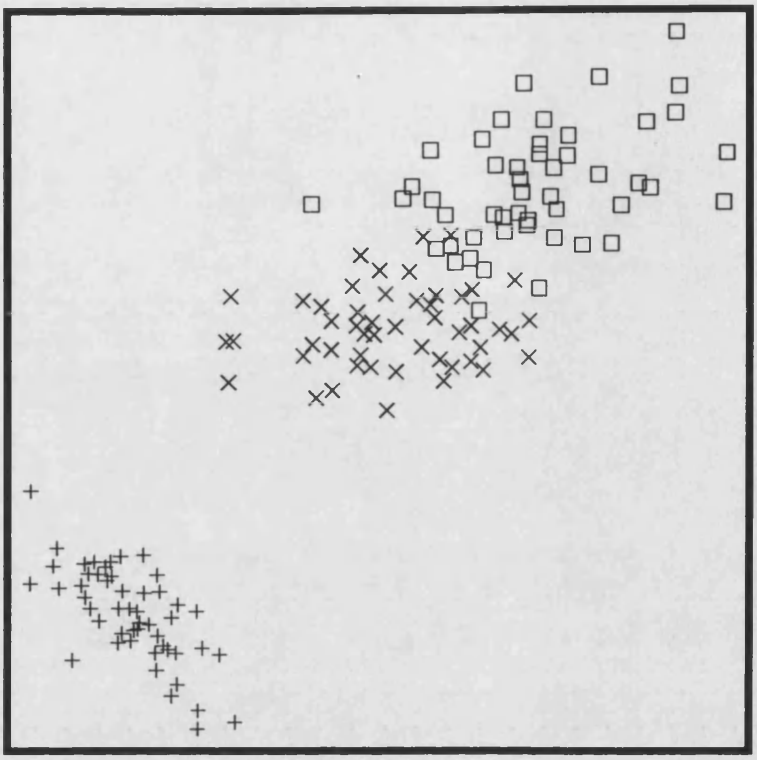

Figure 6.7: Sammon Plot for Iris Data Set

Figure 6.7 shows a Sammon Plot for the classical data set of Fisher[170]; a set of 150 samples of feature dimension four describes three different flower classes, 50 samples per class. It can be seen that the patterns represented by 'plusses' (setosa class), those represented by 'crosses' (versicolor class) and those represented by 'boxes' (virginica class) are clustered into three fairly distinct areas indicating that the patterns contain enough information to perform the classification.

If there is no obvious separation between the classes (in our case stable and unstable) then the composite indices chosen are not likely to be able to classify the stability and they will almost certainly not be robust to changes in the power system operating condition. In this way, the relative clustering of the patterns on a Sammon diagram provides a good indication of the likely success of the ANN screen.

### 6.6.5 Edwards-Sammon Plot

This plot is based on the Sammon plot and has been enhanced by the author to indicate the likely region of classification for patterns that the ANN has not seen before.

For applications where a degree of membership of a class can be determined, it is useful to produce a Sammon plot for the class membership and an associated contour diagram representing the class membership function. For this particular application we can classify a contingency as transiently[1] stable or unstable. However in section 6.3 continuous valued stability indices were investigated, which can be used to provide a degree of membership to the stable or unstable classes.

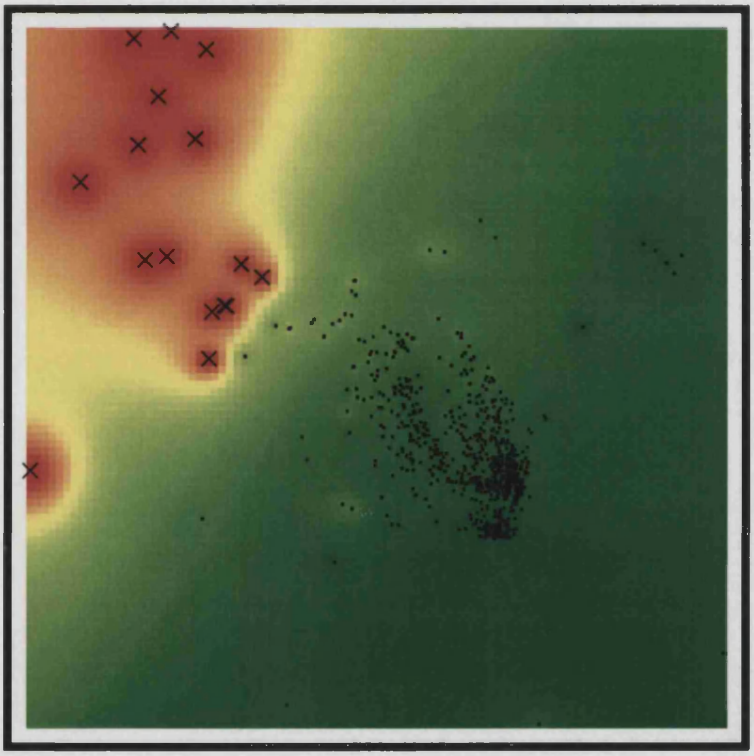

Figure 6.8: Edwards-Sammon Plot for Transient Stability

[1]or oscillatory

Figure 6.8 shows an Edwards-Sammon plot for an ANN transient stability screen developed for the 100 busbar laboratory scale power system model. The surface is visualised by a smooth colour representation of the degree of class membership from in this case green (stable contingency zone) to red (unstable contingency zone). The algorithm for determining the contour plot was determined empirically.

The colour of a point ($x$,$y$) is related to its *class membership*, or *height*, which is determined in the following manner:-

① Calculate the Euclidean distance, $d_i$, from $x$,$y$ (current point) to each of the $i$ patterns in the training set.

② Select the closest $N_p$ patterns to the current point.

③ For each of the $N_p$ points set the $d_j$ to 0.0001 if $d_j$ is less than 0.0001 to prevent numerical problems when ($x$,$y$) is close to the position of an actual pattern on the plot.

④ Use equation 6.49 to calculate the *height* of the current point, $h_{xy}$.

$$h_{xy} = 0.5 + \frac{\sum_{i=1}^{N_p} I_i * W_i * (H_j - 0.5)}{\sum_{i=1}^{N_p} I_i} \tag{6.49}$$

where $I_i$ is an influence factor related to the distance from the current point to the pattern $i$ and is given by

$$I_i = \frac{1}{d_j^2} \tag{6.50}$$

and where $W_i$ is a colour weighting function defined by

$$W_i = 1.0 - \frac{1.0}{1 + e^{5-25d_j}} \tag{6.51}$$

## 6.7 Screening Implementation Methods

In general the contingency screening process will use multiple screens, each tailored to identify a particular security problem. There may also be multiple screens trying to identify the same problem, in which case a voting system can be employed to either take the majority decision or to pass a contingency for evaluation if only one screen identifies it as potentially insecure.

### 6.7.1 Multiple Contingency Screens

Contingency screening for stability violations can be carried out by a single detailed screen which provides all of the discrimination. This approach tends to lead to a relatively computationally intensive screen compared to a coarse filter which may remove only 70% of the stable cases. The adoption of a multi-screen approach as outlined in figure 6.9 uses a number of coarse screens to provide the overall screening. In this manner the least intensive screen can be used to provide some initial screening with more detailed screening being used only on those contingencies which are passed by the coarse screens. The net effect of this approach is to (1) reduce the overall time spent screening the contingencies and (2) to improve the reliability of the contingency screening process.

Within OASIS, the transient and oscillatory screens are used in this multi-screening manner. Those contingencies which are deemed safe by the transient screen are passed to the oscillatory instability screen. Those which pass through this screen are then assumed to produce safe, well damped, electro-mechanical oscillations and are not considered any further.

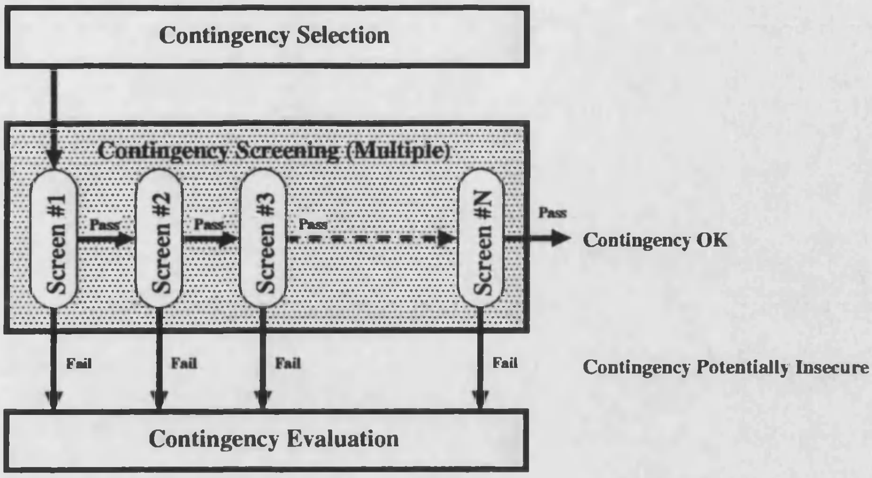


Figure 6.9: Multiple Contingency Screens

### 6.7.2 Voting Methods

Voting methods are often employed in safety critical systems to reduce the probability of mal-operation of the system. The principle behind this approach is to incorporate redundancy within the system by having multiple modules to perform the same task. The results from each module are compared and if one module produces significantly different answers from the rest then its results are ignored and the module flagged up as faulty. One of the most notable examples of this method is employed within the space industry where critical systems within satellites and manned space vehicles must be extremely reliable[171, 172].

For this application, a number of transient screens could be developed and operated in parallel. If any one screen classifies a contingency as unstable then the contingency could be flagged up for detailed evaluation. If the screens used different input features and network topologies then this would further improve the robustness of the screens. The principle drawback to this approach is the computational overhead of running multiple screens.

# 6.8 Performance Evaluation

The performance of a contingency screen can be made on two fronts. Firstly, the performance of the DSA system, incorporating the screens, can be compared to the same system with no screening. Secondly the performance of the screen can be evaluated from the perspective of a pattern classification system and a ROC table can be determined.

## 6.8.1 Performance of Screen

As mentioned previously (5.4.3) a receiver operating table can be constructed to display the performance of an ANN. Such a table can also be used to display the performance of the ANN screen as a whole.

| Actual Stability | Stable | Unstable |
|---|---|---|
| ANN Stable | $\alpha_{ss}$ | $\alpha_{us}$ |
| ANN Unstable | $\alpha_{su}$ | $\alpha_{uu}$ |

Table 6.1: Screen Performance Table

Table 6.1 shows such a performance table. The $\alpha$ values represent the number of contingencies that fall into each of the four categories. For the screen to be a *success* we require that $\alpha_{us}$ is zero, i.e. that no unstable contingencies are mistaken to be stable and that $\alpha_{su}$ is small compared to $\alpha_{ss}$ and $\alpha_{uu}$ so that the screening efficiency is high. We can define this latter quantity by $\eta$, where:

$$\eta = \frac{\texttt{Number of contingencies screened as stable}}{\texttt{Number of stable contingencies}} \tag{6.52}$$

### 6.8.2 Improvement in overall DSA performance

The motivation behind using contingency screening within a DSA system is to reduce the DSA cycle time. Hence, the speedup factor, $\lambda$, of the DSA can be determined by:-

$$\lambda = \frac{\texttt{Operating time of DSA with no screens}}{\texttt{Operating time of DSA with screens}} \tag{6.53}$$

A value of $\lambda$ of over ten or so would represent a considerable improvement in the performance of a DSA system. The cycle time of OASIS, $t_{OASIS}$, with the ANN transient and oscillatory instability screens implemented is given by:-

$$t_{OASIS} = N_s \eta_T t_T + \frac{N_s}{\eta_T} \eta_O t_O + \frac{N_c}{\eta_T \eta_O} t_{SIM} \tag{6.54}$$

where $N_c$ is the total number of selected contingencies. $\eta_T$ and $\eta_O$ are the efficiencies of the transient and oscillatory instability screens respectively. $t_T$ and $t_O$ are the operating times of the transient and oscillatory instability screens and $t_{SIM}$ is the operating time of the contingency evaluator.

## 6.9 Chapter Summary

A method for contingency screening of electro-mechanical instability problems using a numerical integration approach coupled with an ANN has been detailed. A set of composite indices are calculated using the results from a short time domain simulation and presented as inputs to an ANN. The ANN predicts an instability index which is compared with a threshold value to determine whether the contingency is potentially severe.

The performance of the screen should be such that $\alpha_{us}$ is zero and $\eta$ is in excess of 90%. With these conditions met, we can expect an improvement in a DSA cycle time of at least one order of magnitude.

The next chapters give details of the implementation of these screens into OASIS and simulation results on both a laboratory scale and real sized power system model.

Chapter Seven

# Enhancements to OASIS

The enhancements that were made to OASIS involved the modification of parts of the OASIS client and server tasks. This chapter explains the reasons for these changes and gives details of the changes themselves.

## 7.1 Modifications to Client Task

The main modification to the client task was the incorporation of a module to display power system stability in a graphical format. The visualisation of power system security information is an area of active research at the present time. Various techniques to present this information to power system operators in a clear manner have been proposed[102, 173] but the traditional approach of a single line wall diagrams and EMS displays are the norm. The use of single line diagrams is well accepted [174–176] and a full wall diagram of the power system is present within virtually every energy management centre as it provides the power system operators with a clear indication of the activity of circuit breakers, whether busbars are being run split and the current system frequency.

Transient stability problems are by their very nature very localised and as such highly dependent on the local topology of the power system around the generator of interest. Oscillatory instability problems tend to be caused by the outaging of transmission lines between different areas of the power system. This causes the remaining lines to become more highly loaded and can result in poor damping of post-contingency electro-mechanical oscillations. In order to clearly view these problems it was decided to improve OASIS such that the topological and geographical information could be combined with the results of the contingency processing to present a complete picture of the power system stability.

A graphical display method based on the standard topological system map is the natural choice for the display, and is currently used within the NGC to display MW transfer limits and other constraints (Picasso diagrams) [76]. Those items of plant which lead to stability problems (transient or oscillatory) should be clearly shown, and then when used in conjunction with the *Picasso's* will provide a much clearer impression of the system security.

The method that was adopted to indicate those items of plant that are involved in contingencies which lead to instability was to draw them in red. Hence, transmission lines, SVCs and busbars are shown in red if they are involved in contingencies which lead to instability. Transmission lines which when outaged may lead to poor damping on the system are marked as dashed red lines, whereas lines leading to transient instability are marked with solid red lines. Busbars which have machines which are transiently unstable are *ringed* in red to indicate the presence of a generating group which is transiently unstable.

In addition the background of the maps was to be comprised of a patchwork where the colour of each patch is related to the *desired parameter* of the nearest busbar on the map. In this manner an appreciation of the correlation between the pre-contingency parameter, such as busbar voltage magnitude, and the stability is shown.

### 7.1.1 Voltage Profile

In the case of a voltage magnitude profile, sharp patch boundaries correspond to lines with significant voltage difference across then and hence lines with large MVar flows. As the system voltage profile has a large effect on system stability then the inclusion of this information is valuable.

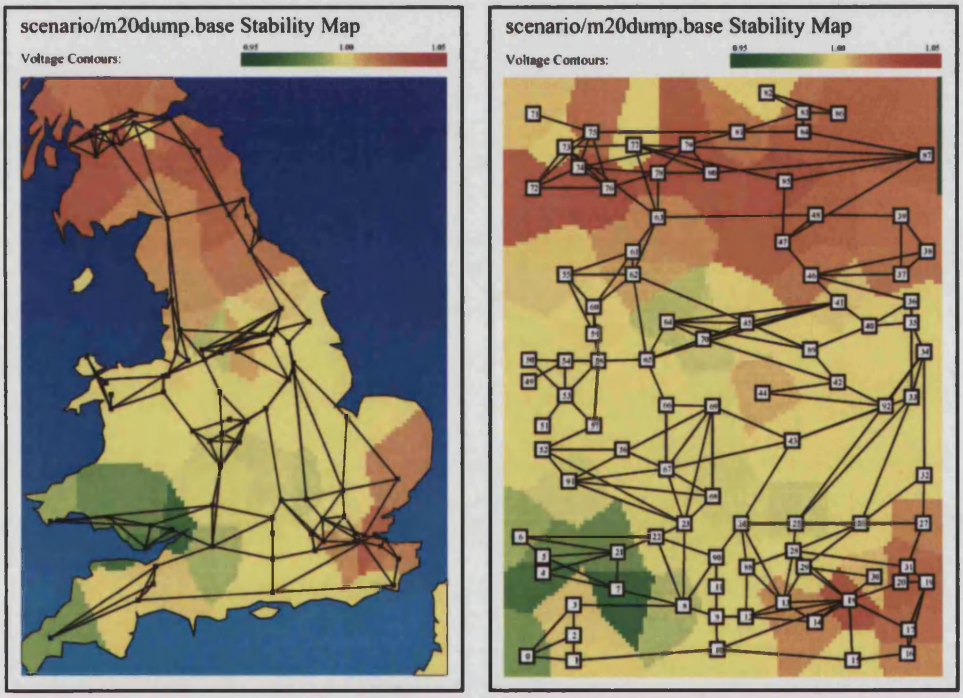


Figure 7.1: Security map with voltage profile

Figure 7.1 shows the geographic and topological maps for the laboratory scale power system model, detailed in 8.1. As expected, the voltage levels are higher in Scotland and the North of England than the South-West of England due to the distribution of the majority of the generation. In particular, the voltage levels in South Wales seem to be relatively low compared to the actual voltage levels on the full NGC system.

This is primarily due to the fact that the generation at Pembroke is not included in the laboratory scale model.

### 7.1.2 MW Injection Profile

The stability maps produced using the net busbar MW injection as a contour allows a comparison between the power generation and local transient instability to be judged. One would expect that those contingencies which may lead to transient instability will occur in the vicinity of large MW generation.

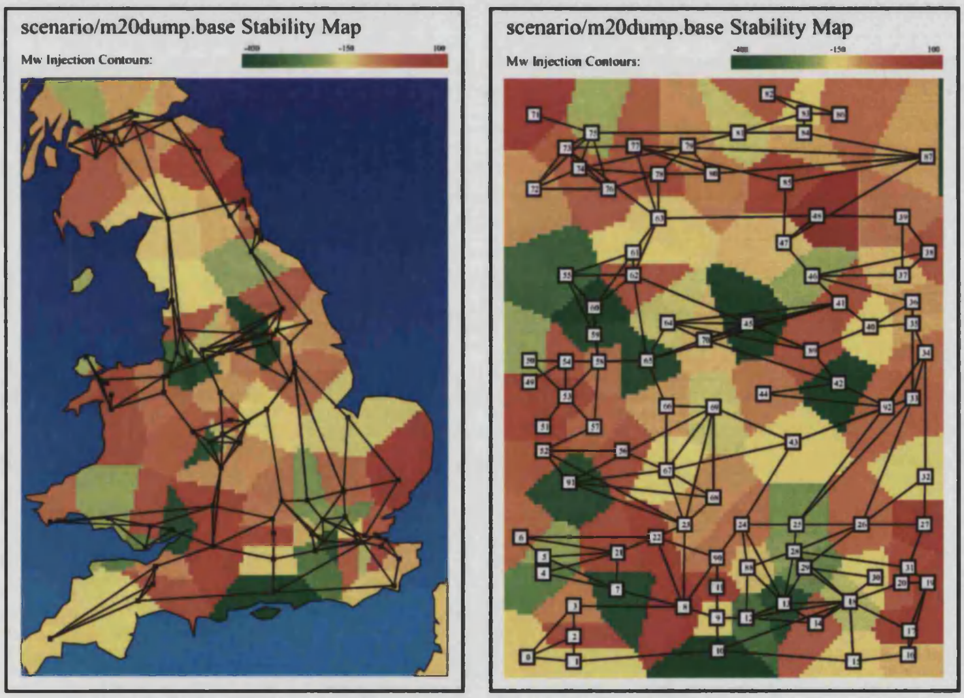


Figure 7.2: Security map with MW injection profile

Figure 7.2 shows the geographic and topological maps for the base case of the laboratory scale model.

### 7.1.3 MVar Injection Profile

The background produced by busbar MVar injections highlights those areas of the power system with power generation and voltage support. Transmission lines that cross a clear boundary in the MVar generation profile are likely to be carrying a large MVar flow, and loss of these lines is likely to result in severe voltage problems in the post-contingency operating point.

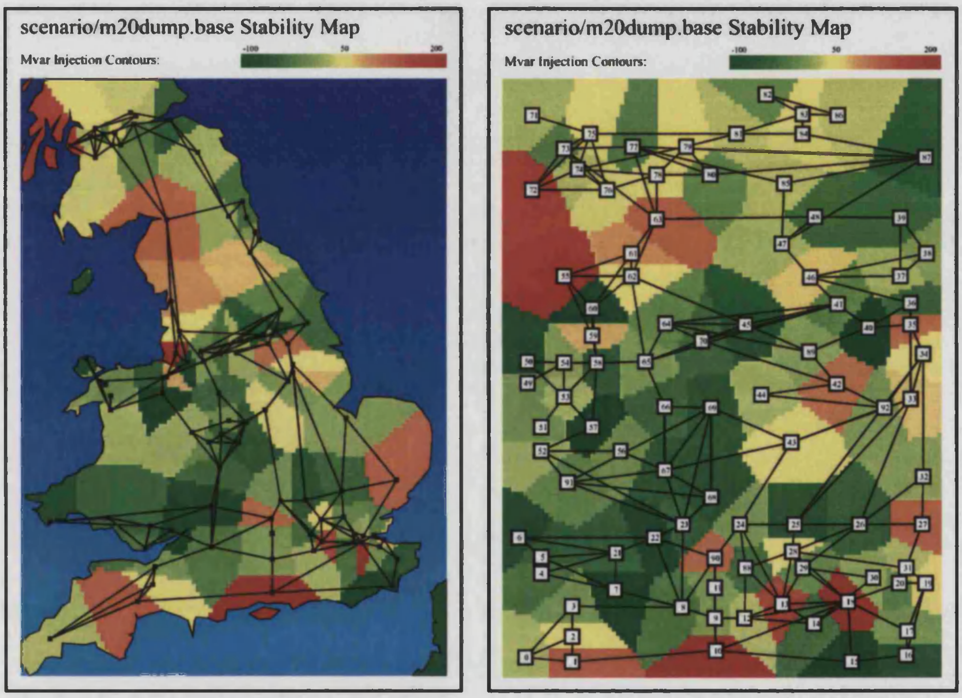


Figure 7.3: Security map with MVar injection profile

Figure 7.3 shows the security maps using this profile.

## 7.2 Modifications to Server Task

The integration of the stability screens into the server task of OASIS required substantial additions to the server task. The basic operation of the server task was extended to allow the generation of composite indices, the inclusion of the ANNs and the threshold comparison.

In order to maintain a high degree of flexibility it was decided that the transient and oscillatory instability screens should be uploaded to each server task from the client, as opposed to being hard-coded into the server. This allows different screens to be loaded into the server task depending on the power system model being used. The main disadvantages of this approach are that (1) there is the initial overhead of building the internal representation of the screen on startup and (2) the slightly slower operation of the screen, due to the slightly less optimal internal representation. However, the much greater flexibility of this approach outweighs these slight disadvantages. From a coding (implementation) perspective, this required the following enhancements to the server task.

- Additions to the PVM interface to allow the screens to be loaded and flags set to allow testing of the screens and generation of training data.
- The incorporation of a load flow within the server tasks.
- The addition of a composite indices module.
- The incorporation of a module to simulate an ANN and perform the stability index comparison.

Figure 7.4 shows the main blocks within the new client task. The new modules are described in more detail in the following sections.

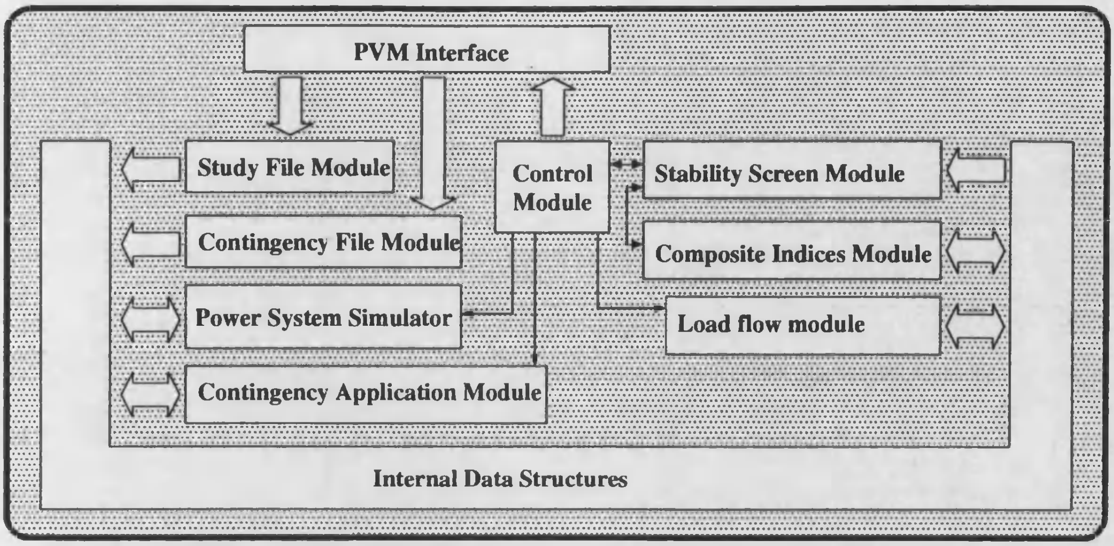


Figure 7.4: Block diagram of new server task

### 7.2.1 PVM Interface

Message handling within PVM applications involves sending and receiving messages, each of which has an associated `integer` tag to indicate the nature of the contents. The changes to the PVM interface involved adding routines to process messages of the following (new) tag types.

`MT_TSS` — this was added to indicate that the received message is a transient instability screen. The message is then extracted from the PVM buffer and stored.

`MT_OSS` — this was added to indicate that the received message is an oscillatory instability screen. The message is then extracted from the PVM buffer and stored.

`MT_TEST` — this was added to allow any the screens to be tested. A flag is set to store the results from the screens and compare them with the results obtained using a full time-domain simulation.

MT_GENDATA — this was added to indicate that the values of the composite indices defined in the screen files are to be written to the stderr stream. This stream is re-directed within oasis to a log file. By defining a screen with all (nearly 2000) composite indices as inputs the training database can be generated. Upon writing the data, the simulation continues to determine the actual transient and oscillatory instability indices. These values are then written to the same stream, and the process repeated for the next contingency.

### 7.2.2 Load Flow Module

Load flow routines have formed the basis of power system static security analysis and have taken many different forms. In the late 1970s and early 1980s, fast decoupled routines became popular [177], although recent trends have favoured fully coupled implementations due to the increased accuracy, improved convergence and the advances in computing power.

The load flow routine (Complex Power Flow - CPF) implemented as part of the OASIS project is based on a standard formulation such as that described in [105]. The set of simultaneous power equations which defines the system's state are non-linear. They are therefore solved via a set of successive linear approximations based on first order Taylor expansions of the power equations.

The solution routine requires assigning some initial estimate to all the busbar voltages and angles (the slack bus is typically assigned to $1\angle 0$) and calculating the initial real and reactive power mismatches. Should any of these be above the set tolerance, the Jacobian is formed and solved for updates of voltages and angles upon which new estimates of the power mismatches are obtained. While convergence is not obtained, the Jacobian is again formed and new updates of voltage magnitude and phase are found.

The core routines to build the admittance matrix, form the Jacobian and solve the power flow were extracted from CPF and inserted into a single module, `lf.c`. Functions were then written to provide the loadflow with the pre-contingency voltage vector as the starting point for the loadflow. The results from the loadflow were then stored to be used in the calculation of the composite indices.

### 7.2.3 Composite Indices Module

The implementation of the composite indices module was performed in a similar structure to the set notation described earlier (see section 6.4.2).

Figure 7.5 shows the basic control flow for the construction of the composite indices. A separate function exists for each statistical function, which then uses the information contained in *set B* and *set C* to build the composite index. The numerical measurements are provided by a call to the *variable-functions* which interface to the OASIS data structures. This description is intended to provide a brief flavour of the implementation. In practice the ANSI 'C' source code (`ci.c`) uses function and data pointers to improve the efficiency.

### 7.2.4 Stability Screen Module

Each stability screen is defined in a screen definition file which is loaded into the server task upon initialisation. The definition file contains the following information concurrently and in plain ASCII format.

① The neural network architecture and connection weights in the same format as an SNNS[178] network definition file. This allows the ANNs to be trained using SNNS and then saved into this format, all ready for including in a screen definition file.

② The definition of the composite indices to be used for the screen is specified using the set notation described earlier (see section 6.4.2).

③ The normalisation limits for each composite index are then included, to ensure that the range of the values of each composite index are the same as used in training the ANN.

④ The stability threshold value is included to allow a binary classification to be achieved.

The functions coded within this module (`screen.c`) perform the decoding of the definition file, the implementation of an ANN and the stability comparison required by each of the screens. The following sections provide a brief indication of the data structures and key functionality of this module.

#### 7.2.4.1 Data Structures

The primary data structure within this module concerns the internal representation of each ANN. The fundamental building block of ANNs, neurons, was used as the basis for the data storage and has the format shown below.

```
typedef struct Neuron {
        float act;
        float bias;
        char st;
        int Nsources;
        int SourceId[MAX_CONNECTIONS];
        float SourceWt[MAX_CONNECTIONS];
        float Output;
} Neuron;
```

The current activation value (`act`) and bias (`bias`) values are followed by a character indicating whether the neuron is in the input, hidden or output layer. The number of source neurons (`Nsources`) is used to store the number of neurons that contribute their output to the activation of the neuron. The arrays `SourceId` and `SourceWt` are the identifier and connection weights for these source neurons. `Output` is the current value of the output of the single output layer neuron.

### 7.2.5 Operation

The decoding of the screen definition file begins with reading the number of neurons from the storage buffer. A section of memory, equal in size to the number of neurons in the screen multiplied by the size of the `Neuron` data structure, is allocated and the bias values and other topology information stored into this array of `Neurons`. The screen initialisation is then complete.

For on-line operation, once the composite indices have been calculated, the inputs are normalised and presented to the input layer neurons. The output of each of the input layer neurons are then propagated through the hidden layer neurons to the output layer neuron. The output of the output layer neuron corresponds to the stability index.

The stability comparison is then performed using a simple numerical comparison. If the stability index is less than the threshold value then the contingency is classified as *secure*, else it is classified as *potentially insecure*.

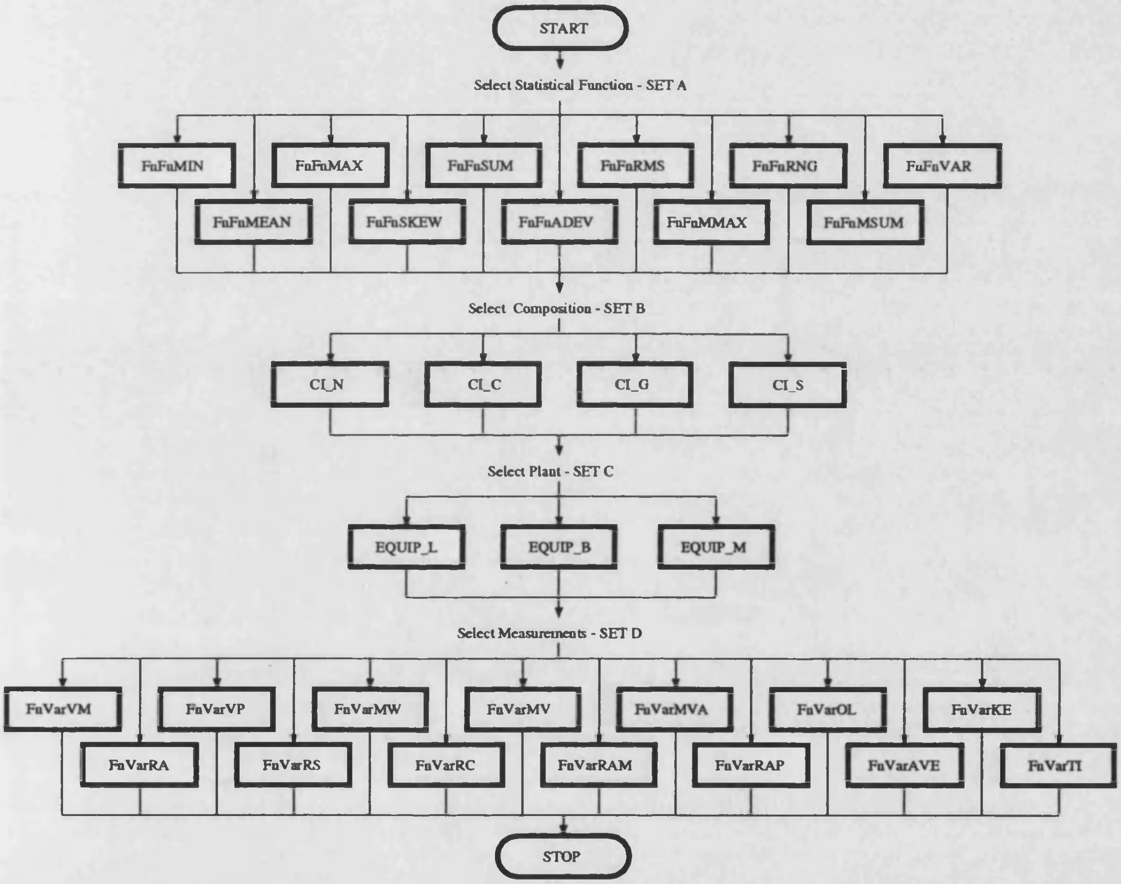


Figure 7.5: Control flow for composite index generation

# Chapter Eight

# Simulation Results

This chapter contains the simulation results that have been obtained using OASIS with the transient and oscillatory instability screens. Results are presented for the laboratory scale power system model as well as snapshots of the full scale UK national grid system which show the speedup of OASIS of approximately 25 times when the stability screens are used.

## 8.1 100 Busbar Model

The standard laboratory scale power system is a 20 machine 100 busbar reduced model of the UK National Grid System. This model is based on a full system snapshot taken from the EMS during a summer night in 1984. Figure 8.1 shows the topological map for this model. The model covers the main 400kV system and extends to cover some of the Scottish system so that the full electro-mechanical interaction between these two systems can be modelled.

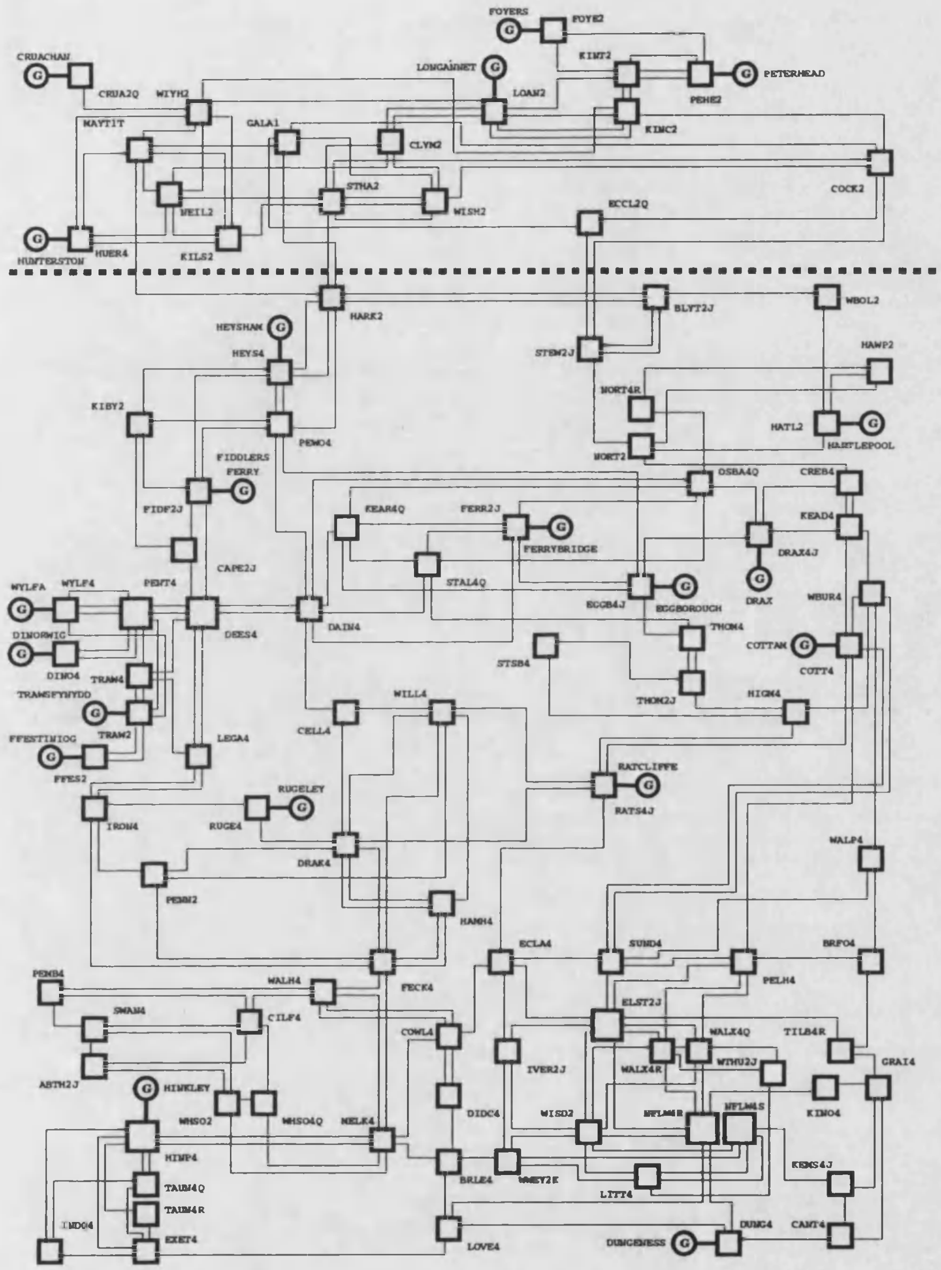


Figure 8.1: 100 Busbar Power System Model

### 8.1.1 Transient Instability Screen

The base case laboratory model was used for generating the training data for the ANN. A total of 1916 composite indices were generated for the 838 training contingencies comprising three phase to ground busbar faults, loss of load, loss of generation and loss of transmission lines. The selection procedure outlined in section 6.5 was applied and resulted in the selection of the 18 composite indices shown in table 8.1 using the set notation discussed earlier in section 6.4.2.

| No | *A* | *B* | *C* | *D* | *E* | No | *A* | *B* | *C* | *D* | *E* |
|---|---|---|---|---|---|---|---|---|---|---|---|
| 1 | S | M | N | MIN | OL | 10 | S | M | C | MIN | RAM |
| 2 | S | M | N | MIN | VM | 11 | S | M | N | MIN | AVE |
| 3 | S | M | N | RNG | VM | 12 | S | M | N | MIN | AVE |
| 4 | S | M | N | VAR | VM | 13 | S | M | N | MIN | AVE |
| 5 | S | M | C | MIN | VM | 14 | S | M | C | MIN | AVE |
| 6 | S | M | C | RNG | VM | 15 | S | M | C | MIN | AVE |
| 7 | S | M | C | VAR | VM | 16 | V | M | N | VAR | VP |
| 8 | S | M | N | MIN | RS | 17 | V | M | C | RNG | VP |
| 9 | S | M | N | MIN | RAM | 18 | V | M | C | ADEV | VP |

Table 8.1: Selected Composite Indices for Transient Instability Screen

These selected indices do not include any line or busbar indices, but when this approach is applied to larger power systems, such as the full national grid system, such indices are selected. 14 of these indices are related to the terminal voltage of the generating sets in the power network, showing the clear link between generator terminal voltage and transient stability. A pattern file was then generated to train the ANN to perform the non-linear mapping from this feature space to the transient instability classification. These patterns were also processed by the Edwards-Sammon algorithm and then displayed on a contour surface based on the stability index as shown in figure 8.2.

The surface is determined from the stability index of each of the patterns and has the effect of highlighting clusters of patterns of a similar stability class. It can be seen that the transiently unstable patterns (crosses) are geometrically well separated from the stable patterns (dots), indicating that the screen is likely to be able to classify the stability and be fairly robust to changes in the power system state and topology.

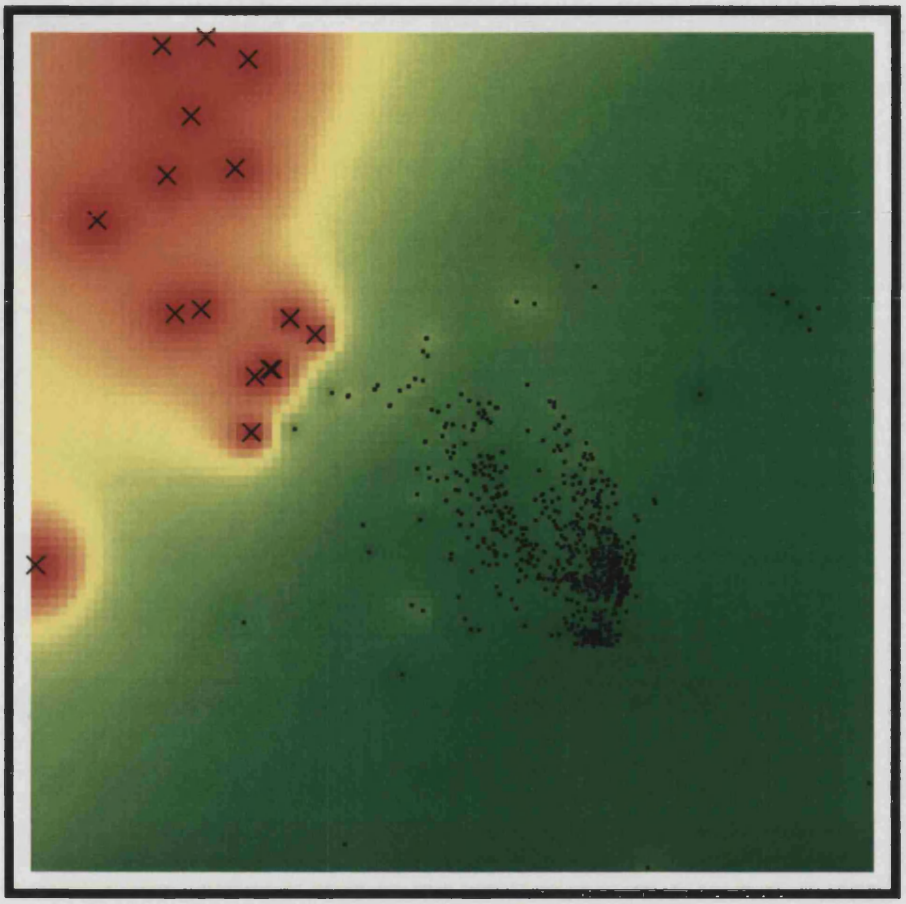

Figure 8.2: Transient Instability Screen Edwards-Sammon Plot for Laboratory Scale Model

The choice of the number of input neurons for the ANN is set by the number of selected features; 18 for this screen. The ANN is required to predict a stability margin, hence one output layer neuron is required. The choice of the number of hidden layer neurons is less well defined. The choice of 10 neurons was made using experience at training a large number of ANNs for a wide variety of applications. In practice, due to the clear separation of the classes on the Edwards-Sammon plot, the ANN will be able to learn and generalise the problem domain well. The choice of the number of hidden layer neurons becomes less critical in these cases.

The ANN was trained using SNNS[178] and a back-propagation algorithm [24]. The training was stopped after 400 iterations when convergence had been achieved.

The threshold value was set to 0.4 because the largest stability index for a stable contingency in the training set was 0.38.

### 8.1.2 Oscillatory Instability Screen

The feature selection process described earlier resulted in the selection of 10 composite indices for the oscillatory instability screen.

| No | *A* | *B* | *C* | *D* | *E* | No | *A* | *B* | *C* | *D* | *E* |
|---|---|---|---|---|---|---|---|---|---|---|---|
| 1 | S | M | N | VAR | RAM | 6 | V | L | C | RMS | MW |
| 2 | S | M | C | VAR | RAM | 7 | V | L | C | MSUM | MW |
| 3 | S | L | N | MSUM | OL | 8 | V | L | C | RMS | MVA |
| 4 | S | L | C | MSUM | OL | 9 | V | L | C | MSUM | MVA |
| 5 | S | L | C | ADEV | MVA | 10 | V | L | C | MSUM | VP |

Table 8.2: Oscillatory Instability Screen Composite Indices for Laboratory Scale Model

Table 8.2 shows the set membership for the 10 selected composite indices. The suitability of these indices at classifying the oscillatory instability problem can be shown by using a Sammon plot, as shown in figure 8.3.

As can be seen from this plot, those patterns represented by 'crosses' (unstable) are well separated from those represented by 'dots' (stable), indicating that the ANN will be able to learn the training data and generalise for other cases that it has not seen before. As before, a simple three layer feed-forward ANN was chosen as the neural network architecture. The selection of 10 composite indices requires 10 input neurons for the ANN. One output neuron is required for the stability index and 8 hidden layer neurons were chosen. The ANN was then trained using SNNS and a back-propagation algorithm with a learning rate of 0.9. The oscillatory instability screen was then tested on a number of different scenario's.

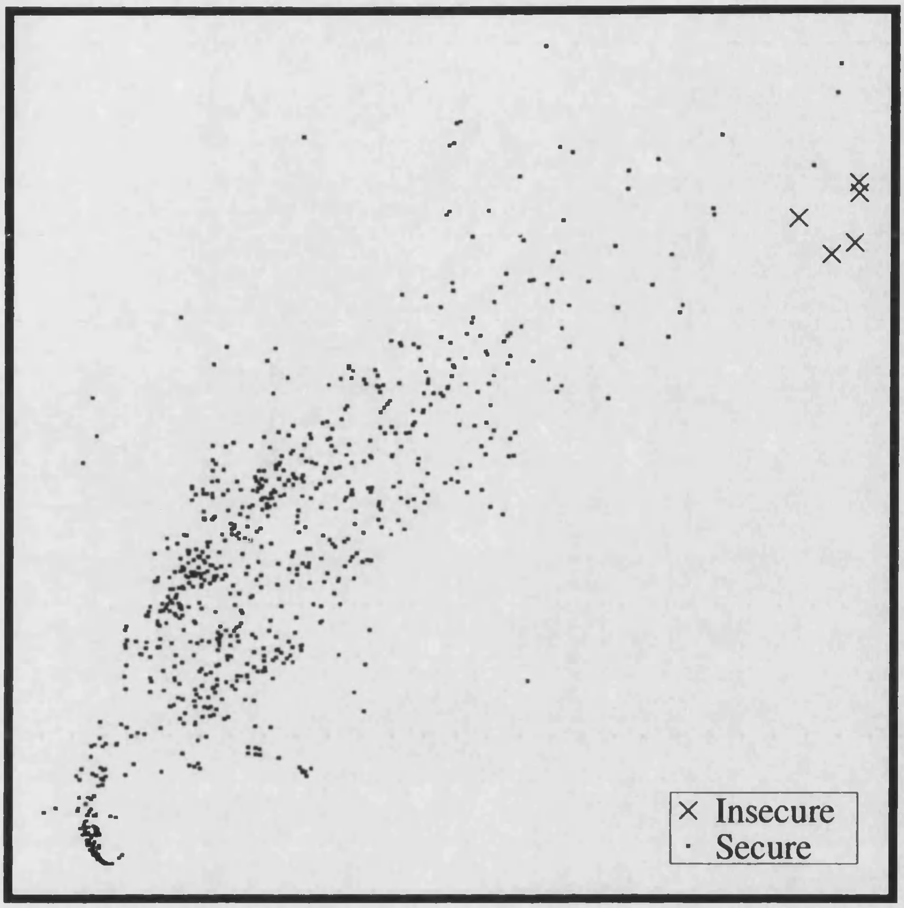


Figure 8.3: Oscillatory Instability Screen Sammon Plot for Laboratory Scale Model

### 8.1.3 Performance Evaluation

Within the laboratory environment a parallel virtual machine consisting of two DEC Alphas and two Silicon Graphics R4000s was used to evaluate the performance of OASIS. The performance of OASIS was then evaluated, using the transient and oscillatory instability screens, on the base case (A) laboratory power system model and a number of scenarios which were constructed from the base case (B–G) as follows:

**Scenario B** — A sudden increase in load on busbars **DRAK4, HAMH, CELL4** and **WILL4** met by reducing the motoring load of the pumped storage units at **Dinorwig** from 1800MW to 1270MW.

**Scenario C** — The same increase in load as (A) met by stopping all 280MW of motoring at **Ffestiniog** and reducing the motoring load at **Dinorwig** from 1800MW to 1530MW.

**Scenario D** — This has the same loading and generation pattern as the base case (A) but the circuits from **PELH4** to **WALP4** and from **PELH4** to **COTT4** are outaged. This has the effect of increasing the power transfer through the remaining circuits into the London area.

**Scenario E** — The loss of one of the England-Scotland circuits between **STEW2J** and **COCK2**.

**Scenario F** — The loss of the generation at Ratcliffe; a total loss in generation of 1176MW.

**Scenario G** — The loss of one of the 400KV circuits between **DEES4** and **PENT4** resulting in an increased impedance between the North-Wales generation and the rest of the system.

| Snapshot | Transient Screen | | | | Oscillatory Screen | | | | OASIS | |
|---|---|---|---|---|---|---|---|---|---|---|
| | $\alpha_{ss}$ | $\alpha_{uu}$ | $\alpha_{su}$ | $\eta(\%)$ | $\alpha_{ss}$ | $\alpha_{uu}$ | $\alpha_{su}$ | $\eta(\%)$ | $\lambda$ | $t_{dsa}$ |
| A | 822 | 16 | 9 | 98.9 | 833 | 3 | 2 | 99.8 | 20.9 | 43 |
| B | 829 | 8 | 0 | 100.0 | 830 | 0 | 8 | 99.0 | 21.5 | 42 |
| C | 821 | 8 | 8 | 99.0 | 830 | 0 | 8 | 99.0 | 20.0 | 45 |
| D | 807 | 16 | 9 | 98.9 | 833 | 3 | 2 | 99.8 | 22.0 | 41 |
| E | 817 | 16 | 5 | 99.4 | 833 | 5 | 0 | 100.0 | 22.0 | 41 |
| F | 802 | 18 | 0 | 100.0 | 826 | 11 | 1 | 99.9 | 23.1 | 39 |
| G | 814 | 19 | 14 | 98.2 | 830 | 6 | 2 | 99.8 | 19.6 | 46 |

Table 8.3: Performance for Laboratory Scale Model

Table 8.3 contains the performance related results using OASIS with both the transient and oscillatory instability screens. For the transient instability screen, the screening efficiency remained above 98% for each of the scenarios used in testing. The number of unstable contingencies mis-classified by the transient screen was zero for all scenarios, meeting the requirement of conservative operation.

The oscillatory instability screen had a performance similar to that of the transient instability screen. In this case, the efficiency remained above 99%. The net effect of using both the transient and oscillatory instability screen within OASIS reduces the cycle time from approximately 15 minutes to 45 seconds - a 20 fold speedup.

### 8.1.4 Contingency Allocation

Figure 8.4 shows details of the OASIS contingency allocation when the PVM was comprised of the four host computers used for the performance evaluation. The total operating time of the DSA was 45 seconds using the screens described above.

It can be seen that those contingencies which required full evaluation took significantly longer to process than those which only required screening. Also, due to the multi-user nature of UNIX systems, the time taken to perform the 30 second time domain simulation (evaluation) varied from both host to host and occasionally from time to time on the same computer. This is due to the unpredictable and variable load demand on the computers due to other user and system programs being executed.

Contingency Allocation 45 secs

| Key | Pvm Hardware Host Name | Arch | Contingencies/Sec Max | Min | Avg | Statistics Idle(s) | No of Ctg | % |
|---|---|---|---|---|---|---|---|---|
| | ALBION | SGI5 | 11.11 | 0.33 | 4.63 | 1 | 207 | 25 |
| | HAYDN | ALPHA | 20.00 | 0.07 | 4.98 | 1 | 222 | 26 |
| | VIOLET | SGI5 | 10.00 | 0.19 | 1.93 | 1 | 86 | 10 |
| | MOZART | ALPHA | 25.00 | 0.58 | 7.20 | 1 | 323 | 39 |

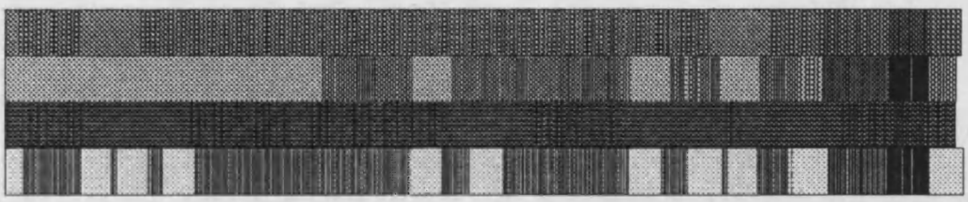

Figure 8.4: Contingency Allocation for Laboratory Scale Model

## 8.2 Full UK Power System Snapshots

The UK Power system is a highly interconnected transmission system with in excess of 7000 kilometres of overhead transmission lines and cables, 21,600 towers, 280 substations and up to 200 large generating units operating at any time. There are two major power interconnections: the first a 275 and 400kV AC link to the Scottish power system and the second a 2000MW DC link with France[26, 27].

During the field trials of OASIS at NGCC (see 3.5) a number of system snapshots were saved to be used in the laboratory for validation of the ANN screens. The number of busbars in each snapshot varied between 900 and 920 and the number of generating units varied from approximately 100 to 150 depending on the load level.

The previous discussion on ANNs (5) explained that ANNs are suited well to interpolation between patterns used for training but not extrapolation. As a consequence it was decided to train the ANN using results obtained for the condition of lowest and highest daily demand and then to examine the performance of the screen for those conditions in between. The lowest daily demand of 28GW occured at approximately 0500 hrs and the daily peak of 48GW occured at 1700 hrs. A total of 6838 training patterns were then generated to be used for training the ANNs.

### 8.2.1 Transient Instability Screen

The selection of the composite indices was performed using 1000 contingencies with the worst transient response. The reason for using a subset of the total training data for the feature selection was to speed up the feature selection process. The majority of contingencies were very stable and hence many of these patterns were very similar in nature. The *mcovar* selection process uses a sequential forward search which is very time consuming for a large number of patterns and hence it was more practical to use a subset of the training cases for the feature selection. The selected indices are shown in table 8.4.

| No | *A* | *B* | *C* | *D* | *E* | No | *A* | *B* | *C* | *D* | *E* |
|---|---|---|---|---|---|---|---|---|---|---|---|
| 1 | S | M | C | MIN | OL | 13 | V | M | C | SKEW | MW |
| 2 | S | M | C | SKEW | PF | 14 | V | M | N | SKEW | KE |
| 3 | S | M | C | SKEW | MW | 15 | V | M | G | SKEW | KE |
| 4 | S | M | G | SKEW | VP | 16 | V | M | C | SKEW | RAP |
| 5 | S | M | C | MAX | VP | 17 | S | L | G | MAX | PF |
| 6 | S | M | C | RNG | VP | 18 | S | L | G | MMAX | PF |
| 7 | S | M | C | MMAX | VP | 19 | S | L | C | MSUM | VM |
| 8 | S | M | N | SKEW | KE | 20 | S | B | C | MMAX | VP |
| 9 | S | M | N | SKEW | RAP | 21 | V | B | N | RNG | VP |
| 10 | S | M | C | SKEW | OL | 22 | V | B | G | SKEW | VP |
| 11 | V | M | N | SKEW | OL | 23 | V | B | C | RNG | VP |
| 12 | V | M | C | SKEW | OL | 24 | V | B | C | MMAX | VP |

Table 8.4: Transient Instability Screen Composite Indices for NGC Model

The selection of only 24 features for the stability classification is a highly significant result. Traditional approaches to applying pattern recognition methods for stability assessment of similar sized power system models are not practical because many more (at least five times as many) features would be required. By selecting only 24 features, it is possible to use an ANN as the core of the pattern classifier. Boxplots for these indices are shown in Appendix A.1. The suitability of these features at performing the stability classification is shown through the Sammon plot in figure 8.5.

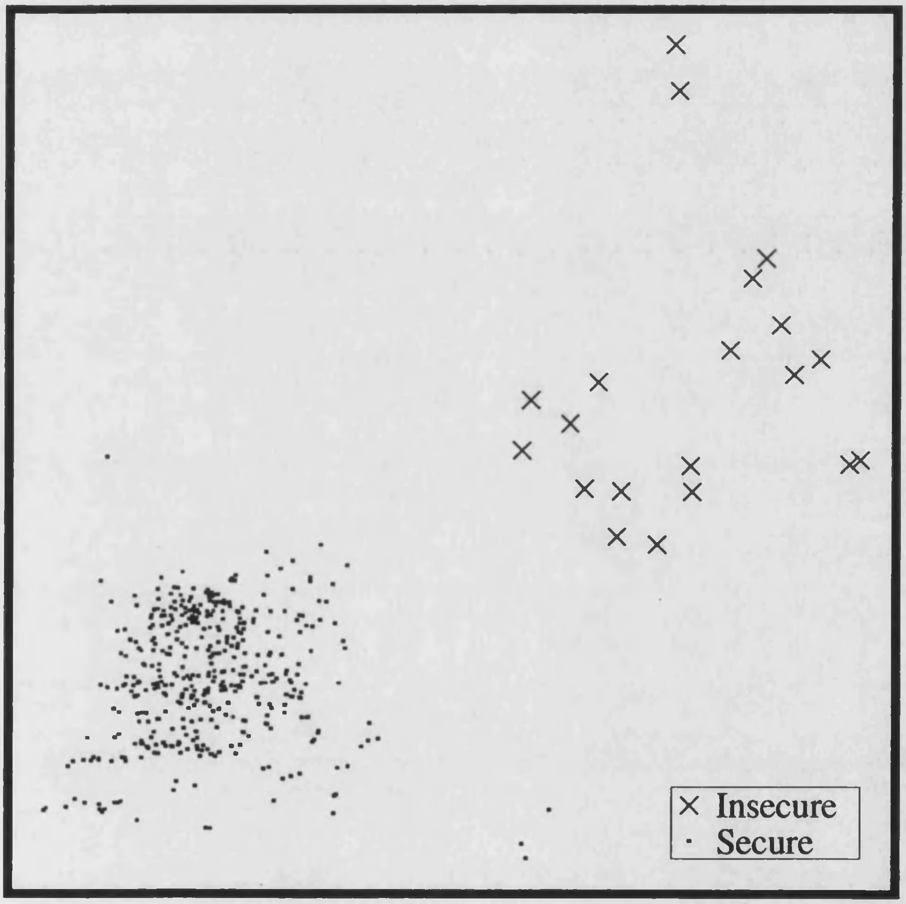


Figure 8.5: Transient Instability Screen Sammon Plot for NGC Model

In this case the unstable patterns again fall into one broad cluster, indicating that the ANN will be able to learn this data. It can be seen that the transiently unstable patterns (crosses) are geometrically well separated from the stable patterns (dots), indicating that the ANN is likely to be able to classify the stability and be fairly robust to changes in the power system state and topology. Hence a standard three layer feed-forward neural network was chosen with 24 inputs, 10 hidden layer neurons and one output neuron. The ANN was trained using SNNS[178] and converged after 5000 iterations. This ten fold increase in the training time over that required for the laboratory scale model due to the larger number of training patterns and connection weights in the ANN. The threshold value was set to 0.4 because the largest stability index for a stable contingency in the training set was 0.37.

### 8.2.2 Oscillatory Instability Screen

The training cases used for the transient screen was also used for the oscillatory instability screen. The 1000 contingencies with the worst oscillatory response were selected to be used for the feature selection. This resulted in the selection of 26 composite indices as shown in table 8.5.

| No | *A* | *B* | *C* | *D* | *E* | No | *A* | *B* | *C* | *D* | *E* |
|---|---|---|---|---|---|---|---|---|---|---|---|
| 1 | ADEV | S | M | PF | S | 14 | SKEW | C | M | RA | V |
| 2 | SKEW | C | M | MW | S | 15 | MIN | C | L | MW | S |
| 3 | SKEW | S | M | MV | S | 16 | MEAN | S | L | MV | S |
| 4 | VAR | N | M | TI | S | 17 | VAR | C | L | MV | S |
| 5 | SKEW | S | M | VM | S | 18 | MAX | S | L | MVA | S |
| 6 | VAR | G | M | RAM | S | 19 | ADEV | C | L | VM | S |
| 7 | MAX | C | M | RAP | S | 20 | MIN | S | L | MW | V |
| 8 | SKEW | C | N | RAP | S | 21 | VAR | C | L | MW | V |
| 9 | RNG | N | M | AVE | V | 22 | RMS | C | L | MVA | V |
| 10 | SKEW | G | M | MV | V | 23 | MAX | N | B | VM | S |
| 11 | VAR | C | M | MVA | V | 24 | ADEV | C | B | VP | V |
| 12 | ADEV | C | M | MVA | V | 25 | MMAX | C | B | VP | V |
| 13 | RMS | N | M | RA | V | 26 | ISLANDING | | | | |

Table 8.5: Oscillatory Instability Screen Composite Indices for NGC Model

These indices are based on a wide selection of power system features. Approximately half of the indices are based on machine parameters including **TI** which is the estimated time to pole slipping. Voltage effects are included by use of terminal voltage magnitudes and AVR voltage errors. Rotor accelerating power was selected for three of the indices. The majority of the remaining indices are based on real and reactive power flows in transmission lines. Two indices were selected based on changes in busbar voltage phase angles. The last index is a *special* index. This is a number which is set to one if there is any islanding in the system, else it is set to zero. Boxplots for these indices are shown in Appendix A.2. Fig.8.6 shows the Sammon plot of the selected features.

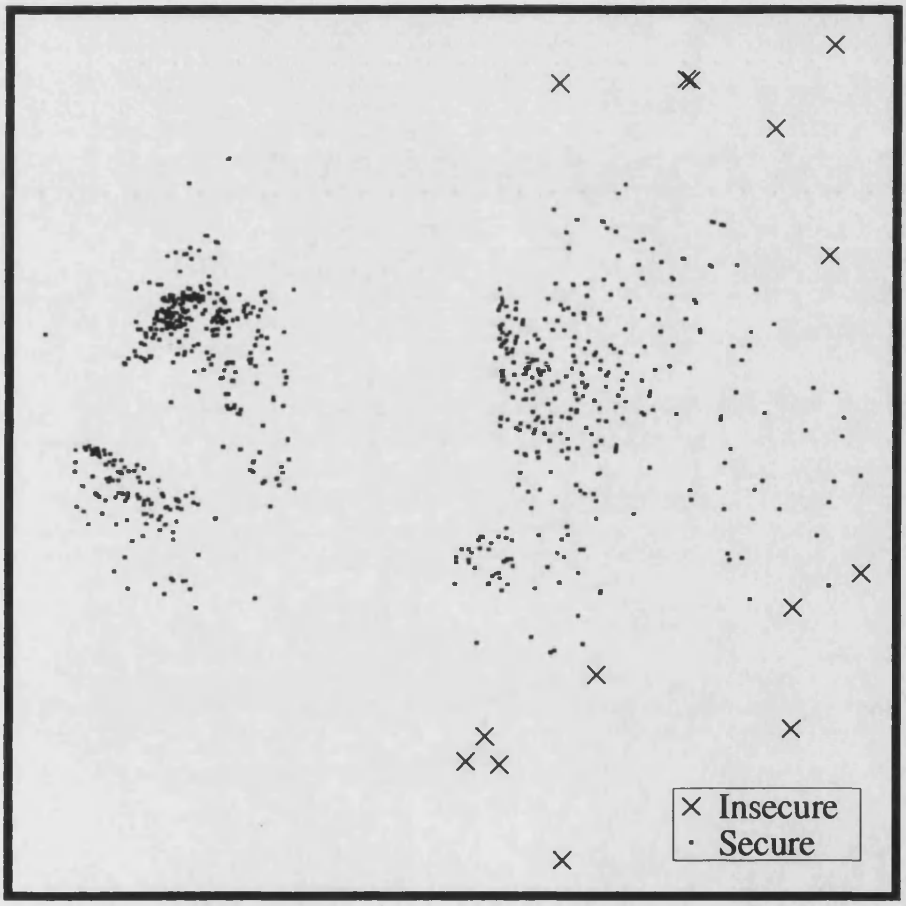


Figure 8.6: Oscillatory Instability Screen Sammon Plot for NGC Model

Again, the *insecure* patterns (crosses) are geometrically fairly well separated from the *secure* patterns (dots), indicating that the screen is likely to be able to classify the stability. A standard three layer feed-forward neural network was chosen with 26 inputs, 13 hidden layer neurons and one output neuron. The ANN was trained and the training was stopped after 1500 iterations when the learning error was approximately zero.

### 8.2.3 Performance Evaluation

Table 8.6 shows the performance of the transient and oscillatory instability screens when tested on several snapshots taken from the EMS of the UK power system. These results were obtained in the laboratory using the processing power of two DEC Alphas and three Silicon Graphics R4000s. The first two columns show the approximate time the snapshot was taken, and the total system load at that time. $N_{ctg}$ is the total number of contingencies selected for analysis. The next two sections contain information on the transient and oscillatory instability screens. The final two columns show the net effect of the incorporation of the screens into OASIS. For the testing of the screens, every contingency was passed through both screens, but for the determination of the speedups, the screens were cascaded, as shown earlier in fig. 6.9

| Snapshot | | | Transient Screen | | | | Oscillatory Screen | | | | OASIS | |
|---|---|---|---|---|---|---|---|---|---|---|---|---|
| t(hrs) | P (GW) | $N_{ctg}$ | $\alpha_{ss}$ | $\alpha_{uu}$ | $\alpha_{su}$ | $\eta$ (%) | $\alpha_{ss}$ | $\alpha_{uu}$ | $\alpha_{su}$ | $\eta$ (%) | $\lambda$ | $t_{dsa}$ |
| 0000 | 31.4 | 3345 | 3313 | 16 | 16 | 99.5 | 3329 | 4 | 12 | 99.6 | 25.1 | 13:22 |
| 0300 | 30.7 | 3348 | 3292 | 20 | 36 | 98.9 | 3321 | 24 | 3 | 99.9 | 24.7 | 13:03 |
| 0600 | 30.5 | 3362 | 3308 | 16 | 38 | 98.9 | 3328 | 2 | 32 | 99.0 | 24.8 | 13:08 |
| 0900 | 39.9 | 3434 | 3399 | 16 | 19 | 99.4 | 3434 | 0 | 0 | 100.0 | 25.2 | 13:33 |
| 1200 | 41.4 | 3452 | 3409 | 16 | 27 | 99.2 | 3452 | 0 | 0 | 100.0 | 24.8 | 13:40 |
| 1500 | 41.1 | 3439 | 3407 | 14 | 18 | 99.5 | 3438 | 0 | 1 | 99.9 | 24.9 | 13:23 |
| 1800 | 45.2 | 3426 | 3395 | 20 | 11 | 99.7 | 3425 | 0 | 1 | 99.9 | 25.0 | 13:29 |
| 2100 | 38.9 | 3416 | 3385 | 16 | 15 | 99.6 | 3416 | 0 | 0 | 100.0 | 25.3 | 13:01 |

Table 8.6: Performance the Instability Screens

For the transient instability screen, the screening efficiency remained above 98%

for all of the test cases. $\alpha_{us}$, the number of insecure contingencies classified as secure was zero for all test cases, meeting the primary requirement of the screen; conservativeness of operation.

The oscillatory instability screen was over 99% efficient, and $\alpha_{us}$ was zero for all the test cases. From an operational perspective it is interesting to note that under the lighter loading conditions oscillatory instability problems (poor damping) were detected. As the load level increases and the system becomes more stressed these problems disappear. This result agrees with operational experience of poor damping on lightly loaded transmission systems.

The overall cycle time of OASIS using both stability screens is shown to be reduced from approximately five and a half hours to approximately 13 minutes by use of the screens. This represents an overall speedup of approximately 25 times which allows OASIS to produce results within an acceptable time frame for on-line operation.

### 8.2.4 Contingency Allocation

Figure 8.7 shows details of the OASIS contingency allocation when the PVM was comprised of the five computers used for the performance evaluation. The total operating time of the DSA was approximately 13 minutes using the screens described above.

As before, it can be seen that those contingencies which required full evaluation took significantly longer to process than those which only required screening. A good example of this case is the first contingency that was processed by **HAYDN**. Also, due to the multi-user nature of UNIX systems, the time taken to perform the screening and 30 second time domain simulations (evaluation) varied from both host

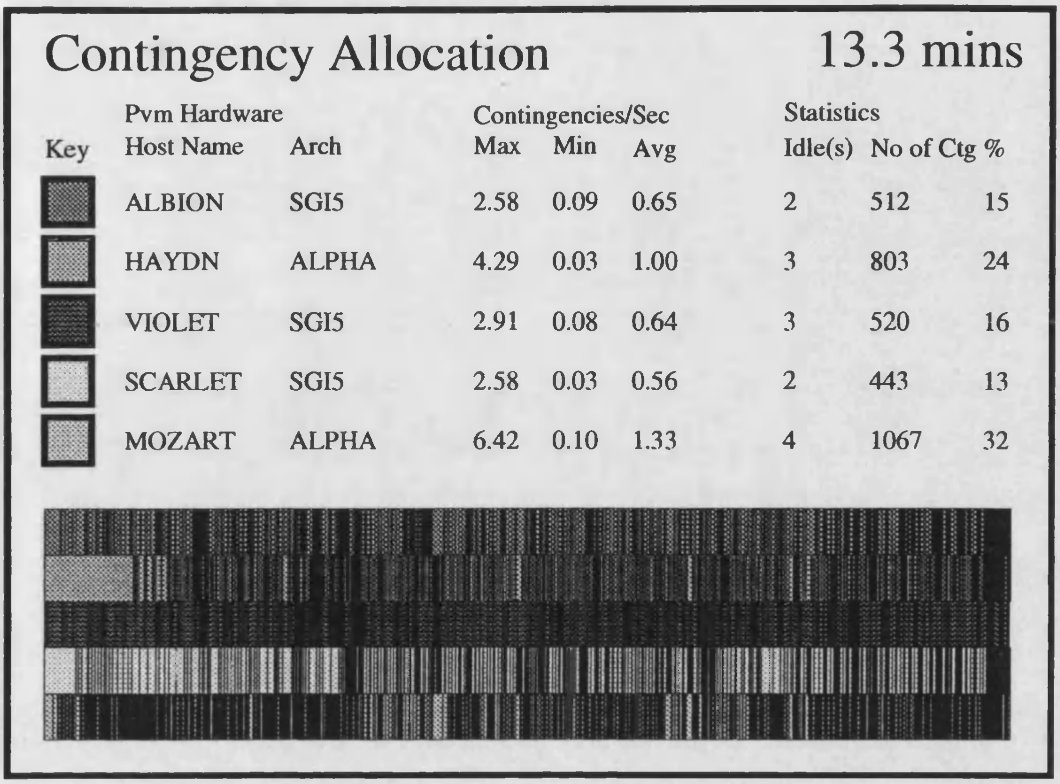


Figure 8.7: Contingency Allocation for Laboratory Scale Model

to host and occasionally from time to time on the same computer. This is due to the unpredictable and variable load demand on the computers due to other user and system programs being executed.

## 8.3 Chapter Summary

The use of the ANN based stability screens within OASIS has been shown to produce an overall reduction in cycle time of at least 20 times on typical networks, due to (1) efficient operation of the screens and (2) due to the low computational demand of the screens.

For the laboratory scale power system model, fewer than 20 composite indices are shown to be capable of classifying the transient (and oscillatory) instability. The net performance benefit of using these screens is shown by the speedup of approximately 20 times, with screening efficiencies of over 98%.

For the snapshots of the UK power system, less than 30 features were required for each stability screen. This represents a significant advance as the traditional dimensionality problems of applying pattern recognition approaches to large power system have been avoided. The overall performance benefit of these screens is seen through a speedup in OASIS of approximately 25 times.

Chapter Nine

# Conclusions

This work has resulted in the development of a general method for fast electro-mechanical stability assessment of large interconnected power systems. It is based on a pattern recognition method and uses a novel feature extraction process to enable easy scaling to both small and large power systems. The pattern classifier is provided by (1) an artificial neural network which predicts a stability index and by (2) a threshold comparison to determine the stability classification.

Stability screens have been developed for both transient and oscillatory instability and incorporated within the OASIS server tasks. The overall speedup of OASIS using these screens represents a significant advance towards achieving full on-line dynamic security assessment.

## 9.1 Overall Approach

The use of the pattern recognition method for contingency screening is shown to produce reliable results in significantly shorter time than is possible by use of a time domain simulation alone. The combination of using composite indices to form the feature vector coupled with a neural network based pattern classifier has resulted in a flexible and robust method for contingency screening.

The implementation of the screens within the server task allows maximum flexibility for both on-line operation and development work. Screens are uploaded to the server task upon initialisation allowing different screens to be used without the need to re-compile the server tasks.

The development of screens for both transient and oscillatory instability detection is crucial as no further contingency screens are required. If only the transient stability screen had been developed then it would still be necessary to run either an eigenvalue analysis or time-domain simulation for each contingency to determine the oscillatory instability.

## 9.2 Composite Indices

Composite indices have been shown to be ideally suited for use as elements of a feature vector for stability assessment. In particular, the novel nature of these features allow the pattern recognition approach to be (1) easily and (2) sensibly scaled to large power systems. This is a highly significant advance over previous work as it overcomes the *curse of dimensionality* which has traditionally prevented pattern recognition techniques being applied to large power systems.

The work of Niebur and others [50, 52, 144] has applied self-organising ANNs to small power systems, i.e. less than 20 busbars, but they suffer from the traditional dimensionality problems as actual power system features are used as inputs. The use of multi-layer perceptron ANNs for stability assessment has been performed for small power systems of typically less than 20 busbars [48, 50, 147]. The only work to approach the same size of power system was carried out by Cauley et al [70]. A similar pattern recognition technique was applied to a 436 busbar system with 88 generating units. With the enhancements that have been made to the generation of composite indices, this concept has been extended to cover transient stability assessment for a system of over 900 busbars and 130 generating sets.

The application of composite indices to the assessment of oscillatory instability problems has made a huge advance over previous work [179]. Typically, ANN applications to *dynamic* security assessment has concentrated on developing ANNs to predict the most positive eigenvalue in the system [149]. This work has been limited to systems with typically less than 20 busbars. The application of ANNs to the oscillatory instability screening of the 900 bus UK system is therefore a significant advance.

## 9.3 Pattern Classifier

Off-line time domain simulations have been successfully used to generate training data for the neural networks. By developing features which produce a clear discrimination between the stability classes, as shown in the Sammon plots, the ANNs are left to determine the simple non-linear mapping to perform the classification. By training the ANNs to predict a stability margin, classification errors at or near decision boundaries are reduced. The conservativeness of the screens can be altered by varying the threshold comparison level in accordance with utility operating policy.

## 9.4 Performance

The improvement in operating performance of OASIS can be split into three broad areas: transient and oscillatory detection and overall speedup.

### 9.4.1 Speedup

The reason for contingency screening is primarily to speed up the time required to fully identify any stability problems in the power system. This speedup is achieved by quickly identifying those contingencies with potential stability problems so that a full evaluation can then be performed by a time-domain simulator.

The artificial neural network based screens developed during this work have been shown to produce a speedup in the total screening and evaluation time of between 20 and 25 times depending on the size of the power system model. This represents a significant speedup and we can conclude that by using these screens with state-of-the-art power system simulator, such as PowSim, for contingency evaluation that full on-line dynamic security assessment can now be performed within the time constraints required for on-line operation within a utilities energy management centre.

### 9.4.2 Transient Instability Detection

These screens were conservative; i.e. $\alpha_{us}$ was zero so that all unstable contingencies were identified by the screen. The low values of $\alpha_{su}$ mean that only a very few stable contingencies are mis-classified as potentially unstable, leading to screening efficiencies of approximately 99% for a wide variety of operating conditions.

One of the main reasons for the high efficiencies are that (1) the composite index based features provide very good discrimination of the post-contingency stability of the power system and (2) that transient stability problems usually occur soon after the contingency termination point and therefore their effects are evident before the point.

### 9.4.3 Oscillatory Instability Detection

As with the transient screens, the oscillatory instability screens are also conservative in nature with $\alpha_{us}$ zero; i.e. no unstable contingencies were mis-classified as stable. The efficiency of the screens for the laboratory and full size power system model is above 98% for a wide range of operating conditions.

## 9.5 Visualisation of Power System Stability

The main enhancement to the OASIS client task was the incorporation of a module to produce the stability maps, explained earlier in section 7.1. These maps manage to display the natural geographic/topological nature of instability in conjunction with features such as the pre-contingency busbar voltage magnitudes. The net effect is a novel and clear method for displaying stability information which could be very useful for power system operators.

## 9.6 Edwards-Sammon Plots

The enhancements that have been made to the basic Sammon algorithm allow visualisation of ANN training data for a continuous valued output. This allows the *smooth* surface that the ANN will learn to be visualised. This represents a powerfull tool, especially when applied to ANN time series prediction problems.

## 9.7 Practical DSA Implementation

The deciding factor for the implementation of a dynamic security assessment system will undoubtedly depend on the results of a cost benefit analysis. In particular, the annual potential savings in constraint costs will have to be compared to the initial capital expenditure on hardware, development costs and continuing maintenance costs.

It seems reasonable that from a utility perspective that the analysis of up to 1000 contingencies within a 15 minute time frame would be, initially at least, a good starting point. If we consider a full on-line implementation of OASIS, using the stability screens, within the UK National Grid Control Centre's energy management system then the following technical conclusions can be made.

① Using the single DEC Alpha (about SPECfp 162 and SPECint 114) 1000 contingencies can be assessed in approximately 17 minutes assuming that less than 8 contingencies will require full evaluation.

② During conditions of stress on the system, during storms for example, many more contingencies may be potentially unstable and hence require detailed evaluation. It is during such times that an on-line DSA tool could be of most use and hence enough processing power should be provided to meet the 15 minute update time under these conditions. This may require up to five times more processing power being used within the PVM.

③ In common with the other EMS computers, redundancy is important to ensure continuous reliable operation and to facilitate upgrades without loss of on-line operation. An on-line backup PVM is the minimum that should be provided, and possibly an engineering backup as well (in accordance with the current use of three EMS computers).

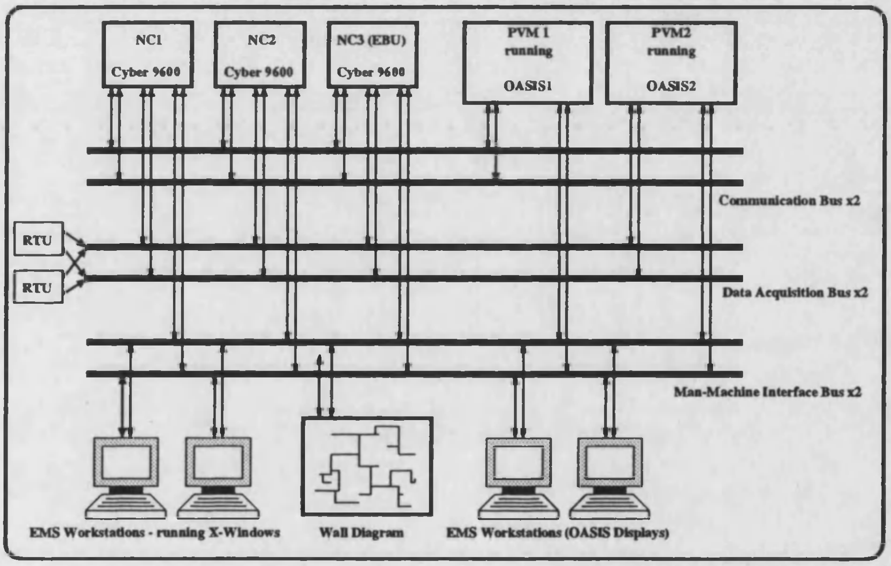


Figure 9.1: Setup for OASIS at NGCC

Figure 9.1 shows the probable hardware configuration for a full version of OASIS running on-line at the UK National Grid Control Centre, taking into account the comments above.

At the end of the day, the capital cost of developing and installing a DSA system within a utilities energy management centre will be considerable. However, the improvement in terms of the reduction of uplift costs and the increase in security will make such an investment worthwhile.

Chapter Ten

# Suggestions for further work

The work described in this thesis has confirmed that the approach of using composite indices and a neural network classifier is well suited to the detection of transient and oscillatory instability. However, certain areas exist where further work is needed to confirm the suitability of this technique for full on-line instability detection and for other similar applications.

## 10.1 Extensive on-line testing of screens

Before any stability screens are likely to be included within a full on-line dynamic security assessment system, confidence in their efficiency and reliability must be obtained. The work described in this thesis has resulted in considerable confidence in their operation, using saved system snapshots, but their performance should also be confirmed by a series of on-line testing within an EMC.

## 10.2 On-line adaption of screens

Within the control and automation fields of engineering, adaptive control techniques are becoming more widely used. The basis of this approach is to optimise the control process further by using the results of actual data obtained from the *plant* that is to be controlled.

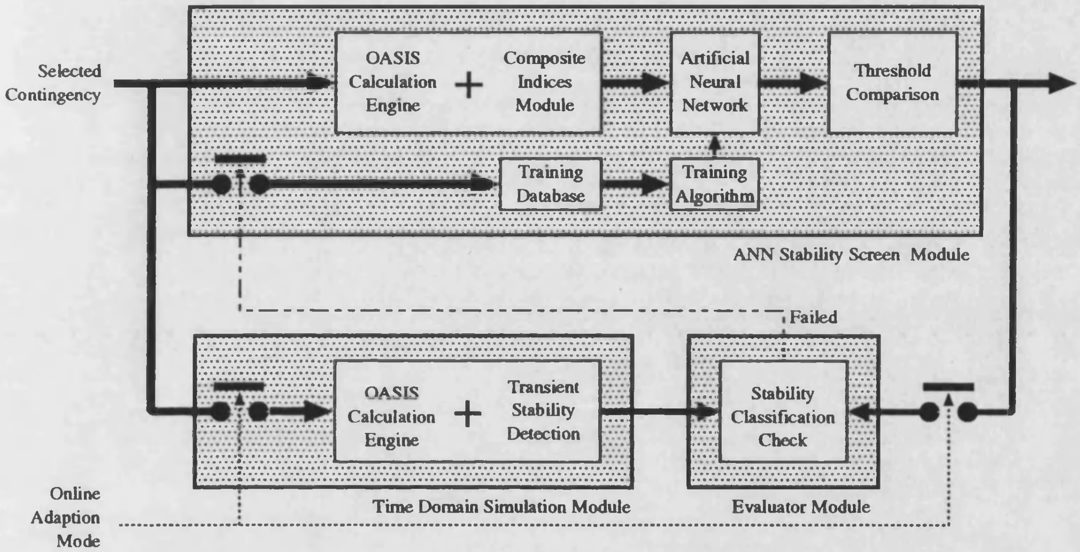


Figure 10.1: Online Adaption of ANN Stability Screen

Figure 10.1 shows a possible approach where the ANN stability screens could be fine tuned by using a real-time power system simulator to evaluate all of the contingencies that have been selected.

Under normal operation the ANN stability screens are used to detect those contingencies which may cause stability problems. In the online adaption mode, a full time domain simulation is also carried out and the results compared to that produced by the ANN screen. If the screen mis-classified the contingency then the ANN inputs are added to the training data set and periodically, the ANN re-trained.

The obvious drawback to this approach is that the DSA operating time will be very slow, but this approach could be used to increase confidence in the ANN screens by performing a comparison of their outputs. This form of supervised testing of the ANN may therefore be useful in the initial stages of acceptance of the screens.

## 10.3 Development of Screens for unusual operating conditions

The work described so far has concentrated on the development of screens for typical operating conditions. From time to time, particularly during poor weather conditions, the power system will be more vulnerable to security violations. From a practical perspective, it may be desirable to train a number of transient and oscillatory instability screens for these more unusual operating conditions, to ensure that the screens remain conservative.

This would require system snapshots, obtained either directly from the EMS or from offline storage to be used to develop the screens.

## 10.4 Application to on-line limit calculation

The main aim of dynamic security assessment is to provide the power system operators with on-line advice to maintain the security of operation of the power system whilst ensuring economic operation. The advice currently provided by OASIS is in the form of a ranked list of contingencies, designed to indicate those area's with stability problems.

The neural network based stability screens described in this thesis could be used as part of a limit calculation function. This function provides the operators with actual MW transfer limits across critical boundaries in the power system. With reference to the UK power system, on-line information on the MW transfer limits between England and Scotland may allow the Scottish import to be increased. The current transfer limits are *conservative* and result in the running of out-of-merit generation adding to the constraint, or *uplift* costs.

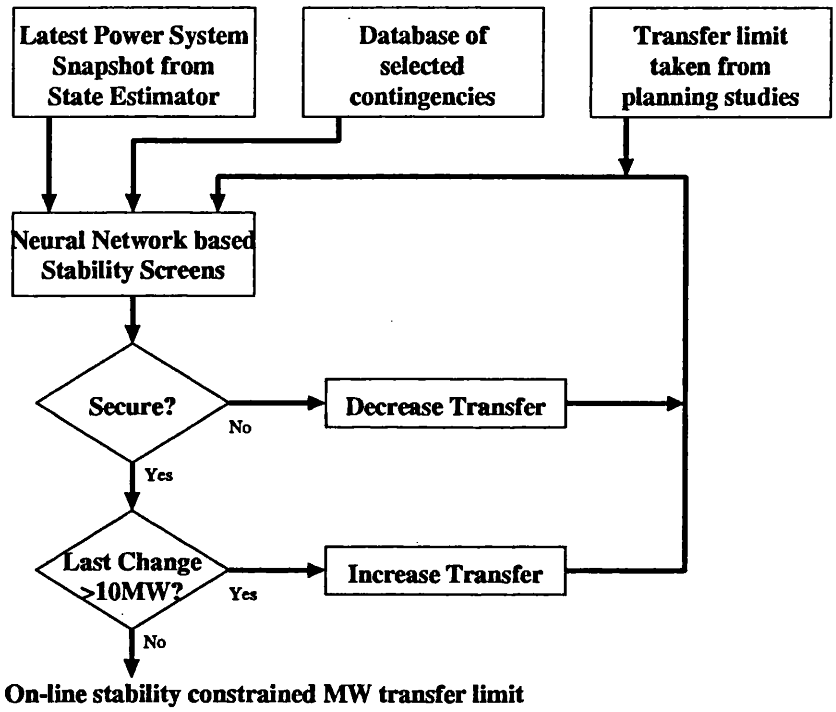


Figure 10.2: Transfer Limit Calculation using Stability Screens

Figure 10.2 shows a flowchart for a possible implementation of a limit calculation function within a dynamic security assessment system. The effects of a database of contingencies on a snapshot latest power system is determined by the stability screens. If the system remains *secure* then the transfer limit is increased, say by 500MW and a new snapshot is assembled. If the system is *insecure* then the transfer limit is reduced and a new snapshot assembled. The process is repeated until the change in MW transfer is within acceptable limits, say 10MW. Although the

ANN does not identify the generating units which experience instability, operator experience can be used to identify those generating units which have to be *backed off* and those generating units which will be used to take up the drop in generation.

This *best estimate* of the transfer limit can then be used to provide constraints for the on-line MW dispatch programs within the EMS. In practice, a small safety margin would be subtracted from the transfer limit to ensure that stability is maintained.

This type of approach, but using the Transient Energy Function, has been tried[89] and seems to produce considerable economic benefit for BC Hydro.

## 10.5 Full on-line dynamic security assessment system

The work that has been undertaken within the Power and Energy Systems Group, at the University of Bath, over the past few years has resulted in the development of a state-of-the-art power system simulator. This work has been extended and has resulted in the development of OASIS, a prototype dynamic security assessment system. The work described in this thesis concerns the development of fast stability screens for OASIS.

Work is currently in progress on the development of a limit calculation module for OASIS and when completed, OASIS will be ready for full trials within an energy management system.

## 10.6 Application to other large engineering systems

The method for the detection of instability in power systems described in this thesis could be applied in a similar manner to the detection of problems within other large engineering systems. The feature extraction and stability classification method are a general approach that could be used in a variety of other industrial applications.

In particular, the authors experience of steel mill automation indicates several areas where this approach would be highly suited. One of the most notable of these involves the detection of the position of the leading edge of steel strip during the rolling process. Traditionally, this relies on the use of infra-red detectors between each rolling mill stand. Because of the hostile environment in these areas (water, grease, dirt, heat etc) these sensors rapidly degrade in performance, and if not cleaned regularly will fail to function. This can lead to large and expensive problems on the mill if the steel strip *cobbles*. This occurs when (usually the leading edge) of the steel strip does not enter a stand properly and causes the upstream strip to lift off the rolling table into the air. At this point the strip can go almost anywhere and usually has to be removed from the stands by being manually cut into small sections by an arc torch. It may well be possible to use information from the stand drives (torque, current etc) to predict the position of the head of the steel strip. With even a temporary mill shutdown of 20 minutes costing many thousands of pounds, the financial rewards could be considerable.

# Bibliography


[1] FERRY, H., *Electricity Supply 1.* Heinemann, 1970.

[2] CHENEY, M., *Tesla - man out of time.* Prentice Hall, 1981.

[3] VON SIEMENS, W., *Inventor and Entrepeneur - Recollections of Werner von Siemens.* P. L. Humphries & Co Ltd, 1980.

[4] SHARLIN, *The making of the electrical age.* Schuman, 1963.

[5] BIS MONTHLY PUBLICATION, 'Spaceflight', tech. rep., British Interpalnetary Society, 1993 Onwards.

[6] BERRIE, T.W., *Power System Economics.* P. Peregrinus & IEE, 1980.

[7] TAYLOR, E. AND BOAL, G., *Electrical Power Distribution.* Arnold, 1966.

[8] CULP, A., *Principles of Energy Conversion.* McGraw Hill, 1979.

[9] HUNT, D., *Handbook of Energy Technology.* Van Nostrand, 1982.

[10] PARKER, S., *McGraw Hill Encyclopedia of Energy.* McGraw Hill, 1977.

[11] NGC, 'NGC Seven Year Statement for the years 1994/5 to 2000/2001', tech. rep., The National Grid Company plc, March 1994.

[12] JONES, B., *New approaches to the design and economics of EHV transmission plant.* Premagon Press, 1972.

[13] ATABEKOV, *The relay protection of high voltage networks.* Premagon Press, 1960.

[14] NEUENSWANDER, J.R., *Modern Power Systems.* Intertext Books, 1971.

[15] HONEYCUTT, R.A., *Electromechanical Devices, Theory, Applications and Troubleshooting.* Prentice Hall, 1986.

[16] HINDMARSH, J., *electrical Machines and their Applications.* Permagon Press, 1970.

[17] KIMBARK, E.W., *Power System Stability VIII.* Wiley, 1956.

[18] SAY, M.G. AND TAYLOR, E.O., *Direct Current Machines.* Pitman, 1980.

[19] WEEDY, B.M., *Electric Power Systems.* Wiley, 1987.

[20] GIARRATANO, J. AND RILEY, G., *Expert systems—principles and programming.* PWS-Kent, 1989.

[21] FU, L., *Neural Networks in Computer Intelligence.* Heinemann, 1994.

[22] ZIMMERMANN, H., *Fuzzy set theory.* Kluwer Academic Publishers, 1991.

[23] HAYKIN, S., *Neural Networks: a comprehensive foundation.* Macmillan, 1994.

[24] ZURADA, J.M., *An introduction to artificial neural systems.* West, 1992.

[25] ORTIZ, S.A., 'The development of interconnected power systems and energy control centers in the united states and brazil', in *Proceedings of Int. Symposium on computerised operation of power systems*, pp. 272–287, 18-20 August 1975.

[26] GRID SYSTEM MANAGEMENT, 'The National Grid Control Center', tech. rep., The National Grid Company plc, July 1994.

[27] GRID SYSTEM MANAGEMENT, 'Grid System Management', tech. rep., The National Grid Company plc, July 1994.

[28] NATIONAL GRID COMPANY PLC, 'Five Center Grid Control Project - Network Applications Demonstration'. NGC document.

[29] DUNNETT, R.M. AND DUCKWORTH, S., 'An experimental study of centralised economic dispatch in the cegb', *IEE 2nd International Conference on Power System Operation and Control*, vol. 1, pp. 7–12, 1986.

[30] THORNTON, L.A., SNYDER, W.L., CHRISTIE, R.D., AND BOWMAN, D.H., 'Energy control system: An advanced approach for translata utilities', *IEEE Trans Pow Sys*, vol. PAS-102, pp. 3446–3452, 1983.

[31] KUNDUR, P., MORISON, G.K., BALU, N.J., AND LAUBY, M.G., 'Advanced software for power system analysis', in *IEE Workshop on 'New Issues in Power System Simulation', Caen, France*, pp. 20–27, 30-31 March 1992.

[32] ALVARADO, F.L. AND TINNEY, W.F., 'State estimation using augmented blocked matrices', *IEEE Trans Pow Sys*, vol. 5, no. 3, pp. 911–921, 1990.

[33] BELL, K., 'State estimation for an on-line dynamic security assessor', tech. rep., Power and Energy Systems Group, School of Electronic and Electrical Engineering, University of Bath, 1993.

[34] SASAKI, H., KUBOKAWA, J., YORINO, N., TAKEHARA, J., AND KITAGAWA, M., 'A parallel computation of state estimation by transputer', *IEE Third International Conference on Power System Monitoring and Control*, pp. 261–263, 1991.

[35] MONTICELLI, A. AND GARCIA, A., 'Fast decoupled state estimators', *IEEE Trans Pow Sys*, vol. 5, no. 2, pp. 556–564, 1990.

[36] EKWUE, A., LI, F., AND MACQUEEN, J., 'An interpolatory demand computation algorithm using half-hour average data', in *Proceedings of 11th Power Systems Computation Conference*, pp. 469–476, 30th August–3rd September 1993.

[37] BAUMAN, T., STRASSER, H., AND LANDRICHTER, H., 'Short term load forecasting methods in comparison : Kohonen learning, backpropogation learning, multiple regression analysis and kalman filters', in *Proceedings of 11th Power Systems Computation Conference*, pp. 445–452, 30th August–3rd September 1993.

[38] HAPP, H.H., 'Optimal Power Dispatch - A comprehensive survey', *IEEE Trans. on Power Apparatus and Systems*, vol. PAS-96, no. 3, pp. 841–850, 1977.

[39] CARPENTIER, J., 'Extended security constrained optimal power flow, a basic tool for integrated secure economic operation', *Proc PSCC 11*, pp. 1265–1278, 1993.

[40] ALSAC, O., BRIGHT, J., PRAIS, M., AND STOTT, B., 'Further developments in lp-based optimal power flow', *IEEE Trans. on Power Systems*, vol. 5, no. 3, pp. 697–711, 1990.

[41] SUN, D.I., ASHLEY, B., BREWER, B., HUGHES, A., AND TINNEY, W.F., 'Optimal power flow by Newton approach', *IEEE Trans Pwr App Sys*, vol. PAS-103, no. 10, pp. 2864–2875, 1984.

[42] CHAI, J.S., ZHU, N., BOSE, A., AND TYLAVSKY, D., 'Parallel newton type methods for power system stability analysis using local and shared memory multiprocessors', *IEEE PES Winter Meeting, 1991*, 1991.

[43] BELL, K.R.W., DANIELS, A.R., AND DUNN, R.W., 'A fuzzy expert system for low-cost security constrained reactive dispatch', in *Proc. Stocholm Power Tech*, pp. 668–673, 18-22 June 1995.

[44] STOTT, B., ALSAC, O., AND MONTICELLI, A.J., 'Security analysis and optimisation', *Proc IEEE*, vol. 75, no. 12, pp. 1623–1644, 1987.

[45] Dewey, A.G. and Tuel, W.G., 'Power system security indices', in *7th Power Systems Computation Conference, Boston, Massachusetts*, pp. 365–373, 23-26 May 1971.

[46] Chang, C.L. and Hsu, Y.Y., 'A new approach to dynamic contingency selection', *IEEE Trans. on Power Systems*, vol. 5, no. 4, pp. 1524–1528, 1990.

[47] Ekwue, A.O. and Laing, W.D., 'Critical evaluation of voltage based contingency selection algorithms for on-line applications', in *10th Power Systems Computation Conference, Graz, Austria*, pp. 835–839, 19-24 August 1990.

[48] Sobajic, D.J. and Yoh-Han, P., 'An artificial intelligence system for power system contingency screening', *IEEE Trans. on Power Systems*, vol. 3, no. 2, p. 647, 1988.

[49] Ekwue, A.O., 'On the ranking of contingencies for on-line applications: Extended formulation', *Electric Power Systems Research*, no. 21, pp. 87–90, 1991.

[50] Pao, Y.H. and Sobajic, D.J., 'Power system static security assessment using the kohonen neural network classifier', in *Power Industry Computer Application Conference*, p. 270, PICA, May 1991.

[51] El-Sharkawi, M.A., Marks, R.J., Damborg, M.J., Atlas, L.E., and Cohn, A.D., 'Artificial neural networks as operator aid for on-line static security assessment of power systems', in *10th Power Systems Computation Conference, Graz, Austria*, p. 895, 19-24 August 1990.

[52] Niebur, D. and Germond, A.J., 'Power flow classification for static security assessment', *The international forum on Application of Neural Networks to Power Systems*, pp. 83–88, 1991.

[53] EKWUE, A.O. AND MACQUEEN, J.F., 'Comparison of load flow solution methods', *Electric Power Systems Research*, vol. 22, pp. 213–222, 1991.

[54] EKWUE, A.O., LAING, W.D., AND MACQUEEN, J.F., 'On-line power systems security assessment', in *IEE Control 91*, pp. 29–31, IEE, 1991.

[55] HOLEN, A., XU, F., AND STOA, P., 'Identification of critical power system contingencies. a heuristic method combining overload and low voltage problems', in *Proceedings of Intelligent System Application to Power Systems*, pp. 179–186, 5th-9th September 1994.

[56] EPRI, 'On-line transient stability assessment', in *EPRI Seminar and Demonstration, Toronto, Ontario, Canada*, EPRI, 6-7 December 1993.

[57] NGC, 'A review of transmission security standards', tech. rep., The National grid Company plc for OFFER, August 1994.

[58] PLUMPTRE, P.H. AND MANNING, P.T., 'The practical analysis of a cegb transmission constraint', in *Universities Power Engineering Conference*, pp. 279–283, 1989.

[59] EPRI, 'Dynamic security assessment for power systems: Research plan', Tech. Rep. EL-4958, EPRI, 1987.

[60] TASK FORCE 39.03, 'Exploring user requirements of expert systems in power system operation and control', *Electra Journal*, vol. 146, pp. 69–83, 1993.

[61] TANAKA, H., TSUCHIMORI, N., WADA, N., KAWAKAMI, J., SUZUKI, M., AND SEKINE, Y., 'Research and development on expert systems applications to power systems in japan', *Elec Pwr and Energy Sys*, vol. 14, no. 2/3, pp. 71–85, 1992.

[62] EL-KADY, FOUAD, A.A., LIU, C.C., AND VENKATARAMAN, S., 'Use of expert systems in dynamic security assessment of power systems', in *10th Power Systems Computation Conference, Graz, Austria*, p. 913, 19-24 August 1990.

[63] DILLON, THARAM, S., AND LAUGHTON, M.A., *Expert system applications in power systems.* Prentice Hall (UK) Ltd, 1990.

[64] CHRISTIE, R.D. AND TALUKDAR, S.N., 'Expert systems for security assessment; a preliminary design', *IEEE Trans. on Power Systems*, vol. 3, no. 2, p. 653, 1988.

[65] XUE, Y., GAO, Z., ZHU, J., AND LIU, J., 'A planning descision support expert system for transient and dynamic security of power systems', in *Second Symposium on Expert Systems Application to Power Systems, Seattle*, pp. 218–224, 17-20 July 1989.

[66] JOHNSON, R.B.I. AND CORY, B.J., 'Expert decision-support in power systems operation', tech. rep., Imperial College of Science and Technology, UK.

[67] HSU, Y.Y. AND SU, C.C., 'A rule-based expert system for steady-state stability analysis', *IEEE Trans Pwr Sys*, vol. 6, no. 2, pp. 771–777, 1991.

[68] R.CRIADO, D.MATAUCO, F.LASHERAS, J.L.FERNANDEZ, P.BASAGOITI, AND J.SERNA, 'Seacon: an on-line expert system for contingency analysis and corrective solutions in transmission', *Elec. Pwr. and Energy Sys.*, vol. 14, no. 4, pp. 303–308, 1992.

[69] CHENG, S., MALIK, O., AND HOPE, G., 'An expert system for voltage and reactive power control of a power system', *IEEE Trans Pwr Sys*, vol. 3, no. 4, pp. 1449–1455, 1988.

[70] Cauley, G., Kumar, A.B.R., Brandwajn, V., and Ipakchi, A., 'Artificial intelligence applications in on-line dynamic security assessment', *Proc PSCC 11*, vol. 2, pp. 881–887, 1993.

[71] Aggoune, M., El-Sharkawi, M.A., Park, D.C., Damborg, M.J., and Marks, R.J., 'Preliminary results on using artificial neural networks for security assessment', *IEEE Trans. on Power Systems*, vol. 6, no. 2, p. 890, 1991.

[72] Sobajic, D.J. and Pao, Y.H., 'Artificial neural-net based dynamic security assessment for electric power systems', *IEEE Trans. on Power Systems*, vol. 4, no. 1, p. 220, 1989.

[73] Ranjit-Kumar, A.B. and El-Sharkawi, M., 'Neural networks for dynamic security assessment of large-scale power systems: requirements overview', in *First international forum on applications of neural networks to power systems, Seattle*, p. 65, 23-26 July 1991.

[74] Pao, Y.H. and Sobajic, D.J., 'Combined use of unsupervised and supervised learning for dynamic security assessment', in *Power Industry Computer Application Conference, Baltimore, Maryland*, pp. 278–284, 7-10 May 1991.

[75] Task Force on Terms & Definitions, System Dynamic Perfrormance Subcommittee, 'Proposed terms & definitions for power system stability', *IEEE Trans. on Power Apparatus and Systems*, vol. PAS-101, no. 7, pp. 1894–1898, 1982.

[76] Branch, O.P., 'The rasm roadshow - an operations guide to running rasm studies', tech. rep., CEGB.

[77] Xue, Y., 'Transient stability limits of interface flows', in *International Federation of Automatic Control : International Symposium on Power Systems modeling and control applications*, 5-8 September 1988.

[78] EPRI EL-367, 'Long Term Power System Dynamics Phase 2', tech. rep., EPRI, 1977.

[79] RUDNICK, H., HUGHES, F.M., AND BRAMELLER, A., 'Steady state instability : simplified studies in multimachine power systems', in *IEEE PICA, Houston, Texas*, pp. 137–144, 17-20 May 1983.

[80] LACHS, W. AND SUTANTO, D., 'Different types of voltage instability', *IEEE Trans. on Power Systems*, vol. 9, pp. 1126–1134, 1994.

[81] BOLTON, K.G.W. AND HODGES, C.J., '32-bit computer based scada system for the Yorkshire Electricity Board', tech. rep., Yorkshire Electricity Board, UK.

[82] EDWARDS, A.R., 'Progress on implementation of scada system', tech. rep., Power and Energy Systems Group, School of Electronic and Electrical Engineering, University of Bath, UK., 1993.

[83] KRUMPHOLZ, G., CLEMENTS, K., AND DAVIS, P., 'Power system observability: A practical algorithm using network topology', *IEEE Trans Pwr App Sys*, vol. PAS-99, no. 4, pp. 1534–1542, 1980.

[84] OCKWELL, G. AND KREGER, R., 'The impact of hardware on open archetecture design', *IEEE Trans. on Power Systems*, vol. 9, pp. 1–5, 1994.

[85] LANGHORNE, C., CARLSON, C., AND CHOWDHURY, S., 'Wide area network performance modeling of distributed energy management systems', *IEEE Trans. on Power Systems*, vol. 9, pp. 730–735, 1994.

[86] CHAN, K.W., EDWARDS, A.R., DUNN, R.W., DANIELS, A.R., AND PADGET, J.A., 'Interactive online dynamic security assessment of large complex power systems part 1 : Contingency analysis', 1995.

[87] CHEUNG, K., PALIZA, R., MA, T., ATHAY, T., AND ZUK, J., 'An expert system guided on-line dynamic security assessment system', in *ISAPS 1994*, no. 1, pp. 263–270, 1994.

[88] DEMAREE, K., ATHAY, T., CHEUNG, K.W., MANSOUR, Y., VAAHEDI, E., CHANG, A.Y., CORNS, B.R., AND GARRETT, B.W., 'An on-line dynamic security analysis system implementation', *IEEE Trans. on Power Systems*, vol. 9, no. 4, pp. 1716–1722, 1994.

[89] MANSOUR, Y., VAAHEDI, E., CHANG, A.Y., CORNS, B.R., GARRETT, B.W., DEMAREE, K., ATHAY, T., AND CHEUNG, K., 'B.c. hydro's on-line transient stability assessment (tsa) model development, analysis and post-processing', *IEEE Trans. on Power Systems*, vol. 10, pp. 241–253, 1995.

[90] KUMAR, A.B.R., BRANDWAJN, V., IPAKCHI, A., AND ADAPA, R., 'Integrated framework for dynamic security analysis', in *Proc. Stocholm Power Tech*, pp. 382–387, 18-22 June 1995.

[91] LAM, B.P., KAZIBWE, W.E., REPPEN, N.G., AND WOODZELL, G.W., 'An investigation of expert systems applications to contingency selection and analysis', in *Second symposium on expert systems applications to power systems, Seattle*, pp. 165–169, 17-20 July 1989.

[92] VEMURI, S. AND USHER, R.E., 'On-line automatic contingency selection algorithms', *IEEE Trans. on Power Apparatus and Systems*, vol. PAS-102, no. 2, pp. 346–354, 1983.

[93] EJEBE, G.C. AND WOLLENBERG, B.F., 'Automatic contingency selection', in *IEEE Trans. on Power Apparatus and Systems*, vol. 98, pp. 97–104, 1979.

[94] IRISARRI, G.D. AND SASSON, A.M., 'An automatic contingency selection method for on-line security analysis', in *IEEE Trans. on Power Apparatus and Systems*, vol. 100, pp. 1838–1843, 1981.

[95] BERRY, T., CHAN, K.W., DANIELS, A.R., AND DUNN, R.W., 'Interactive real-time simulation of the dynamic behavoir of large power systems', pp. 5–10, 1993.

[96] DALE, L.A., *Real-Time Modelling of Multimachine Power System.* PhD thesis, Bath University, School of Electrical Engineering, 1986.

[97] STAGG, T.A., *A Parallel Computer Based Study of the Automatic Control of Power Generation.* PhD thesis, Bath University, School of Electrical Engineering, 1992.

[98] CHAN, K.W., *A Power System Simulator to model the Transient Mode of Operation of the (UK) National Supergrid in real-time.* PhD thesis, Bath University, School of Electrical Engineering, 1992.

[99] HARA, T., KOBAYASHI, N., TAKEI, A., KOYANAGI, K., TANOMURA, K., AND ARAI, J., 'Development of a damping analysis program for multi-generator power systems', *IEEE Trans. on Power Systems*, vol. 9, no. 4, pp. 1803–1810, 1994.

[100] CHEN, Y. AND BOSE, A., 'Direct ranking for voltage contingency selection', in *IEEE Trans. on Power Systems*, no. 4, pp. 1335–1341, 1989.

[101] NYE, A., *Xlib Programming Manual for version 11*, vol. 1. O'Reilly & Associates, Inc, 1 ed., 1988.

[102] MAHADEV, P. AND CHRISTIE, R., 'Envisioning power system data: Vulnerability and severity representations for static security assessment', *IEEE Trans. on Power Systems*, vol. 9, no. 4, pp. 1915–1920, 1994.

[103] EDWARDS, A., 'Discussion of oasis trial results', tech. rep., Power and Energy Systems Group, University of Bath, Bath, UK, 1995.

[104] Chan, K.W., Edwards, A.R., Dunn, R.W., and Daniels, A.R., 'Real-time electromechanical transient simulator for on-line applications', in *Proc. of First International Conference on Digital Power System Simulators – ICDS'95*, pp. 259–263, 5-7 April 1995.

[105] Arrillaga, J. and Arnold, C., *Computer analysis of power systems.* John Wiley & Sons, 1990.

[106] Berry, T., Daniels, A.R., and Dunn, R.W., 'Real time simulation of power system transient behaviour', vol. 336, pp. 122–127, 1991.

[107] Heller, D., *Motif Programming Manual for OSF/Motif version 11*, vol. 6. O'Reilly & Associates, Inc., 1991.

[108] Geist, A.L., Beguelin, A., Donjarra, J.J., Jiang, W., Manchek, R., and Sunderam, V.S., 'PVM3 Users Guide and Reference Manual', tech. rep., Oak Ridge National Laboratory, Oak Ridge, Tennessee 37831, 1994.

[109] Beguelin, A., Donjarra, J.J., Geist, G.A., Manchek, R., and Sunderam, V.S., 'The PVM and HeNCE Projects', tech. rep., Oak Ridge National Laboratory, Oak Ridge, Tennessee 37831, 1993.

[110] Sunderam, V., Geist, G., Dongarra, J., and Manchek, R., 'The pvm concurrent computing system: Evolution, experiences and trends', *Parallel Computing*, vol. 20, pp. 531–545, 1994.

[111] Geist, A., Beguelin, A., Dongarra, J., Jiang, W., Manchek, R., and Sunderam, V., *PVM: A User's Guide and Tutorial for Networked Parallel Computing.* MIT Press, Cambridge, Massachusetts, 1994.

[112] Bach, M., *The design of UNIX Operating System.* Prentice Hall, 1986.

[113] BERRY, T., DANIELS, A.R., AND DUNN, R.W., 'Real time simulation of power system transient behaviour', *Proc. 3rd Int. Conf. 'Power System Monitoring and Control*, vol. 336, pp. 122–127, 1991.

[114] BERRY, T., CHAN, K.W., DANIELS, A.R., AND DUNN, R.W., 'Interactive real-time simulation of the dynamic behavoir of large power systems', in *Proc. IEE of Japan Power & Energy '93*, pp. 5–10, 1993.

[115] SPRATLEY, R.B., 'The transient stability program RASM06', Tech. Rep. CISD/CC/N992, CEGB Computing Centre, 1987.

[116] BERRY, T., DANIELS, A.R., AND DUNN, R.W., 'Parallel processing of sparse power system equations', *IEE Proceedings on Generation, Transmission and Distribution*, vol. 141, no. 1, pp. 68–74, 1994.

[117] KAKIMOTO, N., OHNOGI, Y., MATSUDA, H., AND SHIBUYA, H., 'Transient stability analysis of large-scale power system by lypanov's direct method', *IEEE Trans. on Power Apparatus and Systems*, vol. PAS-103, no. 1, pp. 160–167, 1984.

[118] FOUAD, A.A. AND VITTAL, V., 'State of the art paper : The transient energy function method', *International Journal of Electric Power and Energy Systems*, vol. 10, no. 4, pp. 233–246, 1988.

[119] EL-KADY, M.A., TANG, C.K., CARVALHO, V.F., FOUAD, A.A., AND VITTAL, V., 'Dynamic security assessment utilizing the transient energy function method', *IEEE Trans. on Power Systems*, vol. PWRS-1, no. 3, pp. 284–291, 1986.

[120] LO, K.L. AND HILAL, H., 'Direct assessment of power systems transient stability via lypanov method', in *25th Universities Power Engineering Conference*, pp. 227–230, 1990.

[121] A.Fouad, A., Zhou, Q., and Vital, V., 'System vulnerability as a concept to assess power system dynamic security', tech. rep., Iowa State University, Ames, Iowa 50011, 1992.

[122] Xue, Y., Cutsem, T.V., and Ribbens-Pavella, M., 'Extended equal area criterion justification, generalizations, applications', *IEEE Trans. on Power Systems*, vol. 4, no. 1, pp. 44–52, 1989.

[123] Xue, Y. and Ribbens-Pavella, M., 'Extended equal area criterion : An analytical ultra–fast method for transient stability assessment and preventative control of power systems', *EPES*, vol. 11, no. 2, pp. 131–149, 1989.

[124] 'Artificial neural networks for power systems - a literature survey', tech. rep., CIGRE Task Force 38-06-06, 1993.

[125] Young, D., Lo, K., McDonald, J., Howard, R., and Rye, J., 'Development of a practical expert system for alarm processing', in *IEE Proceedings pt C*, vol. 140, pp. 437–447, 1993.

[126] Akimoto, Y. and Tanaka, H., 'Application of expert system technology to power system stability studies', in *Proceedings of Third Symposium on Expert System Application to Power Systems*, April 1991.

[127] Burt, G.M. and McDonald, J.R., 'Potential advantages of a diagnostic expert system for assisting operator response to system events', tech. rep., University of Strathclyde, UK.

[128] CIGRE Task Force 39.03, 'Exploring user requirements of expert systems in power system operation and control', tech. rep., CIGRE, 1993.

[129] Wehenkel, L., 'Artificial intelligence methods for on–line transient stability assessment of electric power systems', in *Proceedings of First Symposium on Expert System Application to Power Systems*, August 1988.

[130] WEHENKEL, L. AND RIBBENS-PAVELLA, M., 'Decision trees and transient stability of electric power systems', *Automatica*, vol. 27, no. 1, pp. 115–134, 1991.

[131] WEHENKEL, L., PAVELLA, M., EUXIBIE, E., AND HEILBRONN, B., 'Decision tree based transient stability method – a case study', *IEEE Trans. on Power Systems*, vol. 8, pp. 459–469, February 1994.

[132] HATZIARGYRIOU, N., PAPATHANASSIOU, S., PECAS-LOPES, J., AND ACKER, V., 'Pattern recognition versus decision trees methods - a case study in fast dynamic secuirty assessment of autonomous power systems with a large penetration from renewables', in *Proc. of 10th PSCC*, pp. 513–519, 1994.

[133] UCHIDA, N. AND NAGAO, T., 'A new eigen-analysis method of steady state stability studies for large power systems: s matrix method', in *IEEE PICA, Montreall, Quebec, Canada*, pp. 259–265, 18-22 May 1987.

[134] NESS, J.E. AND BORATYNSKA-STADNICKA, D.J., 'A partitioning algorithm for finding eigenvalues and eigenvectors', in *10th Power Systems Computation Conference, Graz, Austria*, pp. 91–98, 19-24 August 1990.

[135] WANG, L. AND SEMLYEN, A., 'Application of sparse eigenvalue techniques to the small signal stability analysis of large power systems', in *IEEE PICA, Seattle, Washington*, pp. 358–365, 1-5 May 1989.

[136] CHAN, K., 'Report on dynamic stability assessment', tech. rep., University of Bath for National Grid Company plc, 1995.

[137] PANG, C.K., PRABHAKARA, F.S., EL-ABIAD, A.H., AND KOVIO, A.J., 'Security evaluation in power systems using pattern recognition', *IEEE Trans. on Power Apparatus and Systems*, vol. PAS-93, pp. 969–976, 1974.

[138] KOIZUMI, K., SAITO, O., SATO, M., MASEGI, K., AND UDO, M., 'Fast transient stability study using pattern recognition', in *5th Power Systems Computation Conference, Cambridge*, pp. 1–15, 1-5 September, 1975.

[139] HAKIMMASHHADI, H. AND HEYDT, T.G., 'Fast transient security assessment', *IEEE Trans. on Power Apparatus and Systems*, vol. PAS-102, no. 12, pp. 3816–3824, 1983.

[140] YAMASHIRO, S. AND KOIKE, T., 'Fast transient security assessment and enhancement of electric power systems using pattern recognition', in *8th Power Systems Computation Conference, Helsinki*, pp. 891–897, 19-24 August 1984.

[141] HAKIM, H., 'Application of pattern recognition in transient security assessment', *Electric Machines and Power Systems*, vol. 20, pp. 1–15, 1990.

[142] FIDALGO, J., LOPES, J.P., MIRANDA, V., AND ALMEIDA, L., 'Fast assessment of transient stability margins by a neural network approach', *Proc PSCC 11*, vol. 1, pp. 81–88, 1993.

[143] SOBAJIC, D. AND PAO, Y., 'On-line transient stability evaluation by associative dichotomous classification', *Proc PSCC 11*, vol. 2, pp. 859–864, 1993.

[144] NIEBUR, D. AND GERMOND, A.J., 'Power system static security assessment using the kohonen neural network classifier', in *Power Industry Computer Application Conference, PICA 91*, p. 270, PICA, May 1991.

[145] CHOWDHURY, BADRUL, H., WILLAMOWSKI, AND BOGDAN, M., 'Security assessment using neural computing', in *First International forum on Applications of neural networks to power systems*, p. 54, 23-26 July 1991.

[146] SONG, Y., QINGYU, Z., AND YINGDUO, H., 'Framework of fast stability assessment of power system by neural network based pattern recognition', *IEE*

*International Conference on Power System Monitoring and Control*, pp. 578–580, 1991.

[147] AGGOUNE, M., ATLAS, L., COHN, D., DAMBOURG, M., EL-SHARKAWI, M., AND MARKS, R., 'Artificial neural networks for power system static security assessment', in *International Symposium on Circuits and Systems, 1989*, pp. 490–494, May 1989.

[148] THOMAS, R., SAKK, E., KU, B., AND CHIANG, H., 'On-line security screening using an artificial neural network', in *International Symposium on Circuits and Systems, 1990*, pp. 2921–2924, May 1990.

[149] MORI, H., TAMARU, Y., AND SENJI, T., 'An artificial neural-net based technique for power system dynamic stability with kohonen model', in *IEEE Trans. on Power Systems*, p. 856, May 1992.

[150] HOBSON, E. AND ALLEN, G.N., 'Effectiveness of artificial neural networks for first swing stability determination of practical systems', *IEEE Trans. on Power Systems*, vol. 9, pp. 1062–1068, May 1994.

[151] ZHOU, Q., DAVIDSON, J., AND FOUAD, A.A., 'Application of artificial neural networks in power system security and vulnerability assessment', *IEEE Trans. on Power Systems*, vol. 9, no. 1, pp. 525–532, 1994.

[152] EBERHART, R.C. AND DOBBINS, R.W., *Neural Network PC Tools.* Academic Press, Inc., 1990.

[153] STUBBS, D., *Neurocomputers.* M.D.Computing, 1988.

[154] ARBIB, M.A., *Brains, Machines and Mathematics.* Springer Verlag, 1987.

[155] DAYHOFF, J., *Neural Network Archetectures: An introduction.* Van Nostrand Reinhold, 1990.

[156] ROSENBLATT, F., 'The perceptron: a probabalistic model for information storage and organisation in the brain', *Psychological Review*, vol. 65, pp. 386–408, 1958.

[157] KOHONEN, T., *Self Organisation and Associative Memory.* Springer-Verlag, 1988.

[158] AIYER, S.V.B., NIRANJAN, M., AND FALLSIDE, F., 'A theoretical investigation into the performance of the hopfield model', *IEEE Trans. on Neural Networks*, vol. 1, no. 2, pp. 204–215, 1990.

[159] MJOLSNESS, E., GARRETT, C.D., AND MIRANKER, W.L., 'Multiscale optimisation in neural nets', *IEEE Trans. on Neural Networks*, vol. 2, no. 2, pp. 263–274, 1991.

[160] BOUZERDOUM, A. AND PATTISON, T.R., 'Neural networks for quadratic optimization with bound constraints', *IEEE Trans. on Neural Networks*, vol. 4, pp. 293–236, March 1993.

[161] CHICHOKI, A. AND UNBEHAUEN, R., 'Neural networks for solving systems of linear equations and related problems', *IEEE Trans. on Circuits and Systems*, vol. 39, pp. 124–138, February 1992.

[162] LEE, B.W. AND SHEU, B.J., 'Modified hopfield neural networks for retrieving the optimal solution', *IEEE Trans. on Neural Networks*, vol. 2, pp. 137–142, January 1991.

[163] LINDEN, A. AND KINDERMANN, J., 'Inversion of multilayer nets', in *Proceedings of International Joint Conference on Neural Networks, Seattle, WA*, pp. 425–430, August 1989.

[164] FIESLER, E., 'Neural network formalization', tech. rep., Institut Dalle Molle d'Intelligence Artificielle Perceptive, Martigny, Suisse, 1992.

[165] PRECHALT, L., 'Answers to questions about Neural Networks', *Newsgroup comp.ai.neural-nets*, 1994.

[166] EL-SHARKAWI, M.A., 'Neural network and its anciliary techniques as applied to power systems', in *Artificial Intelligence applications in power systems*, pp. 3/1–3/6, April 1995.

[167] RAUBER, T.W., BARATA, M.M., AND STEIGER-GARCAO, A.S., 'A toolbox for analysis and visualization of sensor data in supervision', tech. rep., Departmento de Informatica, Intelligent Robotics Group, 285 Monte de Caparica, Portugal.

[168] J. W. TUKEY, R.A.B. AND CLEVELAND, W.S., 'Discussion of graphic comparisons of several linked aspects', *Journal of Computational and Graphical Statistics*, vol. 2, pp. 41–48, 1993.

[169] SAMMON, J.W., 'A nonlinear mapping for data structure analysis', *IEEE Trans. on Computers*, vol. 18, pp. 401–409, 1969.

[170] FISHER, R., 'The use of multiple measurements in taxonomic problems', *Annals of Eugenics*, vol. 7, pp. 179–188, 1936.

[171] LEWIS, B. AND BUNKER, R., 'Max - an advanced parallel computer for space applications', tech. rep., NASA, Jet Propulsion Laboratory, California Institute of Technology, Pasadena, California, USA, 1991.

[172] VOUK, M. AND MCALLISTER, D., 'Software reliability through fault avoidance and fault tolerance', tech. rep., North Carolina State University, Raleigh, North Carolina, USA, 1992.

[173] ALVARADO, F., HU, Y., RINZIN, C., AND ADAPA, R., 'Visualisation of spatially differentiated security margins', in *Proceedings of 11th Power Systems Computation Conference*, vol. 1, pp. 519–525, 1993.

[174] ALVAREZ, C. AND BELENGUER, E., 'Object orientated environment for distribution applications', in *Proceedings of 11th Power Systems Computation Conference*, vol. 1, pp. 155–162, 1993.

[175] ALBA, J., SANCHEZ, J., SANCHEZ, E., AND CENTENO, E., 'A switching operations planner for subtransmission networks', in *Proceedings of 11th Power Systems Computation Conference*, vol. 1, pp. 247–255, 1993.

[176] DO VALE, A.A., GONCALVES, M., AND VALE, Z., 'Improving man-machine interaction in control centers: the importance of a full-graphics interface', in *Proceedings of 11th Power Systems Computation Conference*, vol. 1, pp. 395–401, 1993.

[177] STOTT, B. AND ALSAC, O., 'Fast decoupled load flow', *IEEE Trans Pwr App Sys*, vol. PAS-93, no. 3, pp. 859–869, 1974.

[178] 'Stuttgart neural network simulator version 3.2', tech. rep., Institute for Parallel and Distributed High Performance Systems, University of Stuttgart, Germany.

[179] MORI AND HIROYUKI, 'An artificial neural-net based method for estimating power system dynamic stability index', in *First international forum on applications of neural networks to power systems, Seattle*, p. 129, 23-26 July 1991.

Appendix A

# Box Plots

This appendix contains box plots for the composite indices selected for the transient and oscillatory instability screens for the full national grid system.

## A.1 Transient Stabilty

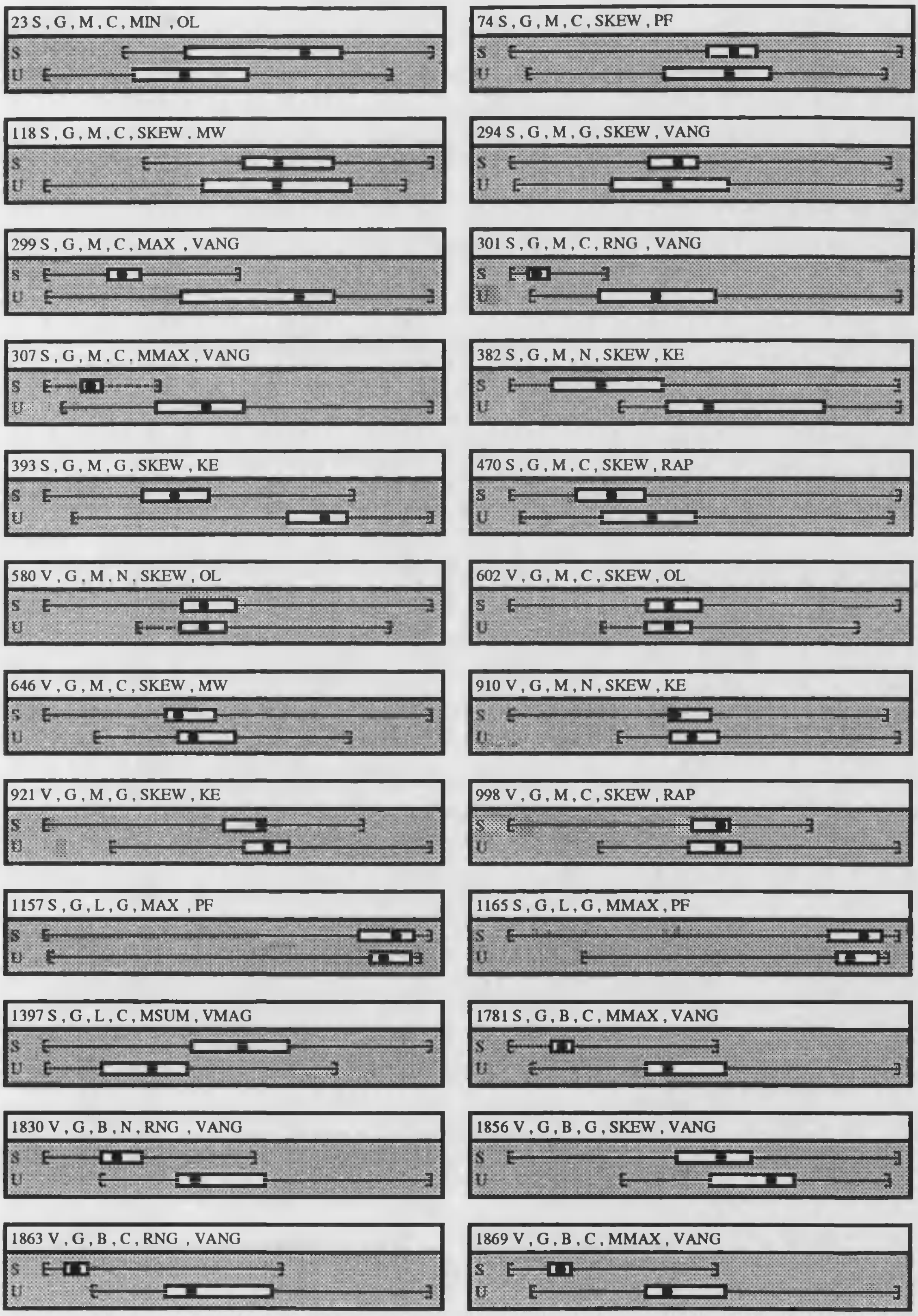
23 S , G , M , C , MIN , OL
74 S , G , M , C , SKEW , PF
118 S , G , M , C , SKEW . MW
294 S , G , M , G , SKEW , VANG
299 S , G , M , C , MAX , VANG
301 S , G , M , C , RNG , VANG
307 S , G , M . C , MMAX , VANG
382 S , G , M , N , SKEW , KE
393 S , G , M , G , SKEW , KE
470 S , G , M , C , SKEW , RAP
580 V , G , M . N , SKEW , OL
602 V , G , M , C , SKEW , OL
646 V , G , M , C , SKEW , MW
910 V , G , M , N , SKEW , KE
921 V , G , M , G , SKEW , KE
998 V , G , M , C , SKEW , RAP
1157 S , G , L , G , MAX , PF
1165 S , G , L , G , MMAX , PF
1397 S , G , L , C , MSUM , VMAG
1781 S , G , B , C , MMAX , VANG
1830 V , G , B , N , RNG , VANG
1856 V , G , B , G , SKEW , VANG
1863 V , G , B , C , RNG , VANG
1869 V , G , B , C , MMAX , VANG

## A.2 Oscillatory Stability

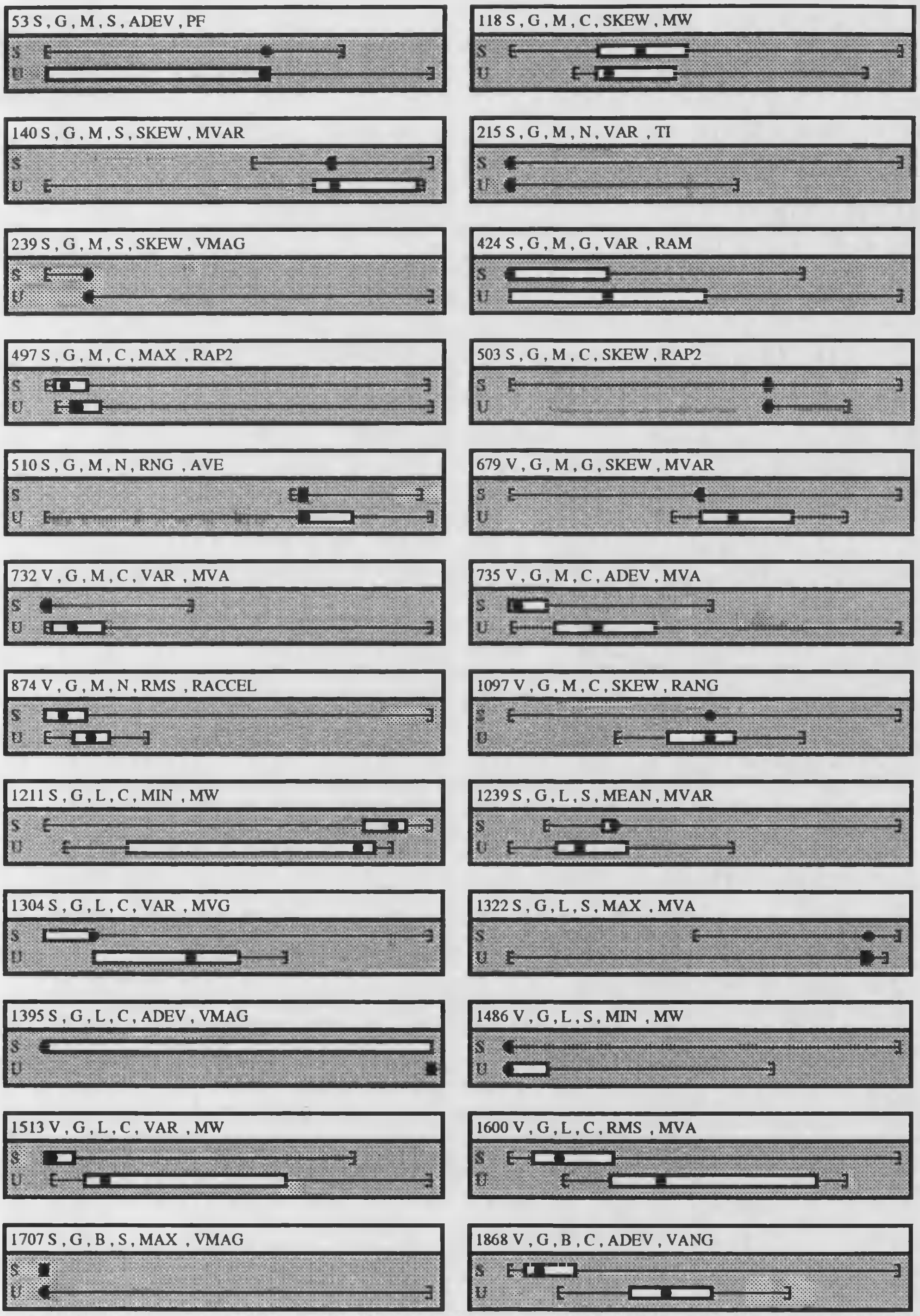
53 S , G , M , S , ADEV , PF
S
U
118 S , G , M , C , SKEW , MW
S
U
140 S , G , M , S , SKEW , MVAR
S
U
215 S , G , M , N , VAR , TI
S
U
239 S , G , M , S , SKEW , VMAG
S
U
424 S , G , M , G , VAR , RAM
S
U
497 S , G , M , C , MAX , RAP2
S
U
503 S , G , M , C , SKEW , RAP2
S
U
510 S , G , M , N , RNG , AVE
S
U
679 V , G , M , G , SKEW , MVAR
S
U
732 V , G , M , C , VAR , MVA
S
U
735 V , G , M , C , ADEV , MVA
S
U
874 V , G , M , N , RMS , RACCEL
S
U
1097 V , G , M , C , SKEW , RANG
S
U
1211 S , G , L , C , MIN , MW
S
U
1239 S , G , L , S , MEAN , MVAR
S
U
1304 S , G , L , C , VAR , MVG
S
U
1322 S , G , L , S , MAX , MVA
S
U
1395 S , G , L , C , ADEV , VMAG
S
U
1486 V , G , L , S , MIN , MW
S
U
1513 V , G , L , C , VAR , MW
S
U
1600 V , G , L , C , RMS , MVA
S
U
1707 S , G , B , S , MAX , VMAG
S
U
1868 V , G , B , C , ADEV , VANG
S
U

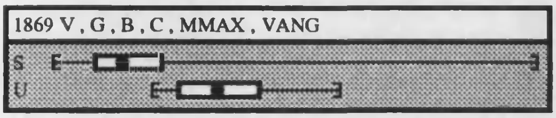
1869 V , G , B , C , MMAX , VANG
S
U

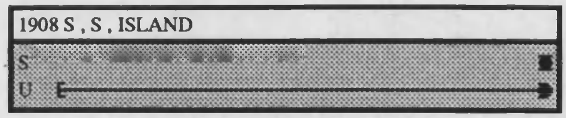
1908 S , S , ISLAND
S
U

# Appendix B

# Published Work

This appendix contains copies of papers which have been published concerning the design and development of the instability screens. Also included are copies of papers that have been submitted for publication for various conferences and proceedings.

① **Transient Stability Assessment using Neural Networks** presented at $29^{th}$ Universities Power Engineering Conference, Galway, Ireland, September 1994.

② **Dynamic Stability Screening of Electric Power Systems using Artificial Neural Networks** presented at $30^{th}$ Universities Power Engineering Conference, Grenwich, England, September 1995.

③ **Transient Stability Assessment using Artificial Neural Networks** accepted for publication in IEE Proceedings, part C, September 1995.

④ **On-line dynamic security assessment using a real-time power system simulator with neural network contingency screens** accepted for presentation at the international conference on advances in power system control, operation and management (APSCOM), November 1995.

⑤ **Interactive On-line Dynamic Security Assessment of Large Complex Power Systems Part 2 : Contingency Screening** submitted to IEEE Power Engineering Society Winter Meeting, January 1996.

# TRANSIENT STABILITY ASSESSMENT USING ARTIFICIAL NEURAL NETWORKS

A.R.Edwards, K.W.Chan, R.W.Dunn, A.R.Daniels

School of Electronic and Electrical Engineering, University of Bath, Avon, UK

## Abstract

This paper discusses a method for fast transient stability assessment of large interconnected power systems. Composite indices, such as the minimum post-contingency busbar voltage magnitude and sum of the changes in rotor angles, provide an effective method for reducing the dimensionality of feature vectors for transient stability classification. Typically, less than 20 composite indices are required to construct a feature vector for a contingency, which can then be classified using an artificial neural network into a transiently stable or unstable contingency.

Simulation results are presented for an IEEE test network as well as a reduced model of the UK National Grid System, and the application of this technique to contingency screening in an Energy Management System is discussed.

## 1 INTRODUCTION

An economic and reliable electric power system is one of the cornerstones of a modern society. The principle aim of the power system is to convey electrical power from generation sites to consumers meeting statutory regulations in the presence of disturbances on the system.

These disturbances, or *contingencies* as they are also known, may be due to failures within the power system or external effects such as lightning strikes. The power system operators must make the minute by minute decisions to keep the power system operating securely and economically, and tools within the Energy Management System (EMS) are provided to assist the operators achieve these goals.

The stability of a power system concerns the nature of the electro-mechanical oscillations within the power system following a contingency, and the loss of synchronism within the power system is of primary concern. Tools for use inside EMSs are being developed to provide the operators with warnings of situations where a probable contingency could lead to transient stability problems. By providing these warnings, operators will be able to move the operating point of the power system to remove these potential problems, or decide on corrective action should the contingency occur.

A number of methods exist for detecting transient stability problems, such as time domain simulation[1], energy function methods [2, 3], expert systems[4, 5] and pattern recognition methods [6, 7]. The method discussed in this paper falls into the pattern recognition class of methods and is shown to provide for a fast method of transient stability screening.

## 2 OUTLINE OF METHOD

The basis of the approach outlined in this paper is to use the calculated power system and generator immediate post contingency states, obtained, by a numerical integration method, as inputs to a transient stability predictor, as shown in figure 1. In this case, the task of predicting a transient stability margin is performed by a feed-forward neural network, trained using the back-propagation algorithm. This stability margin is then classified into either a stable or unstable class by comparison with a pre-determined threshold value.

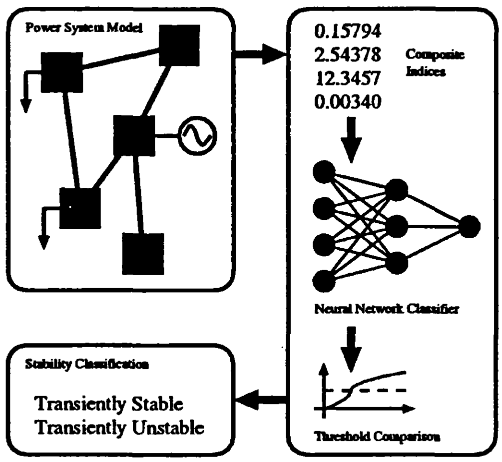


Figure 1: The Basic Approach

The advantage of this method is that there is no need for the computationally intensive numerical integration of the power system state to be carried out beyond the first time step after the contingency to determine whether the power system is transiently stable. The computational overhead of assembling the ANN inputs and propagating the pattern through the ANN is considerably less than that consumed by even one numerical integration iteration on a large power system. It is for this reason that this method is especially suited for contingency screening applications. Using the neural network to predict a stability margin, as opposed to the stability class directly, tends to prevent contingencies near the class boundaries being miss-classified. Those contingencies which pass through the screen will have to be analysed by a full time domain simulation, so the detection of as many of the stable contingencies as possible will have a large effect on the total efficiency of the system.

## 3 OVERVIEW OF ANNs

Artificial Neural Networks (ANNs) have grown from the *perceptron* concept[8] where the problem of how a machine might learn by example was first seriously addressed. The method involves internal reorganisation of the machine from its initial state to a final state where it can not only recognise example patterns that it has *seen* before but also be able to recognise patterns similar to examples that it has seen before.

Recently there has been a confluence of ideas and methods from many sources that has given rise to the area known as **artificial neural net**, or **connectionist net**, research. The common feature of this research area is the concept of using large numbers of heavily connected processing elements, called **neurons**, to process pattern information in a parallel manner. Of the ANNs being used in this area, that of the **feed-forward** layered model is of most interest, particularly as regards the work outlined in this paper, as they are especially suitable for use as pattern classifiers.

A typical feed-forward ANN, is illustrated in figure 2, where a layer represents a topological set of neurons.

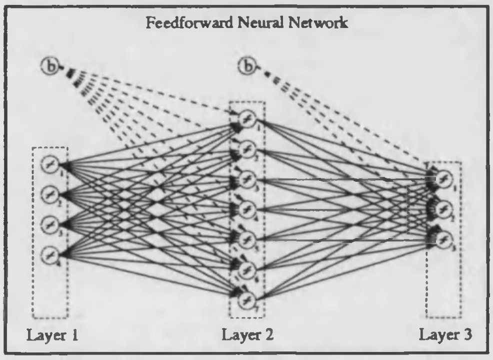


Figure 2: A general feed-forward ANN

The underlying operation of the feed-forward ANN is that patterns are presented to the neurons in the input layer, and the outputs of the input layer neurons are then calculated. These values are then multiplied by connection weights and fed-forward to the inputs of the next layer neurons, and the process repeated until the neurons in the output layer have computed their output values.

There are a variety of **learning** algorithms suitable for a feed-forward ANN, which alter the neuron connection weights such that the training patterns are *learned*. All of these approaches share the same basic method, namely that the ANN is presented with an input pattern and feed-forward propagation is used to calculate the output pattern. This output pattern is then compared to the **desired** output pattern and the error is calculated. Various methods can then be employed to back-propagate the error through the ANN so that when the pattern is propagated through the ANN again, the error has been reduced. One of the most widely used learning algorithms is that of *back-propagation with momentum* which provides a faster learning algorithm than the basic approach.

It is vital that the patterns chosen for training span the range of sets to be classified and are representative of the patterns to be classified, or the ANN will function unreliably.

### 3.1 TRAINING DATA

The training data for the transient stability classifier was generated by a digital simulation of a power system subject to a number of contingencies. The digital power system simulation was performed using PowSim[9, 10], a real-time power system simulator developed at the University of Bath. PowSim provides a 10$^{th}$ order power system model including synchronous machines, AVRs and govenors.

The contingencies used for generating the training patterns were automatically generated for each power system base case considered and comprised:

- 3 phase to ground faults on busbars, with various fault clearing times.
- Loss of single and multiple transmission lines.
- Loss or reduction of load on a busbar.
- Loss of a generator.

In addition, for the NGC based networks used, the contingency database was augmented with further contingencies suggested by NGC engineers.

## 4 COMPOSITE INDICES

The selection of input features for the ANN classifier involved considerable effort in attempting to arrive at a small number of inputs which would allow the transient stability of a large, greater than 50 busbars, power system to be determined.

The inputs to the neural network classifier should contain enough information on the state of the power system so that the transient stability classification is reli-

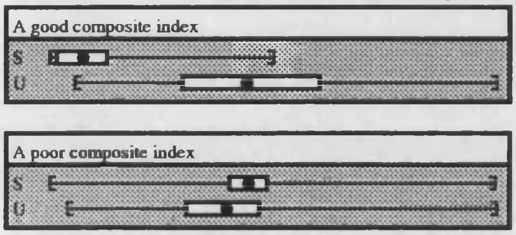


Figure 3: Box Plots for two composite indices

able. The input features, or composite indices, must encode enough information for the ANN to be able determine the degree of stability of the system.

EPRI have shown that indices such as the minimum generator terminal voltage and busbar voltage dip index provide useful discrimination for transient stability assessment[7, 11]. However, the power system model used in the work described here is of a considerably higher modelling complexity and coupled with the use of the 100 busbar reduced NGC network, these indices have been found to be inadequate. Much work has gone into determining indices which provide good discrimination as regards transient stability.

Figure 3 shows box plots[12] of two typical composite indices that were investigated. The plots show the bounds, interquartile ranges and medians of the composite index, on the same scale for the stable and unstable contingencies. The *good* index shows a clear difference in the composite index between the stable and unstable cases, but the *poor* index lacks this discrimination and is therefore likely to be of little use for transient stability classification.

Approximately 270 indices were generated for the networks under consideration. Indices such as the maximum generator rotor speed, sum of changes in rotor angles and the sum of the modulus of generator MVar changes have been found to be useful for the classification, but indices such as the maximum MW output of the generators and the MW export from an area of the power system seem to be less useful.

The selection of a subset of these indices as inputs to the ANN was made using two similar methods. Firstly, each index was ranked according to its ability to perform the classification alone, based on the Euclidean inter-class distance metric. Secondly box plots of the bounds, interquartile ranges and median were produced. The selection process then used this information to determine the best inputs based on as many different types of power system parameters as possible whilst keeping the dimensionality as low as possible.

The stability margin threshold was determined by investigating the performance of the ANN on the training data. The main requirement is to minimise the risk of miss-classifying an unstable contingency as stable, and this was met by lowering the threshold value until all of the unstable contingencies were identified correctly.

# 5 PERFORMANCE

The performance of the neural network transient stability assessor was assessed on three fronts. Firstly, it is essential that the failure rate, $\alpha$, is zero, ie no unstable contingencies are classified as stable. Secondly, the efficiency of the system should be as high as possible. In this case we define the efficiency of the screen, $\eta$ by:

$$\eta = \frac{N_{ns}}{N_s} * 100 \qquad (1)$$

where $N_s$ is the total number of stable contingencies and $N_{ns}$ is the number of contingencies identified as stable by the neural network approach. The final performance measure is the speed advantage of this method compared to a standard two seconds time simulation using PowSim. The performance benefits of this network will be greater for larger networks as the computational requirements for the time simulation of the networks increases rapidly with increased machines and busbars. Also, for systems which may take several seconds to reach instability, a five second time simulation may be required; the operation time of the neural network remains the same and hence its relative performance increases.

## 5.1 IEEE 57 Bus Network

One of the test systems used was based on the IEEE 57 bus loadflow network. At four of the generation sites a generation set was simulated so that the dynamic performance of the system could be simulated. A database of 1414 contingencies was used for training, 11 of which produced transient instability. A database of 278 contingencies were used for testing. Using the feature selection method described earlier, 10 composite indices were chosen as inputs to the neural network.

| Scenario | $\eta$ (%) | $\alpha$ | $N_u$ |
|---|---|---|---|
| Base Case | 99 | 0.0 | 4 |
| 5% Load Increase | 97 | 0.0 | 4 |
| 5% Load Decrease | 98 | 0.0 | 4 |
| Line Bus1-Bus15 Outaged | 95 | 0.0 | 5 |

Table 1: Results for IEEE 57 Bus Network

Table 1 shows the screening results for this study, where $N_u$ is the number of transiently unstable contingencies. For all of the scenarios considered, the failure rate was zero and the efficiency was above 95%. The typical speedup of this method was 4.3 times for a two second time simulation and 7.3 times for a five second simulation.

## 5.2 NGC 100 Bus Network

This network is a 100 bus reduction of the full NGC system including 20 generators. The total number of contingencies used for the training was 2010, of which 222 were transiently unstable. A database of 810 contingencies was used for testing, comprising 80ms busbar faults, single and multiple line outages, loss of load and loss of generation. Using the feature selection method described earlier, 15 composite indices were chosen as inputs to the neural network.

| Scenario | $\eta$ (%) | $\alpha$ | $N_u$ |
|---|---|---|---|
| Base Case | 93 | 0.0 | 13 |
| 5% Load Increase | 94 | 0.0 | 6 |
| 5% Load Decrease | 93 | 0.0 | 10 |
| Line Drax-Eggb Outaged | 81 | 0.0 | 13 |

Table 2: Results for 100 Bus Network

Table 2 shows the screening results for this study. For all of the scenarios considered, the failure rate was zero and the efficiency was above 80%. The typical speedup of this method was 7.9 times for a two second time simulation and 15.8 times for a five second simulation.

# 6 CONCLUSIONS

The use of pattern recognition techniques for transient stability assessment of small power systems has been explored previously, but its application to systems of the order of 100 busbars or more has previously proved difficult. This work shows that a systematic method for the selection of features is required as the number of generators and busbars increases.

The application of a neural network in a transient stability classifier has been shown to give a failure rate of zero and an efficiency of over 80% for a 20 machine 100 busbar power system. In this case, 20% of the stable contingencies will require a full time domain simulation and so the overall speedup of the system will fall to approximately three. However, for higher efficiencies this figure will rise to approximately eight.

This leads us to conclude that this approach may be suited for on-line contingency screening within an energy management system. The next stage is to assess the performance of this method on larger systems. Tests on systems of approximately 800 busbars are still to be carried out, but the results on the 100 bus network indicate that the results will be favourable.

# ACKNOWLEDGEMENT

The continuing technical and financial support of the NGC is gratefully acknowledged, and in particular that of Dr A.O.Ekwue for his useful comments.

# References

[1] CIGRE task force 38. 02. 09. Assessment of practical fast transient stability methods — state of the art report. Technical report, CIGRE, 1992.

[2] N. Kakimoto, Y. Ohnogi, H. Matsuda, and H. Shibuya. Transient stability analysis of large-scale power system by lypanov's direct method. *IEEE Trans. on Power Apparatus and Systems*, PAS-103(1):160–167, 1984.

[3] M. A. El-Kady, C. K. Tang, V. F. Carvalho, A. A. Fouad, and V. Vittal. Dynamic security assessment utilizing the transient energy function method. *IEEE Trans. on Power Systems*, PWRS-1(3):284–291, 1986.

[4] L. Wehenkel and M. Ribbens-Pavella. Decision trees and transient stability of electric power systems. *Automatica*, 27(1):115–134, 1991.

[5] Y. Akimoto, H. Tanaka, J. Yoshizawa, D.B. Klapper, and K. A. Wirgau W. W. Price. Transient stability expert system. *IEEE Trans Pwr Sys*, 4(1):312–320, 1989.

[6] C. K. Pang, F. S. Prabhakara, A. H. El-Abiad, and A. J. Kovio. Security evaluation in power systems using pattern recognition. *IEEE Trans. on Power Apparatus and Systems*, PAS-93:969–976, 1974.

[7] G. Cauley, A. B. R. Kumar, V. Brandwajn, and A. Ipakchi. Artificial intelligence applications in on-line dynamic security assessment. *Proc PSCC 11*, 2:881–887, 1993.

[8] F. Rosenblatt. The perceptron: a probabalistic model for information storage and organisation in the brain. *Psychological Review*, 65:386–408, 1958.

[9] L. A. Dale, A. R. Daniels, and I. A. Erinmez. The real-time modelling of the operation of complex power systems. In *Proc. 21$^{st}$ Universities' Power Engineering Conference*, pages 181–183, 1985.

[10] T. Berry, K. W. Chan, A. R. Daniels, and R. W. Dunn. Interactive real-time simulation of the dynamic behavoir of large power systems. In *Proc. IEE of Japan Power & Energy '93*, pages 5–10, 1993.

[11] EPRI. On-line transient stability assessment. In *EPRI Seminar and Demonstration, Toronto, Ontario, Canada*. EPRI, 6-7 December 1993.

[12] R. A. Becker J. W. Tukey and W. S. Cleveland. Discussion of graphic comparisons of several linked aspects. *Journal of Computational and Graphical Statistics*, 2:41–48, 1993.

# DYNAMIC STABILITY SCREENING OF ELECTRIC POWER SYSTEMS USING ARTIFICIAL NEURAL NETWORKS

A.R.Edwards, K.W.Chan, R.W.Dunn, A.R.Daniels

School of Electronic and Electrical Engineering, University of Bath, Avon, UK

## Abstract

This paper discusses a method for fast dynamic stability screening of large interconnected power systems. Composite indices, such as the variance of machine rotor angular momentum between the pre and immediate post contingency operating points, are shown to be especially suited as features for dynamic stability classification. This work uses composite indices as inputs to an artificial neural network to form a dynamic stability screen.

## 1 INTRODUCTION

The trends in today's modern interconnected power systems have resulted in heavier transmission loadings and therefore operation closer to the steady-state limits. The interconnections to neighbouring power systems are often weak and coupled with the large diversity of generation has resulted in many power systems being stability limited, i.e. the stability limits are reached prior to the steady state limits. The majority of these stability limits are due to dynamic stability problems which are caused by attempts to transmit too much real power across a weak boundary within the power network.

In most power systems there tend to be areas of *cheap* generation (A) and more expensive areas of generation (B). At times of large power demand the power system operators increase the online generation in *merit order*, by using the cheapest generation first. When the MW transfer from (A) to (B) exceeds a critical limit then any further increase in load in area B will have to be met by generation in area B. This will require the running of *out-of-merit* generation and will incur a financial penalty in the form of increased constraint costs.

Traditionally, these MW limits are determined by off-line studies performed a day or more ahead and must be *conservative* to take into account possible changes in the power system state. The aim of dynamic security assessment (DSA) is to provide the operators with the on-line security information which will allow the system to be operated in a more economic manner through the running of less *out-of-merit* generation.

At the heart of a DSA system are the algorithms to evaluate the effect on the power system of a set of contingencies. Due to the highly computationally demanding nature of these algorithms, *filters* are used to remove those contingencies which will cause little or no stability problems. This filtering, or *contingency screening* as it is usually referred to, must be a computationally simple (fast) process and 100% reliable which means it will not filter out any unstable contingency, i.e. it must be *conservative*. If a stable contingency is mis-classified by a screen as unstable then this will be revealed by the full contingency evaluation process and merely has the effect of reducing the efficiency of the screen.

Work has been carried out to develop an artificial neural network (ANN) based contingency screens to detect transient stability problems[1]. The work described in this paper extends this technique to the development of a dynamic stability screen (DSS).

## 2 DYNAMIC STABILITY

Dynamic stability analysis concentrates on the stability of the power system subject to small perturbations about its operating point[2], i.e. its small signal stability. In particular, increasing long term oscillations and limit cycles are of interest as these impair the power system security and may lead to islanding.

If the post-contingency operating point of the power system is dynamically unstable, or close to the stability boundary, then the transition from the pre to post-contingency operating point will be characterised by poor damping of the electro-mechanical oscillations. From an operational perspective it is desired that the electro-mechanical oscillations due to a contingency decay away quickly (within approximately one minute) and that the system remains stable. The rate of decay of these oscillations can therefore be used as an indicator of the dynamic stability of the post-contingency operating point, and hence as a dynamic stability index.

### 2.1 Decay of Oscillations

As a quantitative measure of the decay of these oscillations in a power system, the exponential decay rate of an envelope of power system parameters, $p$, is considered to be of the form given in equation 1.

$$p(t) = Ae^{bt} \tag{1}$$

In practice, the envelope of power system parameters such as rotor angle swings will not be a true exponential, however their decay can be approximated by an exponential envelope. The transient decay rate corresponds to the value of $b$ which is a *best fit* on the discrete data obtained by simulation, as shown in figure 1.

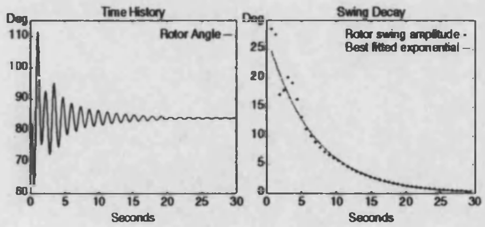


Figure 1: Decay Rate Curves

The decay rate, $b$, can be found by considering a time series of amplitudes of the rotor angle swings, $p$, of the machines in the power system. Taking a logarithm of equation 1 gives:

$$ln(p) = bt + ln(A) \tag{2}$$

This equation yields a linear graph of the logarithm of the rotor angle swing amplitudes versus the simulation time. Therefore, given discrete values of $p$ from a time domain simulation, the method of least squares can be used to fit a *best line* through

Presented at $30^{th}$ Universities Power Engineering Conference, Grenwich, England, September 1994 2

these points, which will correspond to the desired decay envelope. The gradient of this line equals the decay rate $b$. Hence, $b$ can be used as a quantitative measure of the dynamic stability of the post contingency operating point of the power system, i.e. $b$ is a dynamic stability index. Another dynamic stability index that could be used is the most positive eigenvalue[3], but for the purposes of this work the damping index was used as this is more directly related to power system operating conditions.

## 3 OVERVIEW OF ANNs

Artificial neural networks (ANNs), based on the structure of the human brain, are being used with increasing frequency in a wide range of engineering disciplines[4].

An ANN is composed of a set of interconnected *neurons* which produce an output dependent on their input. There are several classes of ANNs, the most popular of which is the feed-forward ANN which is often trained by the *back-propagation* algorithm. A typical feed-forward ANN, is illustrated in figure 2, where a layer represents a topological set of neurons.

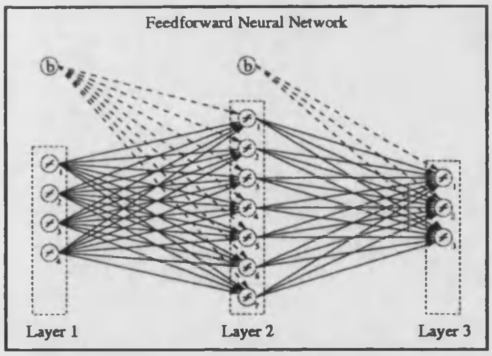


Figure 2: A general feed-forward ANN

The underlying operation of the feed-forward ANN is that patterns are presented to the neurons in the input layer, and the outputs of the input layer neurons are then calculated. These values are then multiplied by connection weights and fed-forward to the inputs of the next layer neurons, and the process repeated until the neurons in the output layer have computed their output values.

An ANN is *trained* to produce the desired input–output (IO) mapping by adapting the connection weights so that IO mapping is achieved for the training data. If the training data is representative of the data to be used by the ANN during normal operation, then the ANN should be able to produce correct outputs for inputs that it has not seen before.

The selection of training data for an ANN is critical. ANNs are very effective at performing classifications when the input pattern falls *between* two or more of the patterns used for training – i.e. they perform well when interpolating between training patterns. Operation of an ANN outside the scope of the training data, i.e. when extrapolation of training data is used, will produce unreliable results. For this application, it is important therefore that realistic contingencies are used for training the ANN and that they cover the likely operating conditions of the ANN.

## 4 DYNAMIC STABILITY SCREEN

This screen is based on a pattern recognition approach[5], see figure 3, and uses a power system simulator[6] to perform a time domain simulation of the contingency up until the power system topology changes are complete. This point in the simulation is referred to as the contingency termination point (CTP). At the CTP a set of numerical values, called *composite indices*, are calculated from the power system state vector and presented as inputs to an ANN. The ANN then predicts the dynamic stability index, $b$, which is compared to a threshold value to determine whether the damping of machine rotor angle oscillations are acceptable.

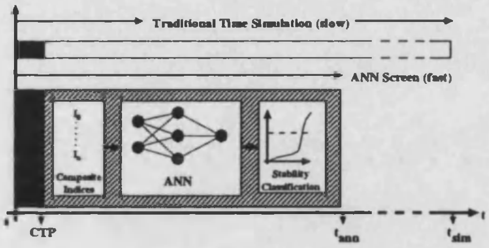


Figure 3: The Basic Approach

With this approach, the computationally intensive operation of simulating the post-contingency state of the power system using a time domain simulator is replaced by the relatively un-intensive process of calculating the composite indices, propagating them through the ANN and comparing the output with a threshold value. This approach makes this method an ideal candidate for use as an online DSS, having an accuracy close to that of a time domain simulator coupled with the speed advantages of a pattern recognition approach[5].

A major factor affecting the robustness of this approach concerns the results obtained close to the stability boundaries. Those contingencies close to the boundary will in practice be either just stable or just unstable and the conventional binary classification into stable or unstable classes looses this information, i.e. does not take into account the degree of stability. By training the ANN to predict the dynamic stability index the errors close to these stability boundaries are greatly reduced as the ANN *surface* is much smoother and consequently the prediction errors in the vicinity of the stability boundary are reduced.

By adopting a continuous valued stability index the issue of the *conservativeness* of the screen can also be controlled. Varying the level of the threshold for stability comparison has the effect of varying the severity of the contingencies which are passed on for detailed time domain simulation evaluation.

## 5 COMPOSITE INDICES

The use of statistical parameters for providing broad information on the state of large systems is widely accepted. Composite indices are used to provide a dimensionality reduction[1] and have been shown to be an effective method for transient stability classification[1]

[1] from say 100 busbar voltage magnitudes to a single numeric value, such as the standard deviation of the voltages

$$I = A \times B \times C \times D \times E \quad (3)$$

Using set notation, equation 3 describes how a set of composite indices, $I$, are formed from the sets of statistical functions and power system variables $A$ to $E$; $\times$ is the product set operator. Table 1 shows the members of each of these five sets.

| No | $A$ | $B$ | $C$ | $D$ | $E$ |
|---|---|---|---|---|---|
| 1 | V | M | N | MIN | VM |
| 2 | S | L | C | MAX | VP |
| 3 | | B | G | SUM | MW |
| 4 | | | S | RMS | MV |
| 5 | | | | RNG | MVA |
| 6 | | | | VAR | OL |
| 7 | | | | MEAN | KE |
| 8 | | | | SKEW | RA |
| 9 | | | | ADEV | RS |
| 10 | | | | MMAX | RC |
| 11 | | | | MSUM | RAM |
| 12 | | | | | RAP |
| 13 | | | | | AVE |
| 14 | | | | | TI |

Table 1: Set Membership

**Set** $A$ contains two members. The first member **V** limits the scope of generation of composite indices to the immediate vicinity of a contingency. Our work has shown that defining the *vicinity* as a topological distance of four busbars from an item of plant involved in the contingency produces good results.

The other member of the set **S** forces the indices to be built from all items of plant in the power system, i.e. the index is system wide.

**Set** $B$ defines the items of plant which are related to the composite index. These may be **B**usbars, **L**ines or **M**achines. For the purposes of the modelling, all transformers, SVCs and quadrature boosters are modelled as lines.

**Set** $C$ contains members which describe how the composite index is to be composed. **N** indicates that the index is to be built using the appropriate measurement at the CTP. **G** indicates that the gradient of the measurement at the CTP is to be used. **C** signifies that the change between the pre-contingency value and the measurement at the CTP is to be used. The set member **S** defines the post contingency steady state value of the composite index, determined by a loadflow, to be used.

**Set** $D$ defines the type of statistical functions to be used to create the composite index. **MIN** and **MAX** are the minimum and maximum values respectively and **SUM** is the sum of the values across all items of plant. **RMS** allows the use of the root mean square function, **RNG** determines the range of the variable and **VAR** calculates the variance. **MEAN** is the mean of all the variables, **SKEW** is the skew and **ADEV** is the absolute deviation. The remaining two use the modulus function: **MMAX** is the maximum modulus of the variable and **MSUM** is the sum of the modulus of all the variables.

**Set** $E$ defines the actual measurements to be constructed from the CTP state vector to form the basis of the composite index. **VM** and **VP** are the voltage magnitude and phase respectively, **MW** and **MV** are the MW and MVAr measurements and **MVA** is the MVA measurement. **OL** is the overload which is the current MVA value divided by the approximate rating. **KE** is the kinetic energy of a machine, **RA**, **RS** and **RC** are the rotor angle, speed and acceleration of machines and **RAM** is the rotor angular momentum. **RAP** calculates the rotor accelerating power, **AVE** is the machine's AVR voltage error and **TI** is the estimated time to instability assuming constant rotor acceleration.

A composite index can then be represented in a manner similar to:

$$i = \{S, L, C, MIN, MV\} \quad (4)$$

which is the *system wide minimum of line MVar flows*. In addition to the indices outlined above, a number of *special* indices were generated which checked for a line outages and islanding.

## 6 SIMULATION RESULTS

Within the laboratory a 100 busbar 20 machine model of the UK power system was used to investigate the performance and reliability of the DSS. This model was derived from a dynamic reduction of a snapshot of the full UK National Grid System taken during a mid-summer night in 1984, which had a very low loading condition and was likely to be susceptible to dynamic stability problems. A number of scenarios (B-G) were constructed from the base case (A) of the model so that the screen could be tested on scenarios which led to more unacceptably damped post-contingency electro-mechanical rotor oscillations.

The training data for the dynamic stability classifier was generated by a time domain simulation of scenario (A) subject to a number of contingencies. The digital power system simulation was performed using PowSim[6], a real-time power system simulator developed at the University of Bath. PowSim provides a 10$^{th}$ order generating plant model including synchronous machines, AVRs and governors. A total of 838 contingencies were used to generate the training data, comprising line, busbar, loss of load and loss of generator contingencies as well as some suggested by NGC engineers which were likely to produce dynamic stability problems.

### 6.1 FEATURE SELECTION

A total of 1916 composite indices were generated as possible features for the ANN for each contingency in the training set. The first stage in the design of the screen involved selection of a small (less than 20) subset of these feature as inputs to the ANN. Univar correlations[7] were performed between the value of each feature versus the stability index for all the contingencies in the training set and those with the highest correlation were selected.

| No | $A$ | $B$ | $C$ | $D$ | $E$ | No | $A$ | $B$ | $C$ | $D$ | $E$ |
|---|---|---|---|---|---|---|---|---|---|---|---|
| 1 | S | M | N | VAR | RAM | 6 | V | L | C | RMS | MW |
| 2 | S | M | C | VAR | RAM | 7 | V | L | C | MSUM | MW |
| 3 | S | L | N | MSUM | OL | 8 | V | L | C | RMS | MVA |
| 4 | S | L | C | MSUM | OL | 9 | V | L | C | MSUM | MVA |
| 5 | S | L | C | ADEV | MVA | 10 | V | L | C | MSUM | VP |

Table 2: Selected Composite Indices for Dynamic Screen

Table 2 shows the set membership for the 10 selected composite indices. The suitability of these indices at classifying the dynamic stability problem can be shown by using a Sammon plot[8], as shown in figure 4.

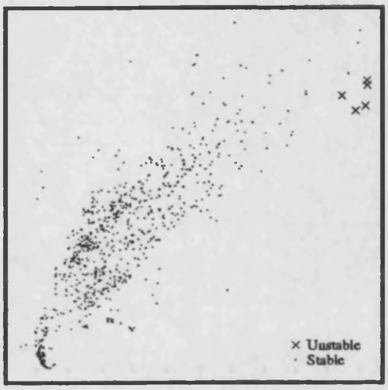


Figure 4: Sammon Plot for Dynamic Screen

As can be seen from this plot, those patterns represented by 'crosses' (unstable) are well separated from those represented by 'dots' (stable), indicating that the ANN will be able to learn the training data and generalise for other cases that it has not seen before.

A simple three layer feed-forward ANN comprising 10 input neurons, 8 hidden neurons and one output neuron was then trained using the back-propagation algorithm[9] with a learning rate of 0.9. The dynamic stability screen was then tested on a number of different scenario's.

### 6.2 PERFORMANCE

The DSS was then tested on the base case (A) and a number of scenarios which were constructed from the base case (B–G) and designed to test the performance of the screen for operating conditions away from the training case.

| Scenario | A | B | C | D | E | F | G |
|---|---|---|---|---|---|---|---|
| N° Stable | 833 | 838 | 838 | 833 | 835 | 833 | 832 |
| N° Unstable | 5 | 0 | 0 | 5 | 3 | 5 | 6 |
| Screening Efficiency | | | | | | | |
| N° Pass | 0 | 4 | 4 | 1 | 5 | 7 | 4 |
| Efficiency (%) | 100.0 | 99.5 | 99.5 | 99.9 | 99.4 | 99.2 | 99.5 |

Table 3: Results for Laboratory Model

Table 3 tabulates the simulation results that were obtained in the laboratory. With all of the scenarios, the screen did not mis-classify any unstable contingencies as stable, thus ensuring that all unstable cases were detected, meeting the primary requirement of a conservative screen. In the unlikely scenario of very large changes in the operating point of the system, such as the outaging of a critical lines between two areas of the power system, the screen may mis-classify some of the unstable contingencies. This is due to the gross dissimilarity between the operating condition and the training case, and under these conditions the screen should be replaced by a time domain simulation.

With the efficiency of a screen being defined as the ratio of the number of contingencies declared stable by the screen to the actual number of stable contingencies, the efficiency of the screen remained above 99% because the number of stable contingencies that passed through the screen (N° Pass) was small. These results indicate that when the dynamic and transient[1] screens are fully integrated into OASIS[6], the cycle time of the DSA will be reduced by a factor of approximately 20.

## 7 CONCLUSIONS

This approach to dynamic stability screening has been shown to be both a fast and efficient method. The training of an ANN to predict a dynamic stability margin produces fewer classification errors and also allows the conservativeness of the screen to be controlled. The application of this technique to the full UK National Grid System is continuing, and the preliminary results are encouraging.

## ACKNOWLEDGEMENT

The continuing technical and financial support of the NGC is gratefully acknowledged, and in particular that of Dr A.O.Ekwue from NGC TSD and the staff of NGC CTC for their useful comments.

## References

[1] A. R. Edwards, K. W. Chan, R. W. Dunn, and A. R. Daniels. Transient stability assessment using neural networks. In *Proc. 29$^{th}$ Universities' Power Engineering Conference, Galway, Ireland*, 1994.

[2] H. Rudnick, F. M. Hughes, and A. Brameller. Steady state instability : simplified studies in multimachine power systems. In *IEEE PICA, Houston, Texas*, pages 137–144, 17-20 May 1983.

[3] L. Wang and A. Semlyen. Application of sparse eigenvalue techniques to the small signal stability analysis of large power systems. In *IEEE PICA, Seattle, Washington*, pages 358–365, 1-5 May 1989.

[4] Artificial neural networks for power systems - a literature survey. Technical report, CIGRE Task Force 38-06-06, 1993.

[5] C. K. Pang, F. S. Prabhakara, A. H. El-Abiad, and A. J. Kovio. Security evaluation in power systems using pattern recognition. *IEEE Trans. on Power Apparatus and Systems*, PAS-93:969–976, 1974.

[6] K. W. Chan, A. R. Edwards, R. W. Dunn, and A. R. Daniels. Real-time electromechanical transient simulator for on-line applications. In *Proc. of First International Conference on Digital Power System Simulators – ICDS'95*, pages 259–263, 5-7 April 1995.

[7] T. W. Rauber, M. M. Barata, and A. S. Steiger-Garcao. A toolbox for analysis and visualization of sensor data in supervision. Technical report, Departmento de Informatica, Intelligent Robotics Group, 285 Monte de Caparica, Portugal.

[8] J. W. Sammon. A nonlinear mapping for data structure analysis. *IEEE Trans. on Computers*, 18:401–409, 1969.

[9] J. M. Zurada. *An introduction to artificial neural systems*. West, 1992.

# Transient Stability Screening Using Artificial Neural Networks within a Dynamic Security Assessment System

A. R. Edwards, K. W. Chan, R. W. Dunn and A. R. Daniels

**Abstract:**
Accurate assessment of transient and dynamic stability provided by an on-line dynamic security assessor allows the power system to be operated closer to its stability limits with considerable economic benefit through the running of less out-of-merit generation. As part of such assessors, contingency screens are used to filter out those contingencies which pose no stability problems. Those contingencies which pass through these filters are evaluated in detail to determine their effects on the system stability. This paper describes an approach where an artificial neural network is successfully used to provide a fast transient stability screen within a dynamic security assessment system. Results are presented for a number of test networks based on a reduced model of the UK National Grid System.

## 1 Introduction

Electric power utilities are usually bound by statutory regulations to provide an economic and reliable supply at all times. As a consequence their power systems must be robust to faults, or *contingencies* as they are usually referred to, due to both external effects such as lightning strikes on overhead transmission lines and internal failures such as insulation breakdown.

The nature of the electro-mechanical oscillations between the power network and the machines connected to it determines the stability of the system. *Transient stability* problems are local effects due to large power imbalances between generators mechanical input power and the available electrical load. Under these conditions, the generator rotor will accelerate and move towards pole-slipping at which point its protection schemes operate and trip the affected machine. The result of transmitting too much power through weak parts of the transmission network moves the system towards *dynamic instability*. Under this condition, large power oscillations occur across the network and if they increase substantially, they will either cause the machines to move towards pole-slipping or cause the weak transmission lines to be tripped due to the operation of protection. The resulting islands will invariably operate at different frequencies and hence be very difficult to re-synchronise and connect.

Most power system utilities are forced to run out-of-merit generation due to stability limitations. Off-line stability studies are performed to determine how much power can be transferred across critical boundaries within the power system whilst ensuring the system is secure for a pre-defined set of contingencies. On-line dynamic security assessment (DSA) tools will provide operators with the actual on-line current stability limits, allowing the power system to be operated closer to these limits. The net effect is that less out-of-merit generation is required resulting in considerable economic savings [1]. In the year 1993/4 the constraint costs on the UK transmission system were approximately £190M [2], some of which was due to stability constraints. Even a small percentage reduction in the amount of out-of-merit generation used will reap large financial rewards; if for two hours during peak loading conditions generation of 100MW can be supplied by a northern generating set bidding at £14/MWh[3] instead of a southern gas turbine bidding at £780/MWh then the saving is over £150K. Financial savings can also be made through less cases of load shedding etc, as the operators are warned of such potential problems in advance and can take preventative control actions. It is the combination of these large financial savings that is the key motivation behind the development of dynamic security assessment systems.

A prototype DSA known as OASIS (On-line Algorithm for System Instability Studies) [4] is under development at the University of Bath and is co-sponsored by the National Grid Company plc, UK. This paper describes a fast transient stability screen for use within OASIS, based on an artificial neural network (ANN) approach.

The authors are with the School of Electronic and Electrical Engineering, University of Bath, Bath BA2 7AY, UK

## 2 Overview Of Existing Approaches

There are four broad approaches used for transient stability assessment:

**Numerical Integration** methods perform a step by step solution of the network and machine equations at discrete intervals in time using numerical integration methods to solve the differential equations. Considerable progress has been made in speeding up these methods [5,6], however they currently remain too slow to be used for contingency screening in an on-line environment such, as a DSA, if a large number of contingencies is to be evaluated. However, this is the most accurate method for stability assessment, and forms the benchmark against which the other stability assessment methods are judged.

**Energy Function Methods** use a stability criterion based on the construction of a Lyapunov function[7] in order to determine the stability of the post-contingency operating point of the system. This method is less computationally demanding than the numerical integration approach but does not achieve the same level of accuracy due to the use of reduced order modeling.

**Expert System Methods** rely on decision trees to assess the system stability in terms of selected pre-contingency parameters[8, 9]. These approaches tend to be less robust to changes in the power system state and can result in mis-classification of unstable contingencies as stable.

**Pattern Recognition Methods** rely on reducing the on-line computational overhead to a minimum at the expense of intensive off-line studies. By performing off-line training of a pattern classifier using results obtained from a time domain simulator, accuracy close to that of a numerical integration method may be achieved within the computational and time constraints of on-line operation making this approach an ideal choice for a stability screen.

The task of pattern recognition consists of defining a pattern vector, $V$, whose components contain sufficient information about the stability of the power system so that a classifier can decide purely on the basis of $V$ what the system stability will be. This vector is then evaluated at many different *representative* operating points of the power system to generate a training data set. The final step is then to determine the classifier function $S(V)$ such that the pattern recognition task becomes:

$$S(V) = \begin{cases} \geq 0 & \text{for a secure V} \\ < 0 & \text{for an insecure V} \end{cases} \quad (1)$$

The lower limit for the classification error depends on the choice of the primary inputs and the feature selection process to determine the inputs to the classifier. Numerous feature extraction methods have been developed[1, 10, 11] but few of these methods are easily scaled to large power system models.

## 3 The Approach

The basis of the approach is shown in Fig.1 and uses a state of the art real-time power system simulator to simulate a contingency up until the power system topology changes are complete. This point in the simulation is known as the contingency termination point (CTP). At the CTP a set of numerical values, *composite indices*, are calculated from the power system states and presented as inputs to an ANN. The ANN then predicts a transient stability margin which is compared to a threshold value to determine the transient stability.

If the time domain simulation is continued beyond the CTP then topology changes may occur as a result of the action of protection equipment but these effects are not part of the contingency, but of the power system's response and hence do not affect the position of the CTP.

With this approach the computationally intensive operation of simulating the post-contingency state of the power system using the power system simulator is replaced by the computationally less intensive process of calculating the composite indices and propagating them through the ANN. This makes this method and an ideal candidate for an on-line transient stability screen, having the accuracy close to that of a numerical integration approach coupled with the speed advantages of the pattern recognition methods. The robustness of this screen to changes in the power system state relies on the selection of composite indices which are as independent of the state as possible and encode the stability information.

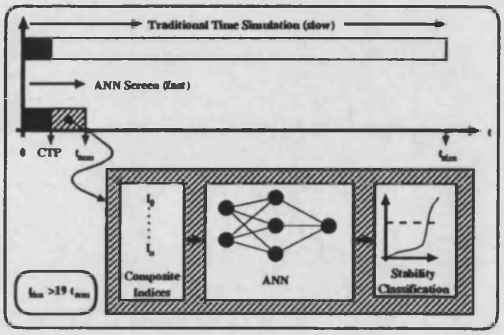


Fig 1: Outline of the approach

### 3.1 Composite Indices

In everyday life we are confronted with statistical indicators of the health of the economy and combinations of these indicators can be successfully used to provide a clear indication of the overall economic health of the country. Similarly, a system with many millions of states can often be successfully classified by a few tens of artificial indicators. This form of feature compression is the motivation behind using composite indices for transient stability screening, and is justified by the results that have been obtained.

$$I = A \times B \times C \times D \times E \quad (2)$$

Using set notation, equation 2 describes how a set of composite indices, $I$, are formed from the sets of statistical functions and power system variables $A$ to $E$; $\times$ is the product set operator. Table 1 shows the members of each of these five sets.

| No | *A* | *B* | *C* | *D* | *E* |
|---|---|---|---|---|---|
| 1 | V | M | N | MIN | VM |
| 2 | S | L | C | MAX | VP |
| 3 | | B | G | SUM | MW |
| 4 | | | | RMS | MV |
| 5 | | | | RNG | MVA |
| 6 | | | | VAR | OL |
| 7 | | | | MEAN | KE |
| 8 | | | | SKEW | RA |
| 9 | | | | ADEV | RS |
| 10 | | | | MMAX | RC |
| 11 | | | | MSUM | RAM |
| 12 | | | | | RAP |
| 13 | | | | | AVE |
| 14 | | | | | TI |

Table 1: Set Membership

**Set** $A$ contains two members. The first member **V** limits the scope of the composite indices to the immediate vicinity of a contingency. Since transient stability problems are local phenomena, the effects on parts of the power system remote from the contingency area are often small. Our work has shown that defining the *vicinity* as a topological distance of four busbars from an item of plant involved in the contingency produces good results.

The other member of the set **S** forces the indices to be built from all items of plant in the power system, i.e. the index is system wide.

**Set** $B$ defines the items of plant which are related to the composite index. These may be **B**usbars, **L**ines or **M**achines. For the purposes of the modelling all transformers, static var compensators and quadrature boosters are modelled as lines.

**Set** $C$ contains members which define which state vector(s) are to be used to construct the composite index. The member **N** indicates that the composite index should be built from the system state vector at the CTP. **C** selects the composite index to be built using the changes between the state vector at the pre-contingency and the CTP state vector. The element **G** indicates that the gradient of the state vector elements at the CTP should be used to build the composite index.

**Set** $D$ defines the type of statistical functions to be used to create the composite index. **MIN** and **MAX** are the minimum and maximum values respectively and **SUM** is the sum of the values across all items of plant. **RMS** allows the use of the root mean square function, **RNG** determines the range of the variable and **VAR** calculates the variance. **MEAN** is the mean of all the variables, **SKEW** is the skew and **ADEV** is the absolute deviation. The remaining two use the modulus function: **MMAX** is the maximum modulus of the variable and **MSUM** is the sum of the modulus of all the variables.

**Set** $E$ defines the actual measurements to be constructed from the CTP state vector to form the basis of the composite index. **VM** and **VP** are the voltage magnitude and phase respectively, **MW** and **MV** are the MW and MVAr measurements and **MVA** is the MVA measurement. **OL** is the overload which is the current MVA value divided by the approximate rating. **KE** is the kinetic energy of a machine, **RA**, **RS** and **RC** are the rotor angle, speed and acceleration of machines and **RAM** is the rotor angular momentum. **RAP** calculates the rotor accelerating power, **AVE** is the machine's automatic voltage regulator's voltage error and **TI** is the estimated time to instability assuming constant rotor acceleration.

$$i = \{\mathrm{S}, \mathrm{M}, \mathrm{C}, \mathrm{SUM}, \mathrm{KE}\} \tag{3}$$

Equation 3 above shows an example of a composite index which is the *system wide sum of the machine kinetic energy changes*. In addition to the indices outlined above, a number of special indices were generated which checked for a line outages and islanding.

The full set of these composite indices was then generated for each of the contingencies in the training set. In addition a transient stability margin was generated for each contingency in this case, based on the maximum rotor angle swing of any of the machines modelled in the power system, found during the simulations. The main reason for the choice of this margin was that it is frequently used within the National Grid Company as a measure of the severity of a transient disturbance, but in practice an energy margin could also be used.

### 3.2 Feature Extraction

The total number of indices generated by this approach was approximately 1900 and hence a semi-automatic selection procedure was required to select those indices which provided the best indicator of the system stability for use as inputs to the ANN. The selection procedure described below has been used with success.

1. Initially, correlations are performed to automatically select the best ten or so indices of the classification, and ten best indices for each contingency are also determined.
2. An initial attempt is then made to train an ANN using only the ten globally selected indices, which highlight any contingencies which are being mis-classified.
3. For these mis-classified contingencies, some of their best individual indices are selected and the process iterated until the ANN trains successfully.

In this work typically less than 30 composite indices proved sufficient to classify the post-contingency stability of the system. The effectiveness of the selected composite indices at performing the required classification can be indicated using a Sammon plot[12]. This algorithm performs a dimensionality reduction from a high order space, equal to the number of selected composite indices, to a lower dimensional space, in this case two dimensions. The criterion for the dimensionality reduction is to reduce, by a gradient descent approach, the differences in the Euclidean distances between patterns in the the high and low spaces as much as possible. In this way the *geometric* separation of the patterns is maintained and therefore we can expect that those classes (stable,unstable) that distinguish well in the high dimensional space maintain this quality also in the lower dimension.

Figure 2 shows a sammon plot for the classical data set of Fisher[13]; a set of 150 samples of feature dimension four describes three different flower classes, 50 samples per class. It can be seen that the patterns represented by 'pluses' (setosa class), those represented by 'crosses' (versicolor class) and those represented by 'boxes' (virginica class) are clustered into three fairly distinct areas indicating that the patterns used contain enough information to perform the stability classification.

If there is no obvious separation between the classes (in our case stable and unstable classes) then the composite indices chosen are not likely to be able to classify the stability and will almost certainly not be robust to changes in the power

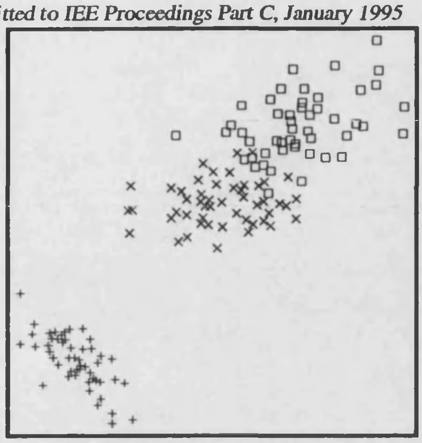

Fig 2: Sammon Plot for Fishers' Data Set

system state or topology. In this way, a sammon plot of the selected indices is a useful guide as to the likely success of training the ANN for this application.

### 3.3 Artificial Neural Network

An ANN was chosen to be the pattern classifier as they have been shown to be successful in other similar applications [14] and because training data was available while classification rules were not.

A standard feed-forward ANN architecture[15] was chosen for a combination of its simplicity, ease of training and fast non-iterative on-line execution. Using off-line time simulations, large numbers of training cases can be generated allowing the ANN classifier to be trained by the back-propagation algorithm. An additional advantage of ANNs is that provision may be made for on-line training of the ANN should its output decision be found to be wrong or should any unexpected system operating condition be reached.

The indices were normalised across the training set before being presented to the ANN for training in order to reduce the possibility of saturation within the ANN structure. These normalisation limits were then applied to all subsequent inputs of the ANN during operation of the DSA.

## 4 Integration into OASIS

OASIS is a dynamic security assessor implemented using Parallel Virtual Machine (PVM) which uses an enhanced real-time power system simulator for contingency evaluation[4]. PVM is a set of utilities and library functions used to create a parallel computing environment that is transparent to the user and can be composed of an arbitrary number of heterogeneous computers. Fig.3 shows the functional block diagram of OASIS which is based on a client-server approach. OASIS can easily be ported to a wide variety of computers since it is implemented using ANSI standard 'C'.

The data input can be from saved power system snapshots, on-line EMS data or from a real-time power system simulator. Within the laboratory environment, the real-time power system simulator is run to mimic the real power system and the

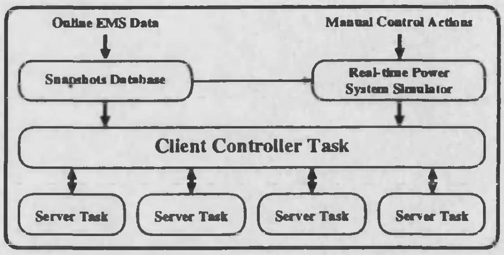


Fig 3: Block diagram of OASIS

effects on stability of simulated control actions on the power system can be seen through changes in the OASIS displays.

The client task controls the contingency processing and provides an X-Window based human-computer interface. The server tasks are based on PowSim, an enhanced real-time power system simulator which has been developed at the University of Bath over a number of years [5,6], which is used for the detailed contingency evaluation. The transient stability screen described in this paper forms part of the server task.

The definition of the transient stability screen, the composite indices to be used and details of the ANN, are specified in a scren definition file to allow maximum flexibility. This file is loaded into the server task at run-time when the server task is initialised by the master. This approach allows a a set of screens to be developed off-line and loaded into OASIS as the power system conditions change. As a result, two additional functional blocks were added to the OASIS server task as shown in Fig.4.

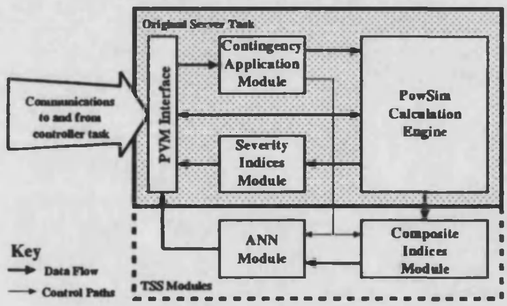


Fig 4: Block diagram of new server task

The first is a module which builds up an internal representation of the ANN defined in the screen definition file. A number of neural network transfer functions were built into the module and the mechanism for propagating the composite indices through the ANN implemented.

The function of the other module is to calculate the composite indices specified in the screen definition file. This required interfacing to the server data structures to obtain the power system state vector and the inclusion of the statistical functions required to compose the composite indices. A facility was also provided to save the composite indices so that off-line training data could be generated.

# 5 Results of Laboratory Studies

Within the laboratory environment, the PVM that was used comprised only two machines: a DEC Alpha 3600/OSF1 2.0 and a Silicon Graphics Indigo R4000/IRIX 5.2. The standard laboratory scale power system is a reduced model of the UK national grid system. This model comprises 20 generating stations connected to a highly interconnected transmission system of 100 busbars and 256 lines. This model was derived by a reduction of a full system snapshot taken from the EMS during a summer night in 1984.

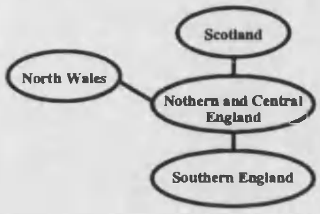


Fig 5: Major areas of UK power system

Figure 5 shows the major areas of the UK power system. The NGC are responsible for power transmission in and between the English and North Wales areas. Power can be imported from the Scottish power system through EHV circuits and also from France (not shown) via a DC link.

## 5.1 Training

The laboratory model was used as the base case for training the transient stability screen. A total of 1916 composite indices were generated for the 838 training contingencies comprising three phase to ground busbar faults, loss of load, loss of generation and loss of transmission lines. The selection procedure outlined in section 3.2 was applied and resulted in the selection of 18 composite indices shown in table 2.

These selected indices did not include any line or busbar indices, but when this approach is applied to larger power systems such indices may be more relevant and therefore be selected. 14 of these indices are related to the terminal voltage of the generating sets in the power network, showing the clear link between terminal voltage and transient stability.

Once these indices were selected, a pattern file was generated to train the ANN. These patterns were also processed by the Sammon algorithm and then displayed on a contour surface based on the stability index as shown in figure 6.

The surface is determined from the stability index of each of the patterns and has the effect of highlighting clusters of patterns of a similar stability. In this example the unstable patterns fall into one broad cluster, indicating that the ANN will be able to learn this data. It can be clearly seen that the transiently unstable patterns (crosses) are geometrically well separated from the stable patterns (dots), indicating that the screen is likely to be able to classify the stability and be fairly robust to changes in the power system state and topology. Hence a standard three layer feed-forward neural network was chosen with 18 inputs, 10 hidden layer neurons and one output neuron. The ANN was trained using a neural netowk simulator and the training was stopped after 400 iterations. The threshold value was set to 0.4 because the largest stability index for a stable contingency in the training set was 0.38.

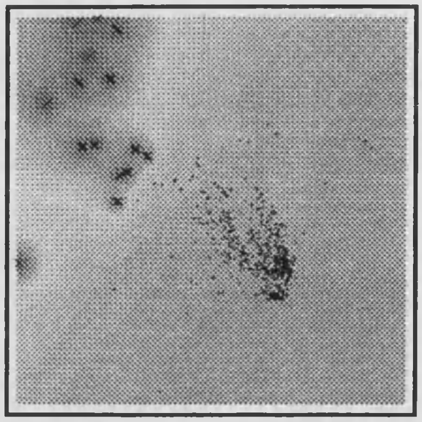

Fig 6: Sammon Plot for Training Data

## 5.2 Testing

The screen was then tested on the base case (A) and a number of scenarios which were constructed from the base case (B–G) as follows:

**Scenario B** — A sudden increase in load of 530MW is met reducing the motoring load of a North Wales pumped storage station from 1800MW to 1270MW. This reduces the net power export from the North Wales area and improvs the transient stability of the system subject to contingencies within this area.

**Scenario C** — The same increase in load as (A) met by stopping all 280MW of motoring at one pumped storage station and reducing the motoring load from 1800MW to 1530MW at another pumped storage station, also within the Noth Wales area. This results in a different generation pattern within the North Wales area.

**Scenario D** — This has the same loading and generation pattern as the base case (A) but includes a double circuit outage between Central and Southern England. This has the effect of increasing the power transfer through the remaining circuits into the southern half of the country.

**Scenario E** — The loss of one of the England-Scotland circuits, increasing the transfer through the remaining curcuits.

**Scenario F** — The loss of 1176MW of generation in central England, being met by increased generation across all major generating stations in the country. This moves many stations closer to their transient stability limits.

**Scenario G** — The loss of one 400KV circuit between the North Wales area and Central England, resulting in increase loading on the remaining circuits. This also has

| No | *A* | *B* | *C* | *D* | *E* | No | *A* | *B* | *C* | *D* | *E* |
|---|---|---|---|---|---|---|---|---|---|---|---|
| 1 | S | M | N | MIN | OL | 10 | S | M | C | MIN | RAM |
| 2 | S | M | N | MIN | VM | 11 | S | M | N | MIN | AVE |
| 3 | S | M | N | RNG | VM | 12 | S | M | N | MIN | AVE |
| 4 | S | M | N | VAR | VM | 13 | S | M | N | MIN | AVE |
| 5 | S | M | C | MIN | VM | 14 | S | M | C | MIN | AVE |
| 6 | S | M | C | RNG | VM | 15 | S | M | C | MIN | AVE |
| 7 | S | M | C | VAR | VM | 16 | V | M | N | VAR | VP |
| 8 | S | M | N | MIN | RS | 17 | V | M | C | RNG | VP |
| 9 | S | M | N | MIN | RAM | 18 | V | M | C | ADEV | VP |

Table 2: Set Membership of Selected Composite Indices

the effect of increasing the impedence between the North Wales generating units and Central England, increasing the susceptability of the North Wales units to transient stability problems.

Table 3 tabulates the results that were obtained using the laboratory PVM. With all of the test cases the screen did not mis-classify any unstable contingencies as stable. This is a very important result and confirms that the screen remained conservative in its stability classification.

With the efficiency of a screen being defined as the ratio of the number of contingencies declared stable by the screen and by the actual number of stable contingencies, the efficiency of the screen remained above 98% because the number of stable contingencies that passed through the screen (N° Pass) was small.

For each of the above simulations, the overall speedup of the DSA by using this stability screen as opposed to the standard 30 second time domain simulation varied between 19 and 25 times. The speedup is also greatly affected by the actual number of unstable contingencies; a large number of these will require more time domain simulations and hence increase the operating time of the DSA with the screen.

## 6 Conclusion

The use of statistical information based on a real power system state vector has been shown to be sufficient for determining the post-contingency stability of a power system. The use of an artificial neural network to predict a transient stability index from this statistical information provides a robust framework for an on-line transient stability screen.

The implementation of this screen within a dynamic security assessor has shown that on-line dynamic security assessment is possible using reasonable computing power.

A transient stability screen is under development for the full UK National Grid System composed of approximately 940 busbars and between 100 and 160 generating units depending on the system load. Preliminary results are very encouraging and indicate that full on-line dynamic security assessment for power systems of this size is now possible.

## 7 Acknowledgement

The authors gratefully acknowledge the contributions of the National Grid Company plc, UK, and in particular the assistance of staff at the National Grid Control Centre and the Technology and Science Laboratory's.

## References

[1] EPRI, 'On-line transient stability assessment', in *EPRI Seminar and Demonstration, Toronto, Ontario, Canada*, EPRI, 6-7 December 1993.

[2] NGC, 'A review of transmission security standards', tech. rep., The National grid Company plc for OFFER, August 1994.

[3] NGC, 'Ngc seven year statement for the years 1994/5 to 2000/2001', tech. rep., The National Grid Company plc, March 1994.

[4] CHAN, K.W., EDWARDS, A.R., DUNN, R.W., AND DANIELS, A.R., 'Real-time electromechanical transient simulator for on-line applications', in *Proc. of First International Conference on Digital Power System Simulators – ICDS'95*, pp. 259–263, 5-7 April 1995.

[5] BERRY, T., DANIELS, A.R., AND DUNN, R.W., 'Parallel processing of sparse power system equations', *IEE Proceedings on Generation, Transmission and Distribution*, vol. 141, no. 1, pp. 68–74, 1994.

[6] BERRY, T., CHAN, K.W., DANIELS, A.R., AND DUNN, R.W., 'Interactive real-time simulation of the dynamic behavoir of large power systems', in *Proc. IEE of Japan Power & Energy '93*, pp. 5–10, 1993.

[7] KAKIMOTO, N., OHNOGI, Y., MATSUDA, H., AND SHIBUYA, H., 'Transient stability analysis of large-scale power system by lypanov's direct method', *IEEE Trans. on Power Apparatus and Systems*, vol. PAS-103, no. 1, pp. 160–167, 1984.

[8] AKIMOTO, Y., TANAKA, H., YOSHIZAWA, J., KLAPPER, D., AND W. W. PRICE, K.A.W., 'Transient stability expert system', *IEEE Trans Pwr Sys*, vol. 4, no. 1, pp. 312–320, 1989.

[9] WEHENKEL, L., PAVELLA, M., EUXIBIE, E., AND HEILBRONN, B., 'Decision tree based transient stability method – a case study', *IEEE Trans. on Power Systems*, vol. 8, pp. 459–469, February 1994.

| Scenario | A | B | C | D | E | F | G |
|---|---|---|---|---|---|---|---|
| N° Stable | 822 | 830 | 830 | 816 | 822 | 813 | 819 |
| N° Unstable | 16 | 8 | 8 | 16 | 16 | 25 | 19 |
| Screening Efficiency | | | | | | | |
| N° Pass | 0 | 1 | 9 | 9 | 5 | 11 | 5 |
| Efficiency (%) | 100.0 | 99.9 | 98.9 | 99.4 | 99.4 | 98.6 | 99.4 |
| Overall DSA Operating Time (min:sec) | | | | | | | |
| OASIS | 19:54 | 20:01 | 20:16 | 19:48 | 19:57 | 21:13 | 19:52 |
| OASIS with Screen | 0:55 | 0:49 | 1:02 | 0:55 | 0:55 | 1:06 | 0:56 |
| Speedup | 21.7 | 24.5 | 19.6 | 21.6 | 21.8 | 19.3 | 21.3 |

Table 3: Results for Laboratory Model


[10] PANG, C.K., PRABHAKARA, F.S., EL-ABIAD, A.H., AND KOVIO, A.J., 'Security evaluation in power systems using pattern recognition', *IEEE Trans. on Power Apparatus and Systems*, vol. PAS-93, pp. 969–976, 1974.

[11] HAKIMMASHHADI, H. AND HEYDT, T.G., 'Fast transient security assessment', *IEEE Trans. on Power Apparatus and Systems*, vol. PAS-102, no. 12, pp. 3816–3824, 1983.

[12] SAMMON, J.W., 'A nonlinear mapping for data structure analysis', *IEEE Trans. on Computers*, vol. 18, pp. 401–409, 1969.

[13] FISHER, R., 'The use of multiple measurements in taxonomic problems', *Annals of Eugenics*, vol. 7, pp. 179–188, 1936.

[14] 'Artificial neural networks for power systems - a literature survey', tech. rep., CIGRE Task Force 38-06-06, 1993.

[15] HAYKIN, S., *Neural Networks: a comprehensive foundation.* Macmillan, 1994.

# ON-LINE DYNAMIC SECURITY ASSESSMENT USING A REAL-TIME POWER SYSTEM SIMULATOR WITH NEURAL NETWORK CONTINGENCY SCREENS

**K.W.Chan, A.R.Edwards, R.W.Dunn, A.R.Daniels**

Power and Energy Systems Group, School of Electronic and Electrical Engineering, University of Bath, Claverton Down, Bath, BA2 7AY,United Kingdom

## Abstract

On-line dynamic security assessment aims to provide power system operators with real-time information on the stability of a power system subjected to a set of probable contingencies. Although this task is several orders of magnitude more complex than static security analysis, recent advancements in computer technology now make such analysis possible within the time constraints required by an energy management system. This paper describes a dynamic security assessment system that has recently been developed and provides details of the artificial neural network based stability screens that are used to improve the performance of the system. Simulation results are presented for various snapshots of the UK national grid system which show that full on-line dynamic security assessment is now practical.

## 1 Introduction

An on-line dynamic security analysis tool will allow the power system to be operated closer to the security limits. Traditionally, security limits have tended to arise from thermal considerations but with increasing demand and more remote generation, and problems associated with its re-enforcement, many transmission systems now suffer from stability constraints.

From an operational perspective, these stability limits are determined in the planning stages and augmented with a safety margin to account for possible variations between the planned study and the actual power system operating state. Dynamic security analysis [1] aims to provide the operators with advice as to (a) the proximity of the operating condition to stability problems and (b) the maximum permissible power flows across critical boundaries in order to remain secure.

A dynamic security assessor (DSA) is comprised of a number of modules to select, screen, evaluate and rank contingencies which may have an adverse effect on power system stability. Contingency *selection* is the process used to identify those contingencies which may lead to stability problems. Contingency *screening* aims to quickly identify those selected contingencies which will produce no adverse effect on the stability of the power system. The remaining contingencies then undergo detailed *evaluation* where the severity of the contingency is determined. The contingencies are then *ranked* in order of severity and presented to the power system operator through the Energy Management System (EMS) displays.

Contingency selection is usually performed off-line using a combination of operational experience and simulated operating conditions. Stability evaluation has traditionally been performed by energy function methods [2] and eigenvalue analysis methods. Recent advancements in the application of artificial intelligence techniques to power system analysis have led to work on applying decision trees and pattern recognition techniques to stability screening. In this study, a pattern recognition technique has been developed which is shown to be well suited to on-line stability screening. The most reliable method for contingency evaluation is to use a full time domain simulation. Numerous contingency ranking algorithms have been developed [3] and to a large extent, the algorithms that are used depend on the operating policy of the utility.

This paper describes a dynamic security analysis system that has undergone field trials at the UK National Grid Control Centre. OASIS (On-line Algorithms for System Instability Studies) has been developed over the last three years in a collaborative venture between the University of Bath, UK, and the National Grid Company, UK. It displays electro-mechanical security information to the operators through an X-Window display.

## 2 Overall Structure of OASIS

OASIS was originally designed as a complementary system working alongside an existing EMS, specialising in on-line electro-mechanical stability analysis. The task of static security analysis, as well as the other EMS functions such as dispatch, are retained by the existing EMS.

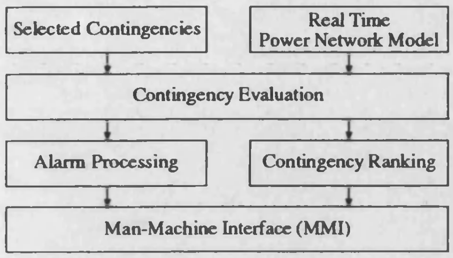


Fig 1: On-Line Dynamic Security Assessor

Approximately every 15 minutes the real-time power network model, comprised of the system topology and operating states, is assembled by the EMS and then fed to OASIS. The effect of the selected contingencies on the updated power system model is then determined, as shown in fig 1. Once all the contingencies have been evaluated, they are ranked according to their severity and then displayed, with any associated alarm messages, to the users through an X-Window based man-machine interface. This process is then repeated when a new updated power system model is made available from the EMS.

## 3 Stability Evaluation

Power systems exhibit non-linear behaviour and consequently may suffer from a wide range of stability problems. In the case of dynamic security assessment, the main interest is in the behaviour of synchronous generators during and immediately after a large system disturbance or contingency. The aim is to detect electro-mechanical transient and oscillatory instability. The time-scale of these phenomena range from milliseconds to minutes or even hours in some extreme cases.

Various methods are available for transient stability analysis. Methods based on transient energy function (TEF) [4] or the extended equal area criterion (EEAC) [5] have often been proposed for use in on-line transient stability assessment applications. Although they are relatively fast in terms of execution speed, the complexity of the power system models and contingency sequences they can cope with are seriously limited.

In the light of recent advancements in computer technology, a modern real-time power system simulator is used within OASIS as the baseline method for contingency evaluation [6, 7]. This simulator is capable of modelling an 80 machine 800 busbar power system in real-time on a standard UNIX workstation. Each machine group is represented by a fifth order voltage behind sub-transient reactance model with second order excitation model and a fourth order prime mover and governor model. A number of non-linearities are modelled such as control limits, non-linear steam flows and magnetic saturation.

For each contingency, the full system is simulated for up to 30 seconds, if no pole-slip is detected. Parameters such as rotor angle are monitored throughout the simulation and transient and oscillatory severity indices are calculated. The transient severity index is calculated based on the time to pole-slip (if there are any) or the magnitude of the first swing and the deviations of the machine frequency and MVA generation from the system frequency and machine MVA rating.

The assessment of oscillatory instability [8] is more difficult than its transient counterpart. Firstly, the term oscillatory instability should be clarified in that it refers to the post-contingency dynamic behaviour of the power system rather than the traditional definition of steady state stability. Slow power oscillations and limit cycles are, primarily, the main concerns. As a result, standard steady state stability analysis methods such as eigenvalue analysis are not adopted in OASIS.

Post-contingency oscillatory problems are manifested through the system damping, and hence the degree of oscillatory instability can be assessed by examining the damping of each machine in the system. As a result of time domain simulation, the time history of the machine rotor swings or accelerations are readily available and can be used to calculate the decay rate of the rotor oscillations. Obviously, cases with growing oscillations, i.e. negative decay rates, are oscillatory unstable and therefore unacceptable. From an operational perspective, any oscillations should decay away quickly, say within a minute i.e. the time constant of these decays is less than 12 seconds. Those contingencies which fail to meet these damping requirements should be reported as cases with poor oscillatory stability and the system oscillation decay rate can be used as an oscillatory severity index.

## 4 Stability Screens

The electro-mechanical stability screens used within OASIS are based on a pattern recognition approach. The real-time power system simulator, used for the detailed contingency evaluation, simulates each contingency up until the topology changes are complete. This point is referred to as the contingency termination point (CTP). A snapshot of the power system state vector at the CTP is then used to construct a feature vector. An artificial neural network (ANN) is then used to predict a stability index which is then compared to a threshold value to determine if the contingency leads to a secure or insecure operating condition.

The choice of stability indices for each screen has been made from practical operational guidelines. The transient stability index was chosen to be the magnitude of the worst machine rotor angle swing in the post-contingency period. Another index that could be used is the transient energy margin [4]. As mentioned earlier, oscillatory stability problems are manifested by poor damping of the post-contingency electro-mechanical oscillations. The time constant of these oscillations can be used as a quantitative measure of the degree of oscillatory instability. Decay time constants of more than 12 seconds can then therefore be identified as being un-acceptably damped.

By training the ANN to predict a stability index, the classification errors in the vicinity of a classification boundary are reduced. This is because there are no discontinuities in the *learning surface* as each contingency has a stability index between zero and one as opposed to only one of the two values. The threshold value should be set so that the desired level of security is achieved. From a transient perspective, it may be operationally desirable to identify all contingencies which lead to rotor angle swings in excess of 100 degrees, say, as transiently poor. Therefore, varying the threshold level allows the utility to control the level of conservativeness of the screens – as the threshold is raised fewer contingencies will be identified as potentially insecure but the faster the DSA will operate.

The power system simulator can also be used to generate training data for the neural networks. This allows detailed modelling of machines and other equipment to be used in the training of the classifier, improving the reliability of the approach still further.

However, the main advantage of this approach is that the demanding task of simulating the whole of the post-contingency operating condition of the power system is replaced by a very small amount of simulation, feature vector calculation and classification. This makes this approach very attractive for on-line use, although this is at the expense of off-line training of the ANNs.

## 4.1 Feature Building

Traditional pattern recognition approaches to stability screening have suffered from the *curse of dimensionality*, namely that for large power systems the feature vectors have a high dimensionality which makes it difficult to construct a pattern classifier. This problem is addressed by the use of features that are based on statistical properties of the power system state vector at the CTP.

The basic approach to feature construction is to apply a standard statistical function, such as *minimum* or *variance*, to a set of power system parameters, such as line power flows or generator terminal voltages. In this way a single numeric value can be derived from a set of power system parameters and can be used as a feature.

## 4.2 Feature Selection

Approximately 2000 statistical features were generated from a time domain simulation for a variety of operating conditions of the power system. The feature selection process involved running a series of correlations to determine those features which were most highly correlated to the required stability classification.

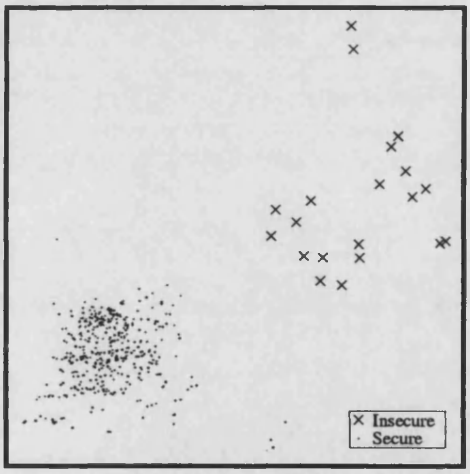


Fig 2: Sammon Plot

The best features selected by each of the selection criteria were then used to form the feature vectors for the screens. The suitability of the feature vectors at performing the classification was confirmed by producing Sammon plots [9] for each screen. If there is a clear separation between the patterns in the two dimensional plot for each stability class then there is a clear geometric separation of the patterns in the higher dimensional feature space. This is an indicator that (a) the features are well suited for the classification and (b) that the neural networks will be able to learn the training data with ease.

Fig 2 shows the Sammon plot for the transient stability screen within OASIS for the 1000 training patterns with the worst transient response. There is a clear separation between the insecure (unstable) and the secure (stable) patterns. As expected, the ANN *learned* this training data in only a few iterations.

The overhead with using multiple screens is very low. The reason for this is that the majority of the time required for the screening process is spent of performing the time domain simulation up to the CTP. The low overhead associated with calculating a few features and propagating them through an ANN takes only approximately 5% of the total screening time. Hence, although only a transient stability screen has been fully developed the inclusion of a screen to detect oscillatory instability problems will not noticeably increase the operating time of OASIS.

## 5 Implementation

One of the design goals of OASIS was an ability to work in an on-line mode with a target cycle time within 15 minutes irrespective of system size and number of contingencies. This requires that OASIS has to be scalable and portable such that more advanced computing systems, which may be general purpose single-processor workstations or dedicated multi-processor computing servers, can be used when they are available.

OASIS follows the client/server model and has been implemented as a set of co-operating tasks running on a heterogeneous computing system. Inter-processor communications and remote task management are supported through the Parallel Virtual Machine (PVM) [10] developed by the Oak National Laboratory. The component tasks of OASIS are founded on the use of Open Systems standards. ANSI C has been used to ensure portability for all all pieces of code. UNIX compatibility has been retained on all computing subsystems. The graphical interface for OASIS is built on X-Windows with MOTIF look and feel. Fig 3 shows the basis software structure of OASIS.

Data input can come directly from an energy management system, saved system snapshots or from a real-time power system simulator mimicking the real power system. This latter feature allows a complete model of a power system and OASIS to be run within the laboratory environment which can be used to train power system operators.

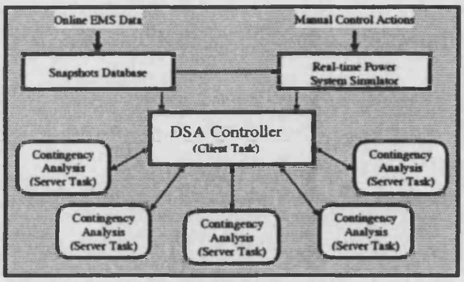


Fig 3: Block Diagram of OASIS

The client task initiates the spawning of one server task on each of the host computers, and then transmits the latest power system snapshot to each of them. The definition of each stability screen is encoded into an ASCII file, defining the composite indices to be used as inputs, the topology of the ANN and the threshold for stability comparison. These files are then uploaded to the server tasks by the client. The client task then enters a contingency allocation loop where a new contingency is allocated to each idle server task.

Upon creation, the server tasks decode the power system snapshot file into the internal data sets required by the power system simulator and build up an internal representation of the stability screens from the screen definition files. The server tasks then perform contingency screening and evaluation for the contingencies specified by the client task. Those contingencies which are selected by the screens as potentially harmful undergo detailed evaluation by the real-time power system simulator [7] to determine the extent of the security violations. When this evaluation is complete each server task calculates an overall severity index and sends this information to the client task. Information on the decay rate of the transients in the system is included in this index to provide a quantitative measure of the degree of oscillatory instability.

When all the contingencies have been evaluated by the server tasks, the client displays the new ranked contingency list to the operator through the Motif X-Window display, as shown in fig 4.

## 6 Experimental Results

The feature selection process for the transient stability screen resulted in the selection of 10 features which are highly suited for transient stability assessment. A feed-forward ANN with 10 input neurons, 8 hidden layer neurons and one output neuron was then trained. Training was stopped

# Interactive Online Dynamic Security Assessment of Large Complex Power Systems Part 2 : Contingency Screening

A.R. Edwards, K.W. Chan, R.W. Dunn and A.R.Daniels
Power and Energy Systems Group, School of Electronic and Electrical Engineering, University of Bath, Bath BA2 7AY, UK

***Abstract*—On-line dynamic security analysis has now become realistic due to advances in computer technology and algorithms for security assessment. This paper presents details of pattern recognition based electromechanical stability screens which have been implemented within a dynamic security assessor. Use of statistical functions of features is shown to overcome the dimensionality problem of applying pattern recognition techniques to large power systems. The low computational cost of this approach coupled with efficient operation has resulted in a significant step towards achieving full on-line dynamic security assessment.**

***Keywords*—Dynamic Security Assessment, Contingency Screening, Pattern Recognition, Artificial Neural Networks**

## I. INTRODUCTION

Dynamic security analysis (DSA) is rapidly evolving from the realm of pure research into a practical engineering tool [1, 2] with significant economic benefit to electric power utilities. The aims of DSA are (1) to assess the security of a power system subject to a set of pre-defined disturbances (contingencies), and (2) to provide the operators with on-line advice to improve the system security while maintaining economic operation. The dynamic security assessment process is split into the following distinct tasks.

*Contingency Selection* — a set of contingencies is chosen for analysis. This may be drawn from a pre-defined list of contingencies or selected from a database of contingencies depending on the system operating condition, expected weather conditions and other factors affecting the system security.

*Contingency Screening* — this process aims to quickly identify those contingencies from the selected list which may lead to a security violation. This is essentially a filtering process which removes those contingencies which pose little or no threat to the security of the power system.

*Contingency Evaluation* — the process where the detailed effects of a contingency on the power system are investigated. A full time domain simulation is currently the most reliable method available for performing detailed evaluation [1, 3].

*Contingency Ranking* — to assist the operator, the contingencies are ranked in order of severity with the most severe contingencies available for display to the operator. The operators can then use this information coupled with their knowledge of the system to move the system towards a more secure operating condition if necessary.

*Limit Calculation* — the on-line calculation of transfer limits between areas of the power system may also be incorporated with DSA systems. This defines the MW transfer constraints which can be coupled into the on-line dispatch tools to reduce generation costs whilst maintaining security.

*Human-Computer Interface* — This is used to display the ranked contingency list and/or transfer limits to the operators, often via an X-Window display similar in style to other EMS applications.

From the DSA perspective, power system stability can be divided into two categories, *transient* and *oscillatory* instability [4]. Contingency screens are required for each of these areas. Fig. 1 shows the practical arrangement of transient and oscillatory instability screens within a DSA system.

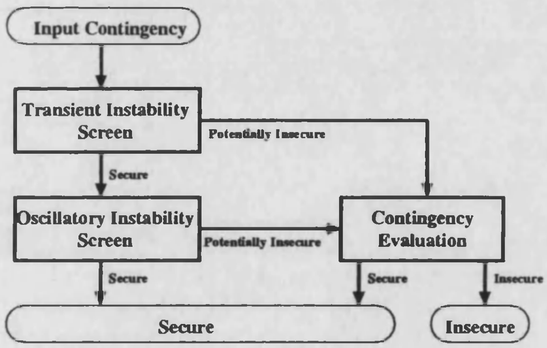


Fig. 1. Stability Screens in a Dynamic Security Assessment System

The stability screens are cascaded so that any contingency that is identified as potentially insecure is passed on to the contingency evaluation module to determine whether it will actually lead to instability in the power system.

OASIS (On-line Algorithms for System Instability Studies) is a DSA system[5] which has been developed in a collaborative venture between the University of Bath, UK, and National Grid Company, UK. OASIS runs on a heterogeneous parallel computing system, and uses multiple copies of a real-time power system simulator[3] for contingency evaluation and is described in detail in a companion paper [6].

The work described in this paper concerns the development of contingency screens to detect both transient and oscillatory insecurity. A pattern recognition approach is adopted where a *stability index* is predicted and compared to a pre-determined threshold value to determine the security classification. This method is shown to be efficient, considerably faster than a time domain simulation and scalable to large power systems. This

Submitted to
IEEE/PES Winter Meeting
January 1996

latter feature is of particular interest as in the past it has limited the application of pattern recognition techniques to only small power systems.

## II. TRANSIENT AND OSCILLATORY INSTABILITY

Transient security concerns the stability of the power system in the event of large changes on the system, such as busbar faults, line outages or the tripping of generating sets. The insecurity is observed as one or more synchronous generators losing synchronism with the rest of the system i.e. pole-slipping. This happens when there is an energy imbalance between the mechanical input power to the generator and the electrical power exported to the transmission system. This imbalance causes the machine's rotor to accelerate and if this is not arrested then pole-slipping will occur.

The maximum amplitude of a rotor angle swing in the post-contingency period can be used as a measure of the transient severity of a contingency. Utility operational guidelines usually recommend that large rotor swings should be avoided to maintain security of operation. For this reason the *maximum rotor swing amplitude* was used as the transient stability index, although the more traditional transient energy margin [7] could also be used.

A power system is often considered to have poor dynamic characteristics if the electro-mechanical oscillations of the generating units do not decay away quickly (within one minute) following a disturbance. The envelope of the amplitudes of these oscillations can be used to provide a quantitative measure of the dynamic, or *oscillatory*, security of the power system. This envelope approximates to an exponential decay (or growth) and by using a *best fit* technique the time constant of the exponential can be determined and used as an oscillatory instability index. To ensure that the oscillations have decayed away after one minute, this decay rate should be kept below 12 seconds.

Oscillatory insecurity, due to insufficient damping in the system, can give rise to long term oscillations which may lead to pole-slipping or limit cycles which will stress generation and transmission plant causing long term damage. This may also cause mal-operation of protection causing further insecurity. By enforcing a limit for the decay of electro-mechanical oscillations the above problems are avoided and the system security is maintained.

## III. PATTERN RECOGNITION APPROACH

The application of pattern recognition techniques to contingency screening is not new[8–10], but recent work [11] has shown considerable progress in the application of artificial intelligence techniques to contingency screening of realistic sized power systems. In particular, the use of *composite indices* as features for stability classification has been shown to provide the basis of a method for avoiding the curse of dimensionality, so often the Achilles heel of the pattern recognition approach. In this work, the concept of composite indices has been extended to allow a set of measurements taken from a power system model to be compressed into a single numeric value by the use of statistical functions. This compression is then shown to avoid dimensionality problems when applied to large power systems, whilst still encoding features characteristic of instability.

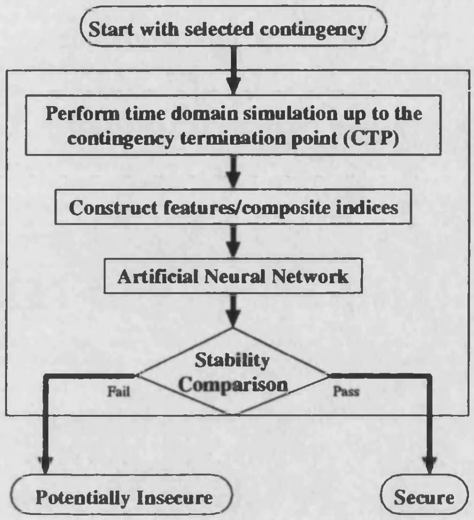


Fig. 2. Structure of Stability Screens

Fig. 2 shows the basic approach for the stability screens. An electro-mechanical power system simulator [3] is used to simulate the effect of a contingency on the power system, until the power system topology changes are complete. This point in the simulation is referred to as the fault clearance or contingency termination point (CTP). For each screen, the features to be used in the pattern recognition process are constructed using both the pre-contingency power system state vector and the power system state vector at the CTP. These features are then presented as inputs to the pattern classifier which classifies the contingency as *secure* or *potentially insecure*.

With this approach, the computationally demanding process of simulating the post-contingency state of the power system is replaced by the trivial task of feature building and pattern classification. In addition, the information stored from simulation of the power system until the CTP is shared amongst the screens, so the overhead involved with implementing multiple screens is fairly small. This approach is therefore an ideal candidate for transient and oscillatory instability screens for use within online dynamic security assessment systems.

### A. Choice of classifier

The pattern classifier that has been adopted is a feed-forward multi-layer perceptron artificial neural network (ANN)[12, 13]. The reason for this choice is threefold. (1) Although explicit rules to determine stability are not well defined, a large number of examples can be generated by applying a database of contingencies to a model of the power system and performing a full time domain simulation. This is the primary reason for choosing an ANN as the pattern classifier. (2) The feature selection process results in features that are highly correlated to the stability index, allowing a simple ANN to be used. (3) A supervised learning technique is appropriate to produce a classifier which predicts the stability index. The use of other ANN architectures is therefore unlikely to achieve any significant advantage over this basic

ANN architecture.

*B. Reliability*

Training an ANN to predict a binary stability classification requires the ANN to learn a discontinuous surface, with the discontinuity being at the stability boundary. Thus, there is a high likelihood of mis-classification for those contingencies which are close to the stability boundary. By predicting a continuous valued stability index, the ANN generalises a smooth surface with no large discontinuities, improving the classification performance around stability boundaries. This stability index is then compared to a *threshold* to determine the stability classification.

In order that the screen remains conservative, the threshold against which the stability index is compared can be lowered. For lower values of the threshold, contingencies which have a lower stability index will be marked as potentially insecure. However, lowering the threshold too much will inevitably impair the performance of the screen as more stable contingencies will be classified as potentially insecure and will therefore undergo full evaluation.

*C. Performance Metrics*

Let the symbol $\alpha_{xy}$ represent the number of contingencies that fall into class $x$ but are classified by a screen as class $y$. Let $s$ represent the class of secure contingencies and $u$ to represent the class of insecure contingencies. For the screen to remain *conservative*, i.e. for all the insecure contingencies to be detected, $\alpha_{us}$, the number of contingencies which are insecure but are classified by the screen as secure, must be zero.

$$\eta = \frac{\alpha_{ss}}{\alpha_{ss} + \alpha_{su}} \tag{1}$$

Equation 1 is used to define the efficiency of a screen, $\eta$. The screen will be 100% efficient if all stable contingencies are correctly classified, and will fall as more stable contingencies are classified as potentially insecure.

The speedup of OASIS obtained by using the screens, $\lambda$, provides a quantitative measure of the overall performance benefit of this approach. The individual speedups of the transient and oscillatory instability screens, $\lambda_t$ and $\lambda_o$, over a full time domain simulation, equivalent to 30 seconds of real time, provide an indication of the relative speeds of both screens.

## IV. COMPOSITE INDICES

Information regarding the post-contingency stability of a power system can be captured by use of a number of composite indices generated in the following manner.

$$i = A \wedge B \wedge C \wedge D \wedge E \tag{2}$$

Equation 2 describes how a composite index, $i$, is formed where $A$, $B$, $C$, $D$ and $E$ are elements of sets where:-

$$A : A \in U_a \tag{3}$$
$$B : B \in U_b \tag{4}$$
$$C : C \in U_c \tag{5}$$
$$D : D \in U_d \tag{6}$$
$$E : E \in U_e \tag{7}$$

- *Set $U_a$* is a set of statistical functions to be used to create the composite index. The members **MIN** and **MAX** are the minimum and maximum functions respectively and **SUM** is the sum of the values across all items of plant. **RMS** allows the use of the root mean square function, **RNG** determines the range of the variable and **VAR** calculates the variance. **MEAN** is the mean of all the variables, **SKEW** is the skew and **ADEV** is the absolute deviation. The remaining two use the modulus function: **MMAX** is the maximum modulus of the variable and **MSUM** is the sum of the modulus of all the variables.
- *Set $U_b$* defines which parameters are to be used in the construction of the composite index. Element **N** indicates that the index is to be built using the appropriate measurement at the CTP. **G** indicates that the gradient of the measurement at the CTP is to be used. **C** signifies that the change between the pre-contingency value and the measurement at the CTP is to be used. The set member **S** defines the post contingency steady state value of the composite index, determined by a loadflow, to be used.
- *Set $U_c$* defines the items of plant which are related to the composite index. These may be Busbars, Lines or Machines. For the purposes of the modelling all transformers, SVCs and quadrature boosters are modelled as lines.
- *Set $U_d$* defines the actual measurements to be constructed from the CTP state vector to form the basis of the composite index. **VM** and **VP** are the voltage magnitude and phase respectively, **MW** and **MV** are the MW and MVAr measurements and **MVA** is the MVA measurement. **OL** is the overload which is the current MVA value divided by the approximate rating. **KE** is the kinetic energy of a machine, **RA**, **RS** and **RC** are the rotor angle, speed and acceleration of machines and **RAM** is the rotor angular momentum. **RAP** calculates the rotor accelerating power, **AVE** is the machine's AVR voltage error and **TI** is the estimated time to instability assuming constant rotor acceleration.
- *Set $U_e$* contains two members. The first member **V** limits the scope of generation of composite indices to the immediate vicinity of a contingency. Since transient stability problems are local phenomena, the effects on parts of the power system remote from the contingency area are negligible. Our work has shown that defining the *vicinity* as a topological distance of four busbars from an item of plant involved in the contingency produces good results. The other member of the set **S** forces the indices to be built from all items of plant in the power system, i.e. the index is system wide.

This is best clarified by considering the example index shown below

$$i = \{\mathrm{SUM}, \mathrm{C}, \mathrm{M}, \mathrm{KE}, \mathrm{S}\} \tag{8}$$

which corresponds to the *sum of the changes in machine kinetic energy changes across the whole system.* In practice, each composite index was divided by the number of items of plant involved in its construction, i.e. the above was divided by the number of machines, in order to reduce the sensitivity of the composite indices to changes in the number of equipment. In this manner, the composite indices are made even more robust to changes in the power system topology and loading.

## V. FEATURE SELECTION

The reliability of pattern recognition techniques is centred on the selection of features that are highly correlated to the desired stability classification and fairly insensitive to other changes, such as the loading level or topology of the power system.

### A. *Selection Criteria*

The composite indices were ranked according to two standard feature extraction algorithms[14]. The first, *univar*, assumes that all the features are independent and performs correlations between each feature and the stability classification. The main advantage of this selection criterion is the low computational cost, because features can be considered sequentially and ranked. The main disadvantage is that although single features may be ranked with a low discriminative power, their multivariate combination might prove to be very discriminative. Also, a number of very similar features may be ranked equally highly, although the benefit of using more than one of them is small.

Secondly, multiple covariance analysis[15] is used to rank the features in order of combined discriminative power. This has a much higher computational cost than the univar algorithm, but the multivariate character of the selection makes this algorithm powerful.

The selected composite indices are chosen from the top 10 of each of the two ranked lists. In general, the multivariate list is used first and augmented with others chosen from the univar list until discrimination is achieved.

### B. *Visualisation of feature space*

The effectiveness of the selected composite indices at performing the required classification can be indicated using a Sammon plot[16]. This algorithm performs a dimensionality reduction from a high order space, equal to the number of selected composite indices, to a lower dimensional space, in this case two dimensions for plotting. The criterion for the dimensionality reduction is to minimise, by a gradient descent approach, the differences in the Euclidean distances between patterns in the the high and low spaces as much as possible. In this way the *geometric* separation of the patterns is maintained and therefore we can expect that those classes, in this case *secure* and *potentially insecure*, that distinguish well in the high dimensional space maintain do so also in the lower dimension.

If there is no obvious separation on the Sammon plot between the classes then the selected composite indices are not likely to be able to classify the stability and will almost certainly not be robust to changes in the power system state or topology. In this way, a Sammon plot of the selected indices is a useful guide as to the likely success of training the ANN for this application.

## VI. RESULTS ON UK POWER SYSTEM

The UK National Grid System operates at up to 400kV and is connected to the Scottish power system by two 400kV and two 275kV overhead lines and by a 2000MW dc link to France. The system is composed of in excess of 7000 kilometres of overhead transmission lines and cables, 21600 towers, 280 substations and up to 200 large generating units. During the trials of OASIS at the UK National Grid Control Centre, a number of system snapshots were saved over a 24 hour period to be used in the laboratory for validation of the screens. The lowest daily demand of 28.5GW was met using 109 large generating units (0500 hrs) and the daily peak of 47.1GW was produced by 147 units (1700 hrs).

These two snapshots were used to provide training data for the ANNs as they cover the demand range for the required operating condition. Applying artificially severe line outage, loss of load and generator tripping contingencies to these snapshots allowed a total of 9098 training patterns to be constructed, with approximately 1900 composite indices each. It was necessary to use artificially severe contingencies in order that stability problems would be encountered when analysing the snapshots obtained from the EMS. The feature selection process described above was then applied to select a small subset of these composite indices to be used as input features to the ANNs.

### A. *Transient Screen*

Table I shows the ten composite indices that were selected using the procedure outlined earlier.

TABLE I
TRANSIENT STABILITY SCREEN FEATURES

| No | *A* | *B* | *C* | *D* | *E* | No | *A* | *B* | *C* | *D* | *E* |
|---|---|---|---|---|---|---|---|---|---|---|---|
| 1 | MIN | N | M | OL | S | 6 | SKEW | G | M | KE | S |
| 2 | MIN | C | M | OL | S | 7 | RNG | C | B | VP | S |
| 3 | RNG | C | M | VP | S | 8 | MMAX | C | B | VP | S |
| 4 | VAR | C | M | VP | S | 9 | ADEV | C | B | VP | V |
| 5 | MMAX | C | M | VP | S | 10 | MMAX | C | B | VP | V |

The selected features are largely based on voltage phase angle changes on machine terminals and busbars. Such changes are directly related to large changes in power flow which are often symptoms of transient instability. Fig. 3 shows the Sammon plot for these features.


Fig. 3. Sammon Plot for Transient Stability Screen

It can be seen that the transiently *insecure* patterns (crosses) are geometrically well separated from the *secure* patterns (dots), indicating that the screen is likely to be able to classify the stability and be fairly robust to changes in the power system state and topology. Hence a standard three layer feed-forward neural network was chosen with 10 inputs, 8 hidden layer neurons and one output neuron. The standard back-propagation algorithm was then used to train the ANN. The threshold value was set to 0.4 because the largest stability index for a secure contingency in the training set was 0.37.

*B. Oscillatory Instability Screen*

For the oscillatory instability screen 16 composite indices, shown in table II, were selected.

TABLE II
OSCILLATORY INSTABILITY FEATURES

| No | *A* | *B* | *C* | *D* | *E* | No | *A* | *B* | *C* | *D* | *E* |
|---|---|---|---|---|---|---|---|---|---|---|---|
| 1 | MIN | N | M | OL | S | 9 | RMS | C | M | VP | V |
| 2 | MIN | C | M | OL | S | 10 | MIN | C | L | MV | S |
| 3 | RNG | C | M | VP | S | 11 | MMAX | N | B | VP | S |
| 4 | MMAX | C | M | VP | S | 12 | MAX | C | B | VP | S |
| 5 | MMAX | G | M | RAM | S | 13 | MMAX | C | B | VP | S |
| 6 | VAR | N | M | RAP | S | 14 | MAX | C | B | VP | V |
| 7 | MSUM | G | M | MW | V | 15 | ADEV | C | B | VP | V |
| 8 | MSUM | G | N | MV | V | 16 | MMAX | C | B | VP | V |

As with the transient stability screen, indices based on voltage phase angle changes are highly correlated to the instability. In addition, indices based on machine rotor angular momentum and accelerating power are shown to be well correlated. Fig.4 shows the Sammon plot of the selected features.

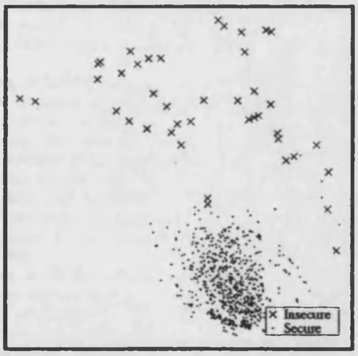


Fig. 4. Sammon Plot for Oscillatory Instability Screen

Again, the *insecure* patterns (crosses) are geometrically well separated from the *secure* patterns (dots), indicating that the screen is likely to be able to classify the stability. A standard three layer feed-forward neural network was chosen with 16 inputs, 10 hidden layer neurons and one output neuron. The ANN was trained and the training was stopped after 1500 iterations.

*C. Performance of Screens*

Table III shows the performance of the transient and oscillatory instability screens when tested on several snapshots taken from the EMS of the UK power system. These results were obtained in the laboratory using the processing power of two DEC ALPHAs and two Silicon Graphics R4000s. The first two columns show the approximate time the snapshot was taken, and the total system load at that time. $N_{ctg}$ is the total number of contingencies selected for analysis. The next two sections contain information on the transient and oscillatory instability screens. The final two columns show the net effect of the incorporation of the screens into OASIS. For the testing of the screens, every contingency was passed through both screens, but for the determination of the speedups, the screens were cascaded, as shown in fig. 1

For the transient instability screen, the screening efficiency remained above 98% for all of the test cases. $\alpha_{us}$, the number of insecure contingencies classified as secure was zero for all test cases, meeting the primary requirement of the screen; conservativeness of operation. The individual speedup of OASIS by using the transient stability screen, for the evaluation of transient stability *only*, was approximately 25 times.

The oscillatory instability screen was approximately 96% efficient, and $\alpha_{us}$ was zero for all the test cases. The individual speedup was slightly lower than that for the transient screen, due to the slightly lower efficiency of the screen.

The overall cycle time of OASIS using both stability screens is shown to be reduced to approximately 10 minutes by use of the screens. This represents an overall speedup of approximately 25 times which allows OASIS to produce results within an acceptable time frame for on-line operation.

## VII. CONCLUSIONS

The following conclusions can be drawn from the results presented.

1. The traditional problem of a high dimension feature space when applying pattern recognition techniques to stability assessment of large power systems has been avoided by the use of composite indices.
2. These indices produce features that are sufficiently loosely correlated to the loading and topology of the power system whilst remaining highly correlated to the power system stability. This allows the classifiers to be used over a wide range of power system operating conditions.
3. A simple pattern classifier, such as a simple feed-forward ANN, can be used resulting in a considerable on-line speed advantage over a full time domain simulation.
4. The efficiency of the screens results in very few secure contingencies being classified as potentially insecure, further increasing the speed advantage of this approach.
5. No contingencies that are insecure are classified by either screen as secure.

These screens are therefore highly suited to implementation within a dynamic security assessment system and reduce the on-line operating time to such an extent that a practical DSA implementation is now feasible.

## VIII. ACKNOWLEDGEMENT

The authors are grateful to the Engineering and Physical Sciences Research Council (UK) and the National Grid Company plc (UK) for supporting this research project.

REFERENCES

[1] K. Demaree, T. Athay, K. W. Cheung, Y. Mansour, E. Vaahedi, A. Y. Chang, B. R. Corns, and B. W. Garrett, "An on-line dynamic security

TABLE III
PERFORMANCE OF STABILITY SCREENS

| Snapshot | | | Transient Screen | | | | | Dynamic Screen | | | | | OASIS | |
|---|---|---|---|---|---|---|---|---|---|---|---|---|---|---|
| Time (hrs) | Load (GW) | $N_{ctg}$ | $\alpha_{ss}$ | $\alpha_{uu}$ | $\alpha_{su}$ | $\eta$ (%) | $\lambda_t$ | $\alpha_{ss}$ | $\alpha_{uu}$ | $\alpha_{su}$ | $\eta$ (%) | $\lambda_d$ | $\lambda$ | $t_{dsa}$ |
| 0000 | 31.4 | 3345 | 3313 | 16 | 16 | 99.5 | 27.1 | 3222 | 7 | 116 | 96.5 | 24.9 | 24.7 | 13:20 |
| 0300 | 30.7 | 3348 | 3292 | 20 | 36 | 98.9 | 26.2 | 3211 | 11 | 126 | 96.2 | 24.8 | 24.6 | 12:55 |
| 0600 | 30.5 | 3362 | 3308 | 16 | 38 | 98.9 | 26.3 | 3229 | 0 | 133 | 96.0 | 24.7 | 24.5 | 14:52 |
| 0900 | 39.9 | 3434 | 3399 | 16 | 19 | 99.4 | 27.2 | 3417 | 2 | 15 | 99.6 | 25.4 | 25.1 | 12:31 |
| 1200 | 41.4 | 3452 | 3409 | 16 | 27 | 99.2 | 26.8 | 3314 | 2 | 136 | 96.1 | 24.7 | 24.5 | 14:45 |
| 1500 | 41.1 | 3439 | 3407 | 14 | 18 | 99.5 | 27.2 | 3321 | 2 | 116 | 96.6 | 24.9 | 24.6 | 14:29 |
| 1800 | 45.2 | 3426 | 3395 | 20 | 11 | 99.7 | 27.6 | 3306 | 4 | 116 | 96.6 | 24.8 | 24.6 | 14:17 |
| 2100 | 38.9 | 3416 | 3385 | 16 | 15 | 99.6 | 27.1 | 3330 | 9 | 77 | 97.7 | 25.1 | 24.9 | 13:15 |


analysis system implementation", *IEEE Trans. on Power Systems*, vol. 9, pp. 1716–1722, 1994.

[2] A. B. R. Kumar, V. Brandwajn, A. Ipakchi, and R. Adapa, "Integrated framework for dynamic security analysis", *in Proc. Stocholm Power Tech*, pp. 382–387, 18-22 June 1995.

[3] T. Berry, K. W. Chan, A. R. Daniels, and R. W. Dunn, "Interactive real-time simulation of the dynamic behavoir of large power systems", *in Proc. IEE of Japan Power & Energy '93*, pp. 5–10, 1993.

[4] System Dynamic Perfromance Subcommittee Task Force on Terms & Definitions, "Proposed terms & definitions for power system stability", *IEEE Trans. on Power Apparatus and Systems*, vol. PAS-101, pp. 1894–1898, 1982.

[5] K. W. Chan, A. R. Edwards, R. W. Dunn, and A. R. Daniels, "Real-time electromechanical transient simulator for on-line applications", *in Proc. of First International Conference on Digital Power System Simulators – ICDS'95*, pp. 259–263, 5-7 April 1995.

[6] K. W. Chan, A. R. Edwards, R. W. Dunn, A. R. Daniels, and J. A. Padget, "Interactive online dynamic security assessment of large complex power systems part 1 : Contingency analysis", 1995.

[7] M. A. El-Kady, C. K. Tang, V. F. Carvalho, A. A. Fouad, and V. Vittal, "Dynamic security assessment utilizing the transient energy function method", *IEEE Trans. on Power Systems*, vol. PWRS-1, pp. 284–291, 1986.

[8] C. K. Pang, F. S. Prabhakara, A. H. El-Abiad, and A. J. Kovio, "Security evaluation in power systems using pattern recognition", *IEEE Trans. on Power Apparatus and Systems*, vol. PAS-93, pp. 969–976, 1974.

[9] K. Koizumi, O. Saito, M. Sato, K. Masegi, and M. Udo, "Fast transient stability study using pattern recognition", *in 5th Power Systems Computation Conference, Cambridge*, pp. 1–15, 1-5 September, 1975.

[10] S. Yamashiro and T. Koike, "Fast transient security assessment and enhancement of electric power systems using pattern recognition", *in 8th Power Systems Computation Conference, Helsinki*, pp. 891–897, 19-24 August 1984.

[11] G. Cauley, A. B. R. Kumar, V. Brandwajn, and A. Ipakchi, "Artificial intelligence applications in on-line dynamic security assessment", *Proc PSCC 11*, vol. 2, pp. 881–887, 1993.

[12] J. M. Zurada, *An introduction to artificial neural systems*, West, 1992.

[13] Cigre Task Force 38-06-06, "Artificial neural networks for power systems", *Electra*, vol. 159, pp. 76–101, 1995.

[14] T. W. Rauber, M. M. Barata, and A. S. Steiger-Garcao, "A toolbox for analysis and visualization of sensor data in supervision", Technical report, Departmento de Informatica, Intelligent Robotics Group, 285 Monte de Caparica, Portugal.

[15] W.W. Cooley and P.R. Lohnes, *Multivariate data analysis*, Wiley, New York, 1971.

[16] J. W. Sammon, "A nonlinear mapping for data structure analysis", *IEEE Trans. on Computers*, vol. 18, pp. 401–409, 1969.


## IX. BIOGRAPHIES

**Anthony R. Edwards** was born in Northampton, UK in 1970. He received his BEng Hons. Degree in Electronic and Electrical Engineering from the University of Bath, UK in 1991, before taking a position as a systems engineer with CEGELEC Projects Ltd, UK. He returned to the University of Bath a year later and is currently a PhD student in the Power and Energy Systems Group. His research interests are centred on artificial intelligence techniques applied to on-line dynamic security assessment.

**Ka Wing Chan** was born in Hong Kong, 1965. He received his BSc Hons. and PhD Degrees in Electronic and Electrical Engineering from the University of Bath, UK in 1988 and 1992 respectively. He is currently a researcher in the Power and Energy Systems Group, School of Electronic and Electrical Engineering, University of Bath. His general research interests are in the areas of distributed and parallel processing, artificial intelligence techniques, power system stability and security.

**Rod W. Dunn** was born in Glasgow, UK in 1959. He received his BSc and PhD in Electrical Engineering from the University of Bath in 1981 and 1984 respectively. He became a lecturer in computing and control at the University of Bath and is now a member of the Power and Energy Systems Group. His research interests include parallel and real-time computing, power system modelling and control using AI methods. He has published over 30 technical papers and is involved in the IEE UK.

**Richard A. Daniels** was born in Plymouth, UK in 1933. He received his degrees from the University of Bristol and he is currently a senior lecturer at the University of Bath. He has wide ranging research interest based on the real-time modelling and control of complex engineering systems with particular emphasis on power systems and road and rail transport systems.

# Index


## A

ANN Contingency Screening ,
  Advantages, 92
  Composite Indices, 102
  Composite Indices Selection, 115
  Drawbacks, 93
  Online Adaption, 167
  Performance Evaluation , 125
  Performance Metrics, 125
  Robustness, 93
  Why neural nets?, 90

## B

Biological Neural Networks, 71
Box Plots, 118
Boxplots ,
  Oscillatory, 194
  Transient, 192

## C

Client Task ,
  Modifications, 128
Composite Indices ,
  Base Indices, 106
  Introduction, 102
  Selection, 115
  Set Notation, 103
  Statistical Functions, 112
  Why use them?, 103
Conclusions, 158
Conclusions ,
  Classifier, 160
  Composite Indices, 159
  DSA Implementation, 163
  Edwards-Sammon Plot, 163
  Oscillatory Instability Detection, 162
  Overall Approach, 159
  Speedup, 161
  Stability Maps, 162
  Transient Instability Detection, 161
Contingencies ,
  Robustness of System, 10
Contingency ,
  Definition, 9
  Evaluation, 25
  Ranking, 25
  Screening, 24
  Selection, 24
Contingency Allocation ,
  Laboratory Model, 148
  UK national grid system, 155
Contingency Evaluation ,
  Time Simulation, 43
Contingency Ranking, 43
Contingency Screening ,
  Definition, 56
  Eigenvalue Analysis, 63
  Energy Function Methods, 58
  Implementation Methods, 123
  Introduction, 56
  Multiple screens, 123
  Numerical Integration Method, 57
  On-line Adaption, 167
  Outline, 41
  Pattern Recognition Method, 64
  Performance Evaluation, 125
  Traditional Approaches, 57
  Voting Methods, 124
Contingency Selection, 41
Critical Clearing Time, 62
Curse of Dimensionality, 67

## D

Decay Rate ,
  Rotor Oscillations, 43

Decision Trees, 63
Dispatch, 17, 21
Dispatch ,
General, 24
NGC, 12
Dynamic Security Assessment ,
Block Diagram, 39
Computational Requirements, 30
Expert Systems, 31
Financial Rewards, 30
Introduction, 29
Neural Networks, 31
Performance Improvement, 126
Requirements, 40

**E**

Edwards-Sammon Plots, 121
Eigenvalue Analysis, 63, 98
Electricity Supply ,
Demand Forecasting, 10
Generating Sets, 10
Spinning Reserve, 10
Synchronised, 10
Energy ,
Consumption, 1
Conversion, 5
Energy Management Systems ,
Dispatch, 24
Outline, 20
SCADA, 22
Security Assessment, 24
State Estimation, 23
UK NGCC, 21
Equal Area Criterion, 62
Expert Systems, 62

**F**

Feature Selection ,
Box Plots, 118
Edwards-Sammon Plots, 121
General, 115
Sammon Plots, 119
Further Work ,
On-line Adaption, 166
On-line DSA, 170
Other Applications, 171

**I**

Instability Indices ,
Eigenvalues, 98
First Swing Magnitude, 97
Introduction, 96
Maximum Rotor Swing, 97
Pole Slip Proximity, 97
Stability Indicator, 96
Transient, 96
Transient Decay Rate, 99
Transient Energy Margin, 97

**L**

Limit Calculations, 44
Loadcurve, 13
Lypanov Methods, 58

**M**

Merit Order, 3, 12, 14

**N**

National Grid System, 2
National Grid System ,
Demand, 13
EMS, 21
Generating Companies, 12
History, 3
Interconnections, 11
Oscillatory instability, 34
Pool, 14
Statutory Regulations, 16
Structure, 5, 11
National Grid System System ,
Generation capability, 14
Neural Networks ,
Application Areas, 87
Artificial, 73
Back-Propagation Algorithm, 76
Biological Basis, 71
Choice of Model, 79
Dendrites & Axons, 72
Feature Extraction, 80
Formal Methods, 86
Generalisation versus Memorisation, 80
Hopfield Model, 78

Inversion, 81
Kohonen Networks, 77
Multi-layer perceptrons, 75
Performance Metrics, 81
Size of Model, 79
Sources of Information, 88
The perceptron, 74
Tools, 85
NNS, 85
SNNS, 85

## O

OASIS, 31
OASIS ,
Contingency Details, 51
Contingency Evaluation, 52
Contingency Processing, 48
Contingency Screening, 52
Full on-line implementation, 163
Hci, 49
Introduction, 45
Ranked Contingency List, 50
Server Initialisation, 48
Server Task, 51
On-line Adaption, 166
On-line DSA, 170
On-line testing, 167
Operator Interface, 44
Optimal Power Flow, 24
Other Applications, 171

## P

Pattern Recognition Method ,
Dimensionality Problems, 67
Outline, 64
Previous Work, 65
Performance, 161
Performance Metrics, 125
Power System ,
Blackout, 6
Definition, 2
Generation, 2
Grid Supply Points, 12
Operational Aims, 9
Protection, 4, 20
Transmission, 3
Power System Controls ,
Automatic Voltage Regulators, 19
Governor Action, 17
Low Frequency Relays, 17
Protection, 20
Quadrature Boosters, 18
Static Compensators, 19
Synchronous Compensators, 19
Tap Changing Transformers, 19
Power System Operation ,
Stability, 37
Power System Stability ,
Voltage, 36
Published Work, 197
Published Work ,
APSCOM95, 224
IEE Proceedings, 224
IEEE Power Engineering Society, 224
UPEC94, 198
UPEC95, 224
PVM, 47

## R

Results ,
Full UK Power System, 149
Laboratory Scale Model, 141

## S

Sammon Plots, 119
Screen Definition File, 136
Security Assessment, 24
Security Assessment ,
AC Load-flows, 25
DC Load-flows, 25
On-line, 26
Security Levels, 11, 26
Static, 25
Security Maps ,
General, 129
MVar Injection Profile, 132
MW Injection Profile, 131
Voltage Profile, 130
Server Task ,
Composite indices module, 136
Load flow module, 135

Modifications, 133
PVM interface, 134
Stability screen module, 136
Stability ,
Definition, 31
Dynamic, 32
General, 6
Limits, 25
NGC Operating Standard, 37
Oscillatory, 32, 34
Steady State, 32, 36
Transient, 32, 33
Voltage, 19, 33
Stability Indices ,
Oscillatory, 98
Stability Margin, 62
System Vulnerability, 60

## T

Thesis ,
Structure, 7
Transient Energy Function, 58

## U

UK Power System ,
Interconnections, 149
Plant, 11, 149

## V

Visualisation ,
Edwards-Sannon Plots, 121
Sammon Plots, 119